Early differentiation dynamics of the trophoblastic lineage and its cross-communication with the embryo

Early differentiation dynamics of the trophoblastic lineage and its cross-communication with the embryo

Javier Frías Aldeguer
born on the 17th of October 1987 in Madrid, Spain

The work described in this thesis was performed at the Hubrecht Institute for Developmental Biology and Stem Cell Research (the Royal Netherlands Academy of Arts and Sciences, KNAW) and the department of Complex Tissue Regeneration of MERLN institute for Technology-Inspired Regenerative Medicine (Maastricht University, The Netherlands).

Layout by Javier Frías Aldeguer
Printed by Ridderprint. www.ridderprint.nl

ISBN: 978-94-6375-317-3

Early differentiation dynamics of the trophoblastic lineage and its cross-communication with the embryo

Dissertation

to obtain the degree of Doctor at the
Maastricht University,
on the authority of the Rector Magnificus, Prof.dr. Rianne M. Letschert
in accordance with the decision of the Board of Deans,
to be defended in public
on Thursday, April 11, 2019 at 10:00 hours

by

Javier Frías Aldeguer
born on the 17th of October 1987 in Madrid, Spain

Promotor:
Prof. Dr. C.A. van Blitterswijk

Co-Promotor:
Dr. N.C. Rivron

Assessment committee:
Prof.Dr. R.M.A. (Ron) Heeren (chair)
Prof. Dr. A. (Alfonso) Martínez Arias, Cambridge, UK
Prof.Dr. H.G. (Han) Brunner
Dr. A.P.A (Aafke) van Montfoort
Prof. Dr. J. (Janet) Rossant, Toronto, Canada

Table of contents

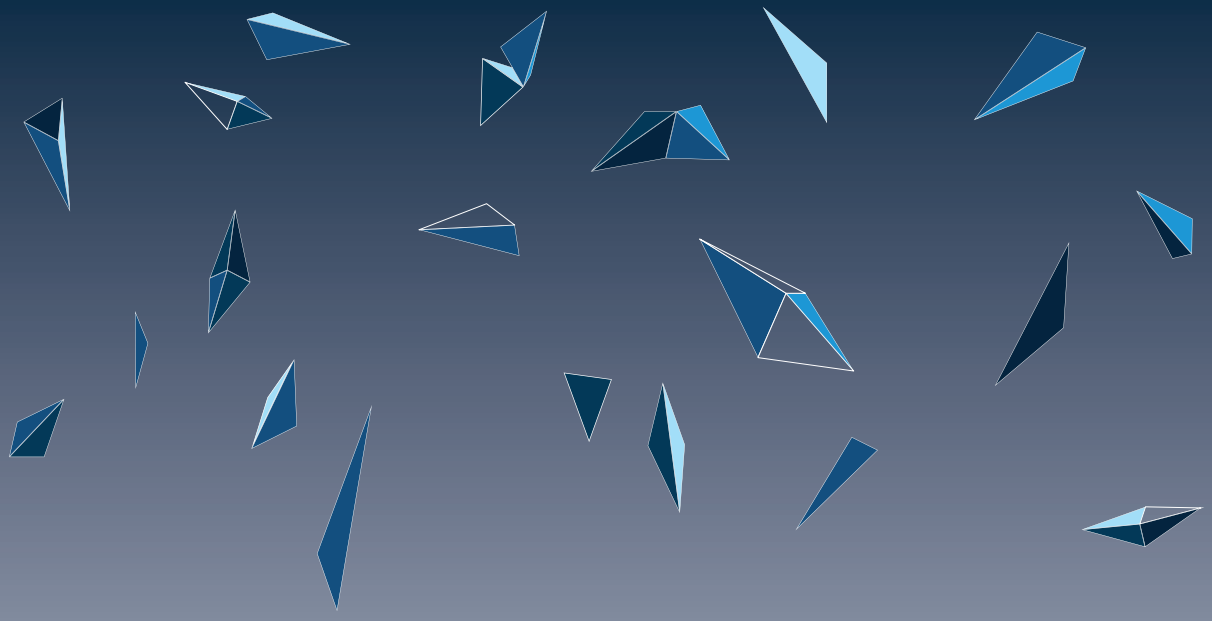

Chapter 1.
General introduction to the trophoblastic lineage

1

1.1 Introduction

The biology of the mouse preimplantation conceptus has been thoroughly studied in the last decades. At the time of implantation in the mother's endometrium, the first and second lineage segregations have already occurred, resulting in an structure that consists of both embryonic and extraembryonic lineages. The embryonic lineage has been on the main scope of research due to its potential applications in regenerative medicine, but we still have many unanswered questions concerning the extraembryonic trophoblastic lineage, responsible for attachment of the conceptus to the mother's womb and mediating the exchange of nutrients among other numerous functions.

In recent years many lines of research have increased their interest in making use of 3D cultures. The development of embryoid bodies (EBs) was one of the earliest examples. EBs have been extremely useful in helping us understand the differentiation dynamics of the embryonic lineage, but more complex models are now required to study its interaction with other lineages or tissues. Such requirement applies to the vast majority of fields, which start to combine multiple initial cell types that allow for studying their crosstalk, leading to models more representative of the in vivo situation. One of the fields taking advantage of such trend is developmental biology, which in recent years has been able to witness the development of new models that will help us gain further insight into the early stages of mouse and human development.

The evident interest of the scientific community on embryonic lineage is justified by the potential use of ESCs in therapeutics, but in the recent years, new models combining embryonic and extraembryonic compartments have been developed, giving us new tools for studying some developmental processes such as conceptus implantation. In this aspect, mouse models can be extremely informative allowing us to make discoveries that could potentially be applied to humans. However, as species we are far less efficient when it comes to reproduction: about 60% of the human zygotes fail to develop correctly before 20 weeks. Implantation is one of the key processes reducing our efficiency in obtaining a progeny. The main mediator of implantation is the trophectoderm, the outer extraembryonic structure of the blastocyst which will eventually lead to the formation of the placenta, organ responsible (among other functions) of the exchange of nutrients between embryo and mothers blood. Importantly, embryonic lethality has often been linked to trophoblastic defects (Perez-garcia et al., 2018).

In this chapter we intend to summarize what is known about the trophoblastic lineage including its crosstalk with the embryonic compartment as well as what we know about its role in implantation and new developments in the field.

1.2 Pre-implantation and trophectoderm development

After fertilization the mouse conceptus will go through different stages before is ready for implantation (**Fig. 1**). Initially, once the oozyte is fertilized, the zygote will undergo a series of symmetrical divisions, until the 8-cell stage. Until this stage, all the cells within the conceptus (blastomeres) are totipotent, meaning that they are capable of differentiating into all possible lineages, including the 3 embryonic germ layers and extraembryonic structures. The next stage is known as the morula (E2.5 dpc) and is the stage at which the first lineage commitment takes place. Between 8 and 16 cell stage, the blastomeres start compacting, increasing the cell to cell contact, mainly due to the formation of adherent and tight junctions, protein structures

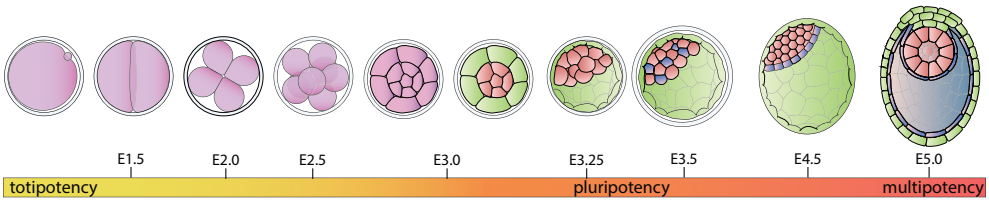

Figure 1. Mouse pre-implantation development. The different stages of early embryonic development from fertilization to the early post-implantation conceptus. Until morula compaction, all blastomeres remain totipotent. At 3 days post-coitum (E3) the first lineage segregation occurs. The blastomeres within the morula, become committed to the Inner Cell Mass (Red) or Trophectoderm (green). The trophectoderm starts cavitating, leading to the formation of a cystic structure known as the blastocyst (E3.25-E4.5dpc). At E3.5, the second lineage commitment takes place within the ICM. Cells differentiate into the Epiblast lineage (red) or the Primitive Endoderm (blue). At E4.5, the blastocyst has hatched from the zona pellucida and is ready to implant.

that contain e-cadherin and Zo1 respectively as principal components. This cellular compaction results in a polarization of the outer cells, while the inner cells remain completely surrounded. Multiple factors influence this first lineage commitment and this cell fate decision is thought the result of a complex set of inputs including apical-basal polarity, orientation of the time of cell division, inheritance of the polarity complexes upon cell division, mechanical forces and signaling pathway activity. Hippo is one of the main pathways that orchestrate the first lineage segregation as a response to such polarization, leading to the formation of Trophectoderm (TE), which is the precursor of the placenta, and the Inner Cell Mass (ICM), which is the precursor of the remaining extraembryonic and embryonic structures. The role of this pathway was discovered when it was observed that embryos with a Tead4 Knockout could not form TE (Nishioka et al., 2008; Yagi et al., 2007). Tead proteins are transcription factors inhibited by YAP, the downstream effector of the hippo pathway. Even though Hippo plays a pivotal role, other pathways such as Notch come into play (Rayon et al., 2014) during this process. One of the key target genes transcribed by Tead4 is Cdx2, the main driver known to determine TE identity. Tead4 knockouts fail to express Cdx2 (Nishioka et al., 2008), but Cdx2 knockouts do form a primordial TE, although such TE has a decreased epithelial integrity only being capable to form a small cavity. These Cdx2 KO embryos fail to implant (Strumpf et al., 2005). Such observations suggest that TE integrity is partly regulated via Cdx2 and that it controls the potential for the blastocyst to implant in utero. Apart from driving the expression of other transcription factors important for the TE identity, Cdx2 has also been reported to transcriptionally repress Oct4 and Nanog (Niwa et al., 2005; Niwa, Miyazaki, & Smith, 2000), a mechanism that ensures the exclusivity in the lineage commitment. Together with Cdx2, other master regulators such as Eomes, Gata3 (Ralston et al., 2010; Russ et al., 2000), Tcfap2c and Elf5 control the expression of other TE related genes. Eomes Knockout embryos are capable of implanting but collapse shortly after (Russ et al., 2000; Strumpf et al., 2005). Knockouts for the other genes mentioned lead to failures later in development such as lack of the formation of some of the TE-derived structures. Although there appears to be a hierarchical expression governing the expression timing of these genes, they all seem to behave as part of the regulatory network, similar to the one of pluripotency related genes in ESCs: these genes regulate their own expression, and they all act in symphony by binding together to the promoters of many other target genes (Chuong, Rumi, Soares, & Baker, 2013). Apart from the already mentioned genes, Klf5 seem to have an important role during the commitment to the TE lineage. Knockouts for Klf5 undergo TE cell arrest in the early blastocyst , lack expression of Cdx2 and Eomes and are incapable of TSC line derivation (Lin, Wani, Whitsett, & Wells,

2010) suggesting that Klf5 acts upstream of Cdx2.
Upon TE commitment, the trophoblasts start expressing adherence and tight junction proteins that will lead to its own epithelialization, a critical event for the process of cavitation. TE cells also express high levels of Na+/K+ ATPases and aquoporins as well (components of the fluid transporting machinery), which results in the formation of the blastocoel. This cavitation event, facilitated by the epithelial phenotype of the TE makes the embryo develop into a cystic structure that will give name to the next developmental stage, the blastocyst (E3-4.5). It is only after the initiation of cavitation, around 3 dpc, that cells within the ICM and TE become fully committed to their lineage (Ziomek, Johnson, & Handyside, 1982).
While the TE is still increasing its cell number and forming a larger cavity, at e3.5, the second lineage commitment will take place within the ICM, giving rise to the Epiblast (Epi) and Primitive Endoderm (PrE) lineages. Cells differentiating into such lineages appear first in a salt-and-pepper distribution. After the commitment occurs, PrE cells will migrate to the surface of the previously known ICM, forming a monolayer of cells between epiblast and the blastocoel cavity.
From the fertilized egg until the late blastocyst, the conceptus is surrounded by the Zona pellucida, a structure that protects the conceptus during the very early stages of development and prevents its attachment during its journey towards the uterus. Once the blastocyst stage is reached, the conceptus will hatch from the zona pellucida and will undergo the steps of attachment to the endometrium and implantation.
Upon implantation, the TE will differentiate leading to the formation of the extraembryonic ectoderm (ExE) and the ectoplacental cone (EC), structures that will eventually generate all the different cell types that form the mature placenta.

1.3 Lineage segregation models

Given our interest in the trophoblastic lineage, we are particularly interested in the events leading to its commitment. Up to three different models trying to explain the first lineage segregation have been suggested (**Fig. 2**).

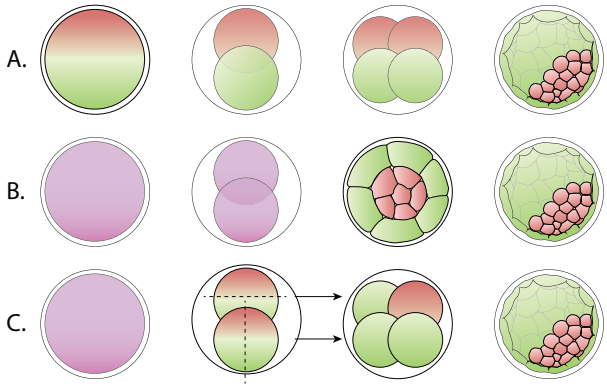

Figure 2. Lineage segregation models. A. Pre-patterning model: This model proposes the existence of polarized lineage determinants as early as in the one-cell embryo. B. The inside-out model: This model suggest that the location of each cell within the morula determines the lineage they commit to. C. The cell polarity model: This model claims that the differential inheritance of apical domains (dependent on the plane of cell division) defines the fate of the daughter cells. Figure adapted from Wennekamp et al., 2013

1.3.1 The Pre-patterning model

This model suggest the existence of asymmetries already present before the first cell division after fertilization occurs (Dalcq, 1957) and it's a model imported from observations made in other animal models such as drosophila melanogaster, c. elegans and xenopus laevis. Those asymmetrically located determinants would be differentially inherited by the daughter cells and would imply a divergent fate for each sister cell. One of the stimuli proposed to trigger these asymmetries would be the spermatozoid entry site (Piotrowska & Zernicka-Goetz, 2001), but only recently some of those determinants have been proposed to generate a bias for a particular blastomere to preferentially become committed to one of the two resulting lineages (Goolam et al., 2016). One of those factors proposed is Sox21, for which a lower expression would correlate with extra-embryonic fate. One of the main evidences against this model were obtained after performing experiments in which blastomeres isolated from the 2, 4 or 8-cell stage lead to formation of new mini blastocyst that included both lineages (A K Tarkowski & Wróblewska, 1967; Andrzej K. Tarkowski, 1959).

1.3.2 The inside-out model

This model proposes that the location of each cell within the morula determines its fate. This model is supported by the discoveries involving the hippo pathway (Nishioka et al., 2009). But it has also been proven that morula cells display molecular heterogeneities that are not explained by this model (Dietrich & Hiiragi, 2007; Plusa, Piliszek, Frankenberg, Artus, & Hadjantonakis, 2008; Ralston & Rossant, 2008).

1.3.3. The cell polarity model

Discoveries involving the presence of apical domains in blastomeres at the 8-cell stage, which implied a differential distribution of villi and organelles (Ducibella & Anderson, 1975), lead to the proposal of this model (Johnson & Ziomek, 1981). These apical domains are asymmetrically inherited based on the orientation of the cell division, resulting in the blastomeres inheriting the apical domains to be biased towards committing to the TE lineage. These experiments have not been proven yet in vivo.
Nowadays it is accepted that none of this models by itself is sufficient to explain the entirety of events taking place during the first lineage segregation, but the observations that led to the proposal of each model suggest that initial asymmetries, differential localization and cell polarity are all involved in the process. We are particularly interested in the hippo pathway (Fig. 3), mainly because is the first event to trigger transcriptional activation of genes restricted to the extraembryonic compartment. Hippo seems to be the first responder to differences in cell polarity, and acts downstream of several processes such as cell to cell adhesion mediated by e-cadherin (Kim, Koh, Chen, & Gumbiner, 2011), the expression of which is observed at the end of the 8-cell stage.

1.4 The blastocyst niche

After the first lineage segregation, the proper development of the different lineages still depends on a permanent crosstalk between compartments, making the blastocyst act as a niche (**Fig. 4**). Such crosstalk is often carried out by secreted proteins. This is the case of the ICM

secreted proteins Fgf4 and Nodal, which have been shown to be critical for the TE by helping maintaining an undifferentiated state, and dramatically affecting TE cell proliferation (Dardik, Smith, & Schultz, 1992; Guzman-Ayala et al., 2004; Tanaka, 1998). Those two signaling molecules activate the Erk branch of the MapK pathway and the Smad2/3 pathways respectively in the TE, both before and after implantation. Importantly, Fgf4 is also the protein that will reinforce the second lineage commitment within the ICM by inducing development of the PrE. After this event, Fgf4 will continue to be expressed by the Epiblast cells. Even though Fgf4 Knockout blastocysts have been reported to be morphologically normal, the embryos fail shortly after implantation (Feldman, Poueymirou, Papaioannou, DeChiara, & Goldfarb, 1995). However, when the Fgfr2 is targeted, both ICM and TE lineages originated but the embryos showed implantation defects (Arman, Haffner-Krausz, Chen, Heath, & Lonai, 1998), including an improper orientation upon implantation. The results obtained by these reports suggest that Fgf signaling plays important roles in the maintenance of TE identity, rather than its commitment.

Another critical factor is LIF, necessary for maintaining ICM and ESC identity, and for the process of implantation, a TE mediated process (Stewart, 1994). LIF is mainly expressed by the uterine endometrium, but we (Rivron et al., n.d.) and other researchers have detected its expression along with other activators of the Stat pathway (Il11) in the blastocyst. Stat3 KO embryos fail to develop further than E6.5, but upon derivation of ESCs lines a lower proliferation is observed (Takeda et al., 1997).

More recently, the blastoid model for preimplantation development, has proven that this cross-communication between embryonic and extraembryonic compartments is necessary for morphological processes such as trophoblast proliferation, self-renewal and cavitation (Rivron et al., 2018), partially due to Nodal/Bmp4 signaling originating from the ICM.

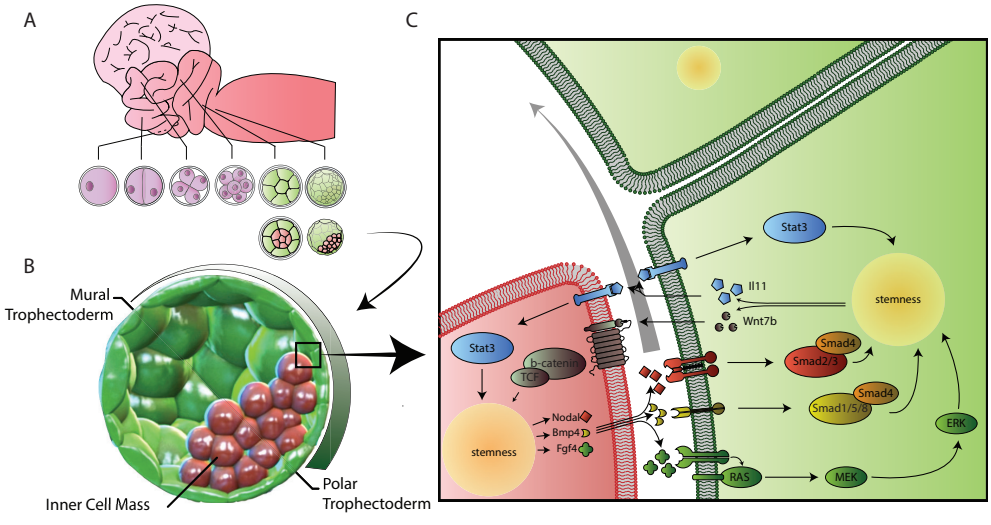

Figure 4. Cross-communication between embryonic and extraembryonic compartments of the mouse blastocyst. A. Diagram of the different stages of the pre-implantation conceptus as it travels from the infundibulum towards the uterus. B. The blastocyst includes ICM and TE. C. Active communication between both compartments takes place, being the potency of the trophectoderm dependent on embryonic signals. As the cells in the TE proliferate, the mural TE distances from the ICM becoming less exposed to its signals, resulting in differentiation of the mural TE cells while the polar TE conserves the stem cell pool.

1.5 Axis formation, trophectoderm patterning and embryonic inductions

Given the structure of the blastocyst, there is an obvious morphological asymmetry concerning the TE in relation to the ICM. It is the position of the ICM that, through embryonic inductions, defines a divergent identity between polar (in contact with the ICM) and mural TE (distal). One of the main reported differences between cells in the polar and the mural TE is their mitotic state. It has been observed that the cells in the polar TE are more proliferative than the ones located in the mural TE (Chavez, Enders, & Schlafke, 1984; Copp, 1978; Cruz & Pedersen, 1985; Gardner, 2000), possibly resulting in a proliferation flow of cells from polar to mural TE. The cells in the polar TE are more exposed to signals originating from the ICM. They have a higher mitotic index and are thought to represent the stem cell pool that generates most of the embryonic part of the placenta. On the contrary, cells in the mural TE slow down the mitotic cycle, initiate a switch to endo-replication and differentiate towards giant trophoblast cells. It is thought that these divergent phenotypes are a consequence of the formation of the blastocoel cavity and of a differential exposure to signals coming from the ICM. For instance, for Nodal signaling, the ICM-expressed membrane-bound coactivator named Crypto (Tdgf1) and the proteins Furin and Pace4 (Pcsk6), which are locally-expressed by the TE, are required in order for the Smad1/5/8 pathway to become active (Guzman-Ayala et al., 2004). Since these are not soluble proteins, full nodal activation is only possible in the cells at the interface between ICM and TE. Similarly, Wnt ligands are membrane-bound molecules, which are thought to act locally through short-range gradients. These ligands travel away from its source in a cell-bound manner through cell division, and not through diffusion (Farin et al., 2016).
These differential identities have been more recently characterized at the transcriptome level, using single cell sequencing (Nakamura et al., 2015). After bisection of the blastocysts into a mural and polar half, single cells were isolated and got their transcriptome sequenced, proving that both subpopulations have very distinct transcriptional profile with dramatic differences in cell cycle status.
Altogether, the ICM is thought to act as a reservoir that fuels, shapes, and patterns the TE, to gate-keep the trophoblast stem cell pool (polar TE), while unleashing the formation of a more differentiated subpopulation mediating implantation (mural TE).

1.6 The trophectoderm and its early derivatives: Implantation and anastomosis

The trophectoderm of the preimplantation conceptus creates a cavity that will serve as room for the embryonic compartment to develop after implantation, allows for the polar and mural TE to diverge, and mediates the attachment and implantation into the mother's endometrium. Once implanted, as the precursor of the placenta, the trophoblastic lineage will need to adapt to its new function: mediating interchange of nutrients and waste between embryo and mother. New structures derived from the TE will arise via differentiation, although the stem cell pool will be maintained until at least 8.5dpc (Uy, Downs, & Gardner, 2002).
After attachment, the polar TE continues to proliferate, leading to the formation of two structures: the extraembryonic ectoderm (ExE), which will retain the stem cell pool; and the ectoplacental cone (EC), composed of the most distal cells responsible for the invasion into the uterine wall. At E7.5 the Chorion originates from the ExE and at E8.5 merges with the Allantois, a mesoderm derived structure. Such fusion constitutes the early placenta, which continues its growth until E14.5. At the end of this first placental stage, three structures are

formed: the labyrinth, the junctional zone and a layer of trophoblast giant cells (TGCs). The labyrinth is the region responsible for the exchange of gas, nutrients and waste with the mother's blood. Structurally, the labyrinth is formed by branched villi that increase the surface area of exchange between the fetus and the mother. In this layer, multiple subtypes of trophoblast cells reside, such as TGCs, syncytiotrophoblasts and progenitor cells. The junctional zone, seems to be a structure derived from the ectoplacental cone, and is composed of spongiotrohphoblast and glycogen cells. The function of the spongiotrophoblasts is believed to be partly structural, while the glycogen cells become the main source of IGF2 in the later stages of gestation (Redline, Chernicky, Tan, Ilan, & Ilan, 1993). The parietal layer of TGCs serves as a barrier between fetal placenta and maternal deciduae.

1.7 Understanding implantation

Even though in this thesis we will not focus on the process of implantation, it is important to understand the potential repercussions that the research included in this book might bring.
The use of mouse models for studying implantation is critical, however, many of the molecular mechanisms differ from those in human. Human procreation, in contrast with the mouse, is a process known to be inefficient, being the embryo implantation a particularly suboptimal mechanism. It has been reported that only 30% of the conceptions taking place at the optimal cycle window lead to a live birth (Chard, 1991). This low efficiency makes it necessary to develop new tools that will allow us to increase the chances for a successful pregnancy, for example for couples who go through IVF derived embryo transfer.
The trophoblastic lineage plays pivotal roles in the development of the embryo, including tasks such as supplying the signals needed for an initial undifferentiated embryonic state, executing the implantation into the endometrium of the mother or mediating the nutrient exchange between embryo and the mother. All these critical roles make the trophoblastic lineage just as sensitive to genetic alterations as the embryonic compartment. Many mutations leading to embryonic lethality have been reported to involve placental defects (Perez-garcia et al., 2018).
The process of implantation is particularly delicate and relies on the optimal interaction between the conceptus and the mother's endometrium, ultimately depending on several factors such as the correct morphology of both structures, hormone levels that condition the receptivity of the endometrium as well as the exchange of growth factors and signaling molecules. An aberration affecting any of these factors will potentially result in an implantation failure.
The whole process of implantation is highly dependent on sexual hormone levels, which will oscillate during the menstrual cycle (Kodaman & Taylor, 2004). Upon ovulation, the corpus luteum starts producing progesterone, which conditions the gene expression in the endometrium, changing it into a receptive state. Several molecular pathways such as Stat, Bmp, Hedgehog, Wnt, or Mapk have been reported to become active in response to progesterone and play a key role in implantation and decidualization (K. Y. Lee et al., 2007; Matsumoto, Zhao, Das, Hogan, & Dey, 2002; Mohamed, Dufort, & Clarke, 2004; Monsivais et al., 2017; Paria et al., 2001; Simon et al., 2009; Takamoto, Zhao, Tsai, & DeMayo, 2002). These pathways need to act in symphony in order to reach a successful implantation. Without a doubt, LIF-dependent Stat signaling is the most critical pathway to our knowledge, having a pivotal role in multiple stages of the peri-implantation embryo.
Mice with Lif deficiency have been proven to be infertile due to implantation failure (Stewart, 1994). Lif is expressed as a response to ovarian steroids (Sherwin et al., 2004) and its expres-

sion in the endometrium peaks twice, one prior to implantation that results in priming the endometrium for receptivity, and a second peak at the time of implantation (Song & Lim, 2006). In human, it has been reported that estrogen is not necessary for the process of implantation (Zegers-Hochschild & Altieri, 1995), instead chorionic gonadotrophins seem to be the hormones promoting LIF expression (Licht et al., 1998). In humans, when comparing the LIF expression during the proliferative and secretory phases of the menstrual cycle, infertile women seem to show lower levels than those observed in fertile women (Tawfeek, Eid, Hasan, Mostafa, & El-Serogy, 2012; Wu, Yin, Zhao, Hu, & Chen, 2013). LIF has a positive effect on implantation by affecting both the blastocyst and the uterine wall.

Regarding its effects on the embryo, LIF is responsible for maintenance of the pluripotency of both ICM and TE, but also seems to promote the expression of hGC and prostaglandin in trophoblasts (Horita, Kuroda, Hachisuga, Kashimura, & Yamashita, 2018). Later on LIF, via the Stat pathway will promote TE stem cell differentiation into trophoblast giant cells, which are the cells responsible for the decidual invasion (Hemberger, 2008). LIF also has been reported to downregulate the expression of a variety of metalloproteinase inhibitors (Suman, Shembekar, & Gupta, 2013), allowing then for an extracellular matrix digestion, needed for the invasion.

LIF also affects the uterine wall by changing its morphology and promoting the synthesis of other growth factors important for implantation such as EGF (Song, Lim, Das, Paria, & Dey, 2000), making the endometrium more receptive. The subsequent process of decidualization has also been proven to be affected in LIF deficient mice. In such mice, the stromal cells fail to differentiate into the primary decidual cells, leading to implantation failure (Fouladi-Nashta et al., 2005). A third effect of LIF on implantation involved the recruitment of Leukocytes at the implantation site. This recruitment of immune cells is triggered both by the seminal fluid first (Robertson, 2007), but also by the blastocyst at the time of implantation (Grümmer & Winterhager, 2011). Dendritic cells, natural killers, neutrophils, eosinophils, macrophages and B and T lymphocytes will be recruited (J. Y. Lee, Lee, & Lee, 2011; Schofield & Kimber, 2004) and will influence the tolerance for the blastocyst, angiogenesis, the tissue remodeling, inflammation and compensate for nitric oxide presence. The pro and anti-inflammatory balance resulting of the presence of all these leukocytes, will determine whether the implantation is successful (Sykes, MacIntyre, Yap, Teoh, & Bennett, 2012).

Apart from LIF dependent Stat signaling, other pathways such as Bmp, Hedgehog, Wnt, or Mapk have been reported to play a key role in implantation and decidualization (K. Y. Lee et al., 2007; Matsumoto et al., 2002; Mohamed et al., 2004; Monsivais et al., 2017; Paria et al., 2001; Simon et al., 2009; Takamoto et al., 2002). The agonists for the mentioned pathways are expressed at the endometrial epithelium or stroma as a response to progesterone and estradiol.

Given the complexity of implantation, new improvements in this field are needed and now expected given the new models developed and the recent human trophoblast stem cells derivation (Okae et al., 2018). The use of such models and development of new ones could have a unprecedented impact in the field of assisted reproduction.

1.8 TSCs as in vitro analogues of the Trophectoderm

Both the embryonic and trophoblastic analogues of the blastocyst have been derived in vitro to establish stem cell lines resembling their respective compartments. These stem cell lines are

important tools to model embryonic development in vitro.
First embryonic stem cells (ESCs) were isolated in 1981 from blastocysts cultured in the presence of LIF as in vitro analogues of the ICM (Evans & Kaufman, 1981). TSCs were then derived in 1998 from the ExE of E6.5 embryos and from E3.5 blastocyst (Tanaka, 1998) in the presence of Fgf4. The use of Fgf4 to maintain and expand TSCs is based on its production by the ICM, thus recreating one aspect of the blastocyst niche. As reported in subsequent publications, researchers managed to derive TSCs from different stages up to E8.5 (Uy et al., 2002), suggesting the maintenance of a stem cell pool during early placental development. In fact, apart from being present in the TE of the blastocyst, pockets with undifferentiated trophoblasts can be found in the post-implantation embryo all along these developmental stages, within the ExE and Chorion. Even though it has been proven that there are stem cell populations present in TE derived tissues until e9.5, such stem cell detection is generally based on the expression of some of the classical TSCs lineage related transcription factors (Kuales et al., 2015), two of which lead to lethality when knocked-out only after implantation. The fact that the derivation from different developmental time points lead to apparently identical TSCs, differs with the case of the other cell types that can be derived from the blastocyst. ESCs and XEN (PrE analogues) cells, to this day, can only be derived from the blastocyst. This observation can suggest that the population of TSCs do not fully or exclusively represent the TE stem cells. However, at least part of the derived TSCs grow in colonies and can be expanded indefinitely while remaining multipotent, being capable of chimerizing, or differentiating into all placental cellular subtypes in vitro by upon removal of the potency maintaining factors Fgf4 and TGFb/Activin A (supplied by MEF).
The initial cultures of TSCs made use of high serum content and a layer of embryonic fibroblasts (MEF) or MEF-conditioned medium. This conditioned medium was later substituted by the use of Tgfb or Activin (Erlebacher, Price, & Glimcher, 2004). In a next improvement, fully chemically-defined media conditions were described (Kubaczka et al., 2014; Ohinata & Tsukiyama, 2014). Those chemically-defined culture conditions are based on a media similar to the essential 8 media used for the culture of human ESCs, but supplemented with Fgf4 and Tgfb, or based on the use of a Wnt inhibitor (XAV939), Rock inhibitor (Y27632), Fgf2 and B27 and N2 supplements. Importantly both new culture conditions require the use of Matrigel or Fibronectin coating respectively in order to ensure the attachment of the cells.
TSC cultures have been described as heterogeneous from cell to cell. Although TSCs maintain an undifferentiated state, there are clear morphological differences across cells and colonies. In 2015, Kuales et al., based on the triple positive staining of post-implantation embryos until the stage e9.5, proposed that the bona fide TSCs co-express the transcription factors Cdx2, Eomes and Elf5 (Kuales, Weiss, Sedelmeier, Pfeifer, & Arnold, 2015). One year later another publication tackles the heterogeneity across colonies (Motomura et al., 2016), proving that the small dome-shaped colonies are the ones that retain the multipotent properties. Cells from such colonies would aggregate with 8-cell stage embryos and chimaerize remaining as cells in the polar TE.
The cells described by Ohinata et al are able to contribute to the placenta when they are injected back in a recipient blastocyst, while the ones cultured under conditions described y Kubaczka require a transition to traditional MEF and serum conditions. The placental contributions observed upon injection of TSCs in a foster blastocyst in most of the TSCs related publications are far from being as efficient as the contributions obtained in the embryonic compartment when using ESCs. This suggests that most of the cultures developed to the day, are only capable of maintaining a progenitor state instead of a multipotent one for in vivo

conditions or that the amount of cells with full potential are only a fraction of the culture.
If we take ESCs as an example, the original culture conditions lead to a degree of heterogeneity comparable to the one observed in TSC cultures. Such heterogeneity represents a spectrum of differentiation states. A clear improvement solving this intercellular variation, was the development of the so known 2i media (Ying et al., 2008). This media involves the use of a MEK and GSK3 inhibitors in combination with LIF, and allows for a culture of ESCs in a "ground state". The cells show a phenotype closer to cells in the epiblast of the blastocyst and a less dramatic intercellular heterogeneity.
Equally to its embryonic counterparts (Takahashi & Yamanaka, 2006), two groups managed to obtain induced TSCs (iTSCs) from mouse fibroblasts (Benchetrit et al., 2015; Kubaczka et al., 2015). Both groups claim to obtain an efficient conversion into iTSCs by forcing the expression of 4 transcription factors. The transcription factors Eomes, Gata3 and Tfap2c are required for both protocols. The protocol from Kubaczka needed Ets2 as well, while Benchetrit managed to obtain the conversion with only those three factors but also when Myc is included in the transcription factor cocktail. Interestingly, even though, Cdx2 expression levels were monitored in order to confirm a TSC identity, both publications agreed to report that Cdx2 was not a required transcription factor for the trans-differentiation. This could be interpreted in two different ways: Cdx2 is a factor that is only important for the lineage determination in the absence of other factors, or TSCs represent a different state than that one present in the blastocyst TE.
TSCs can be derived from different time points ranging from E3.5 to E9.5. This is one of the main arguments used to claim that TSCs don't accurately represent the TE stem cells. The embryonic counterparts can only be derived during a narrow time window; this is between the first lineage commitment and implantation. Even though it has been proven that there are stem cell populations present in TE derived tissues until E9.5, such stem cell detection is generally based on the expression of some of the classical TSC lineage related transcription factors (Kuales et al., 2015), two of which lead to lethality when knocked-out only after implantation.
Only recently, human trophoblast stem cells (hTSCs) have been derived for the first time (Okae et al., 2018), opening the door for a research that could potentially improve our understanding of key molecular mechanisms of human embryology. Before this recent discovery, other researchers tried to obtain hTSCs by transdifferentiation from hESCs by exposing them to Bmp4, which lead to expression of trophoblast related genes (Xu et al., 2002). Such conversion lead to two schools of thought supporting or denying the identity of those transdifferentiated cells as extraembryonic.
Before the recent derivation of hTSCs, the closer attempt to derivation from the implantation embryo intended to derive human ESCs from single blastomeres (Zdravkovic et al., 2015). The lines obtained differed from blastocyst derived ESCs showing expression of trophoblastic lineage genes. Apart from those attempts, in vitro analogues of placental progenitors equivalent to later stages in development had been successfully derived (Genbacev et al., 2011), although these couldn't be expanded unlimitedly and had only a limited differentiation potential.

1.9 In vitro models for studying the peri-implantation embryo

ESCs and TSCs have been fundamental to answer key questions in developmental biology, but as we have mentioned the blastocyst acts as a niche, making the in vitro analogues insuf-

ficient to represent the complexity of the situation in vivo. We are therefore in need of more complex models that are able to complement the knowledge we have acquired by experimenting and observing embryo development. It's important to mention that studying embryonic development in vivo also has its limitations such as embryo finite availability, difficulty for genetical studies, or difficult accessibility for studying certain stages of development.

In the recent years, there has been an increased focus on obtaining organoid cultures that resemble the cellular organization and sometimes heterogeneity observed in the organ of interest. As we will observe in later chapters, our lab as managed to develop the blastoid, a new model combining ESCs and TSCs that will help us study in detail certain processes taking place during the blastocyst stage as well as implantation. The blastoid manages to solve some of those limitations related to the use of embryos.

Interestingly, other organoid cultures important for the study of early embryonic development have been developed recently. That is the case of the endometrium organoid (Boretto et al., 2017; Turco et al., 2017). Importantly, such organoids are responsive to sexual hormones and they could be combined with blastocysts making them a potential tool to be combined with blastoids.

While our model focuses on the pre-implantation embryo, other labs have developed new models that replicate certain processes of the early post-implantation embryo. Harrison et al. (Harrison, Sozen, Christodoulou, Kyprianou, & Zernicka-Goetz, 2017) also made use of both ESCs and TSCs in order to generate structures that resemble the early post-implantation development. The structures obtained self-organized and recapitulated key developmental stages such as epiblast rosette formation and formation of the amniotic cavity. These two new models for mouse pre and post-implantation development open a new field called synthetic embryology.

In the human embryology field, the Zernicka-Goetz and Brivanlou labs developed in vitro models for studying human post-implantation development in the absence of maternal tissues (Deglincerti et al., 2016; Shahbazi et al., 2016). These publications, managed to culture human blastocysts being able to reach a later developmental stage, leading to processes such as the formation of the pro-amniotic cavity, appearance of the prospective yolk sac and trophoblast differentiation. The absence of maternal tissues, prove that the first stages after implantation are self-directed.

A similar model was reported in the 70s for mouse, although this protocol failed to be fully reproduced. In Hsu's publications (Y C Hsu, 1971; Y C Hsu, Baskar, Stevens, & Rash, 1974; Yu Chih Hsu, 1973) the mouse blastocyst was cultured in the presence of collagen (that would serve as extracellular matrix for embryo support) and a sequential use of different serums to promote the development of the embryo into the further developed stages. Hsu claimed that with this protocol, the embryos were capable of developing until the early somite stage at E9.5.

Amongst the several applications of these recently reported post-implantation models for early embryonic development, studying the role of the trophoblast lineage in the embryo nutrition would probably be the one with a more straight forward clinical application. It is now well accepted that embryo nutrition during the early stages of its development has a major impact on the health of the adults. This was observed after periods of famine affecting pregnant women that resulted in chronic diseases in the adulthood of the offspring (Roseboom, Rooij, & Painter, 2006). For many years, it was not clear from how early in the embryo development a nutritional deficit would lead to those diseases, but we currently know from studying IVF infants that even the culture medium in which the embryo develops until is ready for implantation, has an impact on the birth weight (Dumoulin et al., 2018; Kleijkers et al., 2016), and

consequently on its adult life.

Goals of this thesis

In further chapters of this thesis, we will study the nature of TSCs by direct comparison with the TE of the E3.5 mouse blastocyst. Along the way we will discover how certain pathways regulate the expression of Cdx2 and use that to our advantage at the moment of generating new culture conditions that make TSCs a more suitable tool for the generation of blastoids. We will also approach long lasting questions regarding the TE axis formation by generating data that might help us understand the dynamics of early trophoblastic differentiation.

Bibliography

Arman, E., Haffner-Krausz, R., Chen, Y., Heath, J. K., & Lonai, P. (1998). Targeted disruption of fibroblast growth factor (FGF) receptor 2 suggests a role for FGF signaling in pregastrulation mammalian development. Proceedings of the National Academy of Sciences of the United States of America, 95(9), 5082–5087. https://doi.org/10.1073/pnas.95.9.5082

Benchetrit, H., Herman, S., Van Wietmarschen, N., Wu, T., Makedonski, K., Maoz, N., … Buganim, Y. (2015). Extensive Nuclear Reprogramming Underlies Lineage Conversion into Functional Trophoblast Stem-like Cells. Cell Stem Cell, 17(5), 543–556. https://doi.org/10.1016/j.stem.2015.08.006

Boretto, M., Cox, B., Noben, M., Hendriks, N., Fassbender, A., Roose, H., … Vankelecom, H. (2017). Development of organoids from mouse and human endometrium showing endometrial epithelium physiology and long-term expandability. Development, 144(10), 1775–1786. https://doi.org/10.1242/dev.148478

Chard, T. (1991). 11 Frequency of implantation and early pregnancy loss in natural cycles. Bailliere's Clinical Obstetrics and Gynaecology, 5(1), 179–189. https://doi.org/10.1016/S0950-3552(05)80077-X

Chavez, D. J., Enders, A. C., & Schlafke, S. (1984). Trophectoderm cell subpopulations in the periimplantation mouse blastocyst. The Journal of Experimental Zoology, 231(2), 267–271. https://doi.org/10.1002/jez.1402310211

Chuong, E. B., Rumi, M. A. K., Soares, M. J., & Baker, J. C. (2013). Endogenous retroviruses function as species-specific enhancer elements in the placenta. Nature Publishing Group, 45(3), 325–329. https://doi.org/10.1038/ng.2553
Copp, A. J. (1978). Interaction between inner cell mass and trophectoderm of the mouse blastocyst. I. A study of cellular proliferation. Journal of Embryology and Experimental Morphology, 48, 109–125.

Cruz, Y. P., & Pedersen, R. A. (1985). Cell fate in the polar trophectoderm of mouse blastocysts as studied by microinjection of cell lineage tracers. Developmental Biology, 112(1), 73–83. https://doi.org/10.1016/0012-1606(85)90120-4
Dalcq, A. M. (1957). Introduction to General Embryology. O.U.P.[Clarendon Press]. Retrieved from https://books.google.nl/books?id=xXwdAAAAIAAJ

Dardik, A., Smith, R. M., & Schultz, R. M. (1992). Colocalization of transforming growth factor-alpha and a functional epidermal growth factor receptor (EGFR) to the inner cell mass and preferential localization of the EGFR on the basolateral surface of the trophectoderm in the mouse blastocyst. Developmental Biology, 154(2), 396–409.

Deglincerti, A., Croft, G. F., Pietila, L. N., Zernicka-Goetz, M., Siggia, E. D., & Brivanlou, A. H. (2016). Self-organization of the in vitro attached human embryo. Nature, 533(7602), 251–254. https://doi.org/10.1038/nature17948
Dietrich, J.-E., & Hiiragi, T. (2007). Stochastic patterning in the mouse pre-implantation embryo. Development, 134(23), 4219–4231. https://doi.org/10.1242/dev.003798

Ducibella, T., & Anderson, E. (1975). Cell shape and membrane changes in the eight-cell mouse embryo: Prerequisites for morphogenesis of the blastocyst. Developmental Biology, 47(1), 45–58. https://doi.org/10.1016/0012-1606(75)90262-6

Dumoulin, J. C., Land, J. A., Montfoort, A. P. Van, Nelissen, E. C., Coonen, E., Derhaag, J. G., … Evers, J. L. (2018).

Effect of in vitro culture of human embryos on birthweight of newborns, 25(3), 605–612. https://doi.org/10.1093/humrep/dep456

Erlebacher, A., Price, K. a, & Glimcher, L. H. (2004). Maintenance of mouse trophoblast stem cell proliferation by TGF-beta/activin. Developmental Biology, 275(1), 158–169. https://doi.org/10.1016/j.ydbio.2004.07.032
Evans, M. J., & Kaufman, M. H. (1981). Establishment in culture of pluripotential cells from mouse embryos. Nature, 292, 154. Retrieved from http://dx.doi.org/10.1038/292154a0

Farin, H. F., Jordens, I., Mosa, M. H., Basak, O., Korving, J., Tauriello, D. V. F., … Clevers, H. (2016). Visualization of a short-range Wnt gradient in the intestinal stem-cell niche. Nature, 530(7590), 340–343. https://doi.org/10.1038/nature16937

Feldman, B., Poueymirou, W., Papaioannou, V., DeChiara, T., & Goldfarb, M. (1995). Requirement of FGF-4 for post-implantation mouse development. Science, 267(5195), 246–249. https://doi.org/10.1126/science.7809630
Fouladi-Nashta, A. A., Jones, C. J. P., Nijjar, N., Mohamet, L., Smith, A., Chambers, I., & Kimber, S. J. (2005). Characterization of the uterine phenotype during the peri-implantation period for LIF-null, MF1 strain mice. Developmental Biology, 281(1), 1–21. https://doi.org/10.1016/j.ydbio.2005.01.033

Gardner, R. L. (2000). Flow of cells from polar to mural trophectoderm is polarized in the mouse blastocyst. Human Reproduction, 15(3), 694–701. https://doi.org/10.1093/humrep/15.3.694

Genbacev, O., Donne, M., Kapidzic, M., Gormley, M., Lamb, J., Gilmore, J., … Fisher, S. J. (2011). Establishment of human trophoblast progenitor cell lines from the chorion. Stem Cells, 29(9), 1427–1436. https://doi.org/10.1002/stem.686

Goolam, M., Scialdone, A., Graham, S. J. L., MacAulay, I. C., Jedrusik, A., Hupalowska, A., … Zernicka-Goetz, M. (2016). Heterogeneity in Oct4 and Sox2 Targets Biases Cell Fate in 4-Cell Mouse Embryos. Cell, 165(1), 61–74. https://doi.org/10.1016/j.cell.2016.01.047

Grümmer, R., & Winterhager, E. (2011). Blastocyst-mediated induction of endometrial connexins: An inflammatory response? Journal of Reproductive Immunology, 90(1), 9–13. https://doi.org/10.1016/j.jri.2011.02.010

Guzman-Ayala, M., Guzman-Ayala, M., Ben-Haim, N., Ben-Haim, N., Beck, S., Beck, S., … Constam, D. B. (2004). Nodal protein processing and fibroblast growth factor 4 synergize to maintain a trophoblast stem cell microenvironment. Proceedings of the National Academy of Sciences of the United States of America, 101(44), 15656–15660. https://doi.org/10.1073/pnas.0405429101

Harrison, S. E., Sozen, B., Christodoulou, N., Kyprianou, C., & Zernicka-Goetz, M. (2017). Assembly of embryonic and extraembryonic stem cells to mimic embryogenesis in vitro. Science, 356(6334). https://doi.org/10.1126/science.aal1810

Hemberger, M. (2008, March). IFPA award in placentology lecture - characteristics and significance of trophoblast giant cells. Placenta. Netherlands. https://doi.org/10.1016/j.placenta.2007.11.007

Horita, H., Kuroda, E., Hachisuga, T., Kashimura, M., & Yamashita, U. (2018). Induction of prostaglandin E 2 production by leukemia inhibitory factor promotes migration of first trimester extravillous trophoblast cell line , HTR-8 / SVneo, 22(7), 1801–1809.

Hsu, Y. C. (1971). Post-blastocyst differentiation in vitro. Nature, 231(5298), 100–102.

Hsu, Y. C. (1973). Differentiation in vitro of mouse embryos to the stage of early somite. Developmental Biology, 33(2), 403–411. https://doi.org/10.1016/0012-1606(73)90145-0

Hsu, Y. C., Baskar, J., Stevens, L. C., & Rash, J. E. (1974). Development in vitro of mouse embryos from the two-cell egg stage to the early somite stage. Journal of Embryology and Experimental Morphology, 31(1), 235–245. Retrieved from http://www.ncbi.nlm.nih.gov/pubmed/4856485

Johnson, M. H., & Ziomek, C. A. (1981). The foundation of two distinct cell lineages within the mouse morula. Cell, 24(1), 71–80. https://doi.org/10.1016/0092-8674(81)90502-X

Kim, N., Koh, E., Chen, X., & Gumbiner, B. M. (2011). E-cadherin mediates contact inhibition of proliferation through Hippo signaling-pathway components, 2011. https://doi.org/10.1073/pnas.1103345108/-/DCSupplemental. www.pnas.org/cgi/doi/10.1073/pnas.1103345108

Kleijkers, S. H. M., Mantikou, E., Slappendel, E., Consten, D., Echten-arends, J. Van, Wetzels, A. M., … Mastenbroek, S. (2016). Influence of embryo culture medium (G5 and HTF) on pregnancy and perinatal outcome after IVF : a multicenter RCT, 31(10), 2219–2230. https://doi.org/10.1093/humrep/dew156

Kodaman, P. H., & Taylor, H. S. (2004). Hormonal regulation of implantation. Obstetrics and Gynecology Clinics of North America, 31(4), 745–766. https://doi.org/10.1016/j.ogc.2004.08.008

Kuales, G., Weiss, M., Sedelmeier, O., Pfeifer, D., & Arnold, S. J. (2015). A Resource for the transcriptional signature of bona fide trophoblast stem cells and analysis of their embryonic persistence. Stem Cells International, 2015, 17–20. https://doi.org/10.1155/2015/218518

Kubaczka, C., Senner, C., Ara??zo-Bravo, M. J., Sharma, N., Kuckenberg, P., Becker, A., … Schorle, H. (2014). Derivation and maintenance of murine trophoblast stem cells under defined conditions. Stem Cell Reports, 2(2), 232–242. https://doi.org/10.1016/j.stemcr.2013.12.013

Kubaczka, C., Senner, C. E., Cierlitza, M., Ara??zo-Bravo, M. J., Kuckenberg, P., Peitz, M., … Schorle, H. (2015). Direct Induction of Trophoblast Stem Cells from Murine Fibroblasts. Cell Stem Cell, 17(5), 557–568. https://doi.org/10.1016/j.stem.2015.08.005

Lee, J. Y., Lee, M., & Lee, S. K. (2011). Role of endometrial immune cells in implantation. Clinical and Experimental Reproductive Medicine, 38(3), 119–125. https://doi.org/10.5653/cerm.2011.38.3.119

Lee, K. Y., Jeong, J.-W., Wang, J., Ma, L., Martin, J. F., Tsai, S. Y., … DeMayo, F. J. (2007). Bmp2 Is Critical for the Murine Uterine Decidual Response. Molecular and Cellular Biology, 27(15), 5468–5478. https://doi.org/10.1128/MCB.00342-07

Licht, P., Lösch, A., Dittrich, R., Neuwinger, J., Siebzehnrübl, E., & Wildt, L. (1998). Novel insights into human endometrial paracrinology and embryo-maternal communication by intrauterine microdialysis. Human Reproduction Update, 4(5), 532–538. https://doi.org/10.1093/humupd/4.5.532

Lin, S. J., Wani, M. A., Whitsett, J. A., & Wells, J. M. (2010). Klf5 regulates lineage formation in the pre-implantation mouse embryo, 3963, 3953–3963. https://doi.org/10.1242/dev.054775

Matsumoto, H., Zhao, X., Das, S. K., Hogan, B. L. M., & Dey, S. K. (2002). Indian hedgehog as a progesterone-responsive factor mediating epithelial-mesenchymal interactions in the mouse uterus. Developmental Biology, 245(2), 280–290. https://doi.org/10.1006/dbio.2002.0645

Mohamed, O. A., Dufort, D., & Clarke, H. J. (2004). Expression and Estradiol Regulation of Wnt Genes in the Mouse Blastocyst Identify a Candidate Pathway for Embryo-Maternal Signaling at Implantation1. Biology of Reproduction, 71(2), 417–424. https://doi.org/10.1095/biolreprod.103.025692

Monsivais, D., Clementi, C., Peng, J., Fullerton, P. T., Prunskaite-Hyyryläinen, R., Vainio, S. J., & Matzuk, M. M. (2017). BMP7 induces uterine receptivity and blastocyst attachment. Endocrinology, 158(4), 979–992. https://doi.org/10.1210/en.2016-1629

Motomura, K., Oikawa, M., Hirose, M., Honda, A., Togayachi, S., Miyoshi, H., … Ogura, A. (2016). Cellular Dynamics of Mouse Trophoblast Stem Cells: Identification of a Persistent Stem Cell Type. Biology of Reproduction, 94(6), 122–122. https://doi.org/10.1095/biolreprod.115.137125

Nakamura, T., Yabuta, Y., Okamoto, I., Aramaki, S., Yokobayashi, S., Kurimoto, K., … Saitou, M. (2015). SC3-seq: a method for highly parallel and quantitative measurement of single-cell gene expression. Nucleic Acids Research, 43(9), e60. https://doi.org/10.1093/nar/gkv134

Nishioka, N., Inoue, K., Adachi, K., Kiyonari, H., Ota, M., Ralston, A., … Sasaki, H. (2009). Article The Hippo Sig-

naling Pathway Components Lats and Yap Pattern Tead4 Activity to Distinguish Mouse Trophectoderm from Inner Cell Mass. Developmental Cell, 16(3), 398–410. https://doi.org/10.1016/j.devcel.2009.02.003

Nishioka, N., Yamamoto, S., Kiyonari, H., Sato, H., Sawada, A., Ota, M., … Sasaki, H. (2008). Tead4 is required for specification of trophectoderm in pre-implantation mouse embryos. Mechanisms of Development, 125(3–4), 270–283. https://doi.org/10.1016/j.mod.2007.11.002

Niwa, H., Miyazaki, J., & Smith, A. G. (2000). Quantitative expression of Oct-3 / 4 defines differentiation , dedifferentiation or self-renewal of ES cells, 24(april), 2–6.

Niwa, H., Toyooka, Y., Shimosato, D., Strumpf, D., Takahashi, K., Yagi, R., & Rossant, J. (2005). Interaction between Oct3 / 4 and Cdx2 Determines Trophectoderm Differentiation, 917–929. https://doi.org/10.1016/j.cell.2005.08.040
Ohinata, Y., & Tsukiyama, T. (2014). Establishment of trophoblast stem cells under defined culture conditions in mice. PLoS ONE, 9(9). https://doi.org/10.1371/journal.pone.0107308

Okae, H., Toh, H., Sato, T., Hiura, H., Takahashi, S., Shirane, K., … Arima, T. (2018). Derivation of Human Trophoblast Stem Cells. Cell Stem Cell, 22(1), 50–63.e6. https://doi.org/10.1016/j.stem.2017.11.004

Paria, B. C., Ma, W., Tan, J., Raja, S., Das, S. K., Dey, S. K., & Hogan, B. L. (2001). Cellular and molecular responses of the uterus to embryo implantation can be elicited by locally applied growth factors. Proceedings of the National Academy of Sciences of the United States of America, 98(3), 1047–1052. https://doi.org/10.1073/pnas.98.3.1047

Perez-garcia, V., Fineberg, E., Wilson, R., Murray, A., Mazzeo, C. I., Tudor, C., … Mohun, T. (2018). Placentation defects are highly prevalent in embryonic lethal mouse mutants. Nature Publishing Group, 555(7697), 463–468. https://doi.org/10.1038/nature26002
Piotrowska, K., & Zernicka-Goetz, M. (2001). Role for sperm in spatial patterning of the early mouse embryo. Nature, 409(6819), 517–521. https://doi.org/10.1038/35054069

Plusa, B., Piliszek, A., Frankenberg, S., Artus, J., & Hadjantonakis, A.-K. (2008). Distinct sequential cell behaviours direct primitive endoderm formation in the mouse blastocyst. Development, 135(18), 3081–3091. https://doi.org/10.1242/dev.021519

Ralston, A., Cox, B. J., Nishioka, N., Sasaki, H., Chea, E., Rugg-Gunn, P., … Rossant, J. (2010). Gata3 regulates trophoblast development downstream of Tead4 and in parallel to Cdx2. Development (Cambridge, England), 137(3), 395–403. https://doi.org/10.1242/dev.038828

Ralston, A., & Rossant, J. (2008). Cdx2 acts downstream of cell polarization to cell-autonomously promote trophectoderm fate in the early mouse embryo. Developmental Biology, 313(2), 614–629. https://doi.org/10.1016/j.ydbio.2007.10.054

Rayon, T., Menchero, S., Nieto, A., Xenopoulos, P., Crespo, M., Cockburn, K., … Manzanares, M. (2014). Notch and Hippo Converge on Cdx2 to Specify the Trophectoderm Lineage in the Mouse Blastocyst. Developmental Cell, 30(4), 410–422. https://doi.org/10.1016/j.devcel.2014.06.019

Redline, R. W., Chernicky, C. L., Tan, H. Q., Ilan, J., & Ilan, J. (1993). Differential expression of insulin-like growth factor-II in specific regions of the late (post day 9.5) murine placenta. Molecular Reproduction and Development, 36(2), 121–129. https://doi.org/10.1002/mrd.1080360202

Rivron, N. C., Frias-Aldeguer, J., Vrij, E. J., Boisset, J.-C., Korving, J., Vivié, J., … Geijsen, N. (n.d.). Blastocyst-like structures generated solely from stem cells. Nature, 557(7703), 106–111. Retrieved from http://www.ncbi.nlm.nih.gov/sites/entrez?Db=pubmed&DbFrom=pubmed&Cmd=Link&LinkName=pubmed_pubmed&LinkReadableName=Related Articles&IdsFromResult=29720634&ordinalpos=3&itool=EntrezSystem2.PEntrez.Pubmed.Pubmed_ResultsPanel.Pubmed_RVDocSum

Rivron, N. C., Frias-aldeguer, J., Vrij, E. J., Boisset, J., Korving, J., Vivié, J., … Geijsen, N. (2018). Blastocyst-like structures generated solely from stem cells.

Robertson, S. A. (2007). Seminal fluid signaling in the female reproductive tract: lessons from rodents and pigs. Journal of Animal Science, 85(13 Suppl), 36–44. https://doi.org/10.2527/jas.2006-578

Roseboom, T., Rooij, S. De, & Painter, R. (2006). The Dutch famine and its long-term consequences for adult health. https://doi.org/10.1016/j.earlhumdev.2006.07.001

Russ, A. P., Wattler, S., Colledge, W. H., Aparicio, S. A. J. R., Carlton, M. B. L., Pearce, J. J., … Evans, M. J. (2000). Eomesodermin is required for mouse trophoblast development and mesoderm formation, 404(March), 95–99.
Schofield, G., & Kimber, S. J. (2004). Leukocyte Subpopulations in the Uteri of Leukemia Inhibitory Factor Knockout Mice During Early Pregnancy. Biology of Reproduction, 72(4), 872–878. https://doi.org/10.1095/biolreprod.104.034876

Shahbazi, M. N., Jedrusik, A., Vuoristo, S., Recher, G., Hupalowska, A., Bolton, V., … Zernicka-Goetz, M. (2016). Self-organization of the human embryo in the absence of maternal tissues. Nature Cell Biology, 18(6), 700–708. https://doi.org/10.1038/ncb3347

Sherwin, J. R. A., Freeman, T. C., Stephens, R. J., Kimber, S., Smith, A. G., Chambers, I., … Sharkey, A. M. (2004). Identification of Genes Regulated by Leukemia-Inhibitory Factor in the Mouse Uterus at the Time of Implantation. Molecular Endocrinology, 18(9), 2185–2195. https://doi.org/10.1210/me.2004-0110

Simon, L., Spiewak, K. A., Ekman, G. C., Kim, J., Lydon, J. P., Bagchi, M. K., … Cooke, P. S. (2009). Stromal progesterone receptors mediate induction of Indian hedgehog (IHH) in uterine epithelium and its downstream targets in uterine stroma. Endocrinology, 150(8), 3871–3876. https://doi.org/10.1210/en.2008-1691

Song, H., & Lim, H. (2006). Evidence for heterodimeric association of leukemia inhibitory factor (LIF) receptor and gp130 in the mouse uterus for LIF signaling during blastocyst implantation. Reproduction, 131(2), 341–349. https://doi.org/10.1177/0092070306286705

Song, H., Lim, H., Das, S. K., Paria, B. C., & Dey, S. K. (2000). Dysregulation of EGF Family of Growth Factors and COX-2 in the Uterus during the Preattachment and Attachment Reactions of the Blastocyst with the Luminal Epithelium Correlates with Implantation Failure in LIF- Deficient Mice. Molecular Endocrinology, 14(8), 1147–1161. https://doi.org/10.1210/mend.14.8.0498

Stewart, C. L. (1994). Leukaemia Inhibitory Factor and the Regulation of Pre-Implantation Development of the Mammalian Embryo, 238, 233–238.

Strumpf, D., Mao, C., Yamanaka, Y., Ralston, A., Chawengsaksophak, K., Beck, F., & Rossant, J. (2005). Cdx2 is required for correct cell fate specification and differentiation of trophectoderm in the mouse blastocyst, 2093–2102. https://doi.org/10.1242/dev.01801

Suman, P., Shembekar, N., & Gupta, S. K. (2013). Leukemia inhibitory factor increases the invasiveness of trophoblastic cells through integrated increase in the expression of adhesion molecules and pappalysin 1 with a concomitant decrease in the expression of tissue inhibitor of matrix metalloproteinase. Fertility and Sterility, 99(2), 533–542.e2. https://doi.org/10.1016/j.fertnstert.2012.10.004

Sykes, L., MacIntyre, D. A., Yap, X. J., Teoh, T. G., & Bennett, P. R. (2012). The Th1:Th2 dichotomy of pregnancy and preterm labour. Mediators of Inflammation, 2012. https://doi.org/10.1155/2012/967629

Takahashi, K., & Yamanaka, S. (2006). Induction of Pluripotent Stem Cells from Mouse Embryonic and Adult Fibroblast Cultures by Defined Factors, 2, 663–676. https://doi.org/10.1016/j.cell.2006.07.024

Takamoto, N., Zhao, B., Tsai, S. Y., & DeMayo, F. J. (2002). Identification of Indian hedgehog as a progesterone-responsive gene in the murine uterus. Molecular Endocrinology (Baltimore, Md.), 16(10), 2338–2348. https://doi.org/10.1210/me.2001-0154

Takeda, K., Noguchi, K., Shi, W., Tanaka, T., Matsumoto, M., Yoshida, N., … Akira, S. (1997, April). Targeted disruption of the mouse Stat3 gene leads to early embryonic lethality. Proceedings of the National Academy of Sciences of the United States of America.

Tanaka, S. (1998). Promotion of Trophoblast Stem Cell Proliferation by FGF4. Science, 282(5396), 2072–2075. https://doi.org/10.1126/science.282.5396.2072

Tarkowski, A. K. (1959). Experiments on the development of isolated blastomeres of mouse eggs. Nature, 184(4695), 1286–1287. https://doi.org/10.1038/1841286a0

Tarkowski, A. K., & Wróblewska, J. (1967). Development of blastomeres of mouse eggs isolated at the 4- and 8-cell stage. Journal of Embryology and Experimental Morphology, 18(1), 155–180.

Tawfeek, M. A., Eid, M. A., Hasan, A. M., Mostafa, M., & El-Serogy, H. A. (2012). Assessment of leukemia inhibitory factor and glycoprotein 130 expression in endometrium and uterine flushing: a possible diagnostic tool for impaired fertility. BMC Women's Health, 12. https://doi.org/10.1186/1472-6874-12-10

Turco, M. Y., Gardner, L., Hughes, J., Cindrova-Davies, T., Gomez, M. J., Farrell, L., … Burton, G. J. (2017). Long-term, hormone-responsive organoid cultures of human endometrium in a chemically defined medium. Nature Cell Biology, 19(5), 568–577. https://doi.org/10.1038/ncb3516

Uy, G. D., Downs, K. M., & Gardner, R. L. (2002). Inhibition of trophoblast stem cell potential in chorionic ectoderm coincides with occlusion of the ectoplacental cavity in the mouse, 3924, 3913–3924.

Wu, M., Yin, Y., Zhao, M., Hu, L., & Chen, Q. (2013). The low expression of leukemia inhibitory factor in endometrium: Possible relevant to unexplained infertility with multiple implantation failures. Cytokine, 62(2), 334–339. https://doi.org/10.1016/j.cyto.2013.03.002

Xu, R.-H., Chen, X., Li, D. S., Li, R., Addicks, G. C., Glennon, C., … Thomson, J. a. (2002). BMP4 initiates human embryonic stem cell differentiation to trophoblast. Nature Biotechnology, 20(12), 1261–1264. https://doi.org/10.1038/nbt761

Yagi, R., Kohn, M. J., Karavanova, I., Kaneko, K. J., Vullhorst, D., DePamphilis, M. L., & Buonanno, A. (2007). Transcription factor TEAD4 specifies the trophectoderm lineage at the beginning of mammalian development. Development, 134(21), 3827–3836. https://doi.org/10.1242/dev.010223

Ying, Q.-L., Wray, J., Nichols, J., Batlle-Morera, L., Doble, B., Woodgett, J., … Smith, A. (2008). The ground state of embryonic stem cell self-renewal. Nature, 453(7194), 519–523. https://doi.org/10.1038/nature06968

Zdravkovic, T., Nazor, K. L., Larocque, N., Gormley, M., Donne, M., Hunkapillar, N., … Fisher, S. J. (2015). Human stem cells from single blastomeres reveal pathways of embryonic or trophoblast fate specification. Development, 142(23), 4010–4025. https://doi.org/10.1242/dev.122846

Zegers-Hochschild, F., & Altieri, E. (1995). Luteal estrogen is not required for the establishment of pregnancy in the human. Journal of Assisted Reproduction and Genetics, 12(3), 224–228.

Ziomek, C. A., Johnson, M. H., & Handyside, A. H. (1982). The developmental potential of mouse 16-cell blastomeres. The Journal of Experimental Zoology, 221(3), 345–355. https://doi.org/10.1002/jez.1402210310

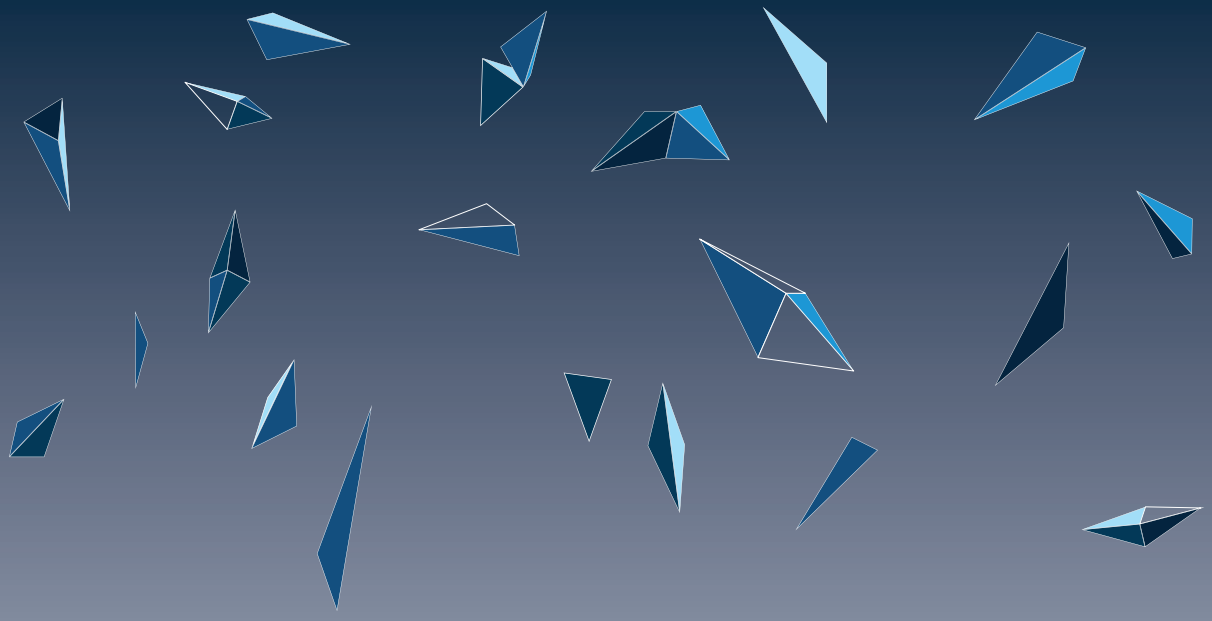

Chapter 2.
The classical cultures of TSCs allow for a wide spectrum of differentiation states

2

2.1 Abstract

During the first stages of the mouse pre-implantation embryo, the first lineage segregation takes place leading to the formation of the Inner Cell Mass (ICM) and the Trophectoderm (TE), precursors of the embryo proper and the placenta respectively. The in vitro analogues for both ICM and TE and have been available for decades and have been instrumental for developmental biologists. While the culture of ESCs has been gradually improving with the purpose of generating new, more reliable models, TSCs have been cultured in very similar conditions ever since they were first derived.
In this chapter, we show how the available TSC cultures lead to a high inter-cellular heterogeneity that includes a range of differentiation states that simultaneously represent different developmental stages. We were able to correlate high CDX2 expression levels with increased in vitro stem cell potential. Developing new culture conditions potentiating CDX2 expression levels might lead to a phenotype more comparable to the TE making TSCs a better tool for the generation of models for studying the trophoblastic lineage.

2.2 Introduction

Before we acquired our understanding of mammalian embryo development, there was a time in which it was necessary to trace the evolutionary roots as viviparous animals. It was during these times at the end of the XIX century that the placenta was the target of studies of zoologists including Ambrosius Hubrecht(Hubrecht 1889). After extensive studies of the early placentation in hedgehogs, based on a comparative embryological approach, he proposed the term trophoblast for the proliferating cells formed from the outer part of the embryo that were in direct contact with the mother's tissues. The term trophoblast comes from the greek meaning trophos- (nourish) and blastos (germ). This term depicts the proposed nutritional role of the outer cells of the conceptus, which form the interface between the maternal tissue and the embryo proper. The trophoblastic lineage is one of the two resulting tissues after the first lineage segregation and will develop into the placenta, organ responsible for nutrient exchange between mother and fetus.
In mice, the trophoblastic lineage is set apart at the morula/early blastocyst stage, in an event termed first lineage segregation. The trophoblast lineage forms the outer trophectoderm (TE) of the blastocyst, which shelters the other precursors (ICM cells) and mediate the implantation into the uterus. Upon implantation, trophoblasts form multiple cell types (e.g. giant trophoblast cells, cytotrophoblasts, syncytiotrophoblasts) including the cells that will mediate anastomosis with the mother's blood vessels to irrigate and nourish the site of implantation. Along development, the trophoblast lineage further develop into the placenta, the organ responsible for actively nurturing the fetus.
The house mouse is currently the most powerful animal model for studying mammalian embryonic development given the possibility to form transgenic animals, the relatively high analogy of its genome with the human one (Lander et al. 2001), the possibility to culture blastocyst-derived stem cells, along with its relatively fast breeding and aging, small scale, and potential for inbreeding. For these reasons, the study of the trophoblastic lineage in mice has been pivotal for our understanding of mammalian development (Cross et al. 2003; Rossant and Cross 2001). In that regard, the derivation of embryonic stem cells (ESCs) (Evans and Kaufman 1981) and of trophoblast stem cells (TSCs) (Tanaka et al. 1998) opened new opportunities to understand early mouse development. TSCs are in vitro analogues of the

early trophoblastic compartment. TSCs primary cell lines derived from the early conceptus (E3-E6.5) proved to be a powerful tool for investigating the molecular, genetic and epigenetic regulations of the trophoblastic lineages. In the recent years, three-dimensional models highlighted their potential to recapitulate aspects of morphogenesis and patterning.
Even though TSCs have been instrumental for our understanding of the trophoblast lineage, a fine understanding of their in vitro states and intercellular heterogeneity needs to be addressed. In this chapter, we focus on describing and characterizing the in vitro states of TSCs.

2.3 Results

2.3.1 CDX2 marks the polar region of the E3.75 blastocyst.

TE and TSCs are characterized by the expression of CDX2, which shows a homogenous expression across the TE in freshly isolated e3.5 blastocysts (**Fig. 1A**). We thus examined the presence of this protein in blastocysts (E3.5+0.25). To prevent the possible role of the uterine environment, we isolated E3.5 blastocysts and cultured them in plain M2 media for 6 hours. The TE of these blastocysts expressed higher levels of CDX2 in the polar region as compared to the mural region (**Fig. 1B**). This observation is consistent with a gradient of differentiation along the polar-mural axis.
Upon dissection of the blastocyst, the mural trophectoderm alone forms trophoblast vesicles that induce decidualization upon in utero transfer. However, these trophoblasts rapidly stop proliferating and generate only few, persistent Giant Trophoblast Cells. Such vesicles, when complemented with ICM cells, can develop into a conceptus, although development is slower than normal (Gardner, Papaioannou, and Barton 1973). This led to the proposition that signals originating from the ICM (embryonic inductions) can revert trophoblasts from a mural to a polar state. These reverted trophoblasts can subsequently form the extra-embryonic ectoderm and a close-to-normal placenta.
The MAPK is important for multiple aspects of blastocyst development (Arman et al. n.d.; Feldman et al. 1995) and multiple ligands and receptors are expressed in the blastocyst (**Fig. 1C-D**). FGF4 is especially produced by the ICM cells (Rappolee et al. 1994). Fgfr2 KO blastocysts induce limited decidualization, random orientation upon implantation, and form only trophoblast giant cells upon in vitro culture (Arman et al. 1998). This suggests that FGF ligands are important embryonic inducers regulating TE development and its implantation potential.
Consistent with that, TSCs are derived by culturing blastocysts with FGF4 and the removal of this protein leads to TSCs terminal differentiation (Tanaka 1998). By using a Cdx2-eGFP fusion reporter line from a mouse line previously published (McDole and Zheng 2012) we observed that CDX2 expression level in TSCs is proportional to the concentration of FGF4 (**Fig. 1E**). On the contrary, Tgfb ligands, which are also important for TSCs maintenance (Erlebacher, Price, and Glimcher 2004)do not regulate a dose-dependent expression of CDX2. We thus tested the response of CDX2 to FGF4 in the TE (**Fig. 1B**). Blastocysts exposed to a high concentration of FGF4 (500 ng/ml for 6 hours) did not increase the expression of CDX2 in the mural trophoblasts. We concluded that FGF4 is not sufficient to regulate CDX2 in the mural trophoblasts. We then postulated that CDX2 expression requires other stimuli exclusively present in the vicinity of the ICM.
In addition, we also stained blastocysts for pERK (active kinase mediator of the pathway) (**Fig. 1B**). Interestingly, both groups showed only a few pERK positive cells in the limit be-

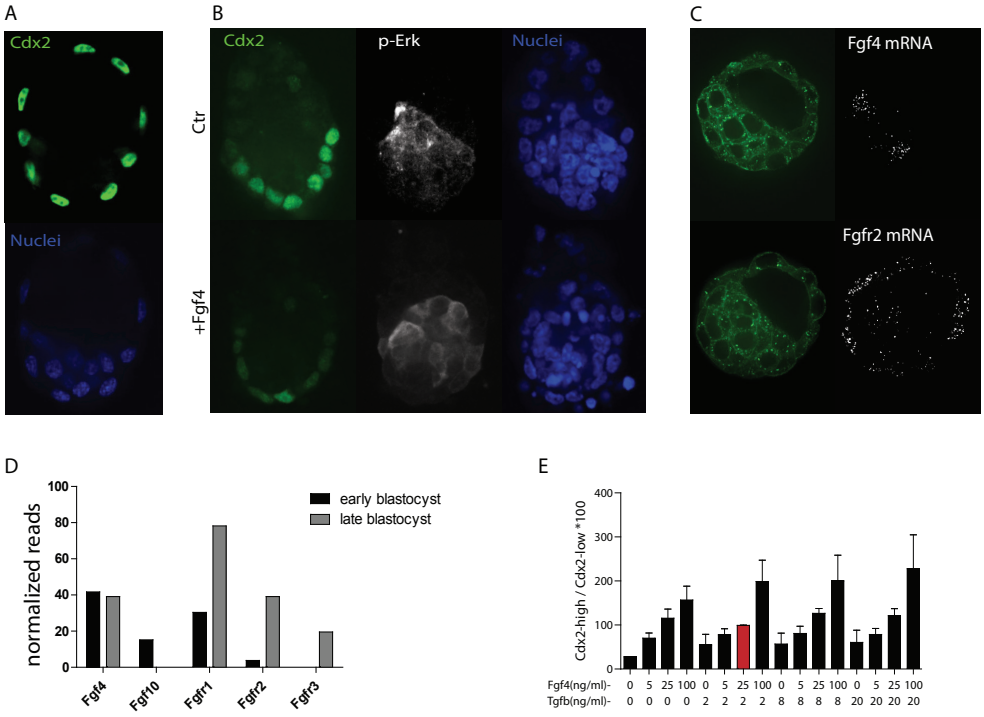

Figure 1. The role of MapK pathway in the trophoblastic lineage A. CDX2 staining of freshly isolated e3.5 blastocyst. B. CDX2 and p-ERK staining of blastocysts isolated at E3.5 and kept in culture for 6 hours in plain media or in the presence of 500 ng/ml of FGF4. C. Single molecule FISH against Fgf4 and Fgfr2 transcripts. D. Detection of MapK related ligands and receptors in the early and late blastocyst. CDX2 expression response to different concentrations of FGF4 and TGFb.

tween polar and mural TE. Internal cells were clearly pERK positive, presumably PrE cells in the ICM. It is known that the MapK pathway acts in pulses and at specific moments of the cell cycle (Ryu et al. 2015). Thus, making a "snapshot" of the phosphorylated status of the pathway is insufficient for determining the activation state across the whole TE. Answering the questions related to the role of the MapK pathway in TE and TSC would require certain tools such as Erk FRET sensors to be tracked by live imaging, inducible KO models, or microfluidic systems that allow for a precise regulation and measurement of the activation of the pathway. Nevertheless, altogether, these experiments suggest Fgf4 to be important to regulate Cdx2 expression but insufficient to revert CDX2 expression loss in the mural trophectoderm.

2.3.2 Single cell analysis reveals mural and polar cells within the TE to have different transcriptional signatures.

Several researchers have demonstrated the different phenotypes between polar and mural trophectoderm, often pointing at differences in the mitotic index (Gardner et al. 1973; Chavez et al. 1984; Copp 1978; Cruz and Pedersen 1985.). In 2015 single cells coming from bisected E4.5

blastocysts, were subjected to single cells transciptome analysis(Nakamura et al. 2015). The authors confirmed a differential phenotype between mural and polar TE cells suggesting a small set of genes to be markers of the polar (Gsto1, Ddah1, Utf1 and Hspd1) or mural TE (Slc2a3, Dmkn, Klf5, Gata2 and Dppa2). We downloaded their dataset from the GEO repository (GSE63266), and used the RaceID and monocle packages for comparing in depth polar and mural transcriptomes (Grun et al. 2016; Muraro et al. n.d.; Trapnell et al. 2014). Unsupervised gene expression clustering confirmed polar and mural cells to have a different transcriptional profile (**Fig. 2A**). Differential gene expression analysis allowed us to find the top differentially expressed genes between the polar and mural cluster of cells (**Fig. 2B**). Among those we could find some genes previously related to an undifferentiated trophoblast state such as Esrrb (Rossant and Cross 2001), or genes reported to mark stem cells in later stages of the placenta such as Ly6a (Natale et al. 2017). Other genes such as Bmp8b (Graham et al. 2014), Ezr (Dard et al. 2001; Korotkevich et al. 2017) or H19 (Zuckerwise et al. 2016) have also been reported to be important in early stages of the trophoblastic lineage. Gene onthology performed using the 1584 differentially expressed genes (fold change>1.5 pvalue<0.05) showed enrichment in biological processes such as cell division, cell cycle, cell migration, in utero development; and pathways such as metabolic pathways, focal adhesions, tight junctions, fatty acid metabolism, hypoxia or MapK, AmpK, hippo and Tgfβ pathways (**Supplementary table 1**).
Monocle is a package for single cell analysis that allows to distribute each cell into a virtual trajectory with a given pseudotime value based on their transcriptional profile. That trajectory tries to explain a biological process such as differentiation. Monocle managed to locate each cell in a trajectory (**Fig. 2C-D**) assigning the polar cells low pseudotime values. The pseudotime values assigned allows us to find genes that define that trajectory (**Fig. 2F**), with genes such as Krt18 (a traditional trophoblastic markers) showing a higher expression in mural cells. When classical trophoblast markers are plotted against pseudotime (**Fig. 2E**) we observed that markers for undifferentiated states such as Esrrb, Elf5 or Sox2 peak with earlier pseudotime values, while differentiation markers like Basp1, Gjb2 or Pparγ peak with higher pseudotime values. Altogether, the analysis of this single cell sequencing data suggests a trajectory of differentiation from the polar to mural trophoblast, and highlights a number of genes and ontologies that define these states.

2.3.3 CDX2 is heterogeneously expressed in TSCs and defines the proliferating and self-renewing cells.

We then looked at CDX2 expression within cultures of TSCs. For these experiments we made use of the CDX2-eGFP fusion reporter knocked-in mouse line previously generated (Mcdole and Zheng 2012) (**Fig. 3A**). A TSC line homozygote for CDX2-eGFP (C3-1, previously derived by Nicolas Rivron) showed a marked CDX2 heterogeneity both via imaging and by FACS (**Fig. 3B and 3D**). This heterogeneity is also observed when performing stainings against CDX2 and EOMES on the F4 TSC line (previously derived at the Rossant lab) (**Fig. 3C**), and occurs both in the presence (Kuales et al. 2015; Tanaka 1998) and in the absence (Kubaczka et al. 2014) of serum.
FACS analysis for live Hoechst staining in the C3-1 line showed that a higher fraction of the CDX2-High TSCs have an enriched G2/M profile as compared to the CDX2-Low cells, which are rather in a G1 phase (**Fig. 3-E**). This observation is consistent with the previous observations that the polar TE cells (which shows higher CDX2 expression) are more proliferative than the mural TE cells.

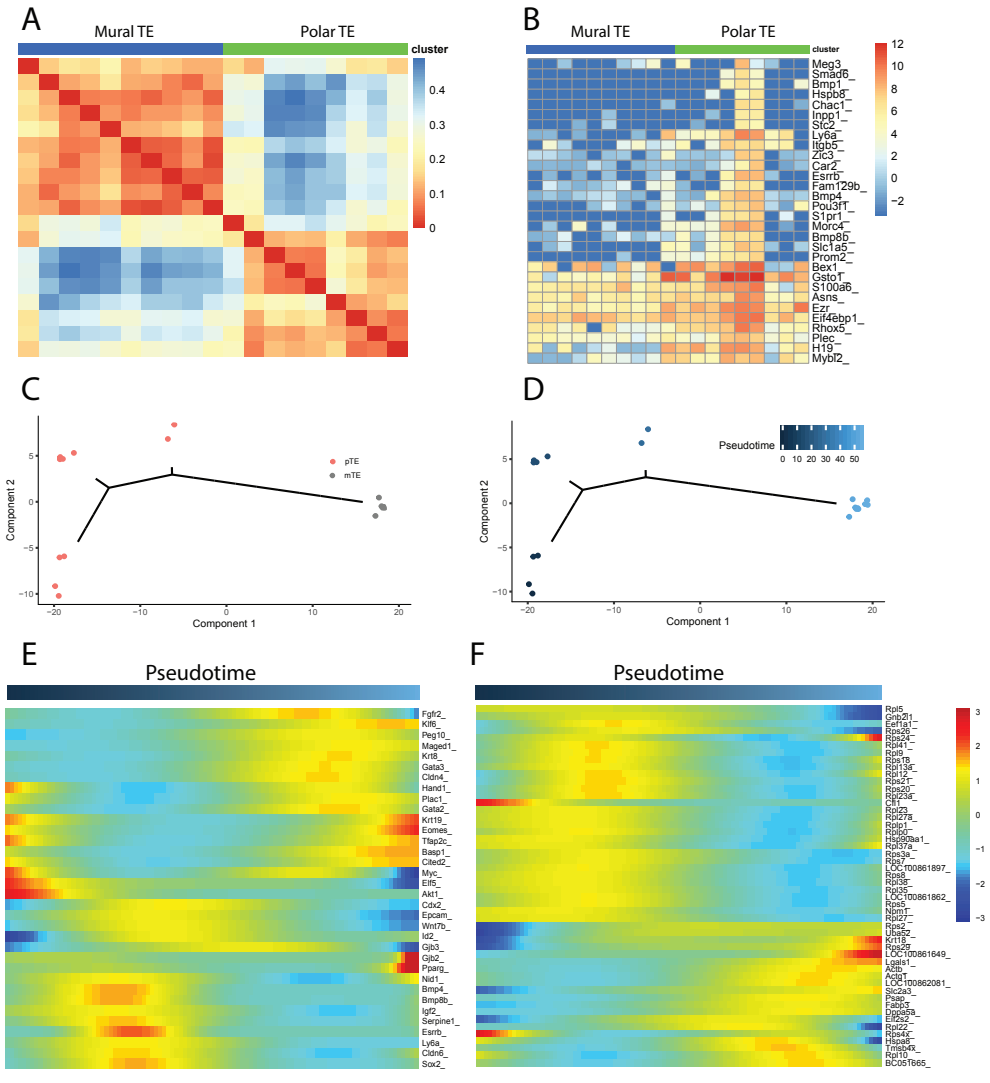

Figure 2. Single cell transcriptome expression on polar and mural TE cells from the E4.5 blastocyst. This dataset has been previously published (Nakamura et al., 2015) (GSE63266). A. Using RaceID, unsupervised clustering analysis of TE single cells confirms the presence of two subpopulations: polar (green) and mural (blue). B. Heatmap showing the expression of the top differentially expressed genes between the polar and the mural cluster. C. Using monocle, single cell trajectory groups polar cells and mural cells separately. D. Monocle assigns mural cells with high pseudotime values. E. Traditional markers for the trophoblastic lineage plotted against pseudotime. F. Top 50 genes defining the pseudotime trajectory.

We then decided to challenge both subpopulations in a functional way. Stem cells are capable of proliferate and self-renew to form colonies. In in vitro studies, a way for assess the capability for a stem cell to proliferate and self-renew is by performing a colony formation assay. We thus plated single cells from both CDX2-High and CDX2-Low subpopulations in

separate wells and counted for the number of wells containing a colony after 7 days of culture. The CDX2-High cells had a significantly higher colony formation potential (**Fig. 3F**, fold change=2.89, pvalue= 0.015).
Altogether, these experiments, along with previous observations in the blastocyst, pinpoint that both TSCs and TE cells are heterogeneous (Kuales et al. 2015; Motomura et al. 2016) for CDX2 expression, proliferation (Chavez et al. 1984; Cruz and Pedersen 1985; Gardner et al. n.d.) and self-renewal.

2.3.4 The CDX2 heterogeneity of TSCs is an intrinsic equilibrium.

We wondered what would be the outcome of sorting and culturing the different CDX2-expressing populations separately. This experiment aimed at finding out whether this CDX2 heterogeneity is an intrinsic property of the culture.
CDX2-High, CDX2-Low and also CDX2-Intermediate populations were sorted, plated in equal numbers, and cultured for a period of 7 days. We tracked the dynamics of each subpopulation by FACS analysis of culture replicates. Results showed that, regardless of the initial population sorted, an equilibrium including remarkably similar subpopulation fractions re-established within less than 7 days (**Fig. 3G**).
These results led us to conclude, that all the CDX2-expresssion is regulated at a population level, and that these sub-populations are present in an equilibrium that is potentially granted by the culture conditions. This suggested that altering the current culture conditions could also potentially alter the proportions of the mentioned CDX2 expression subpopulations. Importantly, these results also suggest that, although the CDX2-High cells seem to have more

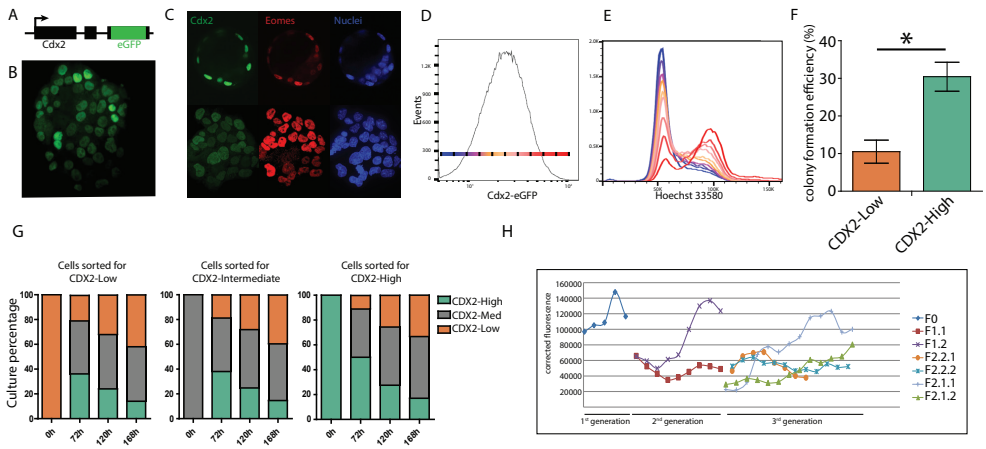

Figure 3. CDX2 expression correlates with stem cell features. A. Cdx2 locus in the Cdx2-eGFP reporter TSC line (McDole et al., 2012). B. CDX2 expression heterogeneity within a CDX2-eGFP TSC colony cultured under Tx conditions. C. CDX2 and EOMES expression comparison between E3.5 blastocyst and TSCs. D. CDX2 expression shows a normal distribution when TSCs are analyzed with FACS. E. Cell cycle state correlated with CDX2 expression. F. Colony formation efficiency of single cells from CDX2-Low and CDX2-High subpopulations after 7 days of culture. Fc=2.89, pvalue=0.015. G. Proportions of each subpopulation tracked over 3, 5 or 7 days of culture after pure subpopulation sorting. H. CDX2-eGFP fluorescence levels tracked over time by live imaging. One cell and its progeny were tracked over 3 generations.

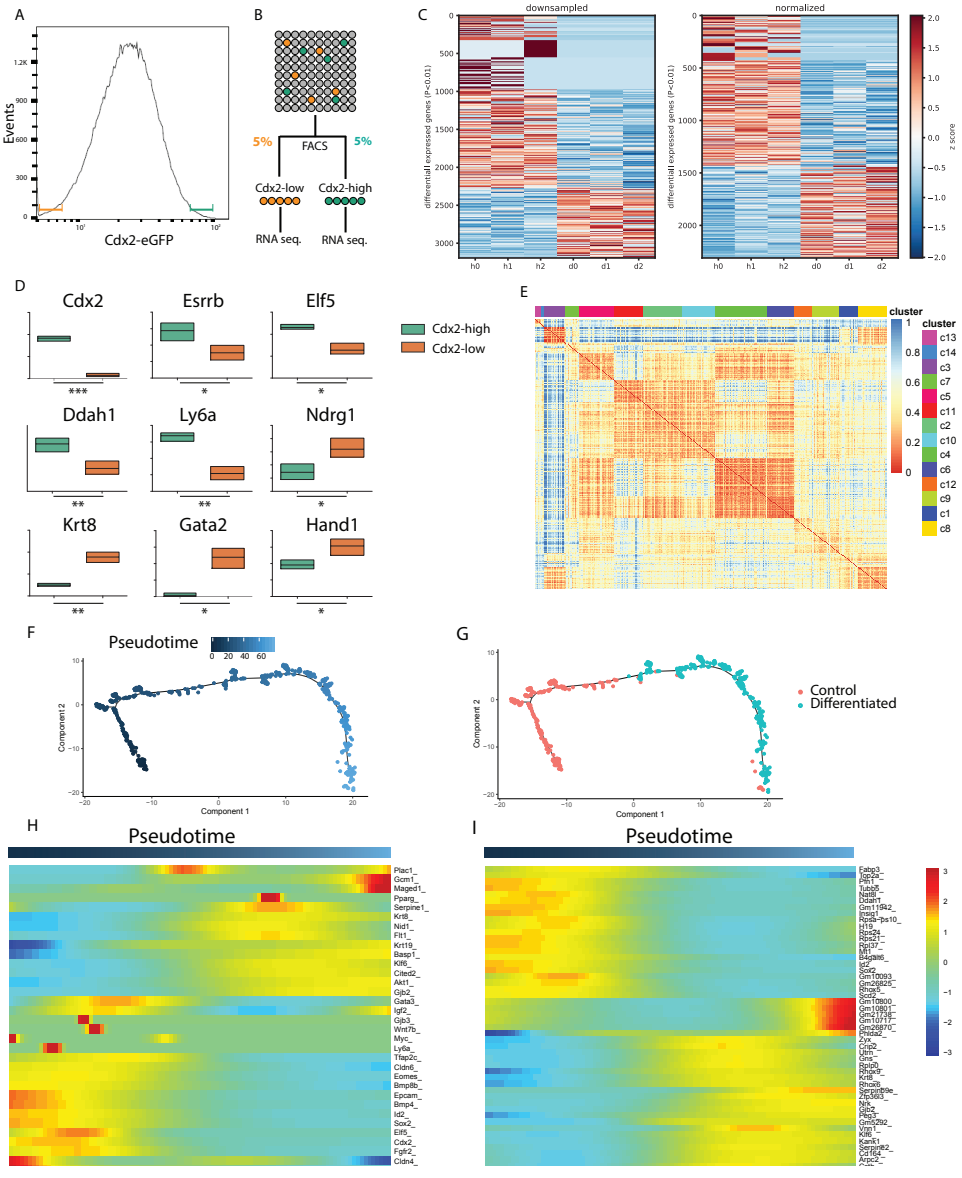

Figure 4. Transcriptome analysis of TSCs cultured in Tx. A-B. Sorting strategy for CDX2-eGFP TSCs. C. Heatmap for differentially expressed genes after downsampling and normalization. D. TSCs markers differentially expressed between CDX2-Low and CDX2-High populations.. * for pvalue<0.05, ** for pvalue<0.01, *** for pvalue<0.001. E. RaceID's unsupervised clustering analysis on single cells from control TSCs cultures. F-G. Pseudotime trajectory obtained with monocle. H. Classical TSCs markers plotted against pseudotime. I. top 50 genes defining pseudotime trajectory.

comparable properties to the ones attributed to cells in the TE, CDX2-Low cells are also capable of reverting to a more potent state, even in the absence of CDX2-High cells or at least upon passaging. The potential to revert to a more potent state is comparable to the potential of mural vesicle to revert to full potential when combined with pluripotent cells (Gardner et al. 1973).
In order to add some insight into the origin of the heterogeneity of CDX2 within colonies, we performed live imaging experiments (C3-1 CDX2-eGFP reporter TSC line). Cdx2 transcripts had been claimed to be asymmetrically distributed at the time of lineage commitment due to a cis-element within the mRNA (Skamagki et al. 2013), therefore we wondered if this mechanism could explain the intercellular heterogeneity for CDX2 protein. Small colonies were tracked for up to 60 hours (**Fig. 3H**). The results showed a substantial fluctuation of CDX2 levels. Although daughter cells would initially have similar CDX2 expression levels, they can acquire an opposed fate, with one of the daughter cells reaching the next cell division with significantly lower CDX2 levels than its sister cell. However, the asymmetric acquisition of different CDX2 levels was not a ubiquitous phenomenon. Such CDX2 fluctuation seemed to be in part linked to accumulation of CDX2 levels during the progression of cell cycle. However, the spatial location of the cell within the colony also seems to contribute to CDX2 expression. Altogether, CDX2 expression seems to be regulated in culture by multiple factors including the moment in the cell cycle, the inheritance upon cell division, and the spatial context in the colony.

2.3.5 The CDX2 populations are transcriptionally different.

In order to better understand the heterogeneity of TSCs, we performed RNA sequencing of TSCs. We were interested in finding out which genes are differentially expressed in CDX2-High TSCs as compared to CDX2-Low cells. Given the normal distribution of the CDX2 expression we sorted for the 5% with higher expression and the 5% with lower expression. Triplicates of the sorted cells underwent RNA extraction and followed Celseq1 protocol for RNA sequencing (**Fig. 4A-B**).
Upon analysis, two clusters were formed, each of them composed by the three replicates. One of the CDX2-Low triplicates showed to be less comparable to the other two, however these differences were not dramatic, therefore we still maintained the replicate as part of the group in the analysis. In order to look for differentially regulated genes, all samples were subjected to down-sampling and normalization, resulting in the normalized results to show a lower variance between each of the triplicates (**Fig. 4C**).
1956 genes were found to be differentially expressed with at least 1.5-fold change and a p-value lower than 0.001 between CDX2-High and CDX2-Low subpopulations. Gene ontology analysis pointed mainly at GO terms related with cell cycle and proliferation for the CDX2-High population, while genes upregulated in the CDX2-Low population included terms like negative regulation of proliferation or placenta development (Supplementary table 2). KEGG pathways analysis pointed at metabolic pathways, cell cycle, p53, Notch and Hippo pathways. Among the differentially expressed genes, we could also find some markers that help us define the differentiation status of each subpopulation. CDX2-High samples showed a higher expression for undifferentiated markers such as Esrrb, Elf5, or Ly6a as well as the polar TE marker Ddah1 (Nakamura et al. 2015) and a lower expression of mural TE related genes such as Ndrg1 (Shi et al. 2013) and Gata2 or the giant trophoblast cells marker Hand1 (**Fig. 4D**) (for all these genes there was a p-value<0.001). The transcriptional profile of CDX2-High

expressing cells is a priori more comparable to an undifferentiated state.
In order to better address the heterogeneity we observe in our TSC cultures we sorted single cells of both control (Kubaczka et al. 2014) and differentiated TSC (after 6 days in the absence of Fgf4 and Tgfb) in order to perform single cell sequencing following the Cel Seq 2 protocol (Hashimshony et al. 2016). RaceID and monocle packages were used for further transcriptome analysis. Unsupervised gene expression clustering grouped the control cells in up to 14 clusters (**Fig. 4F**) suggesting a high degree of heterogeneity. When control and differentiated cells were simultaneously analyzed with monocle, differentiated cells were assigned with high pseudotime values while most of the control cells acquired low pseudotime values (**Fig. 4F-G**). 4.21% of control cells were located among the differentiated cells at the end of the trajectory, suggesting that those cells didn't retain an undifferentiated state. When plotting classical markers for undifferentiated and differentiated trophoblast states against pseudotime (**Fig. 4H**) we can confirm that markers like Esrrb, Cdx2, Elf5 and Sox2 peak with low pseudotime values while markers such as Flt1, Gcm1 or Krt8 have a higher expression in differentiated cells. From monocle we also obtained a set of genes that unbiasedly define the pseudotime trajectory (**Fig. 4I**) which include H19, Id2 or Sox2 for low pseudotime values and Krt8, Serpin9e or Klf6 for high pseudotime values.
Single cell transciptome analysis results confirm the heterogeneity of TSC cultures. The results show that the TSC culture include a small percentage (4.21%) of cells equivalent to 6 day differentiated cells, which are probably discarded upon passaging, along with a large percentage of heterogeneous cells representing a spectrum of differentiation states, and characterized by specific genes.

2.4 Discussion

Our observation regarding the heterogeneity of TSC cultures is in accordance with previous publications.
Initially, when TSC are derived from blastocysts, TE and ICM cells outgrow (**Sup Fig. 1A**) and display multiple morphologies that reflect a range of differentiation status. Some cells differentiate into large giant trophoblast cells (TGCs), while some other cells form smaller, compact clusters reminiscent of stem cell colonies. Upon serial passages, those differentiated cells present at the point of derivation are depleted or dramatically outnumbered by the TSCs that continue growing in colonies (**Sup. Fig. 1B**). However, differentiated cells have been observed in long-term cultures of TSC (Kuales et al. 2015; Motomura et al. 2016), suggesting that the culture conditions allow for differentiation to take place rather than just being a consequence from derivation.
Motomura et al focused on documenting the colony morphology heterogeneity rather than the cell morphology. They concluded that the colonies of small size, compact and with a dome shape show CDX2 positive staining in most cells, and do not show signs of TGC differentiation. These smaller colonies derive into the other colony types eventually (Motomura et al. 2016). They also suggested Elf5 as the potential marker for the true stem cells of the culture based on the enrichment of such gene when compared to other type of colonies. ELF5 is also one of the markers that together with EOMES and CDX2 allows to identify the "bona fide" TSC (Kuales et al. 2015).
The origin of the heterogeneity we and other researchers observed is unknown, however, either time after attachment, or crowding effect could be potential causes. Given what we know about TE lineage commitment and the role that hippo plays, TSCs as analogues of TE,

could also respond to polarity stimuli. However, the hippo pathway is known to be aberrant in most in vitro cultures given the interference of cell culture plate with the cellular mechanical properties. In our stainings, similarly to those published in Motomura's publication, a CDX2 differential distribution can be observed within the colony (**Sup. Fig. 1C**), often being the outer cells of the colony the ones with higher expression levels.

Apart from the intercellular heterogeneity, other features differentiate TSCs from the TE of the blastocyst. One of those differences observed involves the transcription factor SOX2, a factor that might play a role in TE commitment (Keramari et al. 2010). While Sox2 transcripts are detected in the E4.5 TE (Nakamura et al. 2015) (**Fig. 2F**), we were only able to find SOX2 protein expression in the ICM of the blastocyst (**Sup. Fig. 1D**). SOX2 has been reported to be partially regulated by hippo signaling (Wicklow et al. 2014). SOX2 is important for the pluripotency of the embryonic lineage, and a critical factor for generating induced pluripotent stem cells (Takahashi and Yamanaka 2006). Nevertheless, SOX2 is expressed (albeit also in a heterogeneous fashion) in TSCs (**Sup. Fig. 1D**), and our data suggests its expression at the mRNA level to be linked to the undifferentiated state. Given that Sox2 has been reported to be downstream of Fgf signaling (Adachi et al. 2013), we wonder whether an abnormality in this signaling, as compared to TE, causes the aberrant expression.

Trophoblast Stem Cells are widely used in order to study the very early stages in mammalian peri-implantation development, but the knowledge we have acquired in relation to the trophoblastic lineage has, to this day, very limited applications. There are, however, new models that include the use of TSCs, placing them in the scope of researchers. The same way the culture of embryonic stem cells was improved in order to optimize their use, new culture conditions need to be implemented for TSCs, improvements that might be able to reduce the inter-cellular heterogeneity we observe in the available culture conditions. The phenotypical differences observed within the same culture, represent a spectrum of differentiation states that ultimately correspond with different developmental stages making the culture suboptimal for the development of new models that rely on an undifferentiated state. This range of differentiation states within the culture might be a consequence of different factors such as inaccurate or suboptimal signaling pathway activation or excessive crowding effect. Even though differentiation is an innate property of stem cells, we are interested in being able to control its starting point.

Cdx2 is one of the main genes involved in the TE's transcriptional network, being critical for the trophoblastic lineage to pursue its functions. CDX2 controls the expression of several genes that are also important in early stages of the trophoblastic lineage. In this chapter we have proven that higher expression levels of CDX2 correlates with a more undifferentiated state with higher cycling and self-renewal capacity. In order to make a culture of TSCs that result in cells more comparable to those in the TE, we may want to alter the culture conditions and CDX2 appears to be a good marker for us to evaluate the effect of those media modifications.

A culture of TSCs with high fidelity to the TE, could result in the improvement of pre-existing models using TSCs or the development of new ones with potential clinical applications.

2.5 Materials and Methods

• TSC culture.

Unless stated otherwise, TSC are cultured under Tx conditions previously published (Kubacz-

ka et al. 2014). After coating with matrigel, cells are cultured in Tx media, which consists of phenol red free DMEM/F12 (phenol red-free, with l-glutamin) supplemented with insulin (19.4 µg/ml), l-ascorbic-acid-2-phosphate (64 µg/ml), sodium selenite (14 ng/ ml), insulin (19.4 µg/ml), sodium bicarbonate (543 µg/ml), holo-transferin (10.7 µg/ml), penicillin streptomycin, FGF4 (25 ng/ml), TGFβ1 (2 ng/ml) and heparin (1 µg/ml). Cells were routinely passaged using trypsin.

• Immunofluorescence.
Cells in monolayer were fixed using 4%PFA in PBS for 20 minutes at RT followed by 3 washing steps with PBS. A 0.25% triton solution in PBS was used for permeabilization during 30 minutes ar RT,followed by a 1 hour blocking step with PBS+ 10% FBS and 0.1% tween20. Primary antibodies against CDX2 (Biogenes MU392A-5UC), EOMES (Abcam ab23345), pERK (Cell Signalling #4370S) and SOX2 were diluted 1/200 in PBS + 0.1% Tween20, and used for staining O/N at 4C. Stainings involving pERK antibody, also included PhoSTOP in all steps until after the primary antibody incubation. After three washing steps, samples were incubated with the corresponding secondary antibodies for 1 hour at RT. Hoechst was used for counterstaining. All images were analyzed in a PerkinElmer Ultraview VoX spinning disk microscope.

• smFISH.
Samples were fixed using RNAse free 4%PFA in PBS + 1% Acetic Acid during 20 minutes. After fixation, all samples followed the Quantigene ViewRNA kit instructions: After three washes with RNAse free PBS, sampels were incubated for 10 minutes in a detergent solution. After three washes with RNAse free PBS, samples were incubated for 5 minutes at RT with Q protease. After three washes with RNAse free PBS, samples were incubated at 40C for 3 hours (in a humidified chamber) with the probes of interest diluted in Probe set diluent. After 3 washes with wash buffer, samples were incubated at 40C for 30 minutes with preamplifier diluted in amplifier diluent. After 3 washes with wash buffer, samples were incubated at 40C for 30 minutes with amplifier diluted in amplifier diluent. After 3 washes with wash buffer, samples were incubated at 40C for 30 minutes with label diluted in label probe diluent. After 2 washes with wash buffer, they were washed once more for 10 minutes. Samples were then incubated for 15 minutes in RNAse free PBS with Hoechst and WGA as counterstains followed by 3 washes with RNAse free PBS. Blastocysts were carefully placed in mounting media in glass bottom 3.5 mm plates. All samples were imaged with a 63x oil immersion objective in a PerkinElmer Ultraview VoX spinning disk microscope.

• Single Cell Sequencing.
Single, live (Dapi negative) cells were sorted into 384 well plates containing 50 ul of Cel Seq primer and 5 ul of mineral oil to prevent evaporation. Libraries were obtained following a robotized version of the Cel Seq 2 protocol (Hashimshony et al. 2016). After sequencing, transcriptome analysis was performed on RStudio using the monocle pipeline (Trapnell et al. 2014). The dataset for studying mural and polar TE cells from the 4.5 blastocysts was downloaded from the Gene Expression Omnibus repository (GSE63266) (Nakamura et al. 2015). Those cells were analyzed using the monocle and RaceID pipelines (Grun et al. 2016; Grun, Kester, and van Oudenaarden 2014)

• FACS analysis.

A BD FACSCalibur cytometer was sued for all FACS analytical assays. When sorting was required a FACSAria was used. For cell cycle analysis, After trypsinization, 105 TSCs and plTSCs were incubated in 0.5ml of Tx media with 10 ug/ml hoescht 34580 for 30 minutes at 37C. After the incubation time, tubes with cells wre placed on ice and analyzed with a FACS-Canto II.

• Blastocyst isolation.
After crossings between CBA and C57BL/6 strains, 3.5 dpc plugged females were sacrificed and their uterus were flushed with M2 media.

• Fgf4 blastocyst exposure.
A group of 3.5 dpc blastocysts was divided in two groups. The control group was cultured in M2 at 37C for 6 6hours. The other group would be cultured in M2 containing Fgf4 at a concentration of 500ng/ml. After 6 hours, all blastocysts were used for immunofluorescence.

• FACS for FGF dose response.
For studying the CDX2 expression response of C3-1 TSC to Fgf4, 18.000 cell/cm2 were plated. 24 hours later, media was changed to fresh media containing different concentrations of Fgf4. 48 hour after the media change, cells were trypsinized and analyzed via FACS.

• RNA sequencing.
Using a FACSAria, the top 5% and bottom 5% Cdx2 expressing C3-1 cells were sorted into separate tubes and trizol RNA extraction was performed. Samples then followed the Celseq1 protocol.

• Colony formation assay.
C3-1 cultured cells were used for sorting single cells into 96well plates that had been coated with MEF the previous day. Before the sorting, media was change from MEF culture conditions to Tx conditions. One TSC was sorted per well according to their Cdx2 expression level. Media was changed every two days. At the 7th day, wells containing a TSC colony were counted and compared to the total number of wells that had cells sorted in.

• Cdx2 subpopulations re-establishment after sorting.
Cells were sorted according to their Cdx2-expression levels. Each subpopulation was plated separately in a 4 replicates with all the wells initially containing the same number of cells. On days 2, 4, 6 and 7, each of those replicates from each subpopulation was trypsinized and the cells were analyzed by FACS.

Author contribution

Javier Frias Aldeguer wrote the chapter, performed stainings, functional in vitro assays, transcriptome analysis. Anna Alemany Arias contributed to transcriptome analysis. Judith Vivié performed RNA extraction and library preparation for RNA sequencing. Frank Darmis performed live imaging and its analysis. Clemens A. van Blitterswijk and Niels Geijsen helped to direct the project. Nicolas Clement Rivron derived the CDX2-eGFP reporter TSC line, generated the blastocyst bulk sequencing dataset and conceived and directed the research.

Bibliography

Adachi, Kenjiro et al. 2013. "Context-Dependent Wiring of Sox2 Regulatory Networks for Self-Renewal of Embryonic and Trophoblast Stem Cells." Molecular Cell 52(3):380–92.

Arman, E., R. Haffner-Krausz, Y. Chen, J. K. Heath, and P. Lonai. n.d. "Targeted Disruption of Fibroblast Growth Factor (FGF) Receptor 2 Suggests a Role for FGF Signaling in Pregastrulation Mammalian Development." Proceedings of the National Academy of Sciences of the United States of America 95(9):5082–87.

Arman, E., R. Haffner-Krausz, Y. Chen, J. K. Heath, and P. Lonai. 1998. "Targeted Disruption of Fibroblast Growth Factor (FGF) Receptor 2 Suggests a Role for FGF Signaling in Pregastrulation Mammalian Development." Proceedings of the National Academy of Sciences of the United States of America 95(9):5082–87.

Chavez, D. J., A. C. Enders, and S. Schlafke. 1984. "Trophectoderm Cell Subpopulations in the Periimplantation Mouse Blastocyst." The Journal of Experimental Zoology 231(2):267–71.

Copp, A. J. 1978. "Interaction between Inner Cell Mass and Trophectoderm of the Mouse Blastocyst. I. A Study of Cellular Proliferation." Journal of Embryology and Experimental Morphology 48:109–25.

Cross, J. C. et al. 2003. "Genes , Development and Evolution of the Placenta." 123–30.

Cruz, Y. P. and R. A. Pedersen. 1985. "Cell Fate in the Polar Trophectoderm of Mouse Blastocysts as Studied by Microinjection of Cell Lineage Tracers." Developmental Biology 112(1):73–83.

Dard, N. et al. 2001. "In Vivo Functional Analysis of Ezrin during Mouse Blastocyst Formation." Developmental Biology 233(1):161–73.

Erlebacher, Adrian, Kelly a Price, and Laurie H. Glimcher. 2004. "Maintenance of Mouse Trophoblast Stem Cell Proliferation by TGF-Beta/activin." Developmental Biology 275(1):158–69.
Evans, M. J. and M. H. Kaufman. 1981. "Establishment in Culture of Pluripotential Cells from Mouse Embryos." Nature 292:154.

Feldman, B., W. Poueymirou, V. Papaioannou, T. DeChiara, and M. Goldfarb. 1995. "Requirement of FGF-4 for Postimplantation Mouse Development." Science 267(5195):246–49.

Gardner, R. L., V. E. Papaioannou, and S. C. Barton. n.d. "Origin of the Ectoplacental Cone and Secondary Giant Cells in Mouse Blastocysts Reconstituted from Isolated Trophoblast and Inner Cell Mass." Journal of Embryology and Experimental Morphology 30(3):561–72.

Graham, Sarah J. L. et al. 2014. "BMP Signalling Regulates the Pre-Implantation Development of Extra-Embryonic Cell Lineages in the Mouse Embryo." Nature Communications 5(May):5667.

Grun, Dominic et al. 2016. "De Novo Prediction of Stem Cell Identity Using Single-Cell Transcriptome Data." Cell Stem Cell 19(2):266–77.

Grun, Dominic, Lennart Kester, and Alexander van Oudenaarden. 2014. "Validation of Noise Models for Single-Cell Transcriptomics." Nature Methods 11(6):637–40.

Hashimshony, Tamar et al. n.d. "CEL-Seq2: Sensitive Highly-Multiplexed Single-Cell RNA-Seq." Genome Biology 17:77.

Hubrecht, A. A. W. 1889. Studies in Mammalian Embryology: 1. The Placentation of Erinaceus Europaeus, with Remarks on the Phylogeny of the Placenta.

Keramari, Maria et al. 2010. "Sox2 Is Essential for Formation of Trophectoderm in the Preimplantation Embryo." PLoS ONE 5(11).

Korotkevich, Ekaterina et al. 2017. "The Apical Domain Is Required and Sufficient for the First Lineage Segregation in the Mouse Embryo Article The Apical Domain Is Required and Sufficient for the First Lineage Segregation in the Mouse Embryo." 235–47.

Kuales, Georg, Matthias Weiss, Oliver Sedelmeier, Dietmar Pfeifer, and Sebastian J. Arnold. 2015. "A Resource for the Transcriptional Signature of Bona Fide Trophoblast Stem Cells and Analysis of Their Embryonic Persistence." Stem Cells International 2015:17–20.

Kubaczka, Caroline et al. 2014. "Derivation and Maintenance of Murine Trophoblast Stem Cells under Defined Conditions." Stem Cell Reports 2(2):232–42.

Lander, E. S. et al. 2001. "Initial Sequencing and Analysis of the Human Genome." Nature 409(6822):860–921.

Mcdole, Katie and Yixian Zheng. 2012. "Generation and Live Imaging of an Endogenous Cdx2 Reporter Mouse Line." Genesis 50(10):775–82.

McDole, Katie and Yixian Zheng. n.d. "Generation and Live Imaging of an Endogenous Cdx2 Reporter Mouse Line." Genesis (New York, N.Y. : 2000) 50(10):775–82.

Motomura, K. et al. 2016. "Cellular Dynamics of Mouse Trophoblast Stem Cells: Identification of a Persistent Stem Cell Type." Biology of Reproduction 94(6):122–122.

Muraro, Mauro J. et al. n.d. "A Single-Cell Transcriptome Atlas of the Human Pancreas." Cell Systems 3(4):385–394.e3.

Nakamura, Tomonori et al. 2015. "SC3-Seq: A Method for Highly Parallel and Quantitative Measurement of Single-Cell Gene Expression." Nucleic Acids Research 43(9):e60.

Natale, Bryony V. et al. 2017. "Sca-1 Identifies a Trophoblast Population with Multipotent Potential in the Mid-Gestation Mouse Placenta." Scientific Reports 7(1):1–16.

Rappolee, D. A., C. Basilico, Y. Patel, and Z. Werb. 1994. "Expression and Function of FGF-4 in Peri-Implantation Development in Mouse Embryos." Development (Cambridge, England) 120(8):2259–69.
Rossant, Janet and James C. Cross. 2001. "Placental Development: Lessons From Mouse Mutants." Nature Reviews Genetics 2(7):538–48.

Ryu, Hyunryul et al. 2015. "Frequency Modulation of ERK Activation Dynamics Rewires Cell Fate." Molecular Systems Biology 11(11):838.

Shi, Xiao-Hua, Jacob C. Larkin, Baosheng Chen, and Yoel Sadovsky. 2013. "The Expression and Localization of N-Myc Downstream-Regulated Gene 1 in Human Trophoblasts." PloS One 8(9):e75473.

Skamagki, Maria, Krzysztof B. Wicher, Agnieszka Jedrusik, Sujoy Ganguly, and Magdalena Zernicka-Goetz. 2013. "Asymmetric Localization of Cdx2 mRNA during the First Cell-Fate Decision in Early Mouse Development." Cell Reports.

Takahashi, Kazutoshi and Shinya Yamanaka. 2006. "Induction of Pluripotent Stem Cells from Mouse Embryonic and Adult Fibroblast Cultures by Defined Factors." 2:663–76.
Tanaka, S. 1998. "Promotion of Trophoblast Stem Cell Proliferation by FGF4." Science 282(5396):2072–75.

Tanaka, S., T. Kunath, A. K. Hadjantonakis, A. Nagy, and J. Rossant. n.d. "Promotion of Trophoblast Stem Cell Proliferation by FGF4." Science (New York, N.Y.) 282(5396):2072–75.

Trapnell, Cole et al. 2014. "The Dynamics and Regulators of Cell Fate Decisions Are Revealed by Pseudotemporal Ordering of Single Cells." Nature Biotechnology 32(4):381–86.

Wicklow, Eryn et al. 2014. "HIPPO Pathway Members Restrict SOX2 to the Inner Cell Mass Where It Promotes ICM Fates in the Mouse Blastocyst." PLoS Genetics 10(10).

Zuckerwise, Lisa et al. 2016. "H19 Long Noncoding RNA Alters Trophoblast Cell Migration and Invasion by Regulating TβR3 in Placentae with Fetal Growth Restriction." Oncotarget 7(25):38398–407.

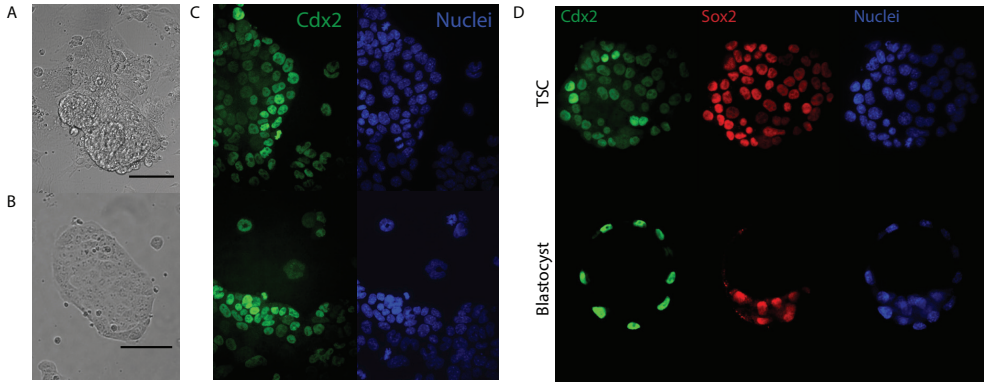

Supplementary Figure 1. TSCs and their heterogeneous CDX2 expression. A. Blastocyst outgrowth for TSC line derivation 4 days after blastocyst plating. B. Morphology of a TSCs colony cultured in Tx conditions. B. Differential distribution of CDX2 expression on large colonies often leads to a higher expression in the colony edges. D. CDX2 and SOX2 expression comparison between Tx cultured TSCs and E3.5 blastocysts.

GO Term	# of genes	%	PValue
cell division	77	5.209743	8.02E-17
cell cycle	101	6.833559	9.97E-15
mitotic nuclear division	58	3.924222	4.59E-13
lipid metabolic process	72	4.871448	8.68E-10
sterol biosynthetic process	13	0.879567	1.24E-07
cholesterol biosynthetic process	14	0.947226	1.35E-07
cholesterol metabolic process	23	1.556157	2.54E-07
cytokinesis	14	0.947226	9.82E-07
positive regulation of cell migration	36	2.435724	1.35E-06
apoptotic process	73	4.939107	2.55E-06
phosphorylation	76	5.142084	4.85E-06
endocytosis	31	2.097429	1.67E-05
transforming growth factor beta receptor signaling pathway	18	1.217862	1.99E-05
regulation of cell shape	26	1.759134	2.01E-05
steroid metabolic process	19	1.285521	2.59E-05
cell migration	31	2.097429	4.77E-05
regulation of cell cycle	22	1.488498	4.79E-05
chromosome segregation	19	1.285521	5.83E-05
response to X-ray	9	0.608931	6.43E-05
isoprenoid biosynthetic process	8	0.541272	1.05E-04
G1/S transition of mitotic cell cycle	15	1.014885	1.10E-04
negative regulation of transcription from RNA polymerase II promoter	81	5.480379	1.20E-04
viral entry into host cell	8	0.541272	1.61E-04
mitotic cytokinesis	10	0.67659	1.90E-04
protein phosphorylation	66	4.465494	2.41E-04
cell proliferation	32	2.165088	2.77E-04
mitotic spindle midzone assembly	5	0.338295	3.65E-04
small GTPase mediated signal transduction	33	2.232747	4.47E-04
mitotic metaphase plate congression	10	0.67659	5.35E-04

Supplementary table 1a. Gene ontology enrichment for differentially regulated genes between polar and mural single cells with fold change higher than 1.5 and pvalue>0.05.

KEGG pathway	# of genes	%	Pvalue
Cell cycle	30	2.02977	1.04E-07
Metabolic pathways	146	9.878214	3.23E-06
Biosynthesis of antibiotics	37	2.503383	1.50E-05
p53 signaling pathway	17	1.150203	5.87E-05
Small cell lung cancer	18	1.217862	3.07E-04
Steroid biosynthesis	7	0.473613	0.002889
Inositol phosphate metabolism	14	0.947226	0.00342
Lysosome	20	1.35318	0.003812
Focal adhesion	29	1.962111	0.00431
Colorectal cancer	13	0.879567	0.004459
Arginine and proline metabolism	11	0.744249	0.004895
AMPK signaling pathway	20	1.35318	0.005959
Proteoglycans in cancer	28	1.894452	0.006294
Mismatch repair	7	0.473613	0.006456
Fatty acid metabolism	11	0.744249	0.006582
Endocytosis	35	2.368065	0.008579
Hippo signaling pathway	22	1.488498	0.00919
Sphingolipid signaling pathway	19	1.285521	0.009965
Arrhythmogenic right ventricular cardiomyopathy (ARVC)	13	0.879567	0.010389
FoxO signaling pathway	20	1.35318	0.010533
Oocyte meiosis	17	1.150203	0.014346
Pathways in cancer	45	3.044655	0.016934
HIF-1 signaling pathway	16	1.082544	0.018704
DNA replication	8	0.541272	0.019475
Apoptosis	11	0.744249	0.02027
Progesterone-mediated oocyte maturation	14	0.947226	0.021041
Regulation of actin cytoskeleton	27	1.826793	0.021819
Phosphatidylinositol signaling system	15	1.014885	0.02251
Hypertrophic cardiomyopathy (HCM)	13	0.879567	0.02316

Supplementary table 1b. Pathway enrichment for differentially regulated genes between polar and mural single cells with fold change higher than 1.5 and pvalue>0.05.

GO Term	# of genes	%	Pvalue
mitotic nuclear division	58	3.080191	1.69E-09
cell division	71	3.770579	1.86E-09
cell cycle	99	5.257568	9.01E-09
regulation of transcription, DNA-templated	269	14.28571	5.80E-07
transcription, DNA-templated	229	12.16144	6.13E-07
positive regulation of apoptotic process	57	3.027084	3.33E-06
positive regulation of transcription from RNA polymerase II promoter	129	6.85077	1.32E-05
chromosome segregation	22	1.168348	2.82E-05
neural tube closure	23	1.221455	3.53E-05
heart development	44	2.336697	6.26E-05
negative regulation of transcription from RNA polymerase II promoter	96	5.098247	1.08E-04
cell-cell adhesion	34	1.805629	1.41E-04
transport	204	10.83378	4.05E-04
DNA repair	48	2.549124	4.09E-04
protein dephosphorylation	26	1.380775	4.91E-04
oxidation-reduction process	87	4.620287	4.93E-04
venous blood vessel morphogenesis	6	0.31864	5.24E-04
mitotic sister chromatid segregation	9	0.477961	5.74E-04
cellular response to insulin stimulus	19	1.009028	6.74E-04
protein ubiquitination	52	2.761551	7.53E-04
negative regulation of JNK cascade	9	0.477961	7.94E-04
cellular response to DNA damage stimulus	58	3.080191	9.44E-04
negative regulation of cell proliferation	54	2.867764	9.53E-04
apoptotic process	74	3.929899	0.001058
organ regeneration	14	0.743494	0.001076
positive regulation of transcription, DNA-templated	74	3.929899	0.001415
DNA methylation on cytosine	10	0.531067	0.001491
response to oxidative stress	24	1.274562	0.001549
determination of adult lifespan	8	0.424854	0.001693

Supplementary table 2a. Gene ontology enrichment for differentially regulated genes between CDX2-High and CDX2-Low cells with fold change higher than 1.5 and pvalue>0.05.

KEGG pathway	# of genes	%	Pvalue
Metabolic pathways	159	8.430541	1.08E-05
Cell cycle	26	1.378579	1.06E-04
Non-alcoholic fatty liver disease (NAFLD)	29	1.537646	3.74E-04
p53 signaling pathway	16	0.848356	8.03E-04
Notch signaling pathway	13	0.68929	1.15E-03
Endocytosis	42	2.226935	1.21E-03
Signaling pathways regulating pluripotency of stem cells	25	1.325557	1.38E-03
Viral carcinogenesis	36	1.908802	1.70E-03
Alzheimer's disease	28	1.484624	4.99E-03
Oxidative phosphorylation	23	1.219512	6.94E-03
Transcriptional misregulation in cancer	26	1.378579	7.94E-03
Thyroid hormone signaling pathway	19	1.007423	1.30E-02
Lysosome	20	1.060445	1.37E-02
HTLV-I infection	37	1.961824	1.84E-02
Inositol phosphate metabolism	13	0.68929	2.28E-02
Axon guidance	20	1.060445	2.37E-02
Progesterone-mediated oocyte maturation	15	0.795334	2.44E-02
Phosphatidylinositol signaling system	16	0.848356	2.82E-02
Protein processing in endoplasmic reticulum	24	1.272534	3.02E-02
Prolactin signaling pathway	13	0.68929	3.07E-02
Carbon metabolism	18	0.954401	3.25E-02
Rheumatoid arthritis	14	0.742312	3.29E-02
TNF signaling pathway	17	0.901379	3.69E-02
Small cell lung cancer	14	0.742312	3.91E-02
Glycosaminoglycan biosynthesis - keratan sulfate	5	0.265111	4.11E-02
Proximal tubule bicarbonate reclamation	6	0.318134	4.39E-02
Parkinson's disease	21	1.113468	4.91E-02
Biosynthesis of antibiotics	28	1.484624	4.96E-02
B cell receptor signaling pathway	12	0.636267	5.00E-02

Supplementary table 2b. Pathway enrichment for differentially regulated genes between CDX2-High and CDX2-Low cells with fold change higher than 1.5 and pvalue>0.05.

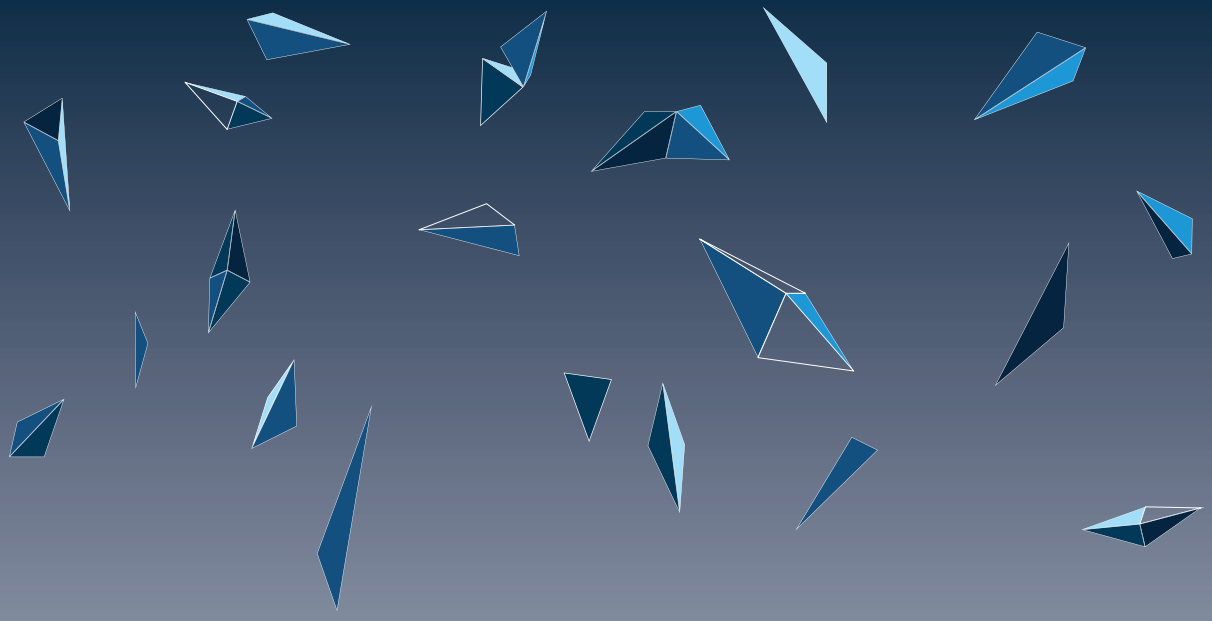

Chapter 3.
Combinatorial screenings for optimization of the TSC culture

3

3.1 Abstract

The development of the mouse embryo relies on the fitness of both embryonic and extraembryonic tissues. The placenta, one of the main extraembryonic organs, is mainly formed by the trophoblastic lineage, which arises at the pre-implantation conceptus as a result of the first lineage segregation, mediates all interactions between embryo and mother. The trophectoderm (TE) is the first trophoblastic structure and is responsible for initial attachment and invasion of the endometrium. One of the genes known to affect the integrity of the TE when mutated is Cdx2, a gene encoding a transcription factor that belongs the core transcriptional network of Trophoblast Stem Cells (TSCs). TSCs represent the in vitro analogues of the TE cells. However, the fidelity at which TSCs represent the TE has been debated. Cultured TSCs show a high degree of inter-cellular heterogeneity leading to different sub-populations equivalent to different developmental stages. We have previously reported CDX2 expression to correlate with stem cell features (proliferation, self-renewal and expression of key genes) and in this chapter, we aim to potentiate CDX2 expression by using soluble compounds that mimic the interaction between ICM/Epiblast and the polar TE. We managed to obtain a number of culture conditions that lead to stable in vitro cultures showing consistently high levels of CDX2 expression without losing the trophoblastic identity. We hypothesize that a TSC culture showing more homogeneous levels of CDX2 will be a better tool to develop or improve in vitro models for the study of the trophoblastic lineage.

3.2 Introduction

ESCs have been on the focus of researchers since their first derivation, which opened a whole new field of research with important potential clinical applications in regenerative medicine. Improving the culture conditions of ESC by including pathway inhibitors maintains them in a so called "ground state", which is less differentiated and less heterogeneous regarding the expression of certain genes (e.g. Nanog). Such culture conditions, referred to as "2i", also elude the need for serum leading to a chemically-defined culture, which is a prerequisite for all clinical applications. These improvements also allowed for fine-tuning the molecular and epigenetic regulatory networks.

We and other researchers have witnessed a similar case of intercellular heterogeneity in the culture of TSCs. In chapter 1, we showed that CDX2, a key player involved in the transcriptional network, is expressed in a heterogeneous fashion similar to the cell states along the polar to mural axis. Several molecular and functional assays suggest that the CDX2-High TSCs retain the stem cell properties (proliferation, self-renewal, transcriptome), while the CDX2-Low are more differentiated. Finally, these states are plastic, representing an intrinsic property of the culture, which might be influenced by the cell cycle state, an asymmetric division, or the position within the colony. Upon observations within the blastocyst, we concluded that the heterogeneity of TSCs reflects aspects of the trophoblast states along the polar-mural axis. Previous work, including ours (Rivron et al., 2018), identified embryonic inductions as regulators of trophoblast differentiation states within the blastocyst. Especially, the blastoid model allowed for the establishment of a list of embryonic inductions regulating trophoblast proliferation, self-renewal, epithelial morphogenesis, and overall the potential for the TE to implant in utero. In this chapter, we hypothesize that altering the culture conditions using our knowledge on embryonic inductions might lead to a culture more homogeneously reflecting

the native state of the polar TE.
We thus developed a systematic screening approach to regulate CDX2 expression and TSCs heterogeneity in vitro. We initially performed target-based screens, which aim for a particular phenotype: high CDX2 expression.

3.3 Results

3.3.1 Crafting a library of potential CDX2 expression modulators

In order to find modulators of Cdx2, we first established a library of potential candidates. This library was created by (1) including ligands that are expressed in the blastocyst niche along with (2) compounds that target pathways active in the TE of the E3.5 blastocyst or (3) modulators of pathways reported to be important for the trophoblastic lineage or for potency maintenance.

Stainings against phosphorylated kinases are relatively easy to perform and can confirm the activation status of certain pathways in the TE. With this method, we can only study a limited number of pathways, but some of those are pivotal in blastocyst biology (MapK, Smad and Stat). Importantly, kinase based activation cascades can happen very quickly and in many cases their activation (displayed as phosphorylation of a protein in the cascade) is only transient. Thus, a negative immunoreactivity does not necessarily imply that the cell in question is not reactive to the pathway of interest.
The Stat pathway's activation status can be assessed by staining for the phosphorylated form of Stat3. The microscopy images of blastocyst stained for p-Stat showed clear immunoreactivity in both compartments of the blastocyst (**Fig. 1A**).
Staining against phosphorylated Erk, would positively mark those cells that have active the Erk branch of the MapK pathway, which is critical to TSC. The Erk ramification is the main branch activated as result of ligands such as Fgf or Egf binding to their corresponding receptors (Arkun & Yasemi, 2018). In the blastocyst, we observe activation in a restricted number of TE cells, with higher immunoreactivity in the layer of the ICM in contact with the blastocoel, presumably PrE cells.
Staining for the phosphorylated form of Smad1/5/8 showed activation of this pathway in all the compartments of the blastocyst. We were unsuccessful in our attempts to stain for phosphor-Smad2/3. However, multiple reports showed this pathway to be critical for TE (Dardik, Smith, & Schultz, 1992; Guzman-Ayala et al., 2004).
There are several potential activators for these pathways, and those ligands are often specific to a particular receptor that would eventually lead to pathway activation. In order to narrow down the candidate compounds for our library, we performed single molecule fluorescent in situ hybridization (smFISH), a technique that allows us identify which cells or compartments express a particular gene of interest. We concluded that specific ligands of the Stat, MapK and SMAD, such as Fgf4 (MapK), Bmp4 (Smad1/5/8), Il11 (Stat) or Nodal (Smad2/3) are expressed in the blastocyst niche (**Fig. 1B**). Importantly, Stat ligands including Il11 and Il6 were previously shown to regulate CDX2 expression levels in TSCs (Rivron et al., 2018). These secreted molecules are clear candidates for the library. Blastocyst RNA sequencing confirmed the presence of those 4 ligands (**Sup. Fig. 1A**).
Given the importance of the MapK pathway for early embryonic development (Hamilton & Brickman, 2014; Meloche, Vella, Voisin, Ang, & Saba-El-Leil, 2004) as proved by the lethal effects observed in mutants for genes involved in the pathway (Arman, Haffner-Krausz, Chen,

Heath, & Lonai, 1998; Feldman, Poueymirou, Papaioannou, DeChiara, & Goldfarb, 1995), other modulators of the pathway such as Egf, HB-Egf (activators) or PD98 (inhibitor) were added to the library.

Other pathways play a role at different stages of trophoblast development. Given our goal of increasing the overall expression of one of the earliest committed genes, we were particularly interested in the pathways involved in the specification of the lineage. From literature, it is known that at least two pathways are involved in the first lineage segregation: Hippo and Notch (Lorthongpanich & Issaragrisil, 2015; Rayon et al., 2014). Hippo is a problematic pathway to work with in in vitro cultures since this signaling is highly dependent on mechanical stimuli, this being greatly disrupted in culture dishes, and by the spatial conformation inherent of colonies. Even though the Hippo pathway relies on a kinase activation cascade, modulators for Lats or Mst (the main kinases involved in the pathway) were unavailable at the time this study was developed. Hippo has nevertheless, been reported to be influenced by other pathways such as MapK (Feng et al., 2017) or by modulating the activity of G coupled protein receptors (Yu, Zhao, et al., 2012) among other pathways. There are several potential modulators for GPCR receptors affecting Hippo signaling (Yu, Mo, & Guan, 2012), including lysophosphatidic acid (LPA), sphingosine 1-phosphate (S1P) (Yu, Zhao, et al., 2012), Thrombin (Mo, Yu, & Gong, 2012), G-1 (Zhou et al., 2015) or Serotonin (Giulietti et al., 2014). Of note, these signaling pathways are strongly interacting intracellularly. For example, these GPCR ligands can also activate Erk and Stat pathways (Oufkir, Arseneault, Sanderson, & Vaillancourt, 2010). The notch pathway generally relies on direct cell-to-cell contact and its activation does not involve the action of kinases. However, it can be modulated by using soluble delta or soluble jagged receptors as activators. The Notch pathway can be tested by using soluble analogues for Delta or Jagged. We thus included LPA, S1P, thrombin, serotonin, and soluble analogues of Delta and Jagged in our library.

An important process mediated by the TE is uterine implantation. As reviewed in chapter one, both TE and endometrium must be in the optimal status for implantation to happen. Sexual hormones are the main signals that will change the endometrium to a receptive status, potentially affecting the embryo as well. Importantly, both Estrogen and Prostaglandin have also be reported to modulate the Hippo pathway (Yu, Zhao, et al., 2012). Prostaglandin E and Estretol, ligands to the Nr3c3 and ER nuclear receptors respectively were thus added to the library.

The Wnt pathway has also been reported to play a role in trophectoderm development in different mammalian species (Krivega, Essahib, & Van de Velde, 2015; Lim et al., 2013; Madeja, Hryniewicz, Orsztynowicz, Pawlak, & Perkowska, 2015). Importantly, an inhibitor for this pathway is used for the culture of TSCs in chemically defined media conditions (Ohinata & Tsukiyama, 2014). In our recent publication(Rivron et al., 2018), we could also establish that the Wnt pathway plays a role in the blastocyst cavitation process, mediated by TE cells. The agonist CHIR99021 and the antagonist XAV939 were thus included in the library in order to explore the direct regulation of Wnt on CDX2 expression.

The Rock pathway has a pivotal role in cytoskeleton dynamics and has also been linked to TSCs, with an inhibitor being used in the Ohinata serum free culture. This pathway has also been reported to affect Hippo signaling and to play a role in the first lineage specification (Kono, Tamashiro, & Alarcon, 2014). An available inhibitor of the Rock pathway is Y-27632.

There are other pathways that play a role in later developmental stages of the trophoblastic lineage. This is the case for Hypoxia or Ppar-γ. The low oxygen concentrations have an impact on placental development (Dunwoodie, 2009). Hypoxia inducible factors are the main drivers of

the response to hypoxia, and they become active when cultured in low oxygen concentrations, but also using other chemical mimetics such as Cocl2(Maxwell & Salnikow, 2004), deferoxamine mesylate (DFO)(G. L. Wang & Semenza, 1993) or 0-Phenannthorline (Xia et al., 2009), making all of them new additions to our library. The Ppar-γ pathway has been related to trophoblast differentiation in later stages of the placental development (Parast et al., 2009) and there are agonist such as Rosiglitazone and antagonist such as BADGE available. Ppar elements heterodimerize with retinoic acid receptors in order to bind to Ppar response elements, suggesting a potential cooperation between both pathways (Barak, Sadovsky, & Shalom-Barak, 2008). Importantly, Retinoic Acid (RA) has also been claimed to promote differentiation of TSCs (Yan et al., 2001).

Other less known pathways such as those involving endocannabinoids have also been stated to play a role in trophoblast biology (J. Wang, Paria, Dey, & Armant, 1999), being capable of interfering with other pathways such as MapK and Stat (Chang et al., 2017; Ibsen, Connor, & Glass, 2017). The agonist ACEA for receptor CB1, Hu-308 for receptor CB2, and the antagonist OMDM-2 were selected for testing together with Jzl184 and Urb597 which will affect the stability of endocannabinoids.

Cholesterol and other lipids have been suggested to have an impact on the crowding effect (Frechin et al., 2015), which can affect Hippo signaling. Therefore, cholesterol and Gm1 were tested.

In other stem cell populations, chromatin modulators have also been used to revert in vitro cultures to states that are more comparable to the in vivo analogues. We thus added compounds such as VPA (Hezroni, Sailaja, & Meshorer, 2011; Yin et al., 2014). A variety of factors that have been reported to affect pluripotency such as ps48 (Zhu et al., 2010), DUPC or DLPC (Guo & Smith, 2010; Heng et al., 2010; Lee et al., 2011) were also included in the library.

The Pka pathway has been shown to regulate differentiation of ESC (Yamamizu et al., 2012), but more importantly, we already showed that a more stable and permeable analogue of cyclic AMP is capable of upregulating the expression of CDX2 in TSCs (Rivron et al., 2018). This pathway is closely related to the metabolic status which plays a role in the transitions between naïve and primed states in human ESCs (Sperber et al., 2015) and in controlling stem cell fate (Folmes & Terzic, 2014). The Pi3K pathway is closely related to the metabolic status, since it is one of the main pathways downstream of insulin or IGF signaling, but also has been linked to play a role in implantation (Busch, Renaud, Schleussner, Graham, & Markert, 2009). This pathway is known to be active in the mouse blastocyst (Riley et al., 2005) and importantly, Insulin is present in the Tx media. 8Br-cAMP, Insulin, IGF and LongIGF were included in the library together with Rapamycin, an inhibitor of the pathway.

All these compounds need to be tested in conditions that allow to clearly observe an effect, thus the screenings were to be performed in serum free condtions. The Tx media does not include serum and it only contains compounds for activating the MapK and the Smad2/3 pathways, in contrast with the chemically defined conditions from Ohinata's publication, where 2 other pathway ligands are included along with B27 and N2 supplements. Importantly, the Tx media, is sufficient to maintain TSC identity only in a suboptimal manner, since in order to obtain placenta contribution, a transition culture in serum containing conditions is necessary. This property of the Tx media potentially allows us to identify new culture conditions that result in TSCs with improved in vivo potential.

The development of the Tx media (Kubaczka et al., 2014) was based on the essential 8 media (Chen et al., 2011), suitable for the culture of human ES. However, the proportion of nutrients in the media was not optimized for TSCs, therefore all components added to the Tx media

such as insulin, sodium selenite, sodium bicarbonate, ascorbic acid and holotransferrin were also to be tested at different concentrations for CDX2 expression.
Hippo signaling is a ubiquitous pathway well known to be influenced by the crowding effect, which partly acts via cytoskeleton. Changing the stiffness of the culture plates has an influence on the mechanical response of TSCs, therefore, plates with different stiffness were also tested for changes in Cdx2 expression.

3.3.2 Screening strategy

In order to quantify CDX2 expression in response to the compounds in the library, we made use of a CDX2-eGFP fusion reporter TSC line derived in the lab from an already available mouse line (Mcdole & Zheng, 2012). Using these TSCs has several advantages. GFP levels are closely correlated with CDX2 expression, which is in contrast with other reporter systems such as P2A or IRES that rely on bicystronic transcripts that results in multiple peptides. IRES systems have been showed to lead to non-proportional presence of the peptides, due to preferential binding to either the mRNA 5' cap or to the internal ribosomal entry site. P2A systems lead to 2 independent peptides but coming from one translation event which means that both final peptides are present at a 1 to 1 proportion. However, in P2A systems, both peptides undergo independent degradation, meaning that one of the two peptides (gene of interest or reporter protein) might be present for a longer time, biasing the readout. The fusion protein reporter solves those two issues. Nevertheless, fusion proteins can lead to miss-folding of the protein of interest due to interference of the reporter protein. In our case, homozygous mice can be obtained, which suggests that the fusion protein does not affect normal CDX2 functioning.
TSCs are generally fed every 48 hours, therefore this is set as the exposure time to the test compounds (**Fig. 1C**). It is expected that some of the compounds in the library will have negative effects on TSCs, not only in their CDX2 expression, but also in their morphology and possibly attachment properties, meaning that it is preferred to plate the TSCs prior to the exposure to the test compounds. Given the influence of crowding effects, the initial number of cells needs to be equal to all test conditions and they need to be equally distributed at the time of plating. After exposure to all test compounds, all wells are trypsinized, quenched, centrifuged and resuspended in the same amount of PBS before the FACS readout. Although suboptimal, an equal time for sample run in the FACS allows for an approximate measurement of the sample cell proliferation. All compounds were tested at multiple concentrations of different orders of magnitude in order to define the optimal concentration needed for a higher CDX2 expression. Those concentrations were selected based on prior publications where the molecule in question was used in any in vitro system or based in the IC50 for small compounds.
With each experiment a set of controls for each two plates was incorporated. The controls include: a control with the same culture conditions all wells were plated with (Tx + FGF4 + TGFβ1+ Heparin) and a negative control on plain Tx. The analysis for each compound is based on the percentage of CDX2-High to CDX2-Low ratio. After selecting for cell singlets and live cells, GFP measurements were represented as a histogram and gates were set as 50% CDX2-high and 50% CDX2-low for the control conditions (Tx medium including FGF4 and TGFβ1). Same gates were applied for all samples CDX2 levels were quantified according to the formula (Cdx2-high/Cdx2-low)*100.

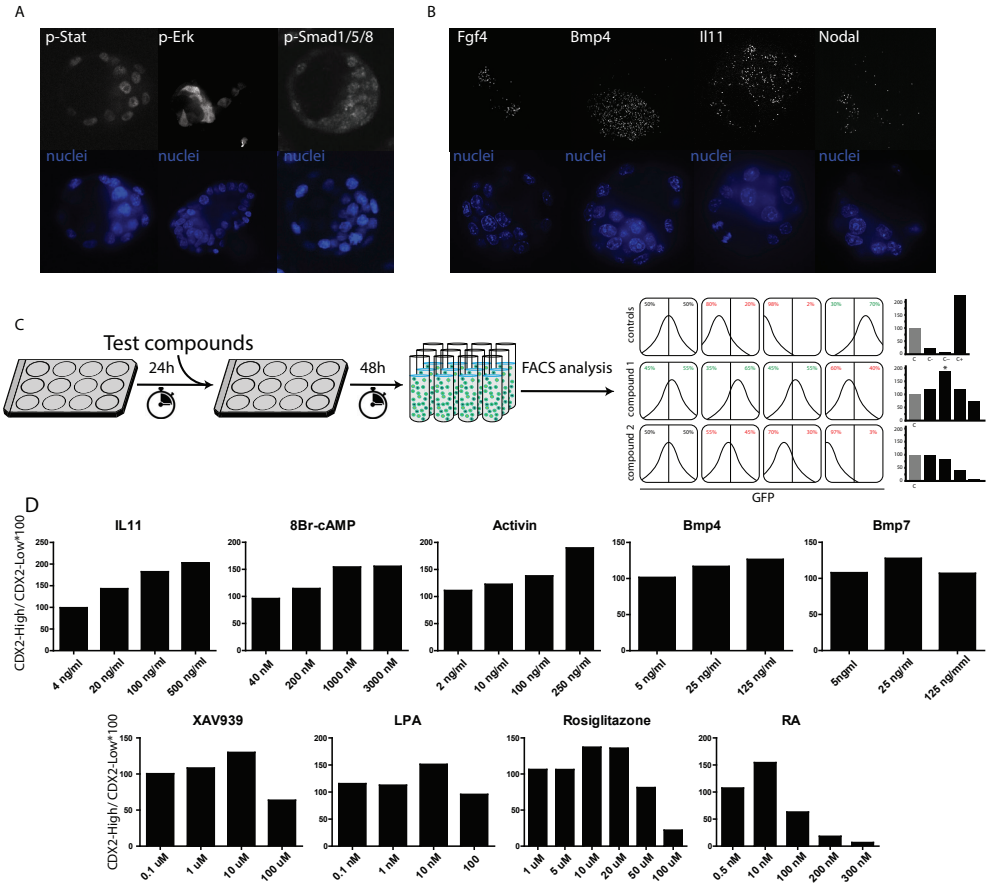

Figure 1. Effect of embryonic signals on CDX2 expression in TSCs. A. Pathway activation stainings performed in freshly isolated E3.5 blastocysts. B. smFISH performed on freshly isolated E3.5 blastocysts allow to detect expression of key pathway ligands. C. Summary of the screening strategy. 24 hours after initial plating of CDX2-eGFP TSCs, media is changed to fresh Tx media including the compound to test. Compounds are tested at 3-5 different concentrations and CDX2-eGFP normal distribution is tracked for CDX2 expression quantification via FACS. D. Positive CDX2 expression modulators induce a higher expression of CDX2 in a dose dependent manner.

3.3.3 Factorial screenings allow us to combine some of the 9 positive modulators of CDX2

Out of 49 compounds tested, 15 showed an induction of CDX2 expression (with a Cdx2-high to Cdx2-low ratio higher than 125%) in a dose dependent fashion (**Sup. table 1** and **Fig. 1D**). Because some of these positive regulators targeted the same pathway, we chose one hit for each pathway. We made an exception for the Smad1/5/8 pathway, since we kept two of the hits for further analysis due to a differential phenotype triggered by each activator. Bmp7 was leading to a more epithelial morphology than the one observed in Bmp4 treated TSC (data not shown). For the Smad2/3 pathway, Nodal was the most potent inductor of Cdx2 expression. However, we chose Activin as the ligand for further test due to the fact that Nod-

al requires the coactivator Cripto to be co-expressed for successful pathway activation, and the expression of Cripto is restricted to the ICM in the blastocyst (Takaoka, Nishimura, & Hamada, 2017). Three Stat pathway activators lead to increase of CDX2 expression in a dose dependent manner, which confirmed our previous results (Rivron et al., 2018). We selected Il11 based on the higher expression achieved (**Fig. 1D**). XAV939 proved to potentiate Cdx2 expression, which is in accordance with the use of this compound in one of the available serum free TSC cultures (Ohinata & Tsukiyama, 2014). Rosiglitazone and retinoic acid were also chosen as hits. Due to the interactions reported to occur between these two pathways, it is particularly interesting to study the effects on TSCs when exposed to both compounds. 8-Br cAMP was confirmed as a positive regulator of CDX2 expression (Rivron et al., 2018). Three GpcR modulators resulted in positive regulation of CDX2 expression in a dose dependent manner, among which Thrombin was the most potent one. However, due to the high costs of this compound, the second most powerful hit was chosen: LPA. DUPC and DLPC also lead to a powerful increase in CDX2 expression, but they dramatically impaired proliferation. sDll1 and PGE also showed a trend in upregulating CDX2 expression, but they didn't reach the threshold established.

These filters resulted in us obtaining 9 potential hits for further tests (**Fig. 1D**).

Our tests increasing the concentration for the Tx components resulted in no increase of Cdx2 expression, therefore we didn't introduce any modifications in the basal Tx recipe (**Sup. table 1**).

These single hits are able to increase overall CDX2 expression by themselves. However, in the blastocyst, these signals are likely to be delivered in combination by the ICM/Epiblast cells to the polar TE cells. It is possible then that combining these hits can further potentiate CDX2 expression; however, it is likely that interactions between some compounds might cause adverse effects on the TSC culture. Given the number of hits, the amount of possible combinations makes it impossible for us to test them experimentally. Factorial design can help us figure out which combination of these factors have a bigger impact on CDX2 expression, suggesting a few experimental conditions for us to test, and then modeling the landscape of combinations. We made use of the JMP software for statistical discovery based on factorial design. This type of designs allows us to identify which are the factors and factor interaction that have a substantial effect on CDX2 expression.

With the software, we generated a design that included testing 21 compound combinations with a D efficiency of around 87% and power of 0,971. The D efficiency states the quality of the design, being 85% the minimum while the power determines how sensitive the design is to detect small interactions between compounds. For each of the 21 combinations generated by the design, each compound was either present at its optimal concentration, 50% of its optimal concentration or absent.

Given that we are trying to find new culture conditions that allow continued expansion of TSCs, we tested these cocktails (named Tx1 to Tx21) in a long-term culture fashion, while tracking the CDX2 changes upon each passage. On passage 1, we followed the same strategy used for the single hit compound screening with an initial 48 hour exposure to the new cocktails. Upon passaging, we quantified cell proliferation and the same number of cells would be used for re-plating for the next passage, the remaining cells would be used for the FACS analysis. After the first passage, each culture would be passaged independently when the cells had reached around 80% confluency, and the cultures would be kept for up to 10 passages. All cocktails were scored using the CDX2-High to CDX2-Low ratio on each passage, allowing us to rank them based on overall CDX2 expression.

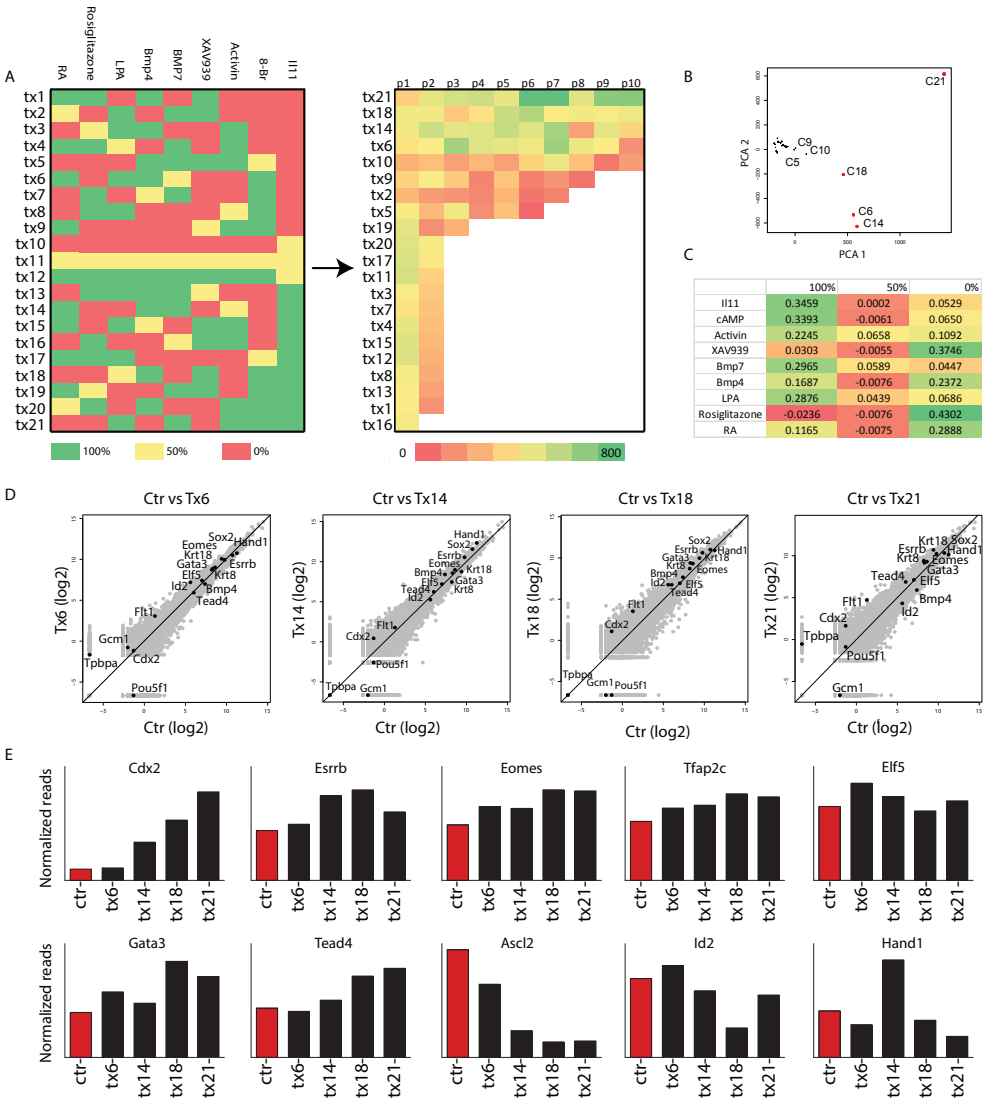

Figure 2. Factorial design for screens combining the single CDX2 modulators. A. Factorial design suggested 21 different compound combinations in which is compound was included at its optimal concentration, 50% of the optimal concentration or absent. 4 combinations allowed for long term culture with the cells displaying consistently high levels of CDX2. B-C. Principal component analysis suggests the effect of each compound at each tested concentration on CDX2 expression. D. Bulk transcriptome analysis allows us to compare the overall expression of key trophoblast markers for each culture conditions. E. Expression of classical markers for the undifferentiated TSC state across all the cultures analyzed.

Even though all the cocktails showed an initial increase in CDX2 expression compared to the control conditions on passage 1, 12 of the cultures collapsed after passage 2, due to a lack of proliferation or attachment (**Fig. 2A**). Three cocktails (Tx2, Tx5 and Tx19) lead to collapse

between passages 2 and 5. Tx9 showed a much lower proliferation rate. We concluded that these cocktails do not allow for the maintenance of stem cells. From the 5 cocktails remaining, Tx10 performed poorly in terms of CDX2 expression when compared with the other 4 conditions.
From the 21 cocktails tested, 18 included 4 or 5 of the hits. The two conditions that included all the compounds (either at its independent optimal concentration or half of it) lead to a quick collapse of the culture despite having the best CDX2-High to low ratio after 48 hours of exposure. From the 18 cocktails that included 4 or 5 compounds, only 4 performed well in terms of culture stability and CDX2 expression levels, suggesting that there might be interactions between the different pathways triggered by these compounds. We were interested in knowing which of these compounds had a bigger impact on CDX2 expression, and we assessed this by comparing CDX2-High to Low ratio from the single hits and the combined cocktails using principal component analysis. PCA suggested that the factors that had a more important role in increasing CDX2 expression were the absence of Rosiglitazone and XAV939 and the presence of Il11, cAMP and Bmp7 at their optimal concentration (**Fig. 2B-C**). Note that these experiments are run using FGF4 and TGFβ1 as a basal cocktail in all conditions.
From the 21 culture cocktails, 4 were stable and showed consistently high CDX2 expression levels. We then tested, via RNA sequencing, whether these cultures still had a trophoblastic identity and if apart from CDX2, they showed clues of being in a more differentiated state. In order to assess this, three replicates of 1000 cells were used for RNA extraction and bulk sequencing.
RNA sequencing results show that all 4 conditions retained trophoblast identity based on the expression of TSC markers (**Fig. 2D**). However minor differences in the expression of those markers could help us filter down which of those conditions lead to a TSC culture more comparable to the polar TE. We were interested in the expression of markers of an undifferentiated state such as, Esrrb, Eomes, Tfap2c, Elf5, Gata3 or Tead4; or markers of trophectoderm derivatives such as Ascl2 (ectoplacental cone), Hand1 (Trophoblast giant cells) and Id2 (**Fig. 2E**). In this sense, cultures Tx18 and Tx21 upregulated stem cell markers and diminished the expression of differentiation related genes.
Apart from the expression profile, the different cultures showed a different cell morphology that was also kept in mind for selecting for cultures to further test. While Tx6 and Tx18 showed a more mesenchymal phenotype, Tx14 and Tx21 displayed a rather epithelial phenotype, which was preferred due to the epithelial nature of the TE.
Consistently high CDX2 expression, higher RNA expression of other stem cell markers, lower expression of differentiation markers and cell morphology pointed at tx21 as a clear candidate. Tx21 included FGF4 (25ng/ml), TGFβ1 (2ng/ml), BMP7 (50 ng/ml), 8Br-cAMP (200 nM), IL11 (100ng/ml), ACTIVIN (100 ng/ml), LPA (10 nM), which effectively regulated CDX2 on a long-term, while maintaining proliferation and an epithelial-like phenotype.

3.3.4 Laminin screens

Tx21 is a fully chemically defined media that maintains high expression levels of CDX2 on a long-term. However, Matrigel is still used for pre-coating the plates. Matrigel contains a variety of extracellular matrix proteins including laminin as a major component. Laminins are formed by 3 chains named α,β and γ (Domogatskaya, Rodin, & Tryggvason, 2012). In mammalians there are 12 chains grouped into α,β or γ and can form up to 60 trimeric combinations. Each cell type expresses a particular subset of those chains. We wondered if different

laminins would have a different effect on CDX2 expression. A set of different laminin coatings commercially available intended for mini-screens was used in order to evaluate their effects on TSC proliferation and CDX2 expression in comparison with classical Tx conditions (**Fig. 3A**). Only laminins 221, 511 and 521 didn't negatively affect proliferation nor CDX2 expression.

From a pre-existing RNA sequencing dataset (Rivron et al., 2018) we confirmed that for the α-subunit, the gene Lama2 was not expressed in the early nor blastocyst stage. Lamc1 was the only γ subunit showing high expression levels. Both Lamb1 and Lamb2 (**Fig. 3B**) genes were detected in the blastocyst at comparable levels, but the Lamb2 levels increased in the late blastocyst stage making laminin 521 our candidate for extracellular matrix coating for culturing TSC.

Importantly, we confirmed that our Tx21 cocktail was still capable of boosting CDX2 expression on TSC cultured on laminin 521 coated plates (**Fig. 3C**). Interestingly, we could observe a synergy between the new CDX2 regulators and laminin 521, leading to a culture with a

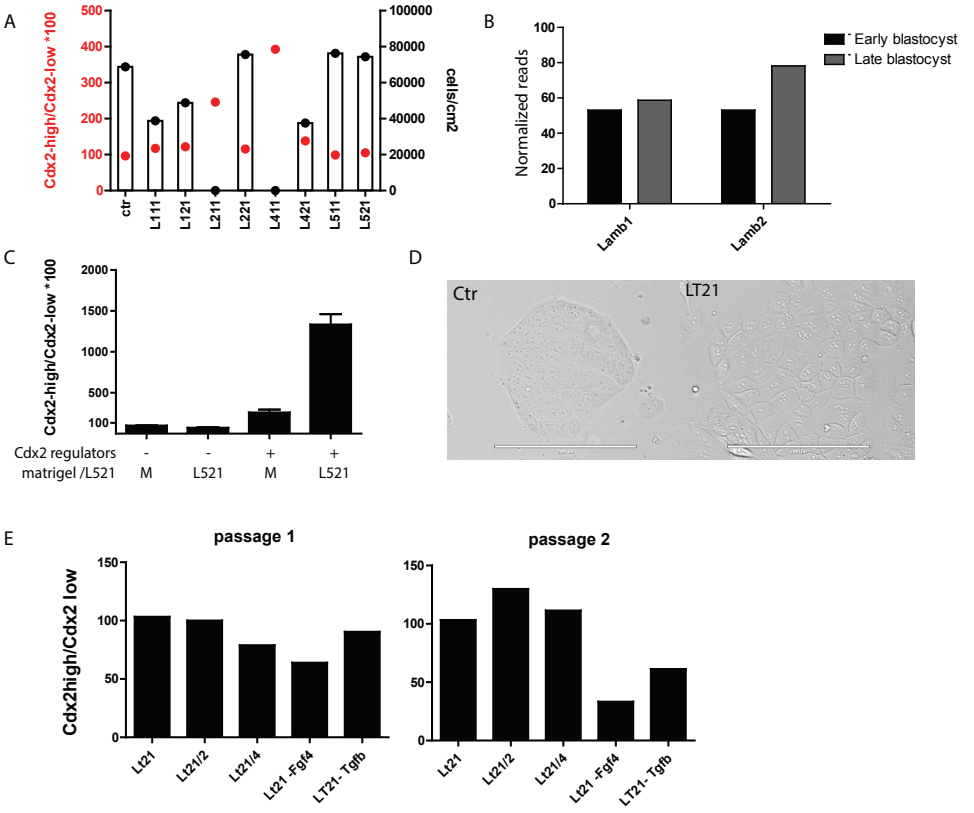

Figure 3. Optimization of the LT21 culture for TSCs. A. CDX2 and proliferation quantification of TSCs cultured under Tx conditions on plates coated with different laminins. B. Lamb1 and Lamb2 expression in bulk samples from early and late blastocysts. C. Combined effect of Tx21 compounds and Laminin521 on CDX2 expression on TSCs. D. Bright field picture of TSCs grown in Tx and LT21 conditions. E. CDX2 expression quantification upon concentration reduction of Tx21 components, removal of FGF4 or removal of TGFB after 1 and 2 passages.

virtually depleted CDX2-Low population. We called these new culture conditions LT21.
Cells cultured in LT21 showed a different colony phenotype, with an apparently more epithelial morphology and maintained high overall CDX2 expression levels (**Fig. 3D**).
Reached this point, it would be interesting to challenge the LT21 culture conditions by changing some of the parameters we initially considered at the beginning of the screenings. Apart from testing all the compounds again, this time taking LT21 as basal conditions, we would be particularly interested in testing culture plates with different stiffness, mainly due to its potential to affect Hippo signaling. This remains to be tested.

3.3.5 LT21 component optimization

The LT21 media includes 7 compounds apart from the laminin for coating, making it a complex cocktail. We wondered if removal of any of the included compounds or reduction of the overall concentrations would affect the CDX2 expression profile. Apart from a possible optimization of the CDX2 expression profile, such compound usage reduction would have a cost benefit. The tests aimed for optimization of the media also included the removal of the two compounds added in the classical cultures: FGF4 and TGFβ1. The same screening strategy was applied for two passages in order to capture the CDX2 expression profile but also a potential quick culture collapse. On the first passage we could observe that reducing the concentration of all new Tx21 compounds to half was still leading to the same CDX2 expression enrichment observed in LT21 conditions. Reducing the concentration of those compounds to one fourth altered the distribution increasing the number of CDX2-Low cells (**Fig. 3E**). Both FGF4 and TGFβ1 removal lead to a dramatic decrease of the CDX2-High subpopulation. From this point onward, LT21 conditions refer to laminin 521 pre-coating plus Tx21 media with the compounds at half of their optimal concentration.

3.6 Discussion

Even though TSCs have been cultured and studied for over two decades, very little is known about pathways leading to increase in the transcription of key players in the transcriptional network. The original cultures of TSCs were successful in retaining the properties of early trophoblast cells in the sense that TSCs were able to differentiate into trophoblast derivatives, they would allow for unlimited expansion in vitro and would lead to placental contribution when injected in the blastocyst.
Even though there have been improvements in the culture of TSC aiming for more defined media, researchers mainly focused on obtaining a culture resembling the classical culture with serum and mouse embryonic fibroblasts rather than obtaining a culture more comparable to TE cells. It is thought that multiple signals originating from the ICM regulate the polar TE, keeping it from differentiating into mural TE.
Few publications have focused on describing the heterogeneity observed in this possibly aberrant culture, but none focused on correcting it. In the previous chapter we identified CDX2 as a good marker for demonstrating a high degree of intercellular heterogeneity, but also as a suitable marker for a more potent stem cell state. We also learned that the available culture conditions regardless of the initial CDX2 subpopulation lead to an equilibrium allowing for this heterogeneity. Our conclusion was that by altering those culture conditions, we might be able to reach a culture in which that equilibrium allows for an enriched CDX2-High culture.
We managed to identify a set of soluble compounds that are independently able to boost the

expression of CDX2, More importantly, factorial design software allowed us to obtain a new combination of growth factors leading to a stable culture with consistently high CDX2 expression. This type of design has been instrumental for our purpose allowing our initial goal to be realistic from an experimental point of view. The fact that combinatorial design was tested in long term cultures has been crucial for us to identify which of those regulators are beneficial in the long term.
Our new culture conditions, named LT21 include a number of soluble compounds that were first screened based on observations made by ourselves (e.g. a list of embryonic inductive signals we previously established) and publications by fellow researchers. Our way to assess the effect of these compounds was purely experimental and required a reporter that was optimal for our purpose, making the screening a relatively straight forward process. A rational way of building our library and the simplicity of the readout lead to a number of hits, that when combined potentiated the expression of CDX2 at a protein level. The results obtained from the conditions suggested by the factorial design proved that the interactions between pathways are key to the outcome of the cultures, and not only in terms of CDX2 expression, but also in terms of maintaining cells capable of attachment and proliferation. These features allowed us to discard most of the suggested cocktails.
Cells react not only to signaling molecules, but also to metabolites or proteins of the extracellular matrix. In our study, even though our main focus was on the signaling molecules, altering the components of the extracellular matrix showed dramatic results. The switch from Matrigel, which contains laminin as a main ingredient, to laminin 521 showed a clear improvement. This suggests either that laminin 521 is not present in Matrigel, or that the rest of impurities play a negative role in our culture of interest. These two options emphasize the importance of performing screenings and of obtaining a defined media culture.
The phenotype of LT21 cultured cells is promising as it shows higher expression of previously known stem markers, but we will only prove that this is a suitable culture by demonstrating the potential of LT21 cultured TSCst experimentally.

3.5 Materials and methods

• TSC culture:

Unless stated otherwise, TSC are cultured under Tx conditions previously published (Kubaczka et al., 2014). After coating with Matrigel, cells are cultured in Tx media, which consists of phenol red free DMEM/F12 supplemented (phenol red-free, with l-glutamin), insulin (19.4 µg/ml), l-ascorbic-acid-2-phosphate (64 µg/ml), sodium selenite (14 ng/ ml), insulin (19.4 µg/ml), sodium bicarbonate (543 µg/ml), holo-transferin (10.7 µg/ml), penicillin streptomycin, FGF4 (25 ng/ml), TGFβ1 (2 ng/ml) and heparin (1 µg/ml). Alternatively, when stated, TSC were cultured in classical TS conditions(Tanaka, 1998) in a media based on RPMI 1640 supplemented with 20% fetal bovine serum, sodium pyruvate (1 mM), b-mercaptoethanol (100 mM), L-glutamine (2 mM), and penicillin and streptomycin (50 mg/ml each), human recombinant FGF4 (25 ng/ml) and heparin (1 mg/ml). Cells were routinely passaged using trypsin. Final LT21 conditions require for a pre-coating of laminin 521 at a concentration of 10 ug/ml diluted in PBS with Mg2+ and Ca2+. Il11 (50 ng/ml), ACTIVIN (50ng/ml), BMP7 (25 ng/ml), LPA (5 nM) and 8Br-cAMP (200 nM) were added on top of the classical Tx media (including FGF4 at 25 ng/ml, TGFβ1 at 2ng/ml and heparin) for the optimized LT21 media.

• Immunofluorescence
Cells in monolayer were fixed using 4%PFA in PBS for 20 minutes at RT followed by 3 washing steps with PBS. A 0.25% triton solution in PBS was used for permeabilization during 30 minutes ar RT,followed by a 1 hour blocking step with PBS+ 10% FBS and 0.1% tween20. Primary antibodies against pSTAT (Cell signaling #9145), Smad (Cell signaling #9511), pERK (Cell Signalling #4370S) were diluted 1/200 in PBS + 0.1% Tween20, and used for staining O/N at 4C. Stainings involving pERK antibody, also included PhoSTOP in all step until after the primary antibody incubation. After three washing steps, samples were incubated with the corresponding secondary antibodies for 1 hour at RT. Hoechst was used for counterstaining. All images were analyzed in a PerkinElmer Ultraview VoX spinning disk microscope.

• smFISH:
Blastocysts were fixed using RNAse free 4%PFA in PBS + 1% Acetic Acid during 20 minutes. After fixation, all samples followed the Quantigene ViewRNA kit instructions: After three washes with RNAse free PBS, sampels were incubated for 10 minutes in a detergent solution. After three washes with RNAse free PBS, samples were incubated for 5 minutes at RT with Q protease. After three washes with RNAse free PBS, samples were incubated at 40C for 3 hours (in a humidified chamber) with the probes of interest diluted in Probe set diluent. After 3 washes with wash buffer, samples were incubated at 40C for 30 minutes with preamplifier diluted in amplifier diluent. After 3 washes with wash buffer, samples were incubated at 40C for 30 minutes with amplifier diluted in amplifier diluent. After 3 washes with wash buffer, samples were incubated at 40C for 30 minutes with label diluted in label probe diluent. After 2 washes with wash buffer, they were washed once more for 10 minutes. Samples were then incubated for 15 minutes in RNAse free PBS with Hoechst and WGA as counterstains followed by 3 washes with RNAse free PBS. Blastocysts were carefully placed in mounting media in glass bottom 3.5 mm plates. All samples were imaged with a 63x oil immersion objective in a PerkinElmer Ultraview VoX spinning disk microscope.

• FACS analysis for screenings:
For all conditions, 18.000 cells/cm2 were plated in 12 well greiner plates previously coated with matrigel diluted 1/100 in DMEM-F12. All conditions were plated in Tx +Fgf4 (25ng/ml), TGFβ1 (2ng/ml) and heparin. 24 hours later, media was replaced with the new condition to test, including a set of controls for every two plates. 48 hours after media change, cells were trypsinized. Trypsin was quenched with soybean trypsin inhibitor, samples were spun down and pellets were resuspended in 250 ul of PBS. For the long term combinatorial screenings, 10 of those 250ul were used for counting the number of cells, and 72.000 cells was used for replating the culture for the next passage.
A BD FACSCalibur cytometer was sued for all FACS analytical assays. When sorting was required a FACSAria was used. All samples were gated first for singlets based on forward and side scaterred reads, then for live cells based on propidium iodide negative staining, and GFP histogram was considered to be 50% Cdx2-low and 50% Cdx2-high in the control situation. The sample ran for 180 seconds on all conditions in order to have an approximate measure of proliferation.

• Blastocyst isolation:
After crossings between CBA and C57BL/6 strains, 3.5 dpc plugged females were sacrificed and their uterus were flushed with M2 media.

• RNA sequencing:
Using a FACSAria, the top 5% and bottom 5% Cdx2 expressing C3-1 cells were sorted into separate tubes and trizol RNA extraction was performed. Samples then followed the Cel Seq1 protocol (Hashimshony, Wagner, Sher, & Yanai, 2012).Transcriptome analysis was performed using the DESeq2 package in RStudio.

• Laminin screens:
Screens were performed in the same was as the soluble compound screening only changing the prior coating of the plates. Laminin (LAMscreen KT202) kit was purchased from biolamina. All laminins were tested at the two suggested concentrations: 5 ug/ml and 10 ug/ml. Laminins were diluted to the mentioned concentration in PBS containing Ca2+ and Mg2+. Coatings can be done for 2 hours at 37C or O/N at 4C. This last condition allows the laminin solution to be reused for one more coating.

Author contribution

Javier Frias Aldeguer performed stainings, smFISH, RNA sequencing analysis, cocktail optimization, part of the screening and wrote the chapter. **Maarten Kip** performed part of the screenings. **Clemens van Blitterswijk** and **Niels Geijsen** helped to direct the project **Nicolas Clement Rivron** derived CDX2-eGFP reporter TSC line, generated the blastocyst bulk sequencing dataset, and conceived and directed the research.

Bibliography

Arkun, Y., & Yasemi, M. (2018). Dynamics and control of the ERK signaling pathway: Sensitivity, bistability, and oscillations. PloS One, 13(4), e0195513. https://doi.org/10.1371/journal.pone.0195513

Arman, E., Haffner-Krausz, R., Chen, Y., Heath, J. K., & Lonai, P. (1998). Targeted disruption of fibroblast growth factor (FGF) receptor 2 suggests a role for FGF signaling in pregastrulation mammalian development. Proceedings of the National Academy of Sciences of the United States of America, 95(9), 5082–5087. https://doi.org/10.1073/pnas.95.9.5082

Barak, Y., Sadovsky, Y., & Shalom-Barak, T. (2008). PPAR Signaling in Placental Development and Function. PPAR Research, 2008, 142082. https://doi.org/10.1155/2008/142082

Busch, S., Renaud, S. J., Schleussner, E., Graham, C. H., & Markert, U. R. (2009). mTOR mediates human trophoblast invasion through regulation of matrix-remodeling enzymes and is associated with serine phosphorylation of STAT3. Experimental Cell Research, 315(10), 1724–1733. https://doi.org/10.1016/j.yexcr.2009.01.026

Chang, X., Bian, Y., He, Q., Yao, J., Zhu, J., Wu, J., … Duan, T. (2017). Suppression of STAT3 Signaling by Delta9-Tetrahydrocannabinol (THC) Induces Trophoblast Dysfunction. Cellular Physiology and Biochemistry : International Journal of Experimental Cellular Physiology, Biochemistry, and Pharmacology, 42(2), 537–550. https://doi.org/10.1159/000477603

Chen, G., Gulbranson, D. R., Hou, Z., Bolin, J. M., Ruotti, V., Probasco, M. D., … Thomson,

J. A. (2011). Chemically defined conditions for human iPSC derivation and culture. Nature Methods, 8(5), 424–429. https://doi.org/10.1038/nmeth.1593

Dardik, A., Smith, R. M., & Schultz, R. M. (1992). Colocalization of transforming growth factor-alpha and a functional epidermal growth factor receptor (EGFR) to the inner cell mass and preferential localization of the EGFR on the basolateral surface of the trophectoderm in the mouse blastocyst. Developmental Biology, 154(2), 396–409.

Domogatskaya, A., Rodin, S., & Tryggvason, K. (2012). Functional Diversity of Laminins. Annual Review of Cell and Developmental Biology, 28(1), 523–553. https://doi.org/10.1146/annurev-cellbio-101011-155750

Dunwoodie, S. L. (2009). The Role of Hypoxia in Development of the Mammalian Embryo. Developmental Cell, 17(6), 755–773. https://doi.org/10.1016/j.devcel.2009.11.008

Feldman, B., Poueymirou, W., Papaioannou, V., DeChiara, T., & Goldfarb, M. (1995). Requirement of FGF-4 for postimplantation mouse development. Science, 267(5195), 246–249. https://doi.org/10.1126/science.7809630

Feng, R., Gong, J., Wu, L., Wang, L., Zhang, B., Liang, G., … Xiao, H. (2017). MAPK and Hippo signaling pathways crosstalk via the RAF-1/MST-2 interaction in malignant melanoma. Oncology Reports, 38(2), 1199–1205. https://doi.org/10.3892/or.2017.5774

Folmes, C. D. L., & Terzic, A. (2014). Metabolic determinants of embryonic development and stem cell fate. Reproduction, Fertility, and Development, 27(1), 82–88. https://doi.org/10.1071/RD14383

Frechin, M., Stoeger, T., Daetwyler, S., Gehin, C., Battich, N., Damm, E.-M., … Pelkmans, L. (2015). Cell-intrinsic adaptation of lipid composition to local crowding drives social behaviour. Nature, 523(7558), 88–91. https://doi.org/10.1038/nature14429

Giulietti, M., Vivenzio, V., Piva, F., Principato, G., Bellantuono, C., & Nardi, B. (2014). How much do we know about the coupling of G-proteins to serotonin receptors? Molecular Brain, 7, 49. https://doi.org/10.1186/s13041-014-0049-y

Guo, G., & Smith, A. (2010). A genome-wide screen in EpiSCs identifies Nr5a nuclear receptors as potent inducers of ground state pluripotency. Development (Cambridge, England), 137(19), 3185–3192. https://doi.org/10.1242/dev.052753

Guzman-Ayala, M., Guzman-Ayala, M., Ben-Haim, N., Ben-Haim, N., Beck, S., Beck, S., … Constam, D. B. (2004). Nodal protein processing and fibroblast growth factor 4 synergize to maintain a trophoblast stem cell microenvironment. Proceedings of the National Academy of Sciences of the United States of America, 101(44), 15656–15660. https://doi.org/10.1073/pnas.0405429101

Hamilton, W. B., & Brickman, J. M. (2014). Erk signaling suppresses embryonic stem cell self-renewal to specify endoderm. Cell Reports, 9(6), 2056–2070. https://doi.org/10.1016/j.

celrep.2014.11.032

Hashimshony, T., Wagner, F., Sher, N., & Yanai, I. (n.d.). CEL-Seq: single-cell RNA-Seq by multiplexed linear amplification. Cell Reports, 2(3), 666–673. Retrieved from http://www.ncbi.nlm.nih.gov/sites/entrez?Db=pubmed&DbFrom=pubmed&Cmd=Link&LinkName=pubmed_pubmed&LinkReadableName=Related Articles&IdsFromResult=22939981&ordinalpos=3&itool=EntrezSystem2.PEntrez.Pubmed.Pubmed_ResultsPanel.Pubmed_RVDocSum

Heng, J.-C. D., Feng, B., Han, J., Jiang, J., Kraus, P., Ng, J.-H., … Ng, H.-H. (2010). The nuclear receptor Nr5a2 can replace Oct4 in the reprogramming of murine somatic cells to pluripotent cells. Cell Stem Cell, 6(2), 167–174. https://doi.org/10.1016/j.stem.2009.12.009

Hezroni, H., Sailaja, B. S., & Meshorer, E. (2011). Pluripotency-related, valproic acid (VPA)-induced genome-wide histone H3 lysine 9 (H3K9) acetylation patterns in embryonic stem cells. The Journal of Biological Chemistry, 286(41), 35977–35988. https://doi.org/10.1074/jbc.M111.266254

Ibsen, M. S., Connor, M., & Glass, M. (2017). Cannabinoid CB1 and CB2 Receptor Signaling and Bias. Cannabis and Cannabinoid Research, 2(1), 48–60. https://doi.org/10.1089/can.2016.0037

Kono, K., Tamashiro, D. A. A., & Alarcon, V. B. (2014). Inhibition of RHO-ROCK signaling enhances ICM and suppresses TE characteristics through activation of Hippo signaling in the mouse blastocyst. Developmental Biology, 394(1), 142–155. https://doi.org/10.1016/j.ydbio.2014.06.023

Krivega, M., Essahib, W., & Van de Velde, H. (2015). WNT3 and membrane-associated beta-catenin regulate trophectoderm lineage differentiation in human blastocysts. Molecular Human Reproduction, 21(9), 711–722. https://doi.org/10.1093/molehr/gav036

Kubaczka, C., Senner, C., Ara??zo-Bravo, M. J., Sharma, N., Kuckenberg, P., Becker, A., … Schorle, H. (2014). Derivation and maintenance of murine trophoblast stem cells under defined conditions. Stem Cell Reports, 2(2), 232–242. https://doi.org/10.1016/j.stemcr.2013.12.013

Lee, J. M., Lee, Y. K., Mamrosh, J. L., Busby, S. A., Griffin, P. R., Pathak, M. C., … Moore, D. D. (2011). A nuclear-receptor-dependent phosphatidylcholine pathway with antidiabetic effects. Nature, 474(7352), 506–510. https://doi.org/10.1038/nature10111

Lim, K. T., Gupta, M. K., Lee, S. H., Jung, Y. H., Han, D. W., & Lee, H. T. (2013). Possible involvement of Wnt/beta-catenin signaling pathway in hatching and trophectoderm differentiation of pig blastocysts. Theriogenology, 79(2), 282–284. https://doi.org/10.1016/j.theriogenology.2012.08.018

Lorthongpanich, C., & Issaragrisil, S. (2015). Emerging Role of the Hippo Signaling Pathway in Position Sensing and Lineage Specification in Mammalian Preimplantation Embryos. Biol-

ogy of Reproduction, 92(6), 143. https://doi.org/10.1095/biolreprod.114.127803

Madeja, Z. E., Hryniewicz, K., Orsztynowicz, M., Pawlak, P., & Perkowska, A. (2015). WNT/beta-catenin signaling affects cell lineage and pluripotency-specific gene expression in bovine blastocysts: prospects for bovine embryonic stem cell derivation. Stem Cells and Development, 24(20), 2437–2454. https://doi.org/10.1089/scd.2015.0053

Maxwell, P., & Salnikow, K. (2004). HIF-1: an oxygen and metal responsive transcription factor. Cancer Biology & Therapy, 3(1), 29–35.

Mcdole, K., & Zheng, Y. (2012). Generation and live imaging of an endogenous Cdx2 reporter mouse line. Genesis, 50(10), 775–782. https://doi.org/10.1002/dvg.22049

Meloche, S., Vella, F. D. J., Voisin, L., Ang, S.-L., & Saba-El-Leil, M. (2004). Erk2 signaling and early embryo stem cell self-renewal. Cell Cycle (Georgetown, Tex.), 3(3), 241–243.

Mo, J., Yu, F., & Gong, R. (2012). Regulation of the Hippo – YAP pathway by protease-activated receptors (PARs) service Regulation of the Hippo – YAP pathway by protease-activated receptors (PARs). Genes & Development, 26, 2138–2143. https://doi.org/10.1101/gad.197582.112

Ohinata, Y., & Tsukiyama, T. (2014). Establishment of trophoblast stem cells under defined culture conditions in mice. PLoS ONE, 9(9). https://doi.org/10.1371/journal.pone.0107308

Oufkir, T., Arseneault, M., Sanderson, J. T., & Vaillancourt, C. (2010). The 5-HT 2A serotonin receptor enhances cell viability, affects cell cycle progression and activates MEK-ERK1/2 and JAK2-STAT3 signalling pathways in human choriocarcinoma cell lines. Placenta, 31(5), 439–447. https://doi.org/10.1016/j.placenta.2010.02.019

Parast, M. M., Yu, H., Ciric, A., Salata, M. W., Davis, V., & Milstone, D. S. (2009). PPARgamma regulates trophoblast proliferation and promotes labyrinthine trilineage differentiation. PloS One, 4(11), e8055. https://doi.org/10.1371/journal.pone.0008055

Rayon, T., Menchero, S., Nieto, A., Xenopoulos, P., Crespo, M., Cockburn, K., … Manzanares, M. (2014). Notch and Hippo Converge on Cdx2 to Specify the Trophectoderm Lineage in the Mouse Blastocyst. Developmental Cell, 30(4), 410–422. https://doi.org/10.1016/j.devcel.2014.06.019

Riley, J. K., Carayannopoulos, M. O., Wyman, A. H., Chi, M., Ratajczak, C. K., & Moley, K. H. (2005). The PI3K/Akt pathway is present and functional in the preimplantation mouse embryo. Developmental Biology, 284(2), 377–386. https://doi.org/10.1016/j.ydbio.2005.05.033

Rivron, N. C., Frias-Aldeguer, J., Vrij, E. J., Boisset, J.-C., Korving, J., Vivié, J., … Geijsen, N. (n.d.). Blastocyst-like structures generated solely from stem cells. Nature, 557(7703), 106–111. Retrieved from http://www.ncbi.nlm.nih.gov/sites/entrez?Db=pubmed&DbFrom=pubmed&Cmd=Link&LinkName=pubmed_pubmed&LinkReadableName=Related Articles&IdsFromResult=29720634&ordinalpos=3&itool=EntrezSystem2.PEntrez.Pubmed.

Pubmed_ResultsPanel.Pubmed_RVDocSum

Rivron, N. C., Frias-aldeguer, J., Vrij, E. J., Boisset, J., Korving, J., Vivié, J., … Geijsen, N. (2018). Blastocyst-like structures generated solely from stem cells.

Sperber, H., Mathieu, J., Wang, Y., Ferreccio, A., Hesson, J., Xu, Z., … Ruohola-Baker, H. (2015). The metabolome regulates the epigenetic landscape during naive-to-primed human embryonic stem cell transition. Nature Cell Biology, 17(12), 1523–1535. https://doi.org/10.1038/ncb3264

Takaoka, K., Nishimura, H., & Hamada, H. (2017). Both Nodal signalling and stochasticity select for prospective distal visceral endoderm in mouse embryos. Nature Communications, 8(1), 1492. https://doi.org/10.1038/s41467-017-01625-x

Tanaka, S. (1998). Promotion of Trophoblast Stem Cell Proliferation by FGF4. Science, 282(5396), 2072–2075. https://doi.org/10.1126/science.282.5396.2072

Wang, G. L., & Semenza, G. L. (1993). Desferrioxamine induces erythropoietin gene expression and hypoxia-inducible factor 1 DNA-binding activity: implications for models of hypoxia signal transduction. Blood, 82(12), 3610–3615.

Wang, J., Paria, B. C., Dey, S. K., & Armant, D. R. (1999). Stage-specific excitation of cannabinoid receptor exhibits differential effects on mouse embryonic development. Biology of Reproduction, 60(4), 839–844.

Xia, M., Huang, R., Sun, Y., Semenza, G. L., Aldred, S. F., Witt, K. L., … Austin, C. P. (2009). Identification of chemical compounds that induce HIF-1alpha activity. Toxicological Sciences : An Official Journal of the Society of Toxicology, 112(1), 153–163. https://doi.org/10.1093/toxsci/kfp123

Yamamizu, K., Fujihara, M., Tachibana, M., Katayama, S., Takahashi, A., Hara, E., … Yamashita, J. K. (2012). Protein kinase A determines timing of early differentiation through epigenetic regulation with G9a. Cell Stem Cell, 10(6), 759–770. https://doi.org/10.1016/j.stem.2012.02.022

Yan, J., Tanaka, S., Oda, M., Makino, T., Ohgane, J., & Shiota, K. (2001). Retinoic acid promotes differentiation of trophoblast stem cells to a giant cell fate. Developmental Biology, 235(2), 422–432. https://doi.org/10.1006/dbio.2001.0300

Yin, X., Farin, H. F., Van Es, J. H., Clevers, H., Langer, R., & Karp, J. M. (2014). Niche-independent high-purity cultures of Lgr5 + intestinal stem cells and their progeny. Nature Methods, 11(1), 106–112. https://doi.org/10.1038/nmeth.2737

Yu, F. X., Mo, J. S., & Guan, K. L. (2012). Upstream regulators of the Hippo pathway. Cell Cycle, 11(22), 4097–4098. https://doi.org/10.4161/cc.22322

Yu, F. X., Zhao, B., Panupinthu, N., Jewell, J. L., Lian, I., Wang, L. H., … Guan, K. L. (2012).

Regulation of the Hippo-YAP pathway by G-protein-coupled receptor signaling. Cell, 150(4), 780–791. https://doi.org/10.1016/j.cell.2012.06.037

Zhou, X., Wang, S., Wang, Z., Feng, X., Liu, P., Lv, X. B., … Guan, K. L. (2015). Estrogen regulates Hippo signaling via GPER in breast cancer. Journal of Clinical Investigation, 125(5), 2123–2135. https://doi.org/10.1172/JCI79573

Zhu, S., Li, W., Zhou, H., Wei, W., Ambasudhan, R., Lin, T., … Ding, S. (2010, December). Reprogramming of Human Primary Somatic Cells by OCT4 and Chemical Compounds. Cell Stem Cell. https://doi.org/10.1016/j.stem.2010.11.015

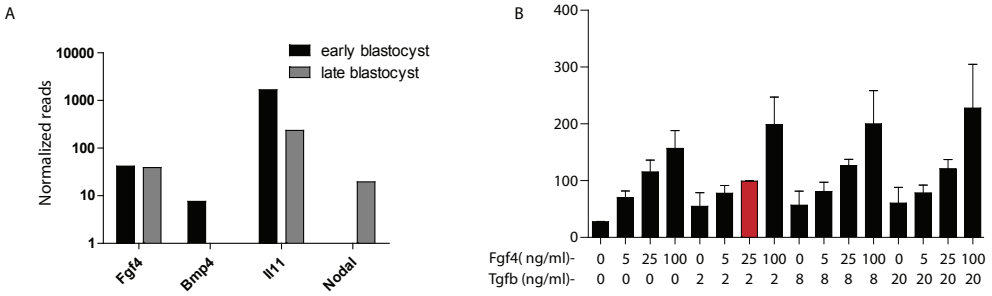

Supplementary Figure 1. A. Expression of the discovered CDX2 modulators in early and late blastocysts. B. CDX2 expression response of TSCs after exposed to different concentrations of FGF4 and TGFb.

3

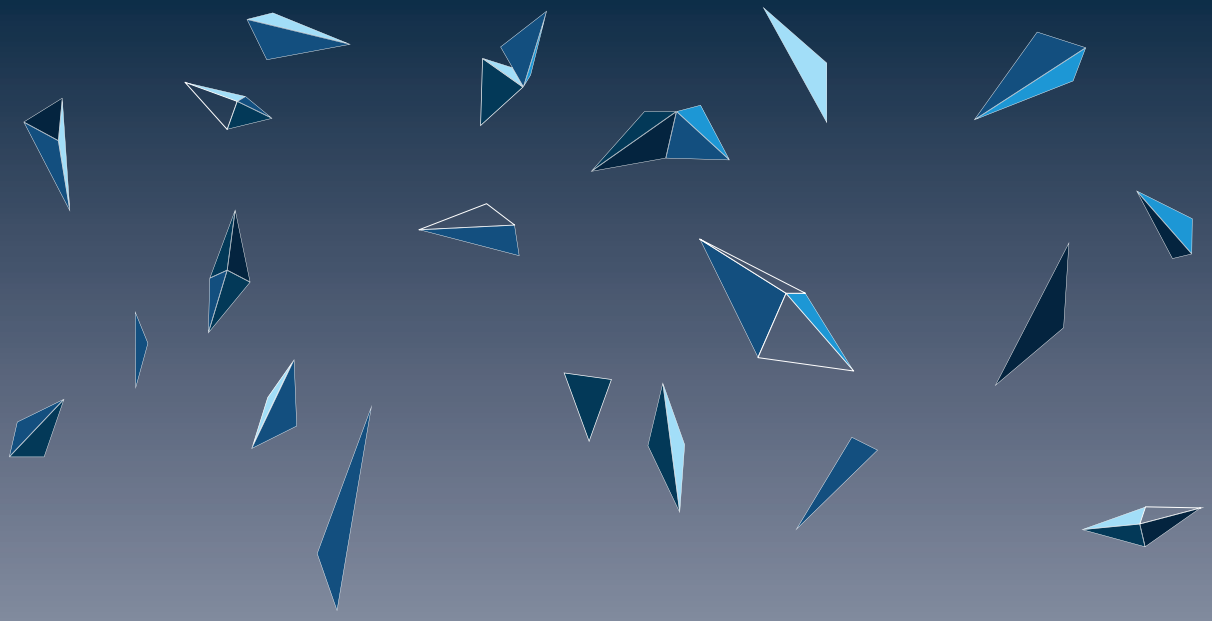

Chapter 4.
Blastoids recapitulate active cross-talk between embryonic and extra-embryonic compartments

4.1 Abstract

The blastocyst (the early mammalian embryo) forms all embryonic and extra-embryonic tissues, including the placenta. It consists of a spherical thin-walled layer, known as the trophectoderm, that surrounds a fluid-filled cavity sheltering the embryonic cells. From mouse blastocysts, it is possible to derive both trophoblast and embryonic stem-cell lines, which are in vitro analogues of the trophectoderm and embryonic compartments, respectively. Here we report that trophoblast and embryonic stem cells cooperate in vitro to form structures that morphologically and transcriptionally resemble embryonic day 3.5 blastocysts, termed blastoids. Like blastocysts, blastoids form from inductive signals that originate from the inner embryonic cells and drive the development of the outer trophectoderm. The nature and function of these signals have been largely unexplored. Genetically and physically uncoupling the embryonic and trophectoderm compartments, along with single-cell transcriptomics, reveals the extensive inventory of embryonic inductions. We specifically show that the embryonic cells maintain trophoblast proliferation and self-renewal, while fine-tuning trophoblast epithelial morphogenesis in part via a BMP4/Nodal–KLF6 axis. Although blastoids do not support the development of bona fide embryos, we demonstrate that embryonic inductions are crucial to form a trophectoderm state that robustly implants and triggers decidualization in utero. Thus, at this stage, the nascent embryo fuels trophectoderm development and implantation.

4.2 Introduction

The first lineage commitment taking place during embryonic development results in the formation of an embryonic and an extraembryonic lineage. The extraembryonic or trophoblastic lineage will develop into the placenta, organ responsible of mediating nutrient exchange between mother and fetus. Because of this, the trophoblastic lineage has been established as a nurturing structure. Nevertheless, in early stages, the trophoblastic lineage relies on the presence of factors produced by the embryonic compartment (Arman, Haffner-Krausz, Chen, Heath, & Lonai, 1998; Tanaka, 1998).

The Blastoid (Rivron et al., 2018), developed in our lab, is a model suitable for studying the pre-implantation mouse embryo. Blastoids are generated exclusively from embryonic stem cells (ESCs) and trophoblast stem cells (TSCs), the in vitro analogues of the inner cell mass (ICM) and the trophectoderm (TE) respectively. Blastoids are phenotypically and morphologically comparable to the E3.5 blastocyst, and are capable of recapitulating aspects of in utero implantation.

The features of blastoids make them an interesting tool for investigating the cross-communication between compartments. In this chapter we make use of gene editing and single cell sequencing on blastoid cells in order to study how both subpopulations interact with each other. In previous chapters, after demonstrating that TSC spontaneously differentiate in Tx cultures, we have shown how there are a number of pathway modulators capable of increasing CDX2 expression, which is one of the main transcription factors controlling the undifferentiated state of TSCs (Strumpf et al., 2005). In our publication (Rivron et al., 2018), we show how maintaining high CDX2 levels in trophoblast is critical for de novo TSCs derivation, and possibly to establish an appropriate cross-talk with ESCs, and forming blastoids.

In this chapter, we will investigate the cross-communication between ESC and TSC in a blastoid context. We will prove that a permanent crosstalk plays a pivotal role for the trophoblast

to perform the in vivo roles of the TE. These include proliferation, cyst expansion, stem cell pool maintenance and implantation.

4.3 Results

4.3.1 ESCs and TSCs cooperate for forming blastocyst-like structures

Blastocysts include a very low number of cells. In order to combine a small number of ESCs and TSCs, hydrogel microchips containing around 1100 microwells were used (Rivron et al., 2012). Each microwell has a diameter of 200 um and round bottom. These properties allow for enclosing a low and relatively reproducible number of cells and facilitate their aggregation. In order to simulate the blastocyst, ESCs must be surrounded by TSCs. This is achieved by sequential seeding. ESCs are first seeded and allowed to aggregate over-night. Then TSCs are dispensed and allowed for forming a structure showing a double layer (**Fig. 1A**) (protocol summary on **Sup. Fig. 1A**). The Rock inhibitor is added at the time of TSCs seeding with the purpose of increasing the engulfment efficiency of TSCs.
Chir99031 (a GSK3 inhibitor, Wnt activator) and 8Br-cAMP (stable and permeable analogue of cAMP) are also included in the blastoid media, delivered at the time of TSCs seeding. These two factors potentiate the cavitation mediated by TSCs (**Fig. 1B**).
The number of cells enclosed by each microwell is one of the main factors affecting blastoid efficiency. The initial number of ESCs and TSCs was optimized for an overall average of 5 and 12 cells per microwell respectively (Rivron et al., 2018). However, when the number of cells per microwell was quantified, the highest blastoid formation efficiency (70%) was observed when 8 ESCs and 21 TSCs were combined (**Fig. 1C**).
During a period of 65h the size of the cavity continues to increase, reaching a fully cavitated structure with TSCs forming a cyst around the ESC aggregate (**Fig. 1D**), making blastoid morphologically comparable to E3.5 blastocysts (**Fig. 1F**). The average diameter of the 24h and 65h blastoids is 76 and 90 micrometer respectively, making the 65h bastoids similar in size to the E3.5 blastocyst.
Importantly, blastoids are permissive for the second lineage commitment to occur within the blastoid's ESCs, as demonstrated by the appearance of cells expressing the primitive endoderm lineage specific marker PDGFRa (**Sup. Fig. 1B**). Upon implantation in the uterus of pseudopregnant females, blastoids trigger a decidualization response in the endometrium, leading to a reaction comparable to the one caused by blastocysts (**Sup. Fig. 1C**). The detection of Aldh3a1 in the mesometrial side of the decidua confirms that blastoids induce some specific aspects of decidualization compared to beads (McConaha, Eckstrum, An, Steinle, & Bany, 2011) (**Sup. Fig. 1D**).
Once the protocol for blastoid formation was developed and its potential to implant was validated we could use it to investigate the interaction between embryonic and extraembryonic compartments.

4.3.2 Internal blastoid communication reverts TSCs and ESCs to a more blastocyst-like state

With the purpose of studying how ESCs and TSCs behave under blastoid conditions we made use of transcriptome analysis. Initially we performed bulk sequencing on 65h blastoids, E3.25 blastocysts, E3.5 blastocysts, ESCs and TSCs. Since blastoids and blastocysts include cells

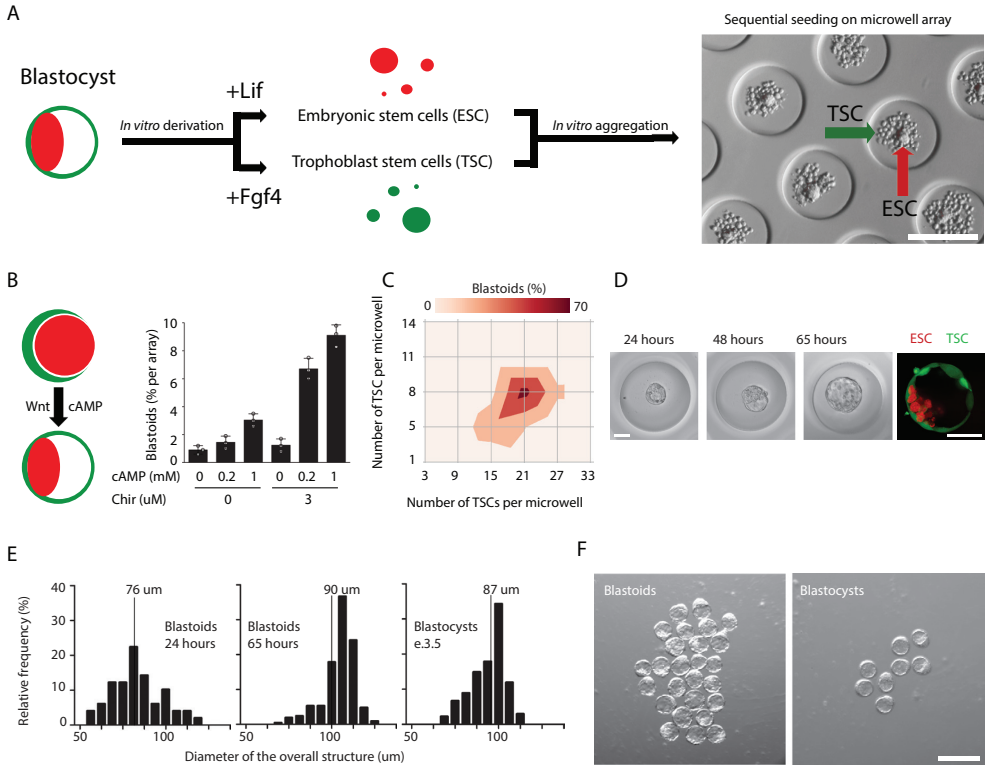

Figure 1. Fig. 1 Embryonic and trophoblast stem cells form blastocyst-like structures in vitro. A. Schematic of blastoid formation. ESCs and TSCs are derived from blastocysts (left), then sequentially combined using a microwell array (right)7. ESCs are seeded to form non-adherent aggregates within 24 h (right, red arrow denotes a 24-h aggregate). TSCs are then added (right, green arrow denotes TSCs upon seeding). Scale bar, 200 μm. B. Aggregates of ESCs engulfed by TSCs were exposed to a WNT activator (3 μM CHIR99021; CHIR) and a cAMP analogue (0.2 or 1 mM 8Br-cAMP; cAMP). Yields of blastoids are shown (measured as the percentage of microwells containing a TSC cyst enclosing an ESC aggregate, 65 h after TSCs addition). 8Br-cAMP plus CHIR99021 generated significantly higher yields of 9% blastoids (P = 0.006, two-sided Student's t-test). n = 3 independent microwell arrays. Error bars are s.d. C. Blastoid yield as a function of the initial number of TSCs and ESCs in individual microwells. 70% of microwells seeded with an optimal number of ESCs and TSCs contain a blastoid. D. Left, evolution of blastoid morphology from 24 to 65 h. Right, blastoids formed with ESCs positive for red fluorescent protein (RFP)-tagged histone H2B (H2B-RFP+ ES cells; red) and TSCs positive for green fluorescent protein (GFP) (GFP+ TS cells; green). Scale bars, 50 μm. E Distribution of the overall diameters of blastoids, at 24 and 65 h, and of blastocysts collected on day E3.5. Bar plots indicate the percentage frequency of specific diameters. n = 50 independent blastoids or blastocysts. Vertical line denotes the median. F. Light microscopy image showing blastoids and E3.5 blastocysts

from both embryonic and extraembryonic lineages, a virtual sample was crafted in silico by combining the transcriptome of ESCs and TSCs in the appropriate ratio based on the amount of cells included in a blastoid (1:3.5). Unsupervised clustering analysis resulted in blastoids to cluster together with E.35 blastocyst and not the E3.25 blastocyst (**Fig. 2A**). Interestingly, virtual blastoids, ESCs and TSCs clustered together independently of blastoids, suggesting that when ESCs and TSCs are combined in vitro in a blastoid context and not in silico, they

undergo through transcriptional changes making the cells more comparable to the in vivo analogues. Gene ontology analysis performed on differentially expressed genes showed enrichment for the MapK, chemokine, p53 and Tgfβ signaling pathways (**Fig. 2B**).
Single cell sequencing was then performed in order to study each compartment separately. Single cells from blastoids were compared to single cells from monolayer cultures (ESCs and TSCs) and to single cells from trophospheres and embryoid bodies (ESCs and TSCs cultured independently in 3D blastoid conditions). Being able to compare the transcriptome of single cells from all those conditions served as a tool to uncouple the effect of the blastoid media from the effect of the ESCs and TSCs cross-communication (**Fig. 2C**). ESCs showed relatively similar expression of pluripotency markers Pou5f1 and Sox2 in all three conditions, but Esrrb showed an upregulation when the ESCs were isolated from blastoids (**Fig. 2D**). Esrrb marks for a more potent state both in the embryonic and the extraembryonic lineage, and together with the markers Elf5 and Eomes demonstrated that trophoblasts from trophospheres differentiate. Trophoblast differentiation markers Basp1, Tead3 and Gata2, supported that hypothesis as they showed upregulation in trophoblasts from trophospheres. Unsupervised clustering analysis showed trophospheres to cluster separately from TSC from 2D cultures and blastoids (**Fig. 2E**).
We wanted to further investigate the differentiated profile of trophospheres and test them functionally for stem cell related properties. When trophoblasts are grown as trophospheres, they show a significantly lower proliferation than when they are combined with ESCs for blastoid formation (**Fig. 2G**). In order to test the self-renewal potential of trophoblasts from trophospheres and blastoids, they were respectively plated on mouse embryonic fibroblasts for re-derivation of TSC lines. After trypsinization of the initial outgrowth, cells were re-plated and allowed to grow. The number of colonies after the first passage was then quantified. Trophospheres lead to a dramatically lower number of colonies than blastoids (**Fig. 2H**) suggesting either a limited self-renewal or an impaired proliferation even after reversion to a 2D culture. As for in vivo potential, trophospheres were tested for in utero implantation on pseudopregnant females. Trophospheres triggered a diminished response in the uterus, indicating a lack of communication with the endometrium (**Fig. 2I**).
These results show that the cross-talk taking place within the blastoid changes ESCs and TSCs to a state more similar to the one ICM and TE display in the blastocyst. Blastoid media infers a transcriptional shift on both cell types. However, in the case of TSC, blastoid culture conditions in the absence of ESCs result in differentiation, dramatically affecting trophoblast proliferation, self-renewal and potential to communicate with receptive endometrium. These results confirm the role of ESCs as a source of factors beneficial for the undifferentiated TSC state.
Gene ontology analysis on differentially regulated genes between blastoid and virtual blastoids, suggested Tgfβ as one of the main pathways affected (**Fig. 2C**). Using single molecule FISH we found the Tgfβ pathway ligands Bmp4 and Nodal to be expressed in the blastocysts and restricted to the ICM of blastocysts (**Fig. 2J**), making them candidates for the active ESC to TSC cross-communication.

4.3.3 Trophoblast epithelial integrity relies on embryonic Tgfβ signals.

In order to validate the role of BMP4 and Nodal as pivotal players on the embryonic to extraembryonic cross-talk, two strategies were followed. First, a gain of function experiment was performed to elucidate whether recombinant BMP4 and NODAL were able to improve

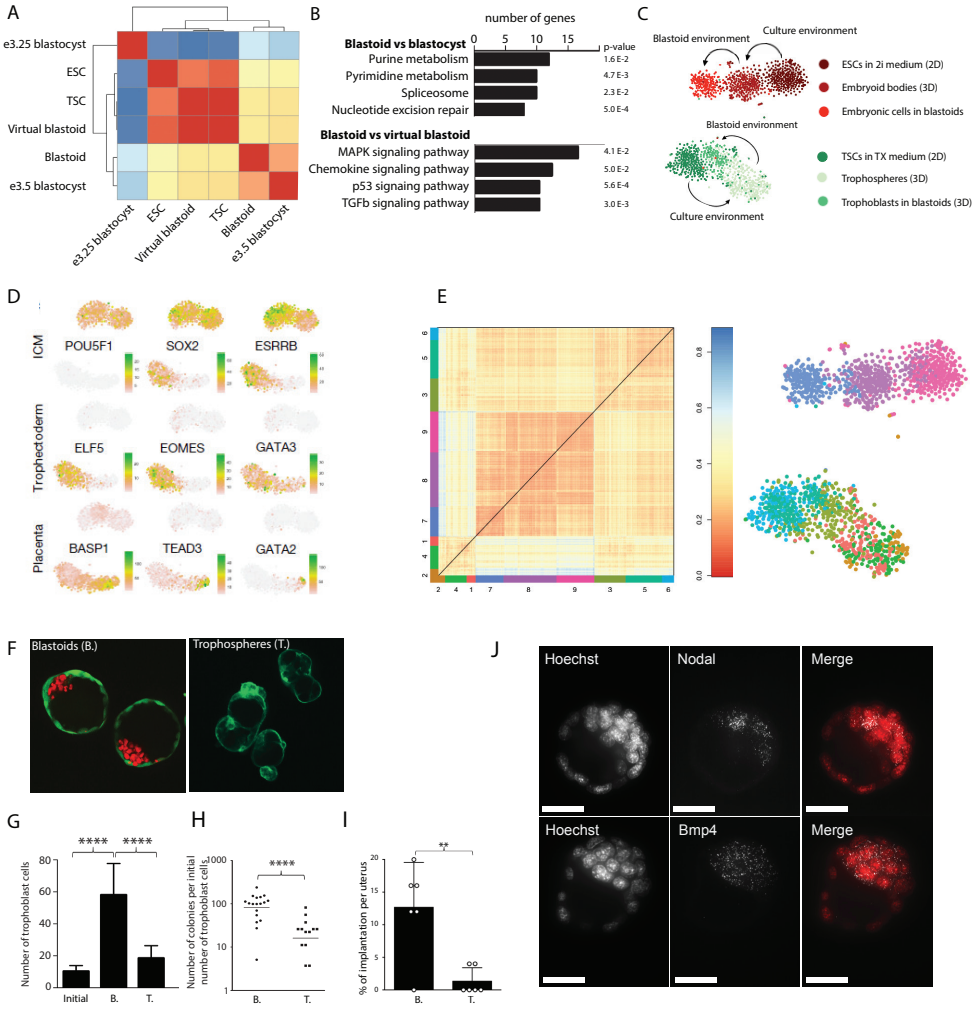

Figure 2. Communication between blastoid embryonic and trophoblast compartments shifts the transcriptome towards an E3.5 blastocyst state. A. Bulk sequencing. Whole-transcriptome distance map. The total number of either blastocysts or blastoids is 50. B. Gene ontology (GO) and KEGG pathways. Genes differentially regulated ($P < 0.05$) were analyzed using DAVID38 and corresponding GO and KEGG pathways are presented. C. t-SNE map representation of transcriptome similarities between 1,577 cells collected from 2D-cultured parental ESCs in 2i medium (316 cells) and parental TSCs in TX medium (290 cells), blastoid cells (367 cells), Trophosphere cells (336 cells) and embryoid body cells (268). Arrows indicate transcriptome shifts due either to the culture environment or to the blastoid environment. D. t-SNE map representation of key transcription factors for the ICM, trophectoderm and placenta. E. Clusters obtained from unsupervised clustering analysis and its corresponding t-SNE map. F. Microscope images of blastoids and trophospheres. G. Number of trophoblasts at the time of TSCs seeding and at the end of blastoid and trophosphere formation protocol. H. Number of TSC colonies after re-derivation of TSCs lines from blastoids and trophospheres. I. Percentage of implantation sites detected after in utero implantation. J. Detection of Bmp4 and Nodal transcripts after smFISH on e3.5 blastocysts.

the integrity of trophospheres. Secondly, knockout ESC and TSC lines were obtained to only deplete the effect of that signaling in a blastoid context.
Trophospheres differ morphologically from blastoids, reaching a smaller size. We took diameter as one of the readouts to evaluate the effect of independent embryonic signals. Trophospheres were exposed to different concentrations of recombinant BMP4 and NODAL independently or combined. The diameter of the cavitated structures was compared to blastoids, blastoids treated with PD0325901 and control trophospheres. Both proteins managed to partially rescue to lower cavity size in the absence of ESCs (**Fig. 3A**). While BMP4 had a linear dose response, NODAL only induced a low response a lower doses. In contrast, when both BMP4 and NODAL were combined, the cavity size increased to up to 80% of the average blastoid cavity size. Interestingly, when we counted the number of trophoblasts included in treated trophospheres, we confirmed that these had not changed in comparison to the untreated ones (**Fig. 3B**). NODAL and BMP4 then affect the swelling of trophospheres and not their proliferation.
We then made Nodal Knockout ESC lines (**Sup. Fig. 2A**). In order to obtained these cell lines, ESCs were transfected with a plasmid including the Cas9 coding sequence and a gRNA. Cultures were co-transfected with two plasmids containing two different gRNAs. They were designed so one gRNA would recognize a region before the start codon of Nodal and another one would target after the start codon. Alternative start codons were also considered to prevent the transcription of a truncated form. We obtained one heterozygous knockout line and one homozygous line, which were then tested for blastoid formation.
Both homozygous and heterozygous lines were significantly less efficient when making blastoids (**Fig. 3C**), leading to structures smaller in size (**Fig. 3D**). This confirms the role of Nodal as an embryonic signal affecting the performance of the trophoblast in a blastoid context. However, we were interested in knowing how Nodal signaling translated into an increased swelling potential in blastoid trophoblasts.
Trophoblasts coming from trophospheres were compared with those coming from BMP4 and NODAL treated trophospheres using single cell sequencing. Klf6 expression was higher not only in blastoids, but also in treated trophospheres when they were compared to untreated trophospheres (**Sup. Fig. 2B**). Klf6, is related to placenta development (Matsumoto et al., 2006) as proven by Klf6 knockout mice to be embryonic lethal manifesting impaired placental development.
In order to validate Klf6 as a mediator of Nodal signaling, we repeated the strategy followed with Nodal. We obtained knockout lines, this time targeting the F4 TSCs. Two different homozygous lines were obtained. The monolayer cultures of the Klf6 -/- lines show a normal phenotype with the cells expressing Cdx2 (**Sup. Fig. 2C**). However, when making blastoids, both Klf6 -/- clones led to a lower blastoid yield (**Fig. 3E-F**). Even though the capacity of Klf6 KO TSC lines to make trophospheres was reduced, they also failed to increase their diameter when exposed to BMP4 and NODAL, confirming Klf6 to be a mediator of the BMP4 and NODAL response (**Fig. 3G-H** and **Sup. Fig. 2D**). Klf6 has been previously reported to have a role in epitheliums (DiFeo et al., 2006), having an impact on e-cadherin expression levels. While the Klf6 -/- clones showed normal e-cadherin expression in 2D cultures (**Sup. Fig. 2C**), this was greatly diminished upon blastoid formation (**Fig. 3I**). E-cadherin plays a very important role in the formation of the TE and its ability to cavitate (Kan et al., 2007), meaning that lower levels of e-cadherin imply a diminished epithelial integrity.
Discovering the Nodal- Klf6 axis confirms the cross-comunication across compartments within the blastoid.

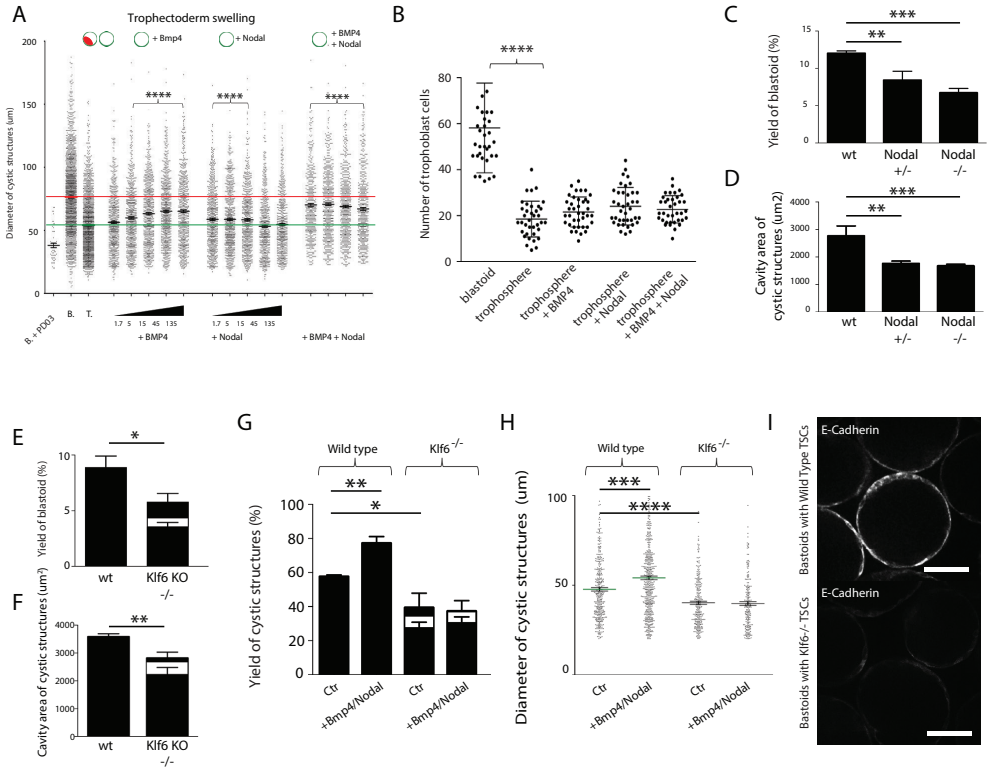

Figure 3. Embryonic inductions regulate trophectoderm proliferation, self-renewal, epithelial morphogenesis and implantation, partially via BMP4 and Nodal. Overall diameter of blastoids, trophospheres and trophospheres exposed to BMP4, Nodal or their combination. Horizontal bars indicate mean of n = 250 independent structures. Error bars denote s.e.m. Combinations of BMP4 and Nodal are (in order): 5 ng/ml BMP4+ 5 ng/ml Nodal; 45 ng/ml BMP+45 ng/ml Nodal; 45 ng/ml BMP4+5 ng/ml Nodal; 45 ng/ml BMP4 + 45 ng/ml Nodal. B. Number of trophoblasts within blastoids, trophospheres and trophospheres stimulated with activators of the TGFβ signaling pathway. n = 30 independent blastoids or trophospheres. P = 0.0001, one-way ANOVA. C-D. Yield (top) and cavity area (bottom) of blastoids formed with wild-type (WT), Nodal+/– and Nodal–/– ES cells. ***P = 2.10–4, two-sided Student's t-test. n = 3 independent microwell arrays. Error bars indicate s.d. E-F. Yield of blastoids formed with wild-type and Klf6–/– TSCs (two clones). Horizontal bars indicate mean yield. *P = 0.01, two-sided Student's t-test. n = 3 independent microwell arrays. C. Cavity area of blastoids formed with wild-type and Klf6–/– TSCs (two clones). Horizontal bars denote the mean cavity area. **P = 0.005, two-sided Student's t-test. n = 3 independent microwell arrays. G. two-sided Student's t-test. n = 3 independent microwell arrays. d, Yield of trophospheres formed with wild-type and Klf6–/– TSCs, and after stimulation with 45 ng/ml BMP4 and 5 ng/ml Nodal. Horizontal bars indicate mean yield. *P = 0.02, **P = 0.001, two-sided Student's t-test. n = 3 independent microwell arrays. H. Diameters of trophospheres formed with wild-type and Klf6–/– TSCs , and after stimulation with 45 ng/ ml BMP4 and 5 ng/ml Nodal. Horizontal bars indicate mean diameter. ***P = 0.001, ****P = 0.0001, two-sided Student's t-test. n = 80. Error bars are s.e.m. I. Immunostaining for E-cadherin (DECMA antibody) in blastoids formed with wild-type and Klf6–/– TSCs. Images are representative of three independent experiments. Scale bars, 50 μm.

4.4 Discussion

The blastoid protocol combines ESCs and TSCs for forming structures that phenotypically and morphologically resemble the E3.5 blastocyst. Blastoids are capable of resembling certain aspects of the pre-implantation embryo. These include cavitation, trophectoderm maturation, second lineage commitment and implantation. The fact that blastoids are capable of reproducing these poorly understood but critical mechanism make the blastoid a suitable model for studying pre-implantation embryonic development. This model has several advantages. Blastoids are produced in large number thanks to the microwell arrays. This allows not only to obtain a large number of structures to use on functional studies, but also makes it possible to detect sub-lethal phenotypes. Because of that, this is a convenient model for screenings. Another benefit of the blastoid is that its formed by combining two cell types that can be cultured independently. This allows us to genetically edit the parental lines independently. Performing lineage specific genetic studies in mice often requires a large time investment and the use of complex recombination mediated systems. The blastoid makes it possible to control a large number of parameters, including the initial number of cells involved. This might help us understand what sort of factors serve as internal control for the embryo to regulate cell numbers, which ultimately translates into size control, a mechanism poorly understood in developmental biology.

Our first discoveries using the blastoid involve a phenotypical switch reverting the in vitro paternal lines to a more in vivo-like phenotype. Importantly, we only observe this phenomenon when both ESCs and TSCs are allowed to interact, proposing the presence of a set of factors (physical, chemical or biological) that allow both cell types to communicate. With this premise and by exploiting some of the advantages of the blastoid, we were able to pintpoint a Nodal-Klf6 dependent axis that regulates the epithelial integrity of trophoblasts as a response to ESCs presence.

In previous chapters, we demonstrated how TSCs cultured in Tx conditions spontaneously differentiate and we showed how this is a result of the Tx culture conditions. By finding a number of CDX2 modulators we were able to develop new culture conditions capable of maintaining the TSCs in a state with high CDX2 expression. We have previously demonstrated that CDX2 levels (Rivron et al., 2018) determine the compatibility between ESCs and TSCs when forming blastoids. Two of the modulators we found to increase CDX2 expression upon development of the blastoid protocol (Il11 and cAMP) were also included in the CDX2 expression screen and ultimately included in the LT21 media. Bmp4, Nodal and Il11 are expressed in the blastocyst, modulate Cdx2 expression in trophoblast and promote an undifferentiated state on trophoblasts.

Keeping in mind that in the blastoid, the communication between both populations is critical for the trophoblast to accomplish their role as implantation mediator, we hypothesize that a pre-culture where the TSCs are exposed to those embryonic signals will make them more comparable to the trophectoderm. In addition, TSCs already exposed to embryonic signals before being seeded in microwells, might be able to more efficiently interact with ESCs. If this is the case, we would expect the blastoid efficiency to increase even when a suboptimal number of cells are pooled within a microwell.

4.5 Materials and Methods

• Cell culture.
TSC are cultured under Tx conditions followed a previously published protocol (Kubaczka et al., 2014). After coating with matrigel, cells are cultured in Tx media, which consists of phenol red free DMEM/F12 supplemented (phenol red-free, with l-glutamin), insulin (19.4 µg/ml), l-ascorbic-acid-2-phosphate (64 µg/ml), sodium selenite (14 ng/ ml), insulin (19.4 µg/ml), sodium bicarbonate (543 µg/ml), holo-transferin (10.7 µg/ml), penicillin streptomycin, FGF4 (25 ng/ml), TGFβ1 (2 ng/ml) and heparin (1 µg/ml). ESC were cultured in B27N2 2i conditions (Ying et al., 2008). After 0.1% gelatin coating cells were cultured in a 1:1 mixture of Neurobasal and DMEM F12 with B27 and N2 supplements, BSA (5mg/ml), non-essential aminoacids, β-mercapto-ethanol and Penn/Strep.

• Blastoid formation.
Full protocol can be found in https://www.nature.com/protocolexchange-/protocols/6579) Agarose microwell arrays were casted using the PDMS stamp and incubated O/N on mES serum containing media. After washing the chips with PBS, a ESC solution of 8000 cells/150 µl is dispensed in the central chip are and allowed to settle. After 15 minutes, an additional 1ml is dispensed. 20 hours later 1 ml of media is removed and a TSC solution of 22000 cells/150 ul is dispensed. After allowing the cells to fall in the microwells, 1 ml of blastoid media is added to the wells. Blastoid media includes 20 µM Y27632 (AxonMed 1683), 3 uM CHIR99021 (AxonMed 1386), 1 mM 8Br-cAMP (Biolog Life Science Institute B007E), 25 ng/ml Fgf4 (R&D systems 5846F4), 15 ng/ml Tgfb1 (Peprotech 100-21), 30 ng/ml Il11 (Peprotech 200-11) and 1 µg/ml heparin (Sigma-Aldricht cat# H3149). An additional dose of cAMP is dispensed 24 hours after TSC seeding. All measurements are performed 65 hours after TSC seeding.

• Knockout line generation.
A plasmid including the Cas9 coding sequence and a gRNA transcription site was used to target ESCs and TSCs. The plasmid included a puromycin resistance expression cassette that allowed us to select for transfected cells. 24 hours after plating, cells were transfected using a combination of 2 plasmids including gRNAs targeting sequences flanking the start codon of the gene to target. 24 hours after transfection, media was change to fresh media with Puromycin. This process was repeated the next day, applying selection for a total of 48 hours. Resistant cells were allowed to grow. TSCs were replated in MEF coated plates to favor their proliferation and attachment. When ESCs and TSCs colonies were large (>40 cells) they were picked under the microscope and replated in 96 well plates (MEF coated for TSCs).
Resistant clones were in later passages palted in duplicates, using one of the replicated for gDNA extraction and further screening for genomic delections by PCR amplification of the region of interest. Primers were designed to flank the gRNA docking sites. Selected TSC lines were then expanded in the absence of MEF.

• smFISH.
E3.5 blastocysts were isolated from pregnant females. After fixation, blastocysts followed the Quantigene ViewRNA kit instructions: After three washes with RNAse free PBS, sampels were incubated for 10 minutes in a detergent solution. After three washes with RNAse free PBS, samples were incubated for 5 minutes at RT with Q protease. After three washes with RNAse free PBS, samples were incubated at 40C for 3 hours (in a humidified chamber) with

the probes of interest diluted in Probe set diluent. After 3 washes with wash buffer, samples were incubated at 40C for 30 minutes with preamplifier diluted in amplifier diluent. After 3 washes with wash buffer, samples were incubated at 40C for 30 minutes with amplifier diluted in amplifier diluent. After 3 washes with wash buffer, samples were incubated at 40C for 30 minutes with label diluted in label probe diluent. After 2 washes with wash buffer, they were washed once more for 10 minutes. Samples were then incubated for 15 minutes in RNAse free PBS with Hoechst and WGA as counterstains followed by 3 washes with RNAse free PBS. Blastocysts were carefully placed in mounting media in glass bottom 3.5 mm plates. All samples were imaged with a 63x oil immersion objective in a PerkinElmer Ultraview VoX spinning disk microscope.

Author Contribution

Javier Frias Aldeguer performed the experiments in Figure 2J, Sup Figure 2A-C, generated the KO cell lines used in Figure 3C-F, and wrote the chapter. **Erik Jacob Vrij** developed part of the high-content imaging assays. **Jeroen Korving** performed the blastocyst complementation assays and the in uteri transfers. **Judith Vivié** helped to prepare the libraries of single cells for RNA sequencing. **Jean-Charles Boisset** contributed to the RNA-sequencing assays. **Roman Truckenmuller** contributed to the design of the microwell array. **Clemens van Blitterswijk**, **Niels Geijsen** and **Alexander van Oudenaarden** helped to direct the project. **Nicolas Clement Rivron** conceived and directed the research, developed the blastoid protocol, designed and performed the experiments in Figure 1, Figure 2A-I, Figure 3, Supplementary Figure 1, and Supplementary Figure 2D, and wrote the Nature publication.

Bibliography

Arman, E., Haffner-Krausz, R., Chen, Y., Heath, J. K., & Lonai, P. (n.d.). Targeted disruption of fibroblast growth factor (FGF) receptor 2 suggests a role for FGF signaling in pregastrulation mammalian development. Proceedings of the National Academy of Sciences of the United States of America, 95(9), 5082–5087. Retrieved from http://www.ncbi.nlm.nih.gov/sites/entrez?Db=pubmed&DbFrom=pubmed&Cmd=Link&LinkName=pubmed_pubmed&LinkReadableName=Related Articles&IdsFromResult=9560232&ordinalpos=3&itool=EntrezSystem2.PEntrez.Pubmed.Pubmed_ResultsPanel.Pubmed_RVDocSum

DiFeo, A., Narla, G., Camacho-Vanegas, O., Nishio, H., Rose, S. L., Buller, R. E., … Martignetti, J. A. (n.d.). E-cadherin is a novel transcriptional target of the KLF6 tumor suppressor. Oncogene, 25(44), 6026–6031. Retrieved from http://www.ncbi.nlm.nih.gov/sites/entrez?Db=pubmed&DbFrom=pubmed&Cmd=Link&LinkName=pubmed_pubmed&LinkReadableName=Related Articles&IdsFromResult=16702959&ordinalpos=3&itool=EntrezSystem2.PEntrez.Pubmed.Pubmed_ResultsPanel.Pubmed_RVDocSum

Kan, N. G., Stemmler, M. P., Junghans, D., Kanzler, B., de Vries, W. N., Dominis, M., & Kemler, R. (2007). Gene replacement reveals a specific role for E-cadherin in the formation of a functional trophectoderm. Development (Cambridge, England), 134(1), 31–41. https://doi.org/10.1242/dev.02722

Kubaczka, C., Senner, C., Ara??zo-Bravo, M. J., Sharma, N., Kuckenberg, P., Becker, A., … Schorle, H. (2014). Derivation and maintenance of murine trophoblast stem cells under defined conditions. Stem

Cell Reports, 2(2), 232–242. https://doi.org/10.1016/j.stemcr.2013.12.013

Matsumoto, N., Kubo, A., Liu, H., Akita, K., Laub, F., Ramirez, F., … Friedman, S. L. (n.d.). Developmental regulation of yolk sac hematopoiesis by Kruppel-like factor 6. Blood, 107(4), 1357–1365. Retrieved from http://www.ncbi.nlm.nih.gov/sites/entrez?Db=pubmed&DbFrom=pubmed&Cmd=Link&LinkName=pubmed_pubmed&LinkReadableName=Related Articles&IdsFromResult=16234353&ordinalpos=3&itool=EntrezSystem2.PEntrez.Pubmed.Pubmed_ResultsPanel.Pubmed_RVDocSum

McConaha, M. E., Eckstrum, K., An, J., Steinle, J. J., & Bany, B. M. (2011). Microarray assessment of the influence of the conceptus on gene expression in the mouse uterus during decidualization. Reproduction, 141(4), 511–527. https://doi.org/10.1530/REP-10-0358

Rivron, N. C., Frias-aldeguer, J., Vrij, E. J., Boisset, J., Korving, J., Vivié, J., … Geijsen, N. (2018). Blastocyst-like structures generated solely from stem cells.

Rivron, N. C., Vrij, E. J., Rouwkema, J., Le Gac, S., van den Berg, A., Truckenmuller, R. K., & van Blitterswijk, C. A. (2012). Tissue deformation spatially modulates VEGF signaling and angiogenesis. Proceedings of the National Academy of Sciences. https://doi.org/10.1073/pnas.1201626109

Strumpf, D., Mao, C., Yamanaka, Y., Ralston, A., Chawengsaksophak, K., Beck, F., & Rossant, J. (2005). Cdx2 is required for correct cell fate specification and differentiation of trophectoderm in the mouse blastocyst, 2093–2102. https://doi.org/10.1242/dev.01801

Tanaka, S. (1998). Promotion of Trophoblast Stem Cell Proliferation by FGF4. Science, 282(5396), 2072–2075. https://doi.org/10.1126/science.282.5396.2072

Ying, Q.-L., Wray, J., Nichols, J., Batlle-Morera, L., Doble, B., Woodgett, J., … Smith, A. (2008). The ground state of embryonic stem cell self-renewal. Nature, 453(7194), 519–523. https://doi.org/10.1038/nature06968

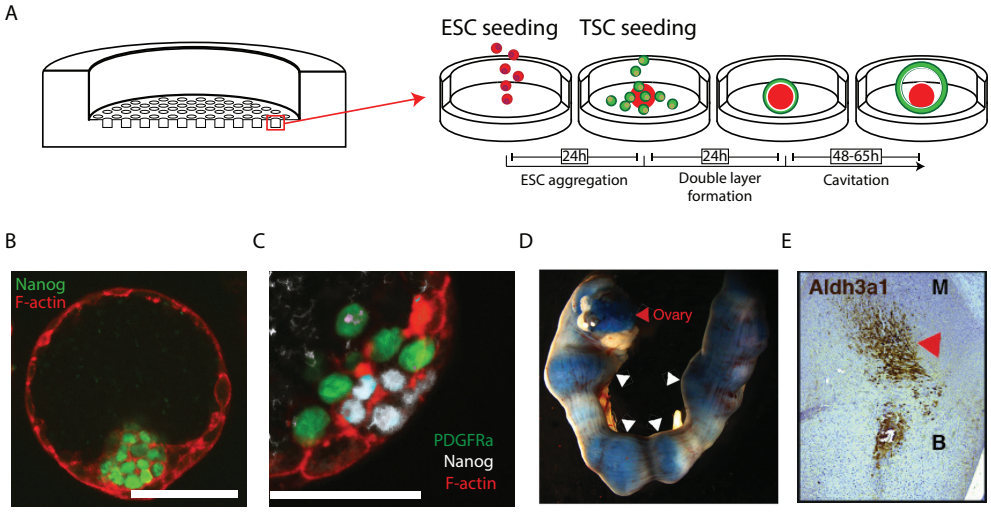

Supplementary Figure 1. A. Summary of Blastoid formation protocol. B. Immunofluorescent staining for NANOG in blastoids counterstained for F-actin. C. Immunofluorescent staining for NANOG and PDGFRa in blastoids counterstained for F-actin. D. Uterus transferred with blastoids at E3.3–E3.5 and explanted at E7.5. Mice are injected systemically with Evan blue dye, revealing typical local vascular permeability of the implantation sites (deciduae: white arrowheads; ovary: red arrowhead). E. Anti-ALDH3A1 staining of a representative decidua induced by a blastoid. B, blastoid implantation site; M, mesometrial side. Red arrowhead denotes the decidua sub-population expressing ALDH3A1.

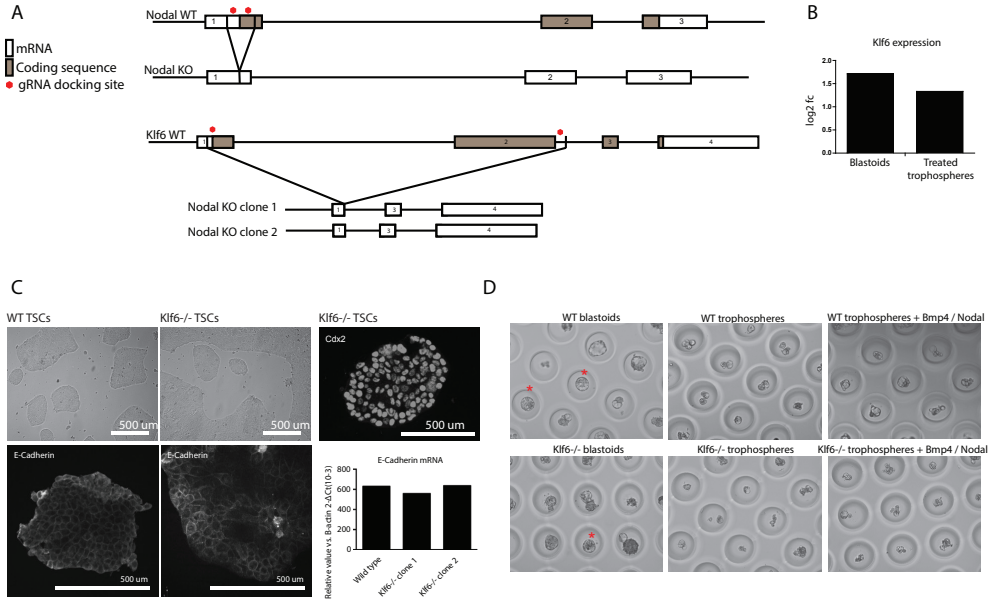

Supplementary Figure 2. A. CRISPR strategy for the generation of Nodal knockout ESCs and Klf6 knockout TSCs. B. Fold change of Klf6 expression in single cells coming from blastoids and Nodal/ Bmp4 treated trophospheres in comparison to untreated trophospheres. C. Bright-field image of wt and Klf6−/− TSCs (top left). Immunostaining for CDX2 in Klf6−/− TS cells (top right). E-cadherin immunostaining (bottom left) and quantitative PCR with reverse transcription (qRT–qPCR) (bottom right) of wild-type and Klf6−/− TSCs. F. Representative pictures of blastoids and trophospheres, and trophospheres stimulated with 45 ng/ ml BMP4 and 5 ng/ml Nodal. Red asterisks denote blastoids, which comply to our definition of cavitated trophoblast structures comprising ESCs, with a circularity greater than 0.9 (circularity = 4π(area/perimeter2)), and a diameter between 70 and 110 μm (see Methods). Comparable results were obtained in three repeated experiments.

4

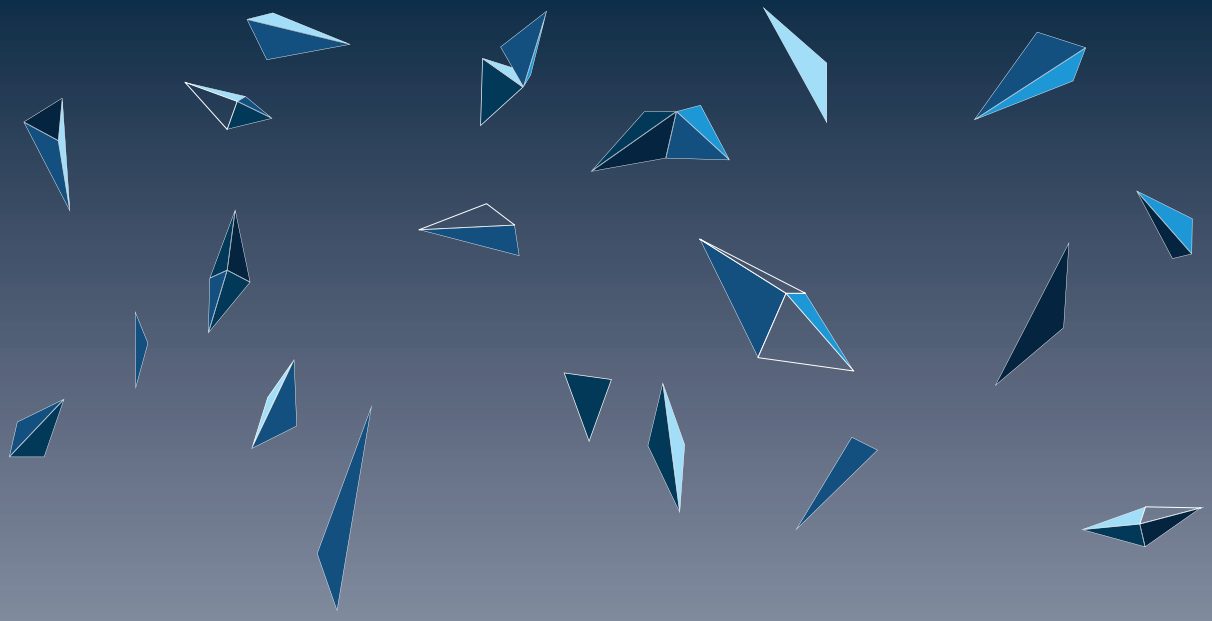

Chapter 5.
TSCs cultured in LT21 conditions resemble a polar-like phenotype

5

5.1 Abstract

Stem Cells (SCs) have been on the main scope of researchers for decades not only due to their potential for therapy but also due to their value as in vitro model. Some of the characteristics of stem cells include self-renewal, proliferation and differentiation potential, and these properties can often be challenged in vitro with a number of classical assays. The study of the trophoblastic lineage relies mainly on the use of trophoblast stem cells (TSCs) as the principal in vitro model. However, as we concluded in prior chapter, such culture is heterogeneous, reflects aspects of the polar and mural trophectoderm (TE) and contains some more differentiated cells. By using our knowledge on embryonic inductions and adequately altering the TSCs culture conditions (LT21), we have been able to increase the overall expression of CDX2, a transcription factor highly expressed in polar TE cells and in the sub-population of TSCs showing enhanced stem cell properties (proliferation, self-renewal, gene expression). In this chapter, we will challenge the TSCs cultured in LT21 conditions for classical assays and for their performance during blastoid formation, a new model that allows us to test the potential of TSCs to communicate with embryonic stem cells (ESCs). Our results indicate that LT21 conditions lead to a phenotypical state that more closely resemble the cells in the proliferating TE. We have thus termed this state polar-like TSCs (plTSCs).

5.2 Introduction

In prior chapters we were able to find a correlation between Cdx2 expression and potency in TSCs. Using CDX2 expression as readout, we managed to develop new culture conditions that allows for consistently high CDX2 levels. Even though transcriptome analysis confirms the undifferentiated trophoblastic identity of the cells obtained in such culture, it is necessary to functionally challenge their potential as stem cells.

There are a number of experimental assays that allow to test the stem cell potential of a given stem cell in vitro culture. Those assays are generally based on the properties of stem cells such as their self-renewal, their unspecialized phenotype and their potential to give rise to specialized cell types. Colony formation assays, cell cycle analysis and tracking gene expression during differentiation are some of the assays most commonly used in vitro for testing the potency of cells, while chimera formation is the assay that will ultimately confirm the potential in vivo. We can now add the blastoid as a new assay for challenging the cross-communication between ESCs and TSCs.

Different TSC lines have different potentials when making blastoids, with the most efficient line allowing us to reach 10% yield. This means that 10% of the microwells include a structure that we define as blastoid. A blastoid is defined based on the morphological parameters of E3.5 blastocysts, as a cystic structure with an outer circularity superior to 0.9 (circularity = $4\pi(\text{area}/\text{perimeter}2)$), and a diameter comprised between 70 and 110 μm, including a single regular cavity lined by a single layer of TS cells and including ES cells. The yields we obtain are partly due to the difficulty to pool precisely the optimal number of ESCs (about 8) and TSCs (about 21) together in the same microwell. Indeed, when looking at the microwells that contain the right number of ESCs and TSCs, the yield is 70% (Rivron et al., 2018). The self-organization process is thus efficient. However, beyond the technical issue of cell seeding, we observe that many structures form that do not fall under the definition of a blastoid, due to the presence of few TSCs forming small clusters on the outer part of the trophoblast cyst. We

suspect that these clusters are TSCs that do not have the capacity to epithelize. These might be more differentiated cells present in the initial TSC culture.
In contrast, ESC cultured in 2i (Ying et al., 2008) conditions have a more predictable behavior. 2i culture conditions are well known to reduce some aspects of intercellular heterogeneity (such as Nanog expression) and a narrower differentiation as compared to ESCs cultured in serum. As mentioned in the previous chapters, classical cultures of TSCs allow for a wide differentiation spectrum. The new TSC culture conditions we aim to obtain must therefore reduce intercellular heterogeneity but also must allow us to obtain cell lines that are consistently efficient in forming blastoids. We previously showed that Epiblast stem cells, which are ESC derivatives developmentally equivalent to a later developmental stage (E3.75), fail to form blastoids due to suboptimal crosstalk with TSCs. Similarly, we hypothesize that a culture of undifferentiated TSCs will display an enhanced intrinsic potential to form blastoids, and/or an enhanced communication with ESCs.
This hypothesis is supported by the increased blastoid yield obtained upon the use of CDX2 regulators (Rivron et al., 2018). Soluble Il11 and cAMP are capable of increasing CDX2 expression not only in 3D during blastoid formation, but also in monolayer culture, particularly in combination with BMP7, LPA and ACTIVIN in laminin pre-coated plates. LT21 conditions result in a culture with consistently high CDX2 expression levels that can potentially improve the potential and efficiency of blastoids.
Although we have demonstrated a correlation between CDX2 and blastoid potential, there are many other genes that form part of the TE transcriptional network that need to be co-expressed for a culture bearing full TE-like potential. From genetic studies, we can establish certain hierarchy in the importance of the key transcription factor, but there are several publications claiming the importance of co-expression of those factors in cultured TSCs for obtaining their full developmental potential (Kuales, Weiss, Sedelmeier, Pfeifer, & Arnold, 2015; Ralston & Rossant, 2008). Upon in vitro line derivation of primary tissue, there is a dramatic change in environmental conditions that often results in phenotypical differences between the cells in vivo and their in vitro analogues, which often result in cultured cells to be locked in a divergent developmental stage. In our case, it is therefore necessary to confirm the potential of TSCs converted to LT21 conditions, but also of those directly derived in such polar-like conditions.
TSCs are theoretically capable of self-renewal, differentiation proliferation and placental contribution upon injection in blastocyst. In order to consider LT21 cultured cells as a polar-like culture, they will need to display not only those properties, but also show active communication with ESCs during blastoid formation.

5.3 Results

5.3.1 LT21 cultured cells display enhanced stem cells properties in comparison with Tx cultured cells

Because the new LT21 culture conditions lead to a stable state with consistently high expression of CDX2, we explored the phenotypic and functional properties of these cells, and attempted to pinpoint their potential as TE analogues. Similar to what we did in the chapter 2, we tested LT21 TSCs for stem cell related assays as compared to Tx cultured TSCs.
•Colony formation and cell cycle
Single and live cells (negative for propidium iodide) (**Sup. Fig. 1A**) were sorted in individual

wells and grown for a period of 7 days. Importantly, these cells were not sorted according to CDX2 levels, meaning that these results were not biased by the lower CDX2 expressing fraction of the control fraction. TSCs cultured in LT21 formed more colonies as compared to TSCs cultured in Tx medium (fc=2.21, p value= 0.0028) (**Fig. 1A**). This reflects a higher propensity for self-renewal. The CFU of LT21 TSCs was also higher as compared to the CFU of the CDX2-high sorted population form Tx medium (fc=1.38) (**Sup. Fig. 1B**).
In chapter 2 we showed a high correlation between CDX2 expression and cell cycle phase (**Sup. Fig. 1C**). We thus compared the cell cycle status of LT21 and Tx TSCs using a FACS assay. LT21 and Tx TSCs showed very similar profiles (**Fig. 1B**), suggesting that the enrichment in CDX2 expression did not imply major changes in the cell cycle. We also did not observe a noticeable difference in overall growth between the two conditions. Altogether, these observations are consistent with CDX2 being a key factor regulating TE self-renewal rather than proliferation.

•Differentiation potential
We then tested the plTSCs for their differentiation potential. We initially plated cells in their corresponding LT21 or Tx culture conditions. After 24 hours, we switched the medium to plain Tx. We assigned replicates for RNA extraction each day, for 4 consecutive days. Removal of the compounds led to differentiation, which we tracked via the expression of markers for extraembryonic structures derived from the TE. The genes Cdx2 and Esrrb are markers of an undifferentiated state. Mash2 marks for the extraembryonic ectoderm, a structure immediately derived from the polar TE, which is thought to be the post-implantation stem cell compartment. Gcm1, Flt1 and Hand1 are markers for syncytiotrophoblasts, spongiotrophoblasts and trophoblast giant cells respectively. Both cultures displayed similar differentiation dynamics (**Fig. 1C**), but the genes of interest were expressed with different amplitudes. LT21 initially showed a higher expression of undifferentiated markers but, upon differentiation, their expression dropped faster than the control culture. A similar profile was observed with Mash2 and Gcm1: LT21 TSCs showed a lower initial expression, but the expression reached faster, a higher peak as compared to Tx TSCs. This suggests that LT21 TSCs have a higher propensity to exit multipotency and to express genes of the post-implantation extra-embryonic ectoderm (the post-implantation stem cell compartment) and syncytiotrophoblasts. In relation to the other differentiation markers, LT21 cultures showed a higher initial expression of the genes Flt1 and Hand1 with somehow maintained expression. We concluded that the differentiation toward spongiotrophoblasts and trophoblast giant cells cannot be achieved in growth factor-free medium. Overall, we concluded that LT21 TSCs remain in an overall less differentiated state, and display a more efficient differentiation toward the post-implantation extra-embryonic ectoderm and syncytiotrophoblasts in serum-free medium deprived of growth factors. Of note, the increased expression of Mash2 upon differentiation is consistent with the idea that TSCs are in vitro analogs of the TE and transition via a ExE-like state upon growth factor removal. The potential for TSCs to form blastoids with the potential to recapitulate aspects of in utero implantation and decidualization also points in that direction.
Altogether, these results suggest that LT21 conditions maintain cells in a proliferative state with enhanced self-renewal, high expression of key TE markers (Cdx2 and Esrrb), and an propensity to rapidly express genes of differentiation. These features are all consistent with the polar state of the TE.

•Derivation of new TSC lines from the 3.5 blastocyst

Here, we should keep in mind that the cells cultured in LT21 conditions, were initially derived from blastocysts using serum cultured conditions (Tanaka, 1998). Upon establishment of the cell lines, these cells were then converted using LT21 culture conditions. We therefore tried to derive new lines directly in LT21 conditions. Although laminins are beneficial for the culture of TSC, the use of mouse embryonic fibroblasts (MEF) is far more efficient for the initial blastocyst attachment in a dish. New lines were successfully derived in Tx21 + MEF conditions for 2 passages. After two passages, cells were plated in laminin coated plates in LT21 conditions, were stable and displayed expression for Cdx2 in a similar fashion to LT21 converted cultures (**Fig. 1D**). When plated directly on laminin 521 pre-coated plates, the blastocysts formed outgrowths that showed a much lower proliferation after 5 days (**Fig. 1E**).
Upon TSC line derivation, cells outgrow from the blastocyst, including some differentiated cells. These differentiated cells are commonly thought to be trophoblast giant cells (TGCs) originating from the mural TE. Here, we tested whether the tx21 media conditions affect the initial differentiation of the outgrowths. Three or four days after initial seeding of the blastocyst, the outgrowths were fixed, stained for CDX2 and EOMES, and counterstained with Hoechst (**Fig. 1F**). In all outgrowths, cells positive for CDX2 were also positive for EOMES. Although results were not statistically significant with the number of outgrowths measured (n=5 for day 3, n=4 for day 4), the derivation in tx21 media tends to diminish the initial appearance of CDX2-/EOMES- cells (for day 3 outgrowths fold change of 1.45, p.value=0.20; for day 4 outgrowths fold change of 1.33, pvalue=0.26 **Fig. 1G**). These results are consistent with a higher maintenance of the polar TE cells, or with a reversal of the mural TE cells in LT21 culture conditions.
Karyotyping of the new TSC lines directly derived in LT21 conditions after 10 passages showed the presence of 41 chromosomes (**Sup. Fig. 1D**), which implies a trisomy for one chromosome, presumable chromosome 19 which is common problem in TSC derivation (Oda et al., 2009). This new line was named pTS1.

•Chimerization potential
True blastocyst-like stem cells have the potential to chimerize the conceptus when injected back in a blastocyst. Upon development, they can contribute to the developing tissues of the embryo proper (ESCs) or of the placenta (TSCs), thus forming chimeras. Of note, the Tx serum-free media did not support any placental contribution upon blastocyst injection (Kubaczka et al., 2014). These TSCs were however able to chimerize the placenta upon reversion to classical serum culture conditions for at least 3 passages. This suggests that Tx culture conditions are minimal and do not compromise the in vivo potential of the cells, but are insufficient to form chimeras. It is also worth mentioning that TSCs cultured in classical serum conditions globally have a limited potential to chimerize the placenta as compared to the potential of ESCs to chimerize the embryo proper. Injected cells usually contribute to a small fraction of the whole organ (Kubaczka et al., 2014; Ohinata & Tsukiyama, 2014). This might be due to the difficulty for the injected cells to attach to the trophectoderm. Indeed, contrary to isolated ICMs, when blastocysts are bisected, the mural trophectoderm pieces are known to not fuse in vitro (Gardner & Johnson, 1972). Injected cells might also have difficulties to contribute to the polar TE, which is hidden behind the ICM. Finally, as we showed in Chapter 2, only few cells with high self-renewing capacity are present in these cultures, which might be able to form chimeras.
In this assay, both converted and newly-derived TSCs formed chimeric placentas (**Fig. 1H**). We did not detect GFP signal in the corresponding non-placental tissues (**Sup. Fig. 1E**). Pla-

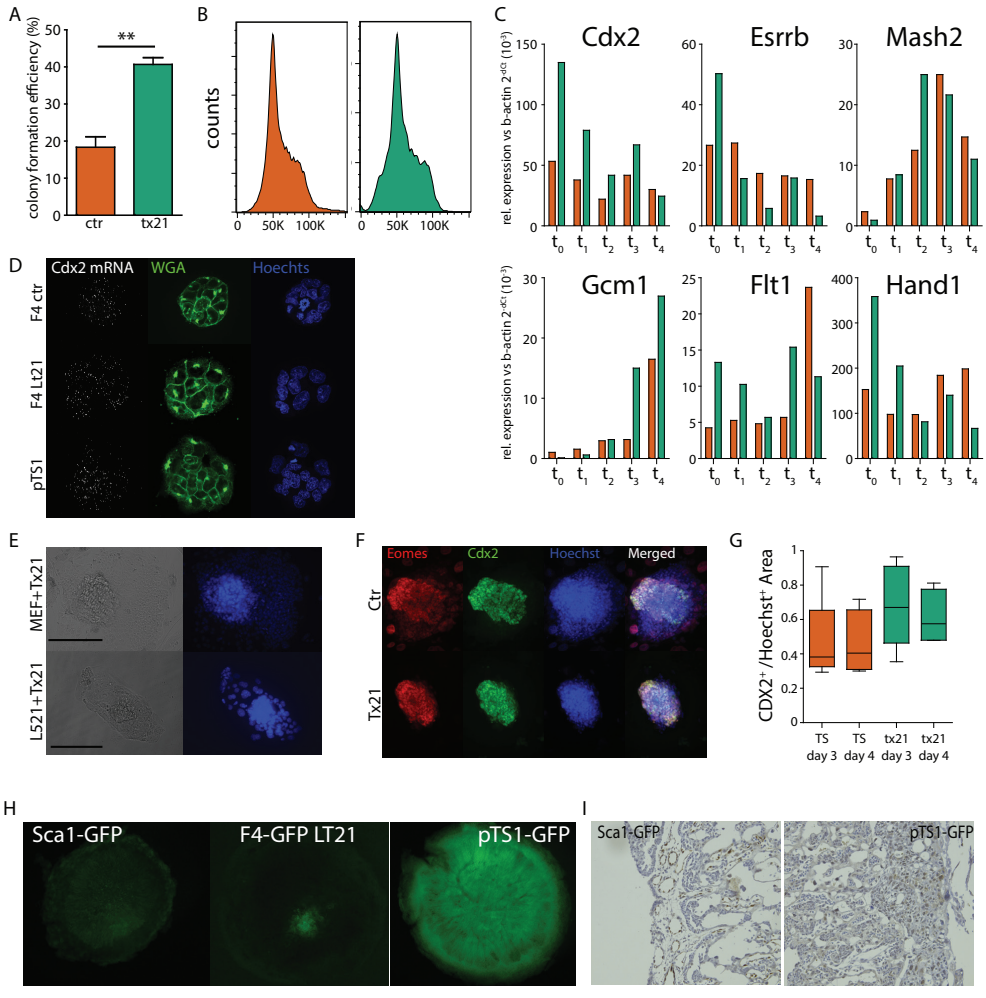

Figure 1. Characterization of the in vitro and in vivo potential of plTSCs. A. Colony formation efficiency for control (orange) and plTSCs(green). fc= 2.21, pvalue=0.0028. B. Cell cycle profile of Control (orange) and plTSCs(green) as measured by Hoechst staining. C. Differentiation dynamics of TSCs originally cultured in Tx (orange) or Lt21 (green) conditions. Original media was switched to plain tx at t0. D. smFISH performed on small colonies from F4 control, F4 LT21 and pTS1 (Lt21 cultured) lines. E. Proliferation comparison of trophoblast 4 days after blastocyst plating on MEF or on Laminin521. Scale is 200 um. F. CDX2 and EOMES staining of blastocysts outgrowths 4 days after blastocyst plating. G. Quantification of initial trophoblast differentiation as measured by CDX2+area in comparison so Hoechst+ area of blastocyst outgrowths. H. Isolated e10.5 placentas after blastocyst injection using F4 GFP Lt21 TSCs (mid) pTS1 (directly derived as plTSCs) (right) as compared to a placenta from Sca1-GFP reporter mice (left). I. Staining against GFP on tissue sections coming from placentas showing TSC contribution.

centas from Sca1-GFP reporter mice were used as a control to assess GFP expression (**Fig. 1H**). We detected GFP expression in a small patch of the placentas issued from blastocyst injected with converted TSCs. However, we observed ubiquitous GFP expression in placentas derived from blastocysts injected with TSC directly derived in LT21 conditions (**Fig. 1H**).

Immunohistochemistry using antibodies against GFP confirmed the presence of placental cells derived from the injected plTSCs (**Fig. 1I**). The immunoreactivity was lower in these sections, probably due to the dim expression in plTSC1 GFP cells, obtained by random integration of a nuclear GFP expressing cassette. Thus, contrary to Tx culture conditions, the LT21 culture condition does not require a reversion to serum conditions and maintain TSCs that can form chimeric placentas. The high chimeric potential of plTSCs (pTS1) might be anecdotic and need to be confirmed. However, in our hands, this is the only line which allowed us to obtain high chimerism of the placenta.

5.3.2 LT21 cultured cells have an enhanced epithelial phenotype

We then investigated the phenotypic changes associated with the LT21 culture conditions. Similar to the classical culture conditions, TSCs cultured under these conditions grow in colonies (**Fig. 2A**). However, they also display a different morphology. Within the colony, the edges of each cell were more apparent, and the cell shape became more polygonal as compared to cells in Tx media (**Fig. 2A**). The TE, as an epithelium relies on the integrity of the cell to cell contacts mediated by tight junctions. This integrity is critical for ensuring the formation of the blastocoel cavity. The expansion of this cavity plays critical roles to separate the polar and mural populations, hatch from the zona pellucida and thus implant into the maternal tissues. E-CADHERIN and ZO-1 are pivotal genes in forming a functional epithelium. Both proteins are expressed and localized in the plasma membrane of LT21 TSCs (**Fig. 2B**).
To characterize the morphology of single cells in an unbiased way, we performed high-content image-based analysis. This allows to measure numerous cell morphological parameters and to correlate them with CDX2 expression levels. For this purpose, we first tested several stains to accurately segment the outer borders of cells, including wheat germ agglutinin (WGA), succinimidyl ester, ZO-1 and E-CADHERIN (**Fig. 2B**). Succinimidyl ester stains for cytosol, leading to no stain in the cell membrane. Even though this staining has been used for this type of analysis before (Battich, Stoeger, & Pelkmans, 2013), for TSC gave suboptimal results since we were unable to distinguish the cytosol of different cells in the central area of the colony. ZO-1 protein staining resulted in very precise outlining of most cells, however, in more crowded areas stain was not observed. WGA staining was satisfactory for our purpose, however, the outline of the cells was unprecise and the signal to noise ratio was not as optimal. E-CADHERIN stainings gave the best results and was thus chosen for cell segmentation.
Stainings for EOMES and E-CADHERIN were performed and samples were counterstained with Hoechst in both Tx and LT21 conditions using CDX2-eGFP cells (**Fig. 2C**). Upon imaging, cells were manually segmented and analysed using Cell profiler.
Upon analysis of the phenotype, a total of 162 morphological features were significantly different between Tx and plTSCs. We ranked these features based on the p-value scores between the two culture conditions (Mann-Whitney U test/random forest) (**Sup. table 1**). We then plotted a distance map based on the top 20% ranked differential features. These features were sufficient to separate the cells in two major clusters (**Fig. 2D**). One cluster was almost fully composed of ctr cells (red x axis index), while the other cluster included mainly plTSCs (blue) but also a sub-population of Tx TSCs. We concluded that the control TSC and plTSC states were morphologically different, and that the Tx culture contained a subpopulation morphologically similar to the plTSCs. This control subpopulation could represent the cells with true stem cell potential.

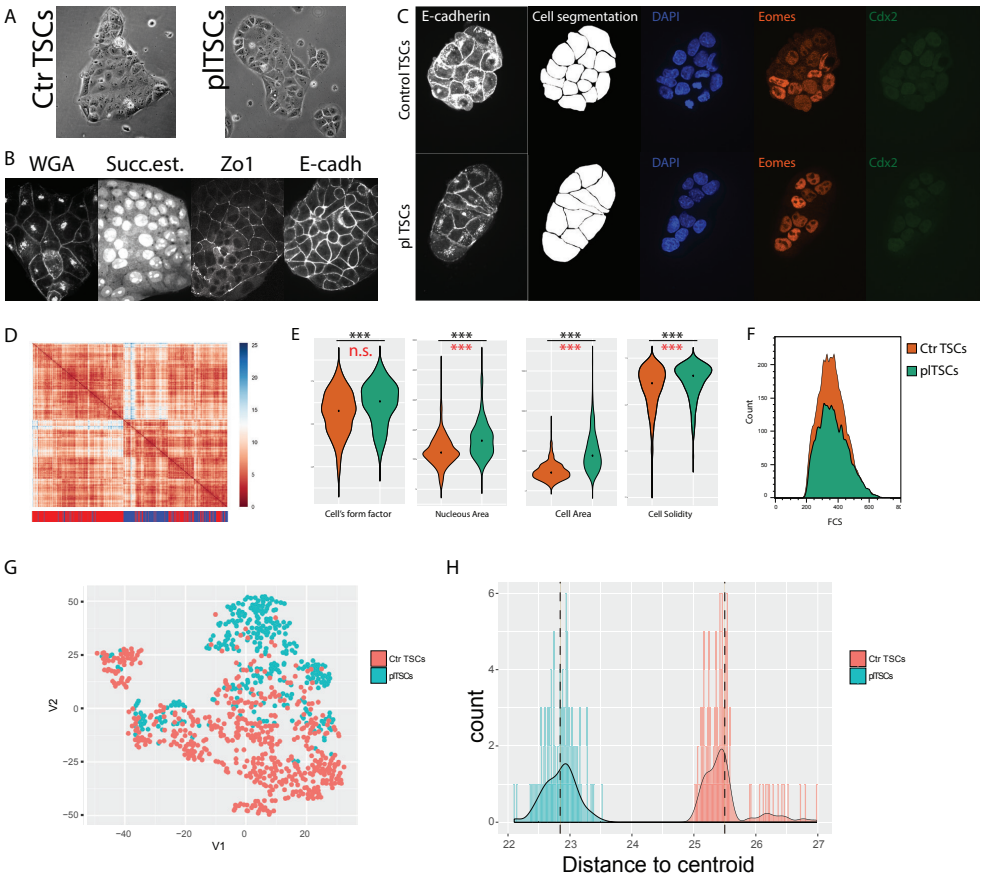

Figure 2. Characterization of TSCs and plTSCs by high content imaging. A. Bright field microcopy image of control and plTSCs F4. Scale bar is 1mm. B. Confocal images of LT21 cultured colonies counterstained with WGA, succinimidyl ester or stained for Zo1 or E-cadherin. C. control and plTSCs stained for E-CADHERIN, EOMES and CDX2 and counterstained with DAPI. Cell segmentation obtained from E-CADHERIN staining is also shown. D. Unsupervised clustering analysis of all control (red) and plTSCs (blue) single cells using only the top 20% differential morphological features. E. Violin plots showing the distribution of values for some of the top ranked differential features. The Statistical analysis performed were unpaired two-tail t-test (black) and F test for variance (red). *** = pvalue<0.001. F. Histogram showing FCS values for control and plTSCs. G. Representative t-SNE map of single cells based on all he features. H. Histogram of the average distance to centroid from 100 different t-SNE maps for control and plTSCs. The vertical line represents the mean distance to centroid across t-SNEs.

The top differential features when comparing both states included cell surface area, solidity (which defines how lobulated a cell is), cell's form factor (which defines the circularity of a cell) and nuclear area (**Fig. 2E**). plTSCs occupy a larger surface area, have a larger nucleus, and a less lobulated, more circular cell shape. We did not observe that plTSCs are more voluminous than Tx cells when in suspension (similar FCS values on a FACS plots, **Fig. 2F**). This suggests that plTSCs are flatter than Tx TSCs when attached on the surface of a dish.
When we use all the features for displaying the single cells in a t-SNE map, we observed that the control cell population showed a wider spread than the LT21 population (**Fig. 2G**). As

an approximation to population heterogeneity we generated 100 different t-SNE maps with different R-Seeds and calculated the average distance of each cell to the centroid of its corresponding population. The average distance to the centroid was obtained for each culture and t-SNE map. The average distance was smaller for plTSCs as compared to Tx TSCs (**Fig. 2H**). We concluded that plTSCs are phenotypically more homogeneous as compared to control TSCs.
Altogether, we concluded that the plTSCs cells are overall phenotypically different and more homogenous as compared to Tx cultured TSCs, being larger, flatter, less lobulated, and with a larger nucleus, features consistent with an enhanced epithelial phenotype. A subpopulation of control TSCs seems to be more comparable to the majority of LT21 cultured TSCs. Whether these few control cells represent the ones with true stem cell potential, remains to be confirmed.

5.3.3. Bulk transcriptome analysis of plTSCS

The increased expression of CDX2 and higher potential to self-renew suggest that plTSCs are in a less differentiated states as compared to Tx cells. To further investigate this possibility, we compared the transcriptome of F4 TSC cultured in tx or LT21 conditions ("converted TSCs"), both in an undifferentiated or differentiated states (TSCs grown without growth factors for 6 days). Differentiated samples clustered separately (**Fig. 3A**). In undifferentiated culture, 299 genes were differentially expressed between Tx and plTSCs (1.5 fold and adjusted p.value < 0.05, **Fig. 3B** and **Sup. table 2**). These genes were enriched for processes including extracellular matrix organization, placenta development and cell adhesion (**Sup. table 3A**). KEGG pathway analysis revealed that Tx and plTSCs differ in the signaling related to ECM-receptor interaction, focal adhesion, regulation of actin cytoskeleton, tight junction and the Pi3K pathway (**Sup. table 3B**). Tight junctions are important in epithelial phenotypes and they play a role in preventing the leakage of solutes and favor transport of selected ions or water. The tight junction genes Tjp2, Cldn4, Cldn6 and Jam2 were upregulated in the plTSCs (**Fig. 3C**). Importantly, Cldn4 and Cldn6 have been shown to be essential for blastocyst formation (Moriwaki, Tsukita, & Furuse, 2007). Cldn4 is also highly expressed upon growth factor deprival. The other tight junction-related genes (Jam2 and Tjp2) reduce their expression upon differentiation (**Fig. 3C**). plTSCs also showed a higher expression of the epithelial cell adhesion molecule Epcam. Thus, consistent with the enhancement of epithelial phenotypic features, plTSCs increase the expression of genes related to epithelial integrity, including key adherens and tight junction molecule Epcam and tight junction molecules Cldn4 and 6.
Among other genes that were differentially expressed, two important genes related to the Smad2/3 pathway were also upregulated in plTSCs: Acvr1, the receptor for Activin and Furin, a protein convertase, which are both necessary for active Nodal signaling in post-implantation conceptus (Guzman-Ayala et al., 2004). Expression of these two genes might potentiate plTSCs to Smad2/3 signaling, a pathway that we previously suggested was important for embryonic to trophoctoderm crosstalk (Rivron et al., 2018). It is unclear to us if the upregulating the expression of the genes is a consequence of Activin being present in LT21 cultures.
Krt8 and Krt18 were also upregulated in plTSCs. These genes are important for TE lineage maintenance. It is worth mentioning that Il11 was also upregulated in plTSCs. Ly6a, a gene previously related to serve as a marker for stem cells in later stages of the placenta (Natale et al., 2017), was also strongly upregulated in LT21 cultured TSCs cultures.
Upon differentiation from LT21 and control culture conditions, 3609 and 4190 genes were

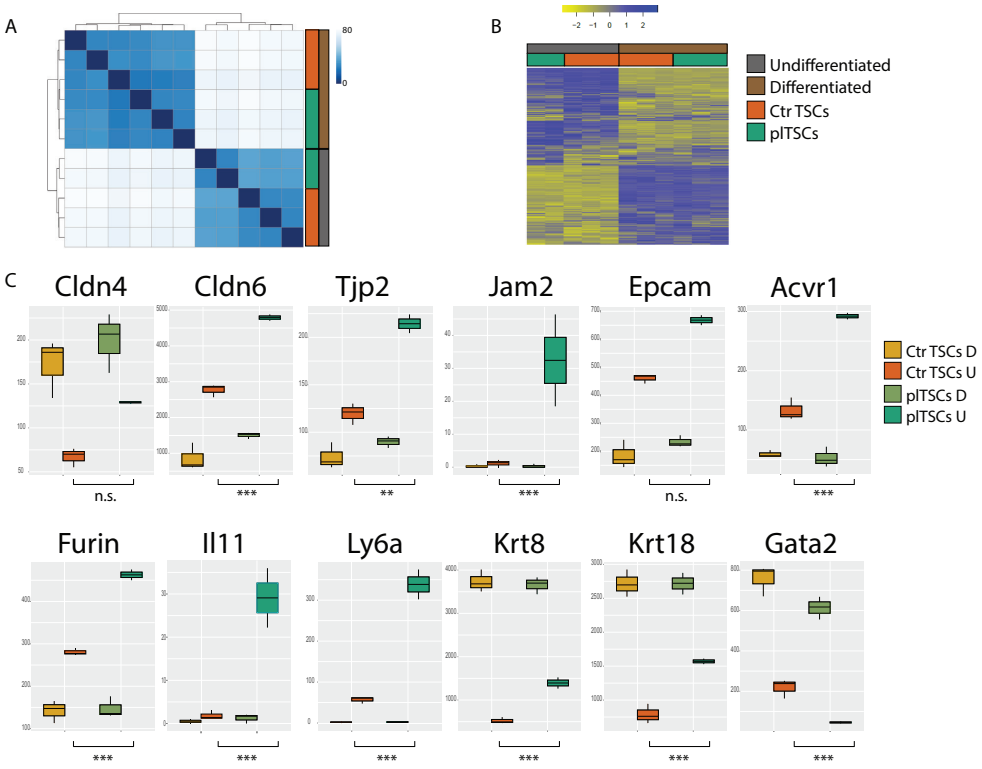

Figure 3. Bulk transcriptome analysis of control and plTSCs. A. Unsupervised clustering analysis of undifferentiated and differentiated cultures of control and plTSCs. B. Heatmap for the differentially regulated genes between undifferentiated and differentiated cultures show both initial cultures to lead to highly comparable differentiated cells. C. Expression of genes related to epithelial phenotypes or differentiation state. *** for adj. pvalue<0.001, ** for pvalue<0.01.

differentially expressed respectively. 3071 genes were common for both cultures. We concluded that, beside different dynamics (**Fig. 1C**), the initial culture conditions do not strongly alter the identity of the differentiated derivatives.

5.3.4. plTSCs more efficiently form blastoids.

In specific chemical and physical conditions, ESCs and TSCs spontaneously organize into structures morphologically and transcriptionally resembling E3.5 blastocysts. Blastoids form through the cross-talk of small, precise number of ESCs and TSCs confined in microwells. The yield of blastoids is about 70% within the microwells that include the correct numer of ESCs and TSCs. However, pooling precise numbers remains difficult, an issue that should be resolved in order to better control the parameters influencing blastoid formation. Here, we reasoned that the presence of multiple sub-populations within TSC cultures might also limit the capacity for cells to organize. The presence of more differentiated TSCs might for example hamper the cross-talk with the ESCs, which is essential for blastocyst and blastoid formation (Gardner & Johnson, 1972; Rivron et al., 2018). The presence of TSCs with a dampened

epithelial phenotype might also limit the capacity to form a TE-like structure. Overall, we speculated that plTSCs might be in a better state to form blastoids.
Measuring all the structures of the microchip (**Fig. 4A**) would allow us to better characterize the consequences of altering any aspect of the blastoid protocol such as changing the initial state of the TSCs. To do so we developed a semi-automated method for measuring the circularity and diameter of each structure within the microwells. A membrane staining using WGA was used to set a threshold for automated shape morphology measurements. This segmentation method permits for circularity and diameter measurements, and thus to more precisely compare the efficiency for blastoid formation (**Fig. 4B**). In parallel, we also took bright field pictures to assess cavitation. This new methods required adjustments for the circularity threshold. When measured manually, the segmentation was performed with the polygonal tool in imageJ, while the semi-automated measuring is performed based on positive pixels at a specific WGA intensity threshold. The outlining of those positive pixels leads to an increase of the perimeter of the shape, thus having an impact on the precision of the circularity measurement. Structures manually segmented with a circularity of 0.9 are equivalent to an automated measured circularity of 0.82. This value is thus used to consider a structure as a blastoid.
We compared both Tx and LT21 cultures of F4 TSC (converted) (**Fig. 4C**). We quantified the yield of trophosphere formation, which we use to describe the autonomous potential of TSCs to organize; and the yield of blastoid formation, which also permits to evaluate the cross-talk with the ESCs. These two measurements thus allows us to separate the response of the TSCs to the blastoid medium from the response to the chemical or mechanical factors originating from the ESCs. plTSCs formed structures with a higher diameter and a higher circularity (pvalue= 0.0191, n=2) (**Fig. 4E**). We quantified an increase in the number of structures with a diameter between 70 and 130 µm and a circularity above 0.82 (for trophosphere mean circularity fc=1.05, pvalue<0.0001, for blastoids mean circularity: mean fc=1.06, pvalue<0.0001, for trophosphere diameter is n.s., for blastoid mean diameter fc=1.06,. **Fig. 4F-G)**, the criteria used to describe a blastoid (Rivron et al., 2018). Trophosphere also formed at a higher rate (**Fig. 4H**). We concluded that plTSCs have an increased intrinsic capacity to cavitate and an increased capacity to respond to the signals present in the blastoid medium. In addition, the improvement in circularity between blastoids formed with plTSCs and ctr TSCs was more acute when compared to the improvement in corresponding trophospheres. These results suggest that plTSCs better respond to the ESCs signals. The number of cells included in blastoids did not change between control and LT21 blastoids (n=22) (**Fig. 4D**) suggesting that the higher diameter is due to enhanced swelling of the cyst.
TSC directly derived from the blastocyst using LT21 conditions (pTS1) performed very similarly to LT21 cultured F4 cells (converted) when it came to all parameters measured independently. However, they performed better in yield (30.5% vs 25.8% and 17.2%). In other words, the TSC line directly derived from the blastocyst in LT21 medium formed more structures that passed the phenotypic criteria for all three measured features and thus qualified as blastoids (**Fig. 4I-M**).
Importantly, similar to our previous observations, blastoids formed from plTSCs showed the correct cellular distribution (**Fig. 4N**) and are permissive for the formation of PrE-like cells (**Fig. 4O**).
These results suggest that plTSCs better respond to the factors present in the blastoid medium, and better communicate with ESC. This results in a more efficient formation of blastoids. Consistent with our previous results in chapter 4 (Rivron et al., 2018), these observations suggest that an increased CDX2 expression and epithelial phenotype positively affect the for-

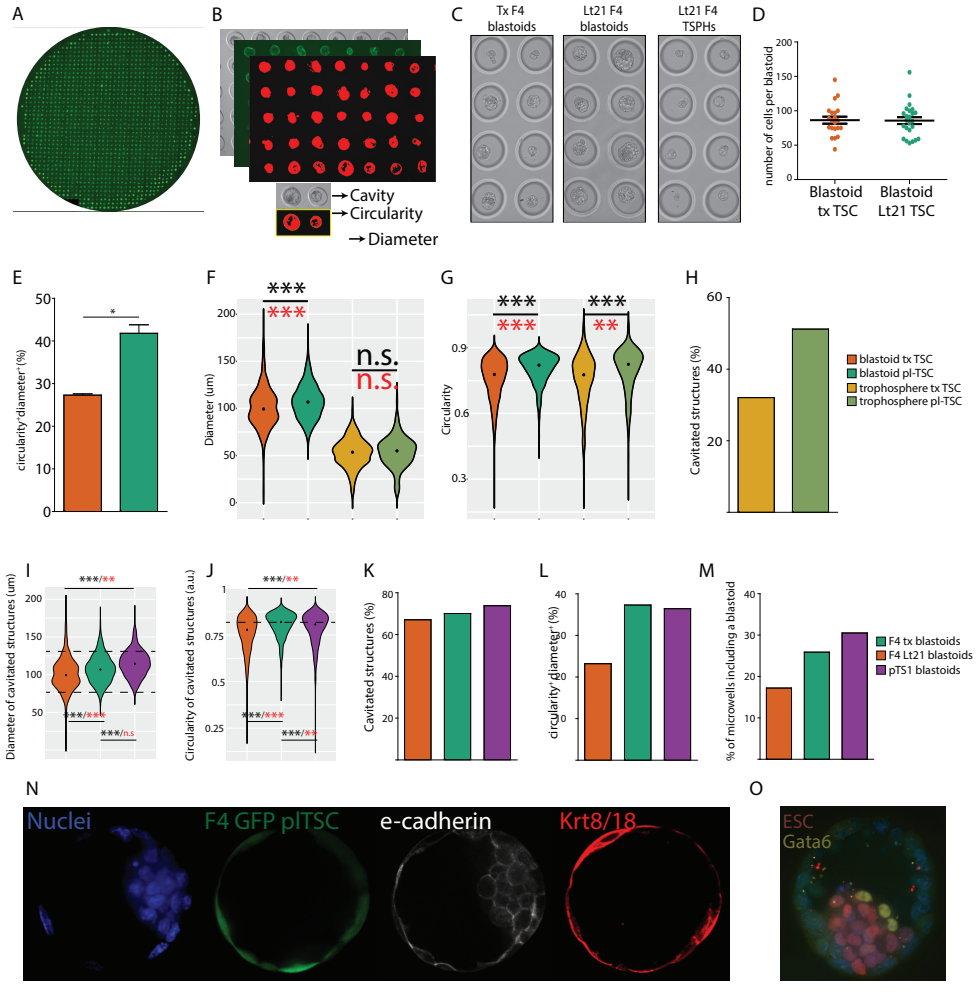

Figure 4. Blastoid efficiency of plTSCs. A. Overview of a microwell array with blastoids. B. Blastoid morphology assessment after WGA counterstain. C. Representative pictures of microwells including control F4 blastoids, LT21 F4 blastoids and LT21 F4 trophospheres. D. Number of cells included in a 65 hour blastoids obtained from control and LT21 F4 TSCs. E. Proportion of structures with a circularity>0.82 and a diameter between 80 and 120um. F. Diameter of all structures included in two microwell arrays for control and LT21 blastoids and trophospheres. G. Circularity of all structures included in two microwell arrays for control and LT21 blastoids and trophospheres.H. Percentage of cavitated structures coming from control and LT21 trophospheres. I. Diameter of cavitated structures from control F4, LT21 F4 and pTS1 blastoids. J. Circularity of cavitated structures from control F4, LT21 F4 and pTS1 blastoids. K. Percentage of cavitated structures from control F4, LT21 F4 and pTS1 blastoids. L. Proportion of structures with a circularity>0.82 and a diameter between 80 and 120um from control F4, LT21 F4 and pTS1 blastoids. N. blastoid yield obtained when using F4, LT21 F4 and pTS1 TSCs. N. Blastoid obtained from LT21 F4 TSCs stained for E-CADHERIN and KRT8/18. O. Blastoid obtained from LT21 F4 TSCs stained for GATA6. Sttatistical analysis are all two-tailed unpaired t-test. ** for pvalue<0.01,*** for pvalue<0.001. In black analysis of the means, in red analysis for F variance.

mation of blastoids.

5.4 Discussion

In this chapter we have managed to confirm that cells cultured in LT21 conditions show enhanced stem cell properties in vitro and are capable of contributing to placenta formation in vivo. These findings imply an improvement of the culture conditions in comparison with the basal Tx media, solving the issue of needing a culture transition in serum + MEF conditions before unlocking the in vivo potential of the TSCs. Importantly the LT21 culture conditions allow for direct derivation of new lines showing a trend for lower levels of initial differentiation. This could suggest plTSCs are able to revert the mural TE to a state capable of self-renewal.
By image based analysis and bulk transcriptome analysis we have characterized cells in the new culture describing their phenotype and transcriptional differences with Tx cultures. We concluded that the LT21 culture conditions result in cells with a less heterogeneous, enhanced epithelial phenotype, showing increased expression of undifferentiated state markers.
Finally plTSCs have a higher capacity to form blastoids with an increased circularity. These results, led us to propose that the TSCs cultured in LT21 conditions are polar-like TSC (plTSCs).
Both converted and directly derived plTSCs increase the efficiency of blastoid formation, making the model more suitable for applications such as genetic or drug screens.
All results included in this chapter support our hypothesis that inductive factors that are secreted by the embryonic compartment of blastocysts lead to a culture of TSCs more potent and with features comparable to the undifferentiated polar TE.

5.5 Materials and methods

• Cell culture.
TSC are cultured under Tx conditions followed a previously published protocol (Kubaczka et al., 2014). After coating with Matrigel, cells are cultured in Tx media, which consists of phenol red free DMEM/F12 supplemented (phenol red-free, with l-glutamine), insulin (19.4 µg/ml), l-ascorbic-acid-2-phosphate (64 µg/ml), sodium selenite (14 ng/ ml), insulin (19.4 µg/ml), sodium bicarbonate (543 µg/ml), holo-transferrin (10.7 µg/ml), penicillin streptomycin, FGF4 (25 ng/ml), TGFβ1 (2 ng/ml) and heparin (1 µg/ml). Alternatively, when stated, TSC were cultured in classical TS conditions(Tanaka, 1998) in a media based on RPMI 1640 supplemented with 20% fetal bovine serum, sodium pyruvate (1 mM), b-mercaptoethanol (100 mM), L-glutamine (2 mM), and penicillin and streptomycin (50 mg/ml each), human recombinant FGF4 (25 ng/ml) and heparin (1 mg/ml). LT21 cultured cells were plated in laminin 521 coated plates (10 ug/ml diluted in PBS with Mg2+ and Ca2+) using Tx media supplemented with Il11 (50 ng/ml), Activin (50ng/ml), Bmp7 (25 ng/ml), LPA (5 nM) and 8Br-cAMP (200 nM) ESC were cultured under 2i conditions (Ying et al., 2008) in gelatin coated plates. Cells were routinely passaged using trypsin.

• TSC line derivation.
E3.5 blastocysts were isolated from pregnant females. Zona pellucida was removed using Tyrode acid solution and then they were placed in MEF coated plates in the presence of Tx or Tx21 media. Media was carefully changed every 48h. The first outgrowth was monitored

daily and was passaged on day 4 or 5 depending on cell growth. Cultures including Tx21 were passaged into MEF coated plates for one more passage since this facilitates attachment of the single cells. Only in passage three they would be converted to LT21 cultures being plated in laminin 521 pre-coated plates. For outgrowth differentiation measuring, staining for CDX2 and EOMES was performed. ImageJ was used for analyzing positive are for each independent staining. CDX2 and EOMES positively stained areas were used for quantifying undifferentiated cells and compared to total DAPI positive area.

• Cell cycle analysis.
After trypsinization, 105 TSCs and plTSCs were incubated in 0.5ml of Tx media with 10 ug/ml hoescht 34580 for 30 minutes at 37C. After the incubation time, tubes with cells were placed on ice and analyzed with a FACSCanto II.

• Colony formation assay.
Singe cells were sorted in MEF coated plates in the presence of either Tx or LT21 media. Media was changed every 48 hours and the number of wells containing colonies was assessed 7 days after sorting.

• TSC differentiation.
TSCs cultured in Tx and LT21 conditions were plates in equal numbers in 5 replicate wells in their corresponding media. 24h after plating, one sample of each group was used for trizol extraction while the rest of the wells had their media changed to Tx without Fgf4, Tgfb and Heparin. A new sample would be used for trizol extraction every 24 hours. After trizol RNA extraction, retrotranscirption was performed using superscript III. qPCR was performed for the target genes using 30ng of RNA for each reaction.

• Blastoid formation.
Full protocol can be found in https://www.nature.com/protocolexchange-/protocols/6579) Agarose microwell arrays were casted using the PDMS stamp and incubated O/N on mES serum containing media. After washing the chips with PBS, a ESC solution of 8000 cells/150 µl is dispensed in the central chip are and allowed to settle. After 15 minutes, an additional 1ml is dispensed. 20 hours later 1 ml of media is removed and a TSC solution of 22000 cells/150 ul is dispensed. After allowing the cells to fall in the microwells, 1 ml of blastoid media is added to the wells. Blastoid media includes 20 µM Y27632 (AxonMed 1683), 3 uM CHIR99021 (AxonMed 1386), 1 mM 8Br-cAMP (Biolog Life Science Institute B007E), 25 ng/ml Fgf4 (R&D systems 5846F4), 15 ng/ml Tgfb1 (Peprotech 100-21), 30 ng/ml Il11 (Peprotech 200-11) and 1 µg/ml heparin (Sigma-Aldrich cat# H3149). An additional dose of cAMP is dispensed 24 hours after TSC seeding. All measurements are performed 65 hours after TSC seeding.

• Immunofluorescence.
Samples were fixed using 4%PFA in PBS for 20 minutes at RT followed by 3 washing steps with PBS. A 0.25% triton solution in PBS was used for permeabilization during 30 minutes ar RT,followed by a 1 hour blocking step with PBS+ 10% FBS and 0.1% tween20. Primary antibodies against CDX2 (Biogenes MU392A-5UC), EOMES (Abcam ab23345), ZO-1 (Fisher scientific # 33-9100), Krt8/18 (DAKO M365201-2), GATA6 (R&D AF1700) or E-CADHERIN (life technologies # 14-3249-82) were diluted 1/200 in PBS + 0.1% Tween20, and used for

staining O/N at 4C. After three washing steps, samples were incubated with the corresponding secondary antibodies for 1 hour at RT. Hoechst was used for counterstaining with or withouth WGA. All images were analyzed in a PerkinElmer Ultraview VoX spinning disk microscope.

• Karyotyping.
TSC were synchronized using Nocodazole, resuspended in a hypotonic KCL solution and fixed with Methanol and Acetic Acid. Cells were then dropped onto coverslips and mounted with prolog for imaging.

• Chimera formation.
After blastocyst isolation from pregnant females, a micromanipulator was used for injecting 10 TSCs in the blastocyst cavity. Those blastocysts were then implanted in one of the uterine horns of pseudopregnant females. Each female had only one of their horns used for implantation and a maximum of 8 blastocysts were used per female. Placenta isolation was performed at E.11.5 (time of implantation was considered as 3.5). Histology was performed on the GFP imaged placentas using an antibody against GFP.

• Single molecule FISH.
TSC plated in glass coverslips were allowed to grow and were then fixed using RNAse free 4%PFA in PBS + 1% Acetic Acid during 20 minutes. After fixation, all samples followed the Quantigene ViewRNA kit instructions: After three washes with RNAse free PBS, samples were incubated for 10 minutes in a detergent solution. After three washes with RNAse free PBS, samples were incubated for 5 minutes at RT with Q protease. After three washes with RNAse free PBS, samples were incubated at 40C for 3 hours (in a humidified chamber) with the probes of interest diluted in Probe set diluent. After 3 washes with wash buffer, samples were incubated at 40C for 30 minutes with preamplifier diluted in amplifier diluent. After 3 washes with wash buffer, samples were incubated at 40C for 30 minutes with amplifier diluted in amplifier diluent. After 3 washes with wash buffer, samples were incubated at 40C for 30 minutes with label diluted in label probe diluent. After 2 washes with wash buffer, they were washed once more for 10 minutes. Samples were then incubated for 15 minutes in RNAse free PBS with Hoechst and WGA as counterstains followed by 3 washes with RNAse free PBS. Blastocysts were carefully placed in mounting media in glass bottom 3.5 mm plates. All samples were imaged with a 63x oil immersion objective in a PerkinElmer Ultraview VoX spinning disk microscope.

• High content imaging.
Each colony was imaged for E-CADHERIN, CDX2, EOMES and Nuclei stainings. E-CADHERIN staining was used for manual cell segmentation in ImageJ. Cell profiler was used for analysis of cells segmentation and the other stainings. Measurements obtained in Cell Profiler were used for further analysis using a Python pipeline. After discarding dividing cells based on the nuclear staining, a total of 500 control cells and 297 plTSCs cells were analyzed.

• RNA sequencing.
For bulk sequencing 1000 control and LT21 cultured cells were used for Trizol extraction RNA extraction from both bulk and single cells was performed following the Cel Seq 2 protocol (Hashimshony et al., 2016). Bulk samples were first normalized and then analyzed using the DESeq2 package on Rstudio. Triplicates for each group (F4 in Tx, F4 in LT21, F4 in Tx

differentiated, F4 in LT21 differentiated) were analyzed. Differentially expressed were those showing an upregulation of 1.5 fold change with a p value lower than 0.05. DAVID gene ontology online tool was used for gene enrichment analysis.

Author contribution

Javier Frias Aldeguer performed all functional assays for TSC and plTSCs, smFISH, new line derivations, stainings, manual segmentation of TSC and plTSC cultures, bulk transcriptome analysis, blastoid experiments and their quantifications, karyotyping and placenta isolation, and wrote the chapter. **Linfeng Li** performed the high content imaging analysis. **Judith Vivié** performed RNA extraction and library preparation for bulk samples. **Jeroen Korving** performed the in utero injections. **Clemens van Blitterswijk** and **Niels Geijsen** helped to direct the project. **Nicolas Clement Rivron** conceived and directed the research.

Bibliography

Battich, N., Stoeger, T., & Pelkmans, L. (2013). Image-based transcriptomics in thousands of single human cells at single-molecule resolution. Nature Methods, 10(11), 1127–1133. https://doi.org/10.1038/nmeth.2657

Gardner, R. L., & Johnson, M. H. (1972). An investigation of inner cell mass and trophoblast tissues following their isolation from the mouse blastocyst. Journal of Embryology and Experimental Morphology, 28(2), 279–312. Retrieved from http://www.ncbi.nlm.nih.gov/pubmed/4672104

Guzman-Ayala, M., Guzman-Ayala, M., Ben-Haim, N., Ben-Haim, N., Beck, S., Beck, S., … Constam, D. B. (2004). Nodal protein processing and fibroblast growth factor 4 synergize to maintain a trophoblast stem cell microenvironment. Proceedings of the National Academy of Sciences of the United States of America, 101(44), 15656–15660. https://doi.org/10.1073/pnas.0405429101

Hashimshony, T., Senderovich, N., Avital, G., Klochendler, A., de Leeuw, Y., Anavy, L., … Yanai, I. (n.d.). CEL-Seq2: sensitive highly-multiplexed single-cell RNA-Seq. Genome Biology, 17, 77. Retrieved from http://www.ncbi.nlm.nih.gov/sites/entrez?Db=pubmed&DbFrom=pubmed&Cmd=Link&LinkName=pubmed_pubmed&LinkReadableName=Related Articles&IdsFromResult=27121950&ordinalpos=3&itool=EntrezSystem2.PEntrez.Pubmed.Pubmed_ResultsPanel.Pubmed_RVDocSum

Kuales, G., Weiss, M., Sedelmeier, O., Pfeifer, D., & Arnold, S. J. (2015). A Resource for the transcriptional signature of bona fide trophoblast stem cells and analysis of their embryonic persistence. Stem Cells International, 2015, 17–20. https://doi.org/10.1155/2015/218518

Kubaczka, C., Senner, C., Ara??zo-Bravo, M. J., Sharma, N., Kuckenberg, P., Becker, A., … Schorle, H. (2014). Derivation and maintenance of murine trophoblast stem cells under defined conditions. Stem Cell Reports, 2(2), 232–242. https://doi.org/10.1016/j.stemcr.2013.12.013

Lin, S. J., Wani, M. A., Whitsett, J. A., & Wells, J. M. (2010). Klf5 regulates lineage formation in the pre-implantation mouse embryo, 3963, 3953–3963. https://doi.org/10.1242/dev.054775

Moriwaki, K., Tsukita, S., & Furuse, M. (2007). Tight junctions containing claudin 4 and 6 are essential for blastocyst formation in preimplantation mouse embryos. Developmental Biology, 312(2), 509–522. https://doi.org/10.1016/j.ydbio.2007.09.049

Nakamura, T., Yabuta, Y., Okamoto, I., Aramaki, S., Yokobayashi, S., Kurimoto, K., … Saitou, M. (2015). SC3-seq: a method for highly parallel and quantitative measurement of single-cell gene expression. Nucleic Acids Research, 43(9), e60. https://doi.org/10.1093/nar/gkv134

Natale, B. V., Schweitzer, C., Hughes, M., Globisch, M. A., Kotadia, R., Tremblay, E., … Natale, D. R. C. (2017). Sca-1 identifies a trophoblast population with multipotent potential in the mid-gestation mouse placenta. Scientific Reports, 7(1), 1–16. https://doi.org/10.1038/s41598-017-06008-2

Oda, M., Tanaka, S., Yamazaki, Y., Ohta, H., Iwatani, M., Suzuki, M., … Shiota, K. (2009). Establishment of trophoblast stem cell lines from somatic cell nuclear-transferred embryos. Proceedings of the National Academy of Sciences of the United States of America, 106(38), 16293–16297. https://doi.org/10.1073/pnas.0908009106

Ohinata, Y., & Tsukiyama, T. (2014). Establishment of trophoblast stem cells under defined culture conditions in mice. PLoS ONE, 9(9). https://doi.org/10.1371/journal.pone.0107308

Ralston, A., & Rossant, J. (2008). Cdx2 acts downstream of cell polarization to cell-autonomously promote trophectoderm fate in the early mouse embryo. Developmental Biology, 313(2), 614–629. https://doi.org/10.1016/j.ydbio.2007.10.054

Rivron, N. C., Frias-aldeguer, J., Vrij, E. J., Boisset, J., Korving, J., Vivié, J., … Geijsen, N. (2018). Blastocyst-like structures generated solely from stem cells.

Russ, A. P., Wattler, S., Colledge, W. H., Aparicio, S. A. J. R., Carlton, M. B. L., Pearce, J. J., … Evans, M. J. (2000). Eomesodermin is required for mouse trophoblast development and mesoderm formation, 404(March), 95–99.

Strumpf, D., Mao, C., Yamanaka, Y., Ralston, A., Chawengsaksophak, K., Beck, F., & Rossant, J. (2005). Cdx2 is required for correct cell fate specification and differentiation of trophectoderm in the mouse blastocyst, 2093–2102. https://doi.org/10.1242/dev.01801

Tanaka, S. (1998). Promotion of Trophoblast Stem Cell Proliferation by FGF4. Science, 282(5396), 2072–2075. https://doi.org/10.1126/science.282.5396.2072

Ying, Q.-L., Wray, J., Nichols, J., Batlle-Morera, L., Doble, B., Woodgett, J., … Smith, A. (n.d.). The ground state of embryonic stem cell self-renewal. Nature, 453(7194), 519–523. Retrieved from http://www.ncbi.nlm.nih.gov/sites/entrez?Db=pubmed&DbFrom=pubmed&Cmd=Link&LinkName=pubmed_pubmed&LinkReadableName=Related Articles&IdsFromResult=18497825&ordinalpos=3&itool=EntrezSystem2.PEntrez.Pubmed.Pubmed_ResultsPanel.Pubmed_RVDocSum

Ying, Q.-L., Wray, J., Nichols, J., Batlle-Morera, L., Doble, B., Woodgett, J., … Smith, A. (2008). The ground state of embryonic stem cell self-renewal. Nature, 453(7194), 519–523. https://doi.org/10.1038/nature06968

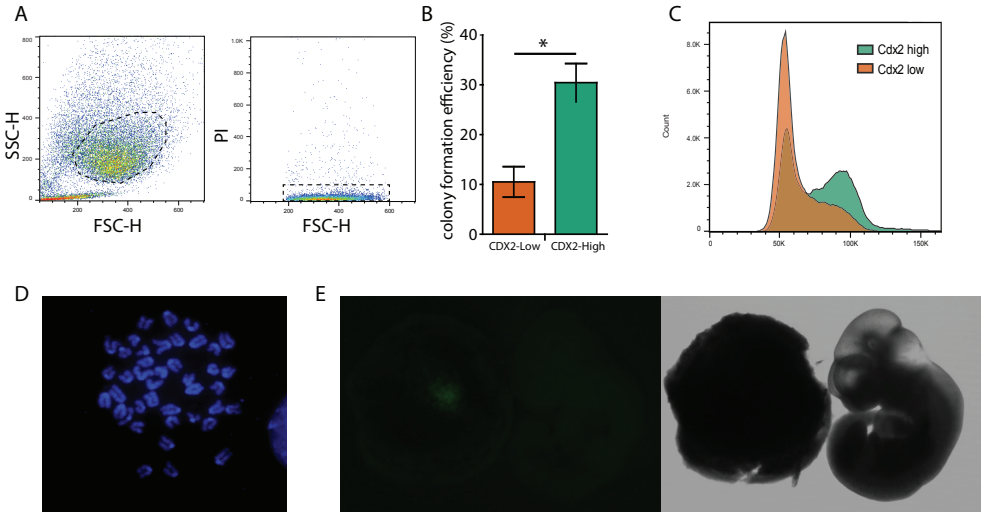

Supplementary Figure 1. A. FACS gating for sorting single TSCs from control and LT21 cultures. B. Colony formation efficiency for CDX2-Low and CDX2-High single cells from control TSC cultures. C. Cell cycle profile comparison of CDX2-Low and CDX2-High TSCs. D. Karyotype analysis of pTS1 plTSCs (directly derived in LT21 conditions) shows the presence of 41 chromosomes. E. F4 LT21 TSCs only contribute to placental tissue after blastocyst injection.

Supplementary table 1

Name of features	#rank	Mann-Whitney values	#rank	Random Forest values
Nuclei_AreaShape_Solidity	1	114.4134593	1	0.047666647
Nuclei_AreaShape_FormFactor	2	85.77308437	4	0.035880732
Cells_AreaShape_Area	3	60.8597356	5	0.030298684
Cells_AreaShape_MeanRadius	4	56.07635707	11	0.018049143
Cells_AreaShape_MedianRadius	5	55.71667553	2	0.036429672
Cells_AreaShape_MaximumRadius	6	54.88878982	3	0.036292954
Cells_AreaShape_MinorAxisLength	7	45.98750301	6	0.030079715
Nuclei_AreaShape_MeanRadius	8	45.41685043	26	0.008777346
Cells_AreaShape_MaxFeretDiameter	9	45.29149364	17	0.013923071
Nuclei_AreaShape_MaximumRadius	10	44.75493868	9	0.020887197
Cells_AreaShape_MinFeretDiameter	11	44.02120268	8	0.025655046
Nuclei_AreaShape_MedianRadius	12	42.65230807	21	0.010672371
Cells_AreaShape_MajorAxisLength	13	41.96066432	10	0.018863862
Cells_AreaShape_Perimeter	14	37.71342279	31	0.007283765
Nuclei_Intensity_MeanIntensityEdge_Cdx2_Nuclei_Mask	15	36.88557464	15	0.015813925
Nuclei_AreaShape_Extent	16	33.2015269	16	0.015319224
Nuclei_AreaShape_Zernike_0_0	17	31.95894481	13	0.016208277
Nuclei_Intensity_MaxIntensityEdge_Cdx2_Nuclei_Mask	18	31.64887363	7	0.026952022
Nuclei_AreaShape_Compactness	19	31.31272308	50	0.004886626
Nuclei_Texture_SumAverage_DAPI_3_00	20	30.17405985	18	0.011002888
Nuclei_Texture_SumAverage_DAPI_3_02	21	30.13523562	12	0.017296462
Nuclei_Texture_SumAverage_DAPI_3_03	22	30.04061233	14	0.015927028
Nuclei_Texture_SumAverage_DAPI_3_01	23	29.96316632	23	0.010288094
Nuclei_AreaShape_MinorAxisLength	24	28.02151391	78	0.003606652
Cells_Mean_Filtered_Nuclei_Distance_Centroid_Filtered_Cells	25	26.61063166	20	0.01075151
Nuclei_Intensity_MinIntensityEdge_Cdx2_Nuclei_Mask	26	26.58200334	27	0.008567637
Nuclei_Distance_Centroid_Filtered_Cells	27	26.09194903	19	0.010896094
Nuclei_Intensity_MinIntensity_Cdx2_Nuclei_Mask	28	25.97898202	25	0.008935692
Nuclei_AreaShape_Zernike_8_8	29	24.21385845	24	0.009337903
Nuclei_AreaShape_Zernike_4_2	30	21.24492987	22	0.010301858
Nuclei_AreaShape_Zernike_4_4	31	20.60321878	42	0.005552254
Nuclei_AreaShape_Zernike_4_0	32	20.55476905	28	0.00816355
Nuclei_AreaShape_Zernike_6_6	33	20.55094659	36	0.006143236
Nuclei_AreaShape_Area	34	20.4586872	68	0.003881279
Nuclei_AreaShape_MinFeretDiameter	35	19.84763707	64	0.003977091
Nuclei_AreaShape_Zernike_3_1	36	18.56361166	30	0.007410389
Nuclei_AreaShape_Zernike_9_7	37	15.88768592	33	0.006325626
Nuclei_AreaShape_Eccentricity	38	15.88434307	29	0.007517246
Nuclei_Intensity_LowerQuartileIntensity_Cdx2_Nuclei_Mask	39	15.0242867	34	0.006265078
Nuclei_Intensity_StdIntensityEdge_Cdx2_Nuclei_Mask	40	14.09201737	41	0.005600092
Nuclei_Intensity_MeanIntensity_Cdx2_Nuclei_Mask	41	13.43977296	35	0.006155201
Nuclei_Intensity_MedianIntensity_Cdx2_Nuclei_Mask	42	12.11737986	32	0.007137528
Nuclei_Intensity_IntegratedIntensity_Cdx2_Nuclei_Mask	43	12.10264162	107	0.003023611
Nuclei_Intensity_UpperQuartileIntensity_Cdx2_Nuclei_Mask	44	10.97029805	39	0.005824278
Nuclei_AreaShape_Zernike_8_4	45	10.6821253	57	0.004455593

Name of features	#rank	Mann-Whitney values	#rank	Random Forest values
Nuclei_AreaShape_Zernike_7_5	46	9.771310093	96	0.00319759
Nuclei_AreaShape_Zernike_9_9	47	9.453245313	38	0.00597094
Nuclei_Intensity_MaxIntensity_Cdx2_Nuclei_Mask	48	9.257184705	45	0.005283245
Nuclei_Texture_DifferenceVariance_DAPI_3_00	49	8.59130945	92	0.003242793
Nuclei_Texture_DifferenceVariance_DAPI_3_01	50	8.388057028	138	0.002540258
Cells_AreaShape_FormFactor	51	8.378518951	37	0.006070457
Nuclei_Texture_DifferenceVariance_DAPI_3_02	52	7.879003002	52	0.004832295
Nuclei_Texture_Variance_DAPI_3_01	53	7.824516902	76	0.00369913
Nuclei_Texture_Variance_DAPI_3_03	54	7.764892936	69	0.003852078
Nuclei_Texture_SumVariance_DAPI_3_01	55	7.705513914	104	0.003062392
Nuclei_Texture_SumVariance_DAPI_3_03	56	7.668336956	102	0.003071898
Nuclei_Texture_Variance_DAPI_3_00	57	7.575440901	151	0.002235395
Nuclei_Texture_Variance_DAPI_3_02	58	7.520595308	129	0.002663331
Nuclei_Texture_DifferenceVariance_DAPI_3_03	59	7.513098907	54	0.004681073
Nuclei_Texture_SumVariance_DAPI_3_02	60	7.40113551	124	0.002777064
Nuclei_Texture_SumVariance_DAPI_3_00	61	7.387760701	118	0.002880118
Nuclei_Texture_DifferenceEntropy_DAPI_3_00	62	6.981760075	58	0.004455588
Nuclei_AreaShape_Zernike_7_3	63	6.710203981	55	0.004609087
Nuclei_Texture_Contrast_DAPI_3_00	64	6.667267094	90	0.003269112
Nuclei_Texture_DifferenceEntropy_DAPI_3_01	65	6.637089725	89	0.003301856
Nuclei_Texture_InverseDifferenceMoment_DAPI_3_00	66	6.507408346	63	0.004009984
Nuclei_Texture_DifferenceEntropy_DAPI_3_02	67	6.353071796	97	0.003175969
Nuclei_AreaShape_Zernike_1_1	68	6.124660023	84	0.003375942
Nuclei_Texture_Contrast_DAPI_3_02	69	6.117951594	119	0.002849608
Nuclei_Texture_Contrast_DAPI_3_01	70	6.063760593	121	0.002825061
Nuclei_Texture_InverseDifferenceMoment_DAPI_3_01	71	6.013153069	136	0.002603564
Nuclei_Texture_DifferenceEntropy_DAPI_3_03	72	5.884359962	71	0.003807639
Nuclei_Texture_InverseDifferenceMoment_DAPI_3_02	73	5.833267697	73	0.003740545
Cells_AreaShape_Solidity	74	5.648005503	46	0.00517327
Nuclei_Texture_InverseDifferenceMoment_DAPI_3_03	75	5.612751966	152	0.002191413
Nuclei_Texture_Contrast_DAPI_3_03	76	5.51024788	79	0.003597744
Nuclei_Texture_Entropy_DAPI_3_00	77	5.379347968	142	0.002390912
Nuclei_Texture_SumEntropy_DAPI_3_01	78	5.280445643	158	0.001663443
Nuclei_Texture_Entropy_DAPI_3_01	79	5.216913185	153	0.002109374
Nuclei_Texture_SumEntropy_DAPI_3_03	80	5.180710674	156	0.001922681
Nuclei_Texture_Entropy_DAPI_3_02	81	5.142206384	95	0.003198572
Nuclei_Texture_InfoMeas1_DAPI_3_00	82	5.03969532	105	0.003024319
Nuclei_Texture_Entropy_DAPI_3_03	83	4.899033329	125	0.002718367
Nuclei_Texture_SumEntropy_DAPI_3_02	84	4.771088746	159	0.001510044
Nuclei_Texture_SumEntropy_DAPI_3_00	85	4.708687059	150	0.002245757
Nuclei_Texture_AngularSecondMoment_DAPI_3_01	86	4.582379465	148	0.002279288
Nuclei_Texture_AngularSecondMoment_DAPI_3_00	87	4.559514306	146	0.002315654
Nuclei_AreaShape_Zernike_5_3	88	4.546965407	65	0.003965135
Nuclei_AreaShape_Zernike_9_5	89	4.508298746	48	0.004965141
Nuclei_AreaShape_Zernike_7_7	90	4.472073354	86	0.003355799

Name of features	#rank	Mann-Whitney values	#rank	Random Forest values
Nuclei_Texture_AngularSecondMoment_DAPI_3_02	91	4.233968167	117	0.002887102
Nuclei_Texture_AngularSecondMoment_DAPI_3_03	92	4.223018247	131	0.002637241
Nuclei_Texture_InfoMeas1_DAPI_3_02	93	4.209899124	108	0.003006287
Nuclei_AreaShape_MaxFeretDiameter	94	3.950692045	59	0.004386371
Nuclei_AreaShape_Perimeter	95	3.753959586	44	0.005341848
Nuclei_AreaShape_MajorAxisLength	96	3.655551055	47	0.005045796
Nuclei_AreaShape_Zernike_6_2	97	3.639921351	49	0.00489988
Nuclei_Texture_InfoMeas1_DAPI_3_01	98	3.554877075	67	0.003899514
Nuclei_AreaShape_Zernike_2_0	99	3.532058923	81	0.003499372
Nuclei_Texture_InfoMeas1_DAPI_3_03	100	2.870737075	145	0.002316226
Cells_AreaShape_Zernike_8_8	101	2.722809417	106	0.003024232
Nuclei_AreaShape_Zernike_5_5	102	2.697242862	91	0.003245544
Cells_AreaShape_Zernike_8_0	103	2.602179806	144	0.002329206
Nuclei_AreaShape_Zernike_2_2	104	2.482649842	53	0.004719766
Nuclei_Texture_InfoMeas2_DAPI_3_00	105	2.435501049	98	0.003169525
Nuclei_AreaShape_Zernike_7_1	106	2.276693737	66	0.003901904
Nuclei_Texture_InfoMeas2_DAPI_3_02	107	2.225385037	83	0.00338507
Cells_AreaShape_Zernike_2_2	108	2.151184001	85	0.003369025
Nuclei_AreaShape_Zernike_8_2	109	2.043162894	72	0.003784586
Cells_AreaShape_Zernike_9_3	110	1.843628112	139	0.002464026
Nuclei_Texture_InfoMeas2_DAPI_3_01	111	1.819192476	75	0.003714064
Nuclei_AreaShape_Zernike_6_0	112	1.808730761	82	0.003454352
Nuclei_AreaShape_Zernike_3_3	113	1.782231156	40	0.005758443
Cells_AreaShape_Zernike_2_0	114	1.712258202	128	0.002677801
Nuclei_Intensity_MADIntensity_Cdx2_Nuclei_Mask	115	1.536775852	74	0.003721226
Nuclei_AreaShape_Zernike_6_4	116	1.534756259	134	0.002609374
Nuclei_Texture_InfoMeas2_DAPI_3_03	117	1.489930307	127	0.002690744
Cells_AreaShape_Zernike_6_0	118	1.446193882	157	0.001921556
Nuclei_Texture_Correlation_DAPI_3_02	119	1.350002592	137	0.002571667
Nuclei_Texture_Correlation_DAPI_3_00	120	1.307974073	116	0.002887153
Cells_AreaShape_Compactness	121	1.10831229	154	0.002023836
Nuclei_AreaShape_EulerNumber	122	1.066932678	160	0
Cells_AreaShape_Zernike_6_4	123	1.045975548	141	0.002419615
Cells_AreaShape_Zernike_7_5	124	1.021948918	135	0.002605692
Cells_AreaShape_Zernike_4_2	125	1.007225832	94	0.003219059
Cells_AreaShape_Zernike_5_3	126	0.948515415	88	0.00331025
Cells_AreaShape_Zernike_5_1	127	0.94806003	133	0.002610832
Nuclei_AreaShape_Zernike_9_1	128	0.930856429	43	0.005414329
Nuclei_Intensity_StdIntensity_Cdx2_Nuclei_Mask	129	0.918529051	60	0.004149195
Nuclei_Texture_Correlation_DAPI_3_01	130	0.872619691	56	0.004504075
Cells_AreaShape_Zernike_8_2	131	0.851599995	77	0.003677443
Cells_AreaShape_Zernike_3_1	132	0.826508831	103	0.003065163
Cells_AreaShape_Zernike_8_6	133	0.783784885	62	0.004012852
Cells_AreaShape_Zernike_7_3	134	0.76157102	132	0.002633205
Cells_AreaShape_Zernike_3_3	135	0.748947267	143	0.002333616

Name of features	#rank	Mann-Whitney values	#rank	Random Forest values
Cells_AreaShape_Zernike_4_0	136	0.74054111	111	0.002977768
Nuclei_AreaShape_Zernike_8_0	137	0.71112037	110	0.002989555
Nuclei_AreaShape_Zernike_9_3	138	0.698476357	122	0.002810464
Nuclei_Texture_Correlation_DAPI_3_03	139	0.642212003	93	0.00322298
Cells_AreaShape_Eccentricity	140	0.603361992	99	0.003156961
Cells_AreaShape_Zernike_9_1	141	0.537734547	109	0.003002378
Cells_AreaShape_Zernike_7_7	142	0.532055097	115	0.00288769
Nuclei_AreaShape_Zernike_5_1	143	0.523299118	120	0.002839024
Cells_AreaShape_Zernike_9_5	144	0.483891834	100	0.003107655
Cells_AreaShape_Zernike_5_5	145	0.470868868	61	0.0040868
Nuclei_AreaShape_Zernike_8_6	146	0.460505764	112	0.002977114
Cells_AreaShape_Zernike_9_9	147	0.428968707	126	0.002703467
Cells_AreaShape_Orientation	148	0.391694612	149	0.002258161
Cells_AreaShape_Zernike_0_0	149	0.387990349	140	0.002441015
Cells_AreaShape_Zernike_7_1	150	0.366507522	123	0.002803583
Nuclei_Intensity_IntegratedIntensityEdge_Cdx2_Nuclei_Mask	151	0.365650774	113	0.002970692
Cells_AreaShape_Zernike_6_6	152	0.358604439	70	0.003820158
Cells_AreaShape_Zernike_8_4	153	0.343500263	80	0.003546406
Cells_AreaShape_Zernike_6_2	154	0.335018587	114	0.002910697
Cells_AreaShape_Extent	155	0.331575038	51	0.004852373
Cells_AreaShape_Zernike_1_1	156	0.330889259	130	0.002653883
Nuclei_Intensity_MassDisplacement_Cdx2_Nuclei_Mask	157	0.330889259	147	0.002312949
Cells_AreaShape_Zernike_9_7	158	0.324085024	87	0.00334513
Cells_AreaShape_Zernike_4_4	159	0.31494261	155	0.001939869
Nuclei_AreaShape_Orientation	160	0.302960226	101	0.003090091

Supplementary table 2 . Genes differentially expressed between Lt21 and Ctr cultures. Genes in read are up regulated in Ctr culture. Genes in black are upregulated in Lt21 cultured cells.

1600014K23Rik	Cldn25	Fxyd6	Ndel1	Slco2a1	Ascl2	Nr0b1
1600029D21Rik	Cldn4	Galnt1	Nid1	Smox	Bmp4	Nrp2
2310067B10Rik	Cldn6	Glrx	Nudt4	Smtn	Calca	Ntf3
AI836003	Clic4	Glul	Nufip1	Snrk	Capn6	Ogt
Aard	Cmtm8	Gm10845	Osgin1	Socs3	Car12	Peg10
Abcb1b	Cntfr	Gm19757	P4hb	Sox17	Casz1	Pfdn4
Abhd6	Col4a1	Gprc5a	Pcsk6	Sox3	Cdc14b	Phlda2
Acan	Col4a2	Grip1	Pdlim1	Sox9	Cdkn1c	Plcg2
Acot7	Copa	Gsto1	Pex26	Sparc	Cited1	Pnpt1
Acpp	Coq10b	Hilpda	Phlda1	Spop	Cse1l	Pygl
Acsbg1	Creb3l2	Hspb1	Pianp	Src	Dgat2	Rae1
Acvr1	Crim1	Igf2	Pim1	Srgn	Dkk1	Rbm38
Ada	Csnk1e	Igfbp4	Pitpnc1	St3gal2	Dkkl1	Rian
Ahnak	Ctla2a	Il11	Plin2	Stard8	Dram1	Rnf114
Akap2	Ctsb	Iqgap1	Pmepa1	Surf4	Epb4.1l2	Rps6ka6
Ano6	Ctsj	Irx1	Prl2a1	Suv39h1	Esx1	Sema5a
Antxr2	Cttnbp2nl	Itga3	Prl7a1	Tes	Fam49a	Shmt1
Anxa2	Cyb5r3	Itgav	Prl8a9	Tfpi	Fbxo21	Slc12a7
Aplp2	Cyp11a1	Itgb3	Pros1	Thbd	Gata2	Slc25a12
Arhgap23	Dab2	Itm2b	Proser2	Tjp2	Gdf6	Slc2a3
Arrdc4	Dcaf12l1	Jam2	Prph	Tmbim6	Gga2	Slc40a1
Atf3	Dctn1	Jund	Prss46	Tmem2	Gjb2	Sorl1
Atp11a	Dmd	Kank1	Psap	Tmsb10	Gldc	Sox2
Atp6v0a1	Dpp9	Klf5	Pvr	Tmsb4x	Gm14295	Stau1
Atxn1	Dppa2	Klf6	Pwwp2b	Tns3	Gsta4	Tex15
Atxn7l1	Dst	Klf9	Rabac1	Tns4	Gstm2	Timp3
Axl	Duoxa2	Krt18	Rap2b	Tomm6	H19	Vnn1
B4galt1	Dusp10	Krt8	Rgs16	Tph1	Hes1	Wls
Basp1	Dusp1	Lad1	Rhou	Tpm4	Hmox1	Zfp771
Bcar3	Efhd1	Lama3	Rhox13	Tsc22d1	Hs3st3b1	
Bhlhe40	Efhd2	Lamc2	Rpl22	Tusc1	Igf2bp2	
Btg1	Elovl7	Lgals3	Rtp3	Ube2h	Igfbp2	
Btg2	Emp1	Litaf	S100a10	Unc5b	Ireb2	
C430049B03Rik	Errfi1	Lmna	S100a6	Upp1	Itih5	
Cald1	Fam129b	Ly6a	Sat1	Vgf	Jam3	
Capns1	Fam214a	Ly6e	Sbno2	Wisp1	Klhl13	
Cd24a	Fat1	Mafk	Sema6a	Wnk1	Ldhb	
Cd44	Fdft1	Mal	Sept11	Zyx	Lpl	
Cd55	Fez2	Map1lc3b	Serinc2	2810008D09Rik	Meg3	
Cdc42ep3	Fn1	Mdfic	Serpinb9e	3830417A13Rik	Mei04	
Cdc42ep5	Fosl2	Mfge8	Serpine1	AU015836	Mid1ip1	
Cdkn1a	Foxl2	Mgat4a	Sft2d2	Aldoc	Mirg	
Cenpm	Foxo4	Msn	Sgk1	Alg13	Nat8l	
Cgnl1	Foxq1	Myof	Slc20a1	Alox15	Ncoa3	
Cited2	Furin	Ncrna00086	Slc38a6	Apoe	Nme4	

5

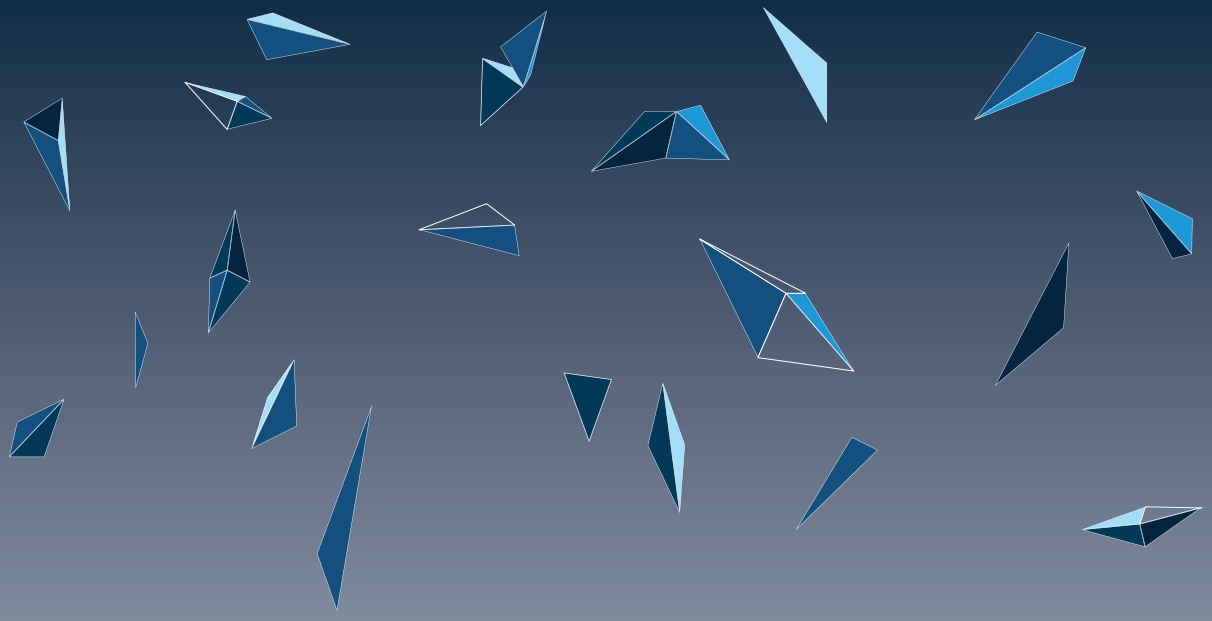

Chapter 6.
Blastoids recapitulate aspects of the TE axis

6.1 Abstract

The trophectoderm (TE) of the mouse blastocyst mediates the attachment into the uterus at the peri-implantation stage (E4.5). For the TE to fulfil its functions, both mural and TE need to diverge phenotypically, with the mural TE initiating attachment to the endometrium and the polar TE being responsible for maintaining the stem cell pool, further invasion and differentiation into all the trophoblast derivatives. The phenotypical differences between mural and polar TE are thus necessary for a successful implantation. While there are multiple reports claiming those differences to exist in terms of proliferation, the molecular signatures of these states and the role of embryonic inductions are poorly defined. Based on transcriptomics data from in vitro cultured polar-like Trophoblast Stem Cells (plTSCs), tomo-sequencing and smFISH of e3.5 blastocysts, we established the molecular basis of the divergent phenotypes between the mural and polar TE, aspects of which blastoids from plTSCs recapitulated.

6.2 Introduction

The polar and mural TE cells that define the first axis of the conceptus have been proposed to display divergent identities based on their mitotic indexes (Gardner, 2000). However, the molecular signatures of these states are poorly defined. Only recently single cell sequencing analysis was applied to the TE of 4.5 blastocysts (Nakamura et al., 2015), results that were able to answer some of the questions regarding the different identities of polar and mural TE. In prior chapters we developed new culture conditions capable of converting Tx cultured TSCs into a state with enhanced stem cell properties. We termed these new cells plTSCs, cells that show higher self-renewal, a more homogeneous and more epithelial phenotype, a more efficient differentiation dynamics, a high potential for in vivo chimerization of the placenta, and a more efficient propensity to cross-talk with ESCs and form bastoids.
In this chapter we focus on investigating the transcriptional state of plTSCs and use this to find new potential markers of a trophoblast undifferentiated state. Together with plTSCs transcriptomics, we will make use of tomo-sequencing of E3.5 blastocysts with the purpose of finding new polar TE markers. Such markers for undifferentiated and polar TE will serve as guide in order to investigate if blastoids obtained from plTSCs show TE axis formation.

6.3 Results

6.3.1 plTSCs RNA sequencing and blastocyst tomo-sequencing reveal molecular signatures of the polar-to-mural axis.

Here, we first used multiple bulk RNA sequencing datasets to infer the transcriptome of these TE states. We reasoned that most polar genes would be (i) downregulated upon a 6 day differentiation process of TSCs or plTSCs (1706 genes with fold change>2 p value<0.05), (ii) upregulated in the plTSCs culture (TSCs cultured in LT21) (237 genes with fold change>2 p value<0.05), while (iii) being expressed in the TE of blastocysts. For this we used an available data set from a prior publication (Nakamura et al., 2015), which detected 16438 genes in single TE cells after RaceID clustering analysis (Grun et al., 2016). These criteria led to 108 putative polar-specific genes (**Sup. Fig. 1**). One of those genes was Ly6a, previously reported to be a marker for trophoblast progenitors in later stages of development (Natale et al., 2017).

We then used the tomo-sequencing method (Junker et al., 2014) to sequence slices of blastocysts along the polar-to-mural axis (**Fig. 1A**). A E3.5 blastocyst was embedded in a polar-to-mural orientation in 2% gelatin and sectioned. Each slice was processed for RNA extraction separately and sequenced.
We first determined in which sections we could detect blastocyst material. This was assessed first by plotting the number of transcripts detected per section (**Sup. Fig. 1A**), which allowed us to select the sections (red line in x axis) including blastocyst material. For one of the sections we could detect only a low number of transcripts in comparison to the adjacent sections (marked with a star) and thus was removed from further analysis.
We used Sox2 as a marker for establishing which sections contained ICM transcripts (**Fig. 1B**). Other markers (Gata6, Krt8 and Eomes) confirmed the correct orientation of the blastocyst at the time of sectioning. Interestingly, Gata6 showed a higher expression in two alternate sections within the ICM, presumably showing the salt and pepper distribution of PrE and Epiblast cells. Of note, the sections including ICM, included also transcripts from the polar region of the TE. Therefore, TE sections were normalized differently than the sections with ICM and TE (details in methods).
We could find very different expression patterns that prove how the TE is indeed formed by cells with divergent identities depending on their location.
The genes following different expression patterns were cross-referenced with prior potential mural or polar markers suggested by Bulk sequencing. We could confirm that Krt8 and Krt18 (**Fig. 1C**), traditional markers for TE, show a higher expression in the mural region of the TE, representing a marker for partial differentiation. We could also confirm an anti-correlation between these cytokeratins and CDX2 in control and cultures of plTSCs (**Fig. 1D**). Gata2 showed a similar expression pattern reaching it expression peak in the most mural section (**Sup. Fig 1B**). Gata2 had already been suggested to be a marker of the mural TE of E4.5 blastocysts (Nakamura et al., 2015). Interestingly, when evaluating the expression pattern of Eomes, our data suggested it to peak in most mural section, which would confirm its role in stages after commitment. We then used smFISH to confirm Eomes expression distribution in E3.5 blastocysts (**Fig. 1E**). This gene was indeed preferentially mural in 3 out of the 4 blastocysts analyzed (**Fig. 1F**).
Tomo-seq data can be used for finding new potential polar TE markers as well as markers of differentiated states. In order to elaborate a list of potential markers we cross-referenced tomo-seq data with our bulk sequencing dataset. Sox2 was considered as a marker for higher expression in the polar half of the TE. When cross-referencing the top 1000 genes following the Sox2 expression pattern with genes dropping upon differentiation of cultured TSC and upregulated in plTSCs cultures compared to control cultures, we obtained 108 genes that could potentially serve as polar markers of the E3.5 trophectoderm (**Sup. table 1**). This list of genes includes genes such as Epcam, Jam2, Upp1, Furin, Klf5, Cldn6, Dppa2, Sox9, Ly6a or Sparc. These genes require validation by smFISH.
Deep sequencing of tomo-seq sections from different, precisely timed pre-implantation blastocyst (E3.25, E3.5, E3.75, E4, E4.25, E4.5), would help us better understand the dynamics of TE axis formation.

6.3.2 Blastoids formed using plTSCs generate aspects of the polar-to-mural axis.

With the purpose of better investigate the transcriptional signature of plTSCs, we performed single cell sequencing. The transcriptome of single plTSCs was compared to single cells from

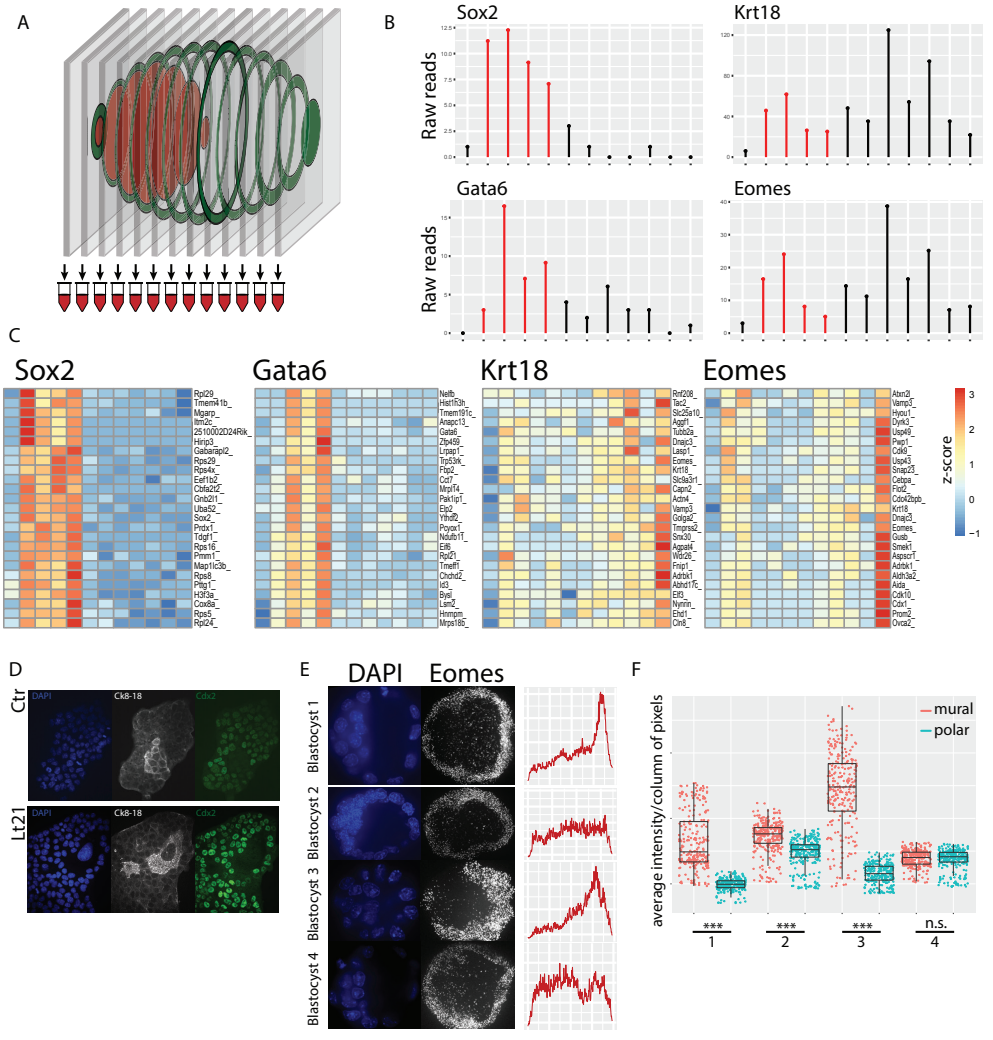

Figure 1. Blastocyst tomo-sequencing allows for finding polarized TE markers. A. Schematic of tomo-sequencing sectioning strategy. B. Raw reads detected for key markers of the ICM, PrE and TE. C. Using key blastocyst markers we can find other genes following similar expression trends across sections. D. TSCs cultured in control and LT21 conditions stained for CDX2 and KRT8/18. E. smFISH for Eomes on E3.5 blastocysts (left and mid) and intensity profile of the z-stack projection (right). F. Jitter plot comparing the average pixel intensity for the most polar and mural segment of the blastocyst.

control and differentiated cultures using monocle (Trapnell et al., 2014).
Monocle locates plTSCs in the opposite end of the trajectory in relation to the differentiated cells (**Fig. 2A**). Interestingly, monocle clusters the cells from control culture into 3 separate subpopulations: one subpopulations clustering with a set of differentiated cells, another subpopulation clustering with the plTSCs and a third subpopulation forming a separate cluster (**Fig. 2B**). This supports our previous observation suggesting that the control culture allows for a wide range of differentiation states. We speculate that the subpopulation of TSCs orig-

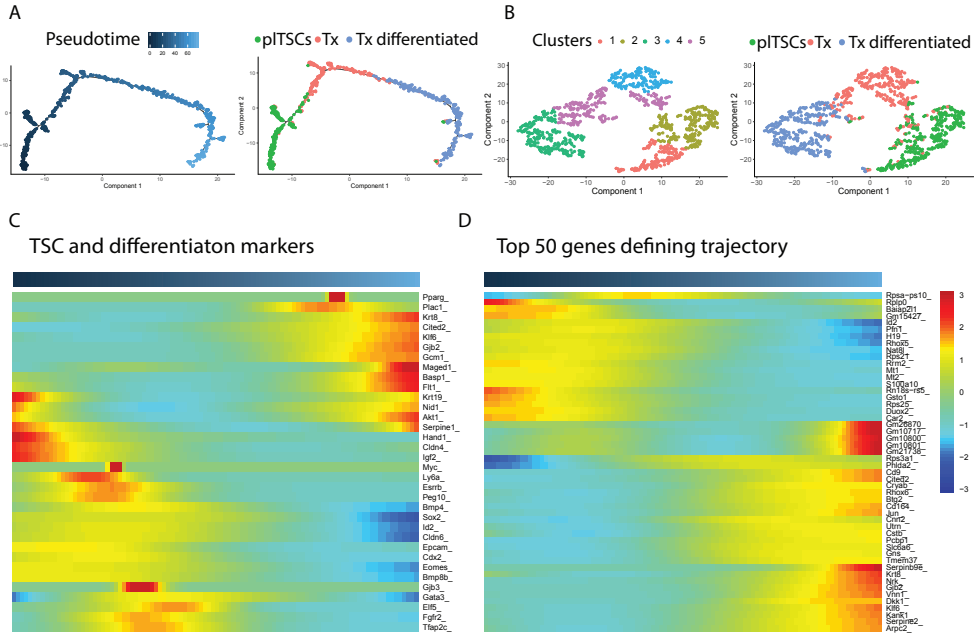

Figure 2. Single cell transcriptome analysis of plTSCs as compared to control and differentiated TSCs. A. Pseudotime trajectory suggested by monocle. B. Clustering analysis of the three cultures obtained from monocle. C. Classical markers of trophoblast differentiated and undifferentiated states plotted against pseudotimes. D. Top 50 genes defining the pseudotime trajectory.

inating from classical culture condition and clustering with a subpopulation of the plTSCs might represent the most potent TSCs, possibly with in vivo potential. The plotting of classical markers for undifferentiated and differentiated trophoblasts confirmed the directionality of the pseudotime values (**Fig. 2C**). We also extracted, in an unbiased way, the top genes defining that trajectory (**Fig. 2D**). Amongst the 50 genes that describe best that trajectory, we found Duox2 and Gsto1. These two genes have been previously reported to be markers for bona fide TSCs (Kuales, Weiss, Sedelmeier, Pfeifer, & Arnold, 2015) and for the polar TE of 4.5 blastocysts (Nakamura et al., 2015). A set of pseudogenes (Gm26870, Gm10717, Gm10800, Gm10801 and Gm21738) show a higher expression with higher pseudotimes. Our results suggest again Krt8 to be upregulated in differentiated cells. Differentiation markers such as Cited2, Gjb2 and Nrk (Imakawa et al., 2016; Morioka, Nam, & Ohashi, 2017; Sood, Kalloway, Mast, Hillard, & Weiler, 2006) peaked at higher pseudotime values as well.

These results suggest that plTSCs are in a more undifferentiated state, showing and revealing stem markers differentially expressed as compared to control and differentiated populations. We then wondered if blastoids formed an axis recapitulating aspects of the gene expression pattern along the polar to mural TE.

Although single cell sequencing can give us candidate genes following the trends we aim to investigate, single molecule FISH is a far more sensitive technique that can allow us to better investigate gene expression patterns. We chose Ly6a, a gene shown to be enriched in plTSCs, both in bulk (**Chapter's 5 Fig. 3C**) and in single cells showing a single peak in pseudotime progressions (**FIg. 2C**). Ly6a was also previously proposed to mark stem cells in later stages

(Natale et al., 2017).
E3.5 blastocysts were used for assessing polarity using smFISH probe sets against Ly6a and Cdx2. Confocal images were taken with a z-step of 0.3 μm. Given the complexity of an analysis performed in 3 dimensions that would require an algorithm capable of segmenting cells and quantifying the number of transcripts in 3D, we decided to quantify a 2 dimension projection of the slices that included the ICM and blastocoel. Those z-stack projections were oriented with polar side at the left and mural side at the right and they were then analyzed for average column pixel intensity, allowing us to plot an average pixel intensity histogram (**Fig. 3A**). An intensity profile was plotted for each embryo and gene (**Fig. 3B**). Each blastocyst is structurally different showing distinct cavity sizes, which implies that a different percentage of the TE is in contact with the ICM for each embryo. In order to compare the expression of polar and mural TE, we then divided the length of the embryo in three segments of equal distance, irrespective of the total diameter. The intermediate segment was considered a transition stage between those theoretical two identities in the TE and therefore was not included in the next analyses. The polar and mural segments of the profile were analyzed by comparing the average pixel intensities of each pixel column included in the segment (**Fig 3D**). E3.5 blastocysts showed a preferential expression for Ly6a in the polar TE (3/3), while Cdx2 did not show a consistent differential expression (1/3 polar, 1/3 mural). We concluded that the expression of Ly6a is higher in the polar region at E3.5. Despite a clearly higher expression of the protein CDX2 in the polar region of E3.5+0.25 blastocysts (**Chapter 2 Fig. 1A**), the RNA is not polarized at E3.5. It is worth mentioning, that images for both genes show some transcript expression within the ICM, but also that noise comes from the blastocoel. This means that a more efficient way of quantifying such differential expression is needed.
When blastoids were used for the same approach (**Fig. 3C and 3E**), Ly6a showed a clear polar TE preferential expression (10/10), while Cdx2 showed polar preference in 7/10 embryos and mural preference in 1/10. These results suggest that blastoids are capable of displaying the TE axis formation as observed between E3.5 and E4.0.
When cultured in monolayers, plTSCs differentiated faster than cell in control cultures. It is therefore possible that in blastoids, trophoblasts from plTSC cultures also more prone to form the TE axis while away from the embryonic inductions. Based on these observations, we concluded that the TE of the blastoids is patterned and of an equivalent to a stage later than E3.5. This hypothesis is supported by our Cdx2 polarity analysis on E4.5 blastocysts, where all embryos analyzed showed a preferential polar expression (**Fig. 3F**).
This data confirms that blastocysts and blastoids form a TE axis noticeable as early as E3.5.

6.3.3 Transcriptome analysis of plTSCs from blastoids confirms the blastoids to form a TE axis.

In order to better understand the TE axis formation in blastoids, single cells sequencing was performed on trophoblasts after blastoids formation and dissociation (**Fig. 4A**). Such blastoids were formed using H2B-RFP ESC and GFP plTSCs in order to allow for FACS sorting of trophoblasts only.
Monocle (Trapnell et al., 2014) organized the cells into a pseudotime trajectory (**Fig. 4B**) and grouped the cells into three clusters (**Fig. 4C**). Cluster 3 is composed by few cells and according to the pseudotime values (**Fig. 4D**), it appears to be a transition between the states groups in clusters 1 and 2. Differential gene expression comparing clusters 1 and 2 revealed a set of genes that monocle used for clustering (**Sup. table 2** and **Sup. Fig. 2**).

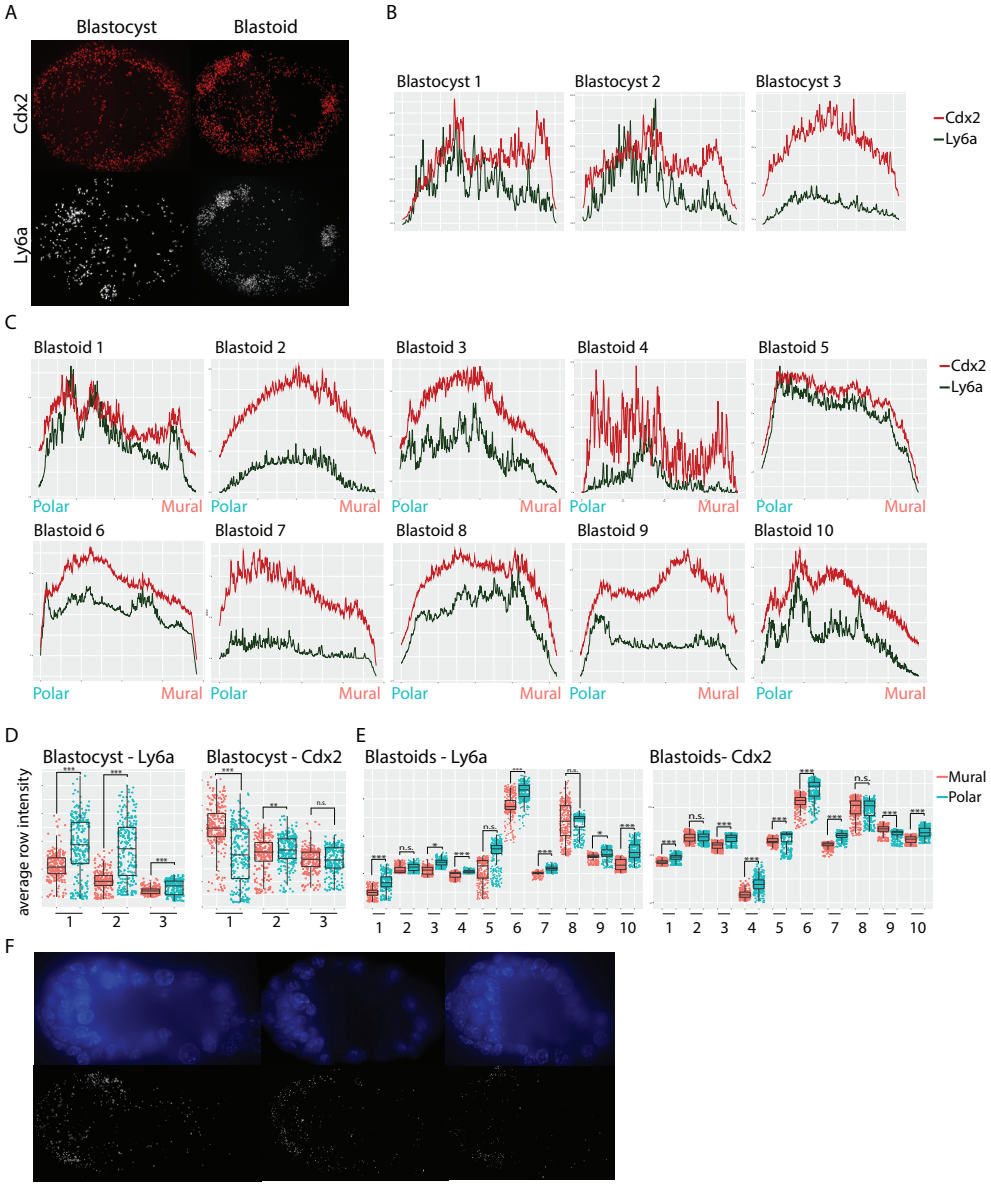

Figure 3. Ly6a is polarized on both blastoids and e3.5 blastocysts. A. smFISH simultaneously performed for Ly6a and Cdx2 detection on e3.5 blastocysts and 65 hour blastoids from plTSCs. B. Average column intensity profile for the three blastocysts analyzed for Cdx2 and Ly6a. C. Average column intensity profile for the 10 blastoids analyzed for Cdx2 and Ly6a. D. Jitter plot comparing the polar and mural segments of each blastocyst. E. Jitter plot comparing the polar and mural segments of each blastoid. For D and E: Each dot represents the value of average intensity for one column of pixels. In coral color all the pixel columns included in the mural segment and in blue those in the polar segment. Significance assessed by two-tailed unpaired t-test . *** for pvalue<0.001 and * for pvalue<0.05. F. smFISH for CDX2 transcript detection on e4.5 blastocysts.

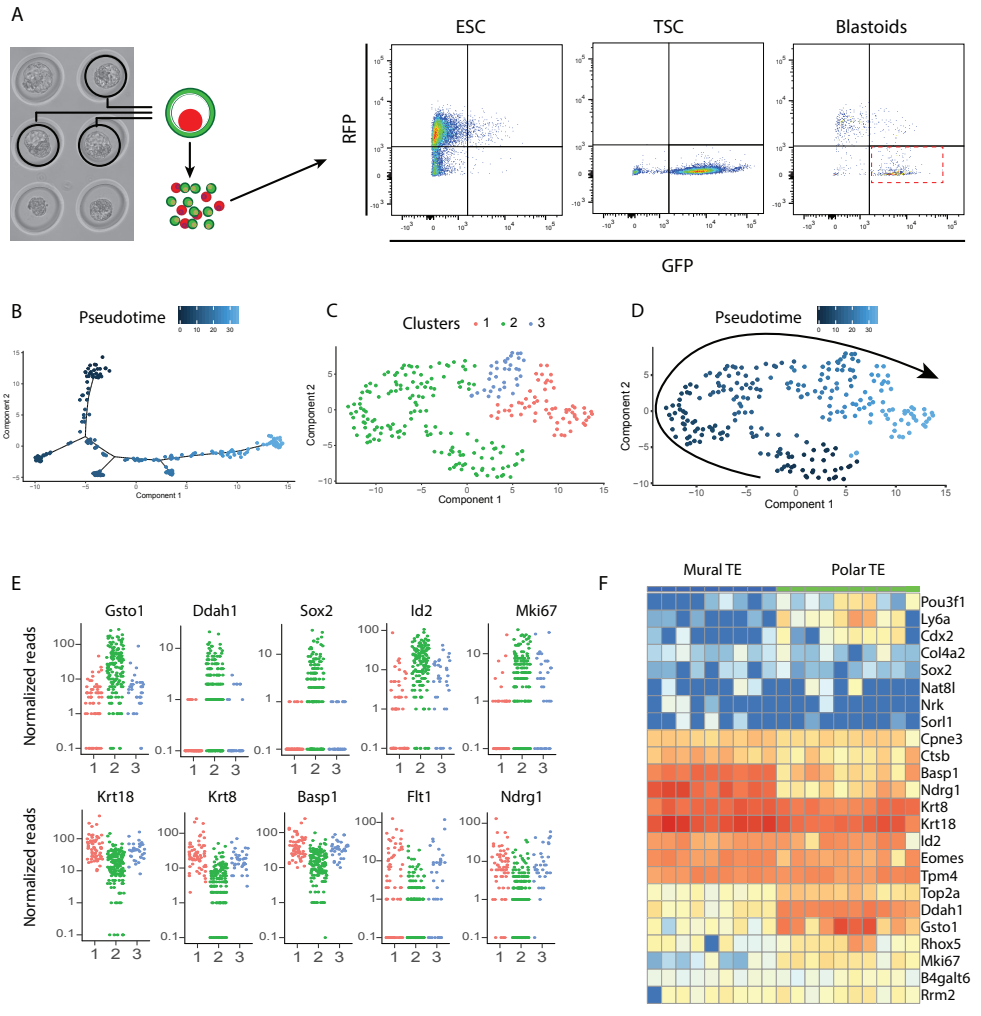

Figure 4. Blastoids from plTSCs show TE axis formation. A. After blastoid selection and dissociation, GFP cells are sorted into single 384 well plates for single cell sequencing. B. Monocle analysis on blastoid cells. C. t-SNE map of single cells grouped by clustering analysis. D. Monocle assigns low pseudotime values to cells in the cluster 2 and high pseudotime values to cells in cluster 1. The arrow indicates the direction of differentiation. E. Jitter plots for the expression of genes reported to be markers of the polar TE and for differentiation markers suggest cluster 2 to represent an undifferentiated population while cluster 1 is differentiating. Importantly, the proliferation marker Mki67 is also upregulated with cluster 2. These genes are found within the top50 differentially expressed genes between clusters 1 and 2. F. The top differentially expressed genes when comparing clusters 1 and 2 were plotted for the single cells obtained from polar and mural TE from Nakamura et al., 2015.

The genes Gsto1, Ddah1 and Utf1, previously reported to be markers of the polar TE of the 4.5 TE (Nakamura et al., 2015), showed a higher expression in cluster 2 (**Fig. 4E** and **Sup. Fig. 2**). Eomes, Sox2 and Id2 also confirm the cluster 2 to be more undifferenciated (**Sup. Fig 2**). Cluster 1 is characterized by higher expression of differentiation markers such as Flt1, Krt8,

Krt18, Ndrg1 (Shi, Larkin, Chen, & Sadovsky, 2013) or Nrk (Sood et al., 2006). Interestingly, mKi67, a marker of proliferation also showed up as upregulated in the cluster 2.
This data suggest that we can find two major subpopulations of trophoblasts isolated from blastoids, one showing a higher expression of markers of an undifferentiated state, and another one with higher expression of differentiation markers. We aimed for validating these two populations by looking at the expression of the polar marker Ly6a. However, this gene is expressed at low levels and its mRNA does not have a polyA tail, which is used as a recognition site to amplify the transcripts (Hashimshony et al., 2016). We thus failed to detect Ly6a in single cell RNA libraries obtained with Cel Seq 2. Differential genes expression confronting clusters 1 and 2 suggested a number of potential markers for studying TE axis formation in blastoids. Apart from the previously mentioned ones, the genes B4galt6, Cpne3, Duox2, Nat8l, Pou3f1, Ppp2r2c, Rhox5, Rrm2, Sorl1 or Top2a show upregulation in the putative polar cluster, while markers like Basp1, Ctsb, Ptsg2 or Slc5a5 were higher in the putative mural cluster. Most of these genes also show a differential expression between polar and mural cells within the E4.5 blastocyst TE (data from Nakamura et al.) (**Fig. 4F**).

6.4 Discussion

Our data confirms the formation of a TE axis noticeable as early as E3.5. Studying the transition between a relatively homogeneous TE and the different subpopulations of the peri-implantation TE would be extremely informative and could help us understand which pathways are involved in the TE axis formation. Blastoids manage to implant but fail to progress shortly after implantation. Blastoids formed from plTSCs seem to be able to form a trophoblastic axis that might result in more suitable extraembryonic compartment possibly capable of further supporting in utero development.
From our smFISH results, given that Cdx2 is polarized in blastoids and E4.5 blastocysts, but not in E3.5, we interpreted that blastoids from plTSCs might accentuate the axis formation or that their trophoblast are now corresponding to the TE of blastocyst later than E3.5. Some of the new markers we find to be polarized could serve us to evaluate the developmental equivalent of the trophoblast of a 65h polarized blastoid.

5.4 Materials and methods

• Cell culture.
TSC are cultured under Tx conditions followed a previously published protocol (Kubaczka et al., 2014). After coating with matrigel, cells are cultured in Tx media, which consists of phenol red free DMEM/F12 supplemented (phenol red-free, with l-glutamin), insulin (19.4 µg/ml), l-ascorbic-acid-2-phosphate (64 µg/ml), sodium selenite (14 ng/ ml), insulin (19.4 µg/ml), sodium bicarbonate (543 µg/ml), holo-transferin (10.7 µg/ml), penicillin streptomycin, FGF4 (25 ng/ml), TGFβ1 (2 ng/ml) and heparin (1 µg/ml). plTSCs were plated in laminin 521 coated plates (10 ug/ml diluted in PBS with Mg2+ and Ca2+) using Tx media supplemented with Il11 (50 ng/ml), Activin (50ng/ml), Bmp7 (25 ng/ml), LPA (5 nM) and 8Br-cAMP (200 nM) ESC were cultured under 2i conditions (Ying et al., 2008) in gelatin coated plates. Cells were routinely passaged using trypsin.

• Blastoid formation.

Full protocol can be found in https://www.nature.com/protocolexchange-/protocols/6579) Agarose microwell arrays were casted using the PDMS stamp and incubated O/N on mES serum containing media. After washing the chips with PBS, a ESC solution of 8000 cells/150 µl is dispensed in the central chip are and allowed to settle. After 15 minutes, an additional 1ml is dispensed. 20 hours later 1 ml of media is removed and a TSC/plTSCs solution of 22000 cells/150 ul is dispensed. After allowing the cells to fall in the microwells, 1 ml of blastoid media is added to the wells. Blastoid media includes 20 µM Y27632 (AxonMed 1683), 3 uM CHIR99021 (AxonMed 1386), 1 mM 8Br-cAMP (Biolog Life Science Institute B007E), 25 ng/ml Fgf4 (R&D systems 5846F4), 15 ng/ml Tgfb1 (Peprotech 100-21), 30 ng/ml Il11 (Peprotech 200-11) and 1 µg/ml heparin (Sigma-Aldricht cat# H3149). An additional dose of cAMP is dispensed 24 hours after TSC/plTSCs seeding. All measurements are performed 65 hours after TSC/plTSCs seeding.

• Blastoid Dissociation.
After blastoid formation, a large number of blastoids was selected based on their morphology (one uniform cavity, highly circular, comparable size to blastocysts and with presence of both ESC and TSC/plTSCs. Selected blastoids were incubated in collagenase (600u/ml) for 30 minutes at 37C in rocking conditions and then 3x TrypLE for another 20 minutes at 37C. After quenching the trypsin with soybean trypsin inhibitor, cells were sorted based on their RFP (ESCs) or GFP (plTSCs) expression on a FACSAria II. Cells were sorted on 384 well plates with each well containing different primer mixtures for further RNA extraction and sequencing.

• Single Cell Sequencing.
Single, live (Dapi negative) cells were sorted into 384 well plates containing 50 nl of Cel Seq primer and 5 ul of mineral oil to prevent evaporation. Libraries were obtained following a robotized version of the Cel Seq 2 protocol (Hashimshony et al., 2016). After sequencing, transcriptome analysis was performed on RStudio using the monocle pipeline (Trapnell et al., 2014). The dataset for studying mural and polar TE cells from the 4.5 blastocysts was downloaded from the Gene Expression Omnibus repository (GSE63266) (Nakamura et al., 2015). Those cells were analyzed using the monocle and RaceID pipelines (Grun et al., 2016; Grun, Kester, & van Oudenaarden, 2014)

• smFISH and Polarity analysis.
E3.5 blastocysts and 65h blastoids were subjected to smFISH using the Quantigene ViewRNA kit from thermofisher. smFISH images were acquired with a Z-step of 0.3 µm on a spinning disk Perkin-Elmer microscope. Only the stacks that included ICM and blastocoel were subjected to further analysis. The analysis was performed on the max Z-projection of those stacks in a polar to mural orientation. Intensity profile was obtained from those projections. Due to morphological differences across blastoids and a potential transition state between polar and mural phenotypes, only the polar and mural third were confronted.

• Blastocyst tomo-sequencing.
Blastocyst was embedded in 4% gelatin bock in an annotated orientation flanked by blue beads that serve as mark for starting sectioning. 8 µm sections were performed and embedded

in Trizol for further RNA extraction and further sequencing. Normalization was applied differently in sections containing the ICM. For those including the ICM, they were normalized according to the median of total transcripts detected in only ICM including sections, while TE only sections were compared t the median of total transcripts detected in only TE including sections.

Author contribution

Javier Frias Aldeguer generated the blastoids, performed the embedding and sectioning of blastocyst for tomo-seq, stainings, smFISH, quantified polarity and analyzed transcriptome expression. **Judith Vivié** performed RNA extraction and library preparation for single cells and tomo-seq sections. **Anna Alemany Arias** and **Annabel Ebbing** supplied the R scripts for transcriptome analysis. **Clemens van Blitterswijk** and **Niels Geijsen** helped to direct the project. **Nicolas Clement Rivron** conceived and directed the research. Data from single cells from E4.5 blastocysts was downloaded from Gene Expression Omnibus: GSE63266 (Nakamura et al., 2015).

5.6 Bibliography

Gardner, R. L. (2000). Flow of cells from polar to mural trophectoderm is polarized in the mouse blastocyst. Human Reproduction (Oxford, England), 15(3), 694–701.

Grun, D., Kester, L., & van Oudenaarden, A. (2014). Validation of noise models for single-cell transcriptomics. Nature Methods, 11(6), 637–640. https://doi.org/10.1038/nmeth.2930

Grun, D., Muraro, M. J., Boisset, J.-C., Wiebrands, K., Lyubimova, A., Dharmadhikari, G., … van Oudenaarden, A. (2016). De Novo Prediction of Stem Cell Identity using Single-Cell Transcriptome Data. Cell Stem Cell, 19(2), 266–277. https://doi.org/10.1016/j.stem.2016.05.010

Guryev, V., Peterson, K. A., Shah, G., Huisken, J., Junker, J. P., & Noe, E. S. (2014). Resource Genome-wide RNA Tomography in the Zebrafish Embryo. https://doi.org/10.1016/j.cell.2014.09.038

Hashimshony, T., Senderovich, N., Avital, G., Klochendler, A., de Leeuw, Y., Anavy, L., … Yanai, I. (2016). CEL-Seq2: Sensitive highly-multiplexed single-cell RNA-Seq. Genome Biology, 17(1), 1–7. https://doi.org/10.1186/s13059-016-0938-8

Imakawa, K., Dhakal, P., Kubota, K., Kusama, K., Chakraborty, D., Karim Rumi, M. A., & Soares, M. J. (2016). CITED2 modulation of trophoblast cell differentiation: insights from global transcriptome analysis. Reproduction (Cambridge, England), 151(5), 509–516. https://doi.org/10.1530/REP-15-0555

Kuales, G., Weiss, M., Sedelmeier, O., Pfeifer, D., & Arnold, S. J. (2015). A Resource for the transcriptional signature of bona fide trophoblast stem cells and analysis of their embryonic persistence. Stem Cells International, 2015, 17–20. https://doi.org/10.1155/2015/218518

Kubaczka, C., Senner, C., Ara??zo-Bravo, M. J., Sharma, N., Kuckenberg, P., Becker, A., … Schorle, H. (2014). Derivation and maintenance of murine trophoblast stem cells under defined conditions. Stem Cell Reports, 2(2), 232–242. https://doi.org/10.1016/j.stemcr.2013.12.013

Morioka, Y., Nam, J.-M., & Ohashi, T. (2017). Nik-related kinase regulates trophoblast proliferation and placental development by modulating AKT phosphorylation. PloS One, 12(2), e0171503. https://doi.

org/10.1371/journal.pone.0171503

Nakamura, T., Yabuta, Y., Okamoto, I., Aramaki, S., Yokobayashi, S., Kurimoto, K., … Saitou, M. (2015). SC3-seq: a method for highly parallel and quantitative measurement of single-cell gene expression. Nucleic Acids Research, 43(9), e60. https://doi.org/10.1093/nar/gkv134

Natale, B. V., Schweitzer, C., Hughes, M., Globisch, M. A., Kotadia, R., Tremblay, E., … Natale, D. R. C. (2017). Sca-1 identifies a trophoblast population with multipotent potential in the mid-gestation mouse placenta. Scientific Reports, 7(1), 1–16. https://doi.org/10.1038/s41598-017-06008-2

Shi, X.-H., Larkin, J. C., Chen, B., & Sadovsky, Y. (2013). The expression and localization of N-myc downstream-regulated gene 1 in human trophoblasts. PloS One, 8(9), e75473. https://doi.org/10.1371/journal.pone.0075473

Sood, R., Kalloway, S., Mast, A. E., Hillard, C. J., & Weiler, H. (2006). Fetomaternal cross talk in the placental vascular bed: control of coagulation by trophoblast cells. Blood, 107(8), 3173–3180. https://doi.org/10.1182/blood-2005-10-4111

Trapnell, C., Cacchiarelli, D., Grimsby, J., Pokharel, P., Li, S., Morse, M., … Rinn, J. L. (2014). The dynamics and regulators of cell fate decisions are revealed by pseudotemporal ordering of single cells. Nature Biotechnology, 32(4), 381–386. https://doi.org/10.1038/nbt.2859

Ying, Q.-L., Wray, J., Nichols, J., Batlle-Morera, L., Doble, B., Woodgett, J., … Smith, A. (2008). The ground state of embryonic stem cell self-renewal. Nature, 453(7194), 519–523. https://doi.org/10.1038/nature06968

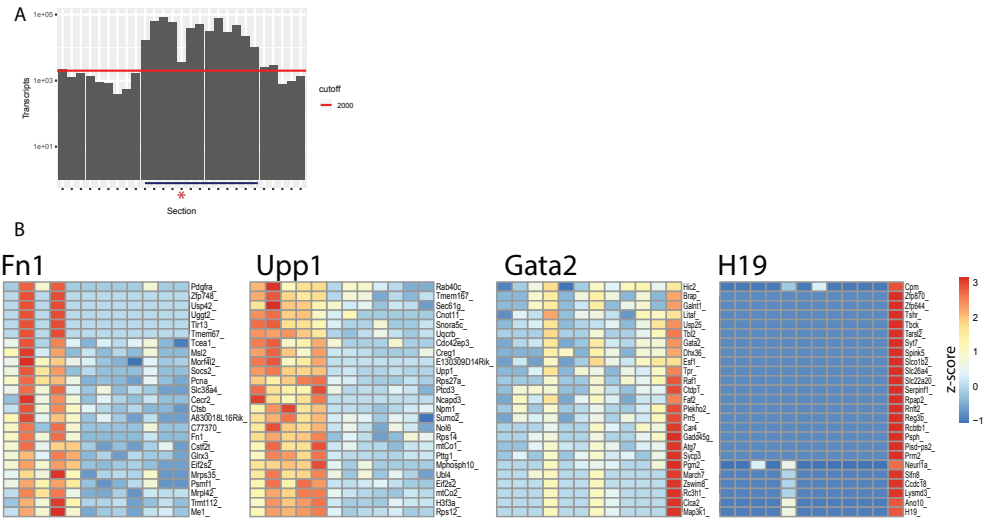

Supplementary figure 1. A. Initial raw reads detected per sample. Samples with a number of transcripts below the threshold bar (red) were not considered to include blastocyst material. Only sections marked with the blue horizontal bar were considered to include blastocyst data. One of the sections (red star) contained significantly less transcripts when compared to the adjacent sections. This section was discarded from further analysis. B. Alternative expression profiles were found in tomo-seq data.

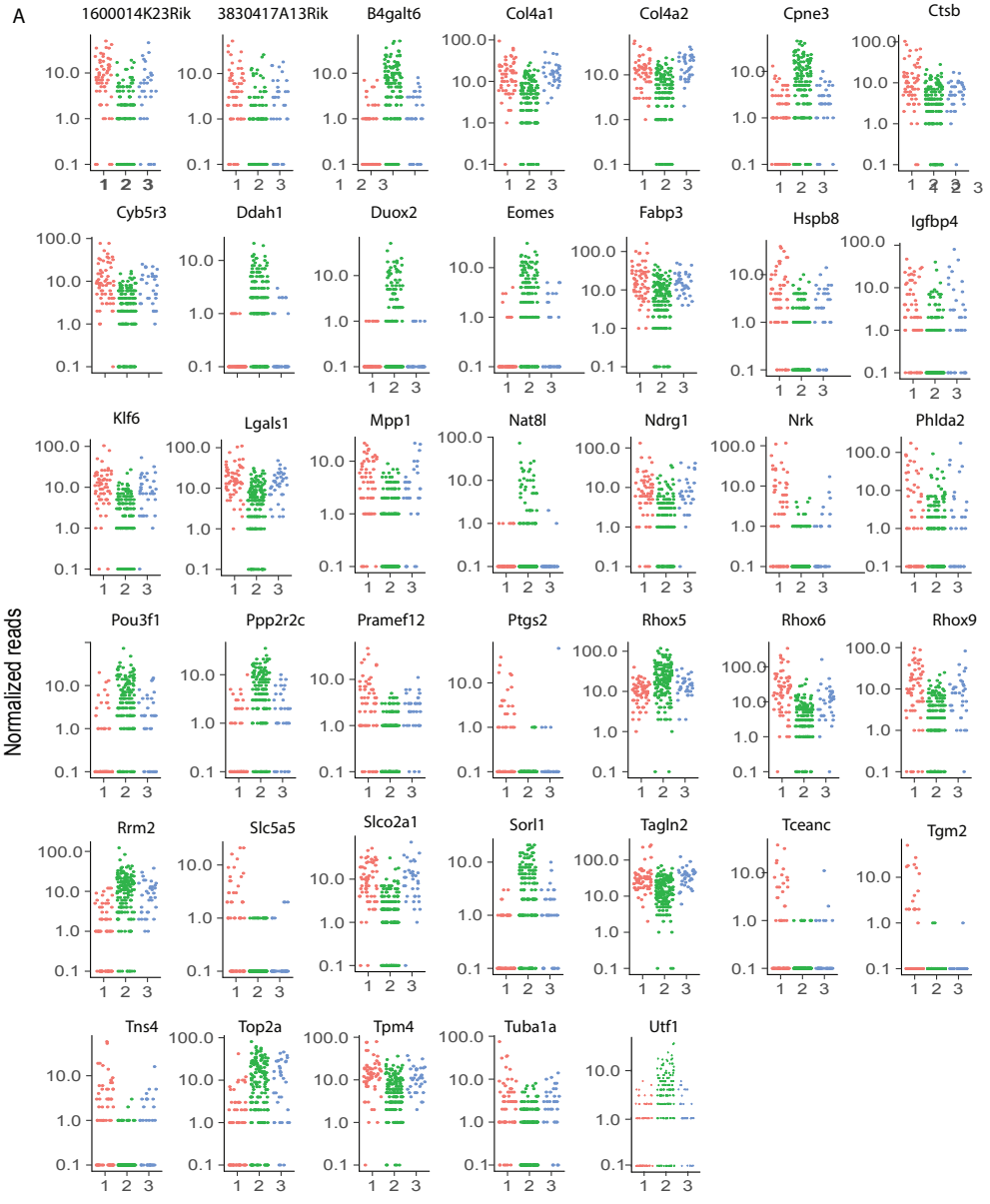

Supplementary figure 2. Jitter plots for the expression of the top 49 (combined with those in figure 4E) differentially expressed genes when comparing clusters 1 and 2.

Creb3l2	Igfbp4	Suv39h1	Fdft1	Acvr1
Rgs16	Prph	Gm10845	Slc38a6	Smox
Mdm2	Il11	Cldn6	Sox9	Fez2
Gsto1	Glul	Gprc5a	Duoxa2	Cdc42ep5
Atp6v0a1	Fn1	Grb10	Lama3	Elovl7
Vgf	Spop	Serinc2	Aard	Socs3
Dpp9	Pwwp2b	Lamc2	Itga3	Slco2a1
Mfge8	Jam2	Crim1	Cd44	Errfi1
Acan	Galnt1	St3gal2	Cttnbp2nl	Cmtm8
Srgn	Surf4	Csnk1e	Mdfic	Cgnl1
Acpp	Tes	Pcsk6	Dppa2	Sc4mol
Tmem2	Foxl2	Coq10b	Axl	Junb
Cd55	Dusp1	Rpl22	Ncrna00086	Ly6a
Abcb1b	Foxq1	Wisp1	Plp2	Pitpnc1
Cd24a	Igf2bp1	Nudt4	Cldn25	Litaf
Tjp2	Upp1	Hand1	Smtn	Lad1
Serpine1	Tpd52	Osgin1	AI836003	Cenpm
Epcam	Furin	1600029D21Rik	Itgav	Sox17
Efhd1	Stard8	Sord	Phlda1	Unc5b
Pmepa1	Acot7	Fat1	Nufip1	Sparc
Arrdc4	Atxn7l1	Dab2	Rps25	
Tomm6	S100a10	Klf5	Sft2d2	

Supplementary table 1. Genes detected in TE(Nakamura et al., 2015), drop upon differentiation, follow Sox2 trend in tomoseq data (up in polar half of the blastocyst)

Rank	pval	qval	gene_name	Rank	pval	qval	gene_name	Rank	pval	qval	gene_name
1	8.86E-166	8.43E-162	Gsto1	47	2.77E-27	5.18E-25	Mpp1	93	3.58E-17	3.30E-15	Syt13
2	4.35E-156	2.07E-152	Rhox6	48	3.89E-27	7.11E-25	Neat1	94	3.94E-17	3.60E-15	Tmem114
3	2.56E-128	8.13E-125	Krt8	49	3.03E-26	5.44E-24	Atrx	95	4.24E-17	3.85E-15	Hs3st3b1
4	3.37E-114	8.02E-111	Krt18	50	7.42E-26	1.31E-23	Peg3	96	5.43E-17	4.87E-15	Utrn
5	1.05E-108	2.00E-105	Id2	51	4.53E-25	7.84E-23	Pim1	97	5.98E-17	5.31E-15	Abca1
6	8.36E-92	1.33E-88	Nrk	52	7.00E-25	1.19E-22	Prss8	98	8.26E-17	7.28E-15	Sin3b
7	6.30E-85	8.56E-82	Flt1	53	2.23E-24	3.66E-22	Kcnq1ot1	99	1.97E-16	1.72E-14	Ralb
8	4.82E-79	5.73E-76	Basp1	54	3.45E-24	5.57E-22	Serpine2				
9	2.90E-74	3.06E-71	Rhox9	55	4.77E-24	7.56E-22	Ube2c				
10	9.40E-66	8.94E-63	Rrm2	56	2.85E-23	4.45E-21	Rhou				
11	3.56E-62	3.08E-59	Phlda2	57	9.82E-23	1.51E-20	Krt19				
12	1.07E-61	8.46E-59	Top2a	58	1.08E-22	1.63E-20	Sord				
13	1.29E-61	9.43E-59	1600014K23Rik	59	1.63E-22	2.43E-20	Fam129b				
14	3.44E-59	2.34E-56	Lgals1	60	5.71E-22	8.23E-20	Tmem64				
15	7.51E-59	4.76E-56	Slco2a1	61	7.05E-22	1.00E-19	Helz				
16	3.31E-55	1.97E-52	Cyb5r3	62	1.64E-21	2.29E-19	Efnb1				
17	7.94E-54	4.45E-51	Klf6	63	2.42E-21	3.34E-19	Utf1				
18	1.69E-53	8.91E-51	Sox2	64	2.85E-21	3.87E-19	Spred2				
19	6.31E-51	3.16E-48	Fabp3	65	3.72E-21	4.99E-19	Clcn5				
20	9.78E-48	4.65E-45	Col4a1	66	3.93E-21	5.19E-19	Gkap1				
21	7.08E-47	3.21E-44	Tceanc	67	5.48E-21	7.14E-19	Slc6a6				
22	2.56E-46	1.11E-43	Tns4	68	5.58E-21	7.17E-19	Jade3				
23	6.69E-46	2.77E-43	B4galt6	69	2.02E-20	2.52E-18	Nrip1				
24	9.08E-46	3.60E-43	Tgm2	70	2.04E-20	2.52E-18	Bmp8b				
25	3.74E-44	1.42E-41	3830417A13Rik	71	2.97E-20	3.62E-18	Eif4ebp1				
26	2.87E-43	1.05E-40	Ndrg1	72	3.36E-20	3.99E-18	Hmmr				
27	9.62E-41	3.27E-38	Eomes	73	4.22E-20	4.95E-18	Lin28a				
28	1.62E-40	5.31E-38	Ptgs2	74	6.68E-20	7.75E-18	Pgap1				
29	5.25E-40	1.67E-37	Ddah1	75	6.92E-20	7.94E-18	Rab15				
30	5.79E-40	1.78E-37	Ctsb	76	7.70E-20	8.72E-18	Elovl5				
31	1.14E-38	3.39E-36	Duox2	77	9.18E-20	1.03E-17	Abhd17b				
32	1.00E-35	2.81E-33	Cpne3	78	1.92E-19	2.12E-17	Bcl9l				
33	6.45E-35	1.75E-32	Sorl1	79	2.27E-19	2.48E-17	G3bp1				
34	7.41E-34	1.96E-31	Tagln2	80	3.92E-19	4.23E-17	S1pr1				
35	8.05E-34	2.07E-31	Igfbp4	81	4.33E-19	4.58E-17	Pbx3				
36	9.89E-34	2.47E-31	Rhox5	82	4.94E-19	5.17E-17	Pmepa1				
37	1.01E-33	2.47E-31	Col4a2	83	1.17E-18	1.21E-16	Cks1b				
38	1.44E-33	3.42E-31	Ppp2r2c	84	1.80E-18	1.84E-16	Serpine1				
39	1.89E-32	4.39E-30	Pramef12	85	2.68E-18	2.71E-16	Ska2				
40	9.93E-31	2.20E-28	Hspb8	86	6.24E-18	6.18E-16	Tmem41a				
41	2.44E-30	5.27E-28	Pou3f1	87	7.43E-18	7.28E-16	Cited2				
42	3.44E-28	7.11E-26	Mki67	88	1.43E-17	1.39E-15	Glrx5				
43	5.67E-28	1.15E-25	Tpm4	89	1.92E-17	1.84E-15	Cebpb				
44	1.23E-27	2.44E-25	Nat8l	90	2.24E-17	2.13E-15	Nid1				
45	1.42E-27	2.76E-25	Tuba1a	91	3.09E-17	2.91E-15	Sox21				
46	2.34E-27	4.46E-25	Slc5a5	92	3.28E-17	3.06E-15	Dusp9				

Supplementary table 2. Top DE genes for cluster 1 vs cluster 2

6

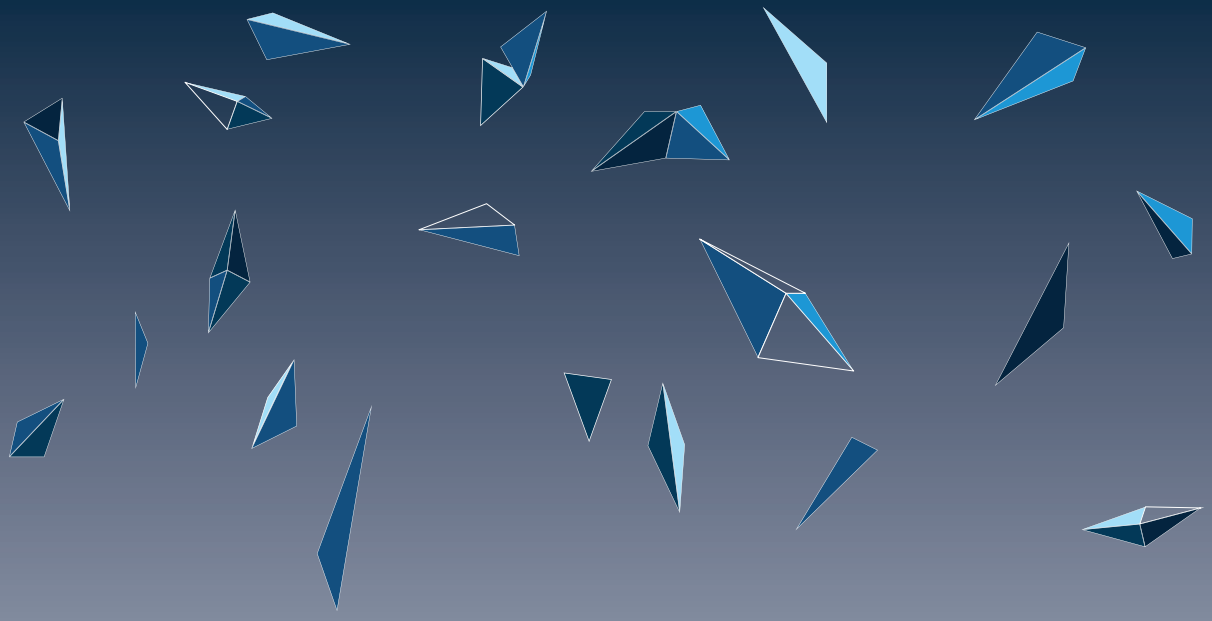

Chapter 7.
Discussion and valorization of results

7

In this chapter we intend to evaluate the findings described in this thesis and put them in a perspective of potential applications in the fields of stem cell biology, developmental biology and the new field of synthetic embryology.

Cutlure of TSC

The traditional culture of TSC makes the use of a feeder layer of cells serum, which often represent an obstacle in the development of new models. This is because these two factors provide a large supply of unknown molecules that might be detrimental for some of the properties we may want to exploit form a particular cell type. The use of feeder layer and serum, also means a potential variability across laboratories due to different batches, that prevent full control of the culture conditions and reproducibility. These two limitations of the classical culture can now be avoided thanks to the development of new conditions such as the Tx media. Although this media eluded the use of serum or feeder cells, it leads to a culture with a high degree of inter-cellular heterogeneity that we hypothesize to represent of spectrum of differentiation states observed along the TE axis and beyond. This same observation was already made in the culture of ESC, the embryonic equivalent of the TSC, a problem that was solved by the development of the so known 2i media.
Such inter-cellular heterogeneity we observe allows us to confirm the role of Cdx2 as a gene controlling the undifferentiated state of TSC. We found Cdx2 expression to be directly correlated with stem cell related properties such as self-renewal and proliferation, making it an ideal gene to act as readout to improve the culture conditions. On the other hand, this heterogeneous culture results in a spectrum of differentiation states limiting the applications of TSC.

Screenings for improving TSC culture

Screenings are an extremely valuable tool in many fields of life sciences, but in cell and developmental biology play a particularly important role, for example in primary cell line derivation. Although researchers generally have candidate factors to add on the culture media when deriving a new cell line (based for example on information acquired from observations made on mutant mice), traditionally several conditions are tested aiming to obtain a cell type showing a phenotype similar to that observed in the cells in vivo. These screenings are relatively simple and rely on testing one compound at the time and are sufficient for a qualitative result: whether the cell type of interest is derived in vitro or not. However, when we use screenings with a quantitative readout aiming to maximize the expression of a particular gene, factorial design becomes a very useful tool, as long as there are multiple single compounds having the desired effect. In our case, several modulators of different pathways were considered as screening "hits" based on our readout (increased Cdx2 expression). Several factors such as feedback loops or pathway crosstalk may play a role when multiple pathways interact, potentially leading to negative effects such as cellular differentiation or toxicity, or in contrary, they could have a cooperative effect. Factorial design of combinatorial screenings help us combine those initial hits and figure out which of the single compounds have a more beneficial effect while preventing us from performing experimentally all the potential combinations, but they also serve as tool for discovering compound or pathway interactions.
From the factorial design we tested 21 cocktails, with 4 of them reaching elevated and stable Cdx2 expression levels but showing different cells morphologies with one of them resulting in the phenotype we aimed for.

In the field of human ESC, there has been a constant search for new culture conditions that allow for culturing the cells in a more naïve state. In a previous publication aiming to upregulate Oct4 expression on hESCs (Gafni et al., 2015), several positive regulators were obtained that were first combined and then subdivided into two pools that were tested separately. Although the cocktail resulted in upregulated in Oct4 expression, with this strategy it is unclear if such expression could have been increased even further, possibly resulting in a different phenotype. We believe factorial design to be underrepresented tool in the optimization of in vitro models, for us it played a pivotal role in the findings described in this book.

The blastoid

This in vitro model for the mouse pre-implantation embryo combines ESCs and TSCs that under specific culture conditions cooperate in order to form structures that morphologically and functionally resemble the E3.5 blastocysts. Interestingly, during the blastoid protocol, the cultured cells switch to a phenotype much more comparable to the one observed of the cells in the embryo, and they help each other maintain an undifferentiated state. We can witness a permanent cross-communication between both compartments and we have successfully delineated it by performing lineage specific knockouts. Importantly, the blastoids are also capable of implanting in the uterus of pseudo-pregnant females, triggering a response in the endometrium only comparable to the one obtained by a blastocyst. However, the development in utero only progresses for one or two days after implantation.

There are some aspects of the blastoid protocol that remain to be improved. One of those is obtaining a more efficient second lineage commitment within the ICM. With the current protocol, this event takes place, however it happens at a low rate. Forming blastoids is highly dependent on the culture of TSCs, which we consider the main factor affecting the blastoid formation efficiency, making the TSCs pre-culture a second factor to solve. Some TSC lines are incapable of cooperating with ESC to form blastoids, and we hypothesize this to be a result of those TSCs not being representative of the blastocyst TE. Obtaining a culture of TSC that shows a higher similarity with the cells in the TE would potentially lead to higher blastoid formation efficiencies and an enhanced cross-communication with the embryonic compartment. Both primitive endoderm formation and a more robust trophoblast epithelium need to be achieved in the blastoid before we consider the blastoid to progress further after implantation.

Potential improvements aside, the blastoid is already a valuable tool for a variety of applications in the fields of developmental and reproduction biology. Blastoids might become an instrumental tool for toxicological and genetic screenings, and if someday a blastoid is capable to lead to live pups, it will make individual cloning possible.

Polar like TSCs in blastoid formation

Combinatorial screenings allowed us to obtain a new culture cocktail with increased Cdx2 expression levels in a stable manner. After further optimization by switching to a fully chemically-defined plate coating and a compound concentration reduction we obtained a culture we call Lt21, that lead to polar-like TSCs (plTSCs) with enhanced stem cell properties and that allows us for direct derivation of new lines.

Importantly cells cultured in these new conditions reach the expectation of being more efficient at forming blastoids both when the cells cultured in TX are converted to polar-like conditions and when they are directly derived in them. In order to be considered a blastoid, a structure must include both cell types with the ESCs engulfed by the TSCs, form a cavity

and reach certain size and circularity. Both blastoids and trophospheres obtained from the use of plTSCs show an increased circularity suggesting this to be an intrinsic property of the plTSCs, but only blastoids show an increased diameter by swelling, which suggests a more efficient crosstalk with the ICM. plTSCs are also more prone to cavitation since they are not as dependent on ESCs to trigger this process. Blastoids obtained from plTSCs cells show correct distribution of compartments and allow for ESCs differentiation into PrE-like cells. These new culture conditions show clear improvements when it comes to improving the efficiency of the blastoid protocol without affecting any other parameters, and we hypothesize this to be a result of an improved epithelial phenotype, a improved expression of the core transcription factors, and a better cross-talk with the ESCs, possibly by being in a more developmentally equivalent state, hence the name polar-like TSC.

Polar-like TSC reduced heterogeneity

As shown on chapter 1, TSCs cultured in Tx conditions display a notorious inter-cellular heterogeneity with cells being present in a partially differentiated state. Although a validated model for properly quantifying culture heterogeneity is lacking, our shows that the LT21 culture conditions partially correct for such heterogeneity, especially when the cell line is directly derived under polar like conditions. That heterogeneity is greatly reduced when it comes to expression of Cdx2 protein, but this also happens in wider terms as suggested by our transcriptome and phenome results.
Transcriptome analysis also allows us to find markers of differentiated and undifferentiated states, such as Ly6a, which we have proven to be preferentially expressed in the polar TE of the blastocysts.

TE axis formation

Over the years many researchers have reported a different, partly reversible phenotype between polar and mural trophectoderm (Chavez, Enders, & Schlafke, 1984; Copp, 1978; Cruz & Pedersen, 1985; Gardner, 2000). Although this different identity has mainly been observed in the late blastocysts (E4.5) we have tried to assess this in the 3.5 blastocysts. For this we have primarily used two tools: blastocyst tomo-sequencing and blastocyst whole mount fluorescent in situ hybridization (smFISH). Each of these techniques has its advantages and its limitations. Tomo-sequencing is a technically difficult experiment to perform due to the size of the tissue and the need for a near perfect orientation upon mounting. However, it allows to obtain genome-wide results without requiring initial candidates. However, the protocol we followed by RNA extraction relies on the presence of PolyA sequences on the mRNA, which are not present in all genes. Bearing this in mind, we are unable to make interpretations involving a large number of genes, including Cdx2 or Nanog. Also, similar to the case of single cell sequencing, we are unable to reliably detect lowly expressed genes such as transcription factors. It could be, nevertheless an extremely useful technique when the goal is to find new markers following a particularly expression pattern. smFISH on the other hand has the limitations of requiring a candidate gene and can be performed for one to three genes at a time only. However, it is a far more sensitive technique when it comes to detect a higher percentage of the transcripts of the gene of interest and allows us to spatially locate them. Combining these two techniques is instrumental for finding new unknown markers.
Although we do see differential gene expression patterns from the results obtained in the blas-

tocyst, we believe that these divergent phenotypes between mural and polar trophectoderm might become more evident in the late blastocyst. Performing multiple tomo-sequencing experiments at different blastocyst stages would allow us to better characterize and therefore understand those divergent fates.

Transcriptomics data from trophoblasts obtained from blastoids show a high heterogeneity when those blastoids have been made from plTSCs, suggesting an efficient axis formation. smFISH polarity data confirms the symmetry breaking to occur in blastoids from plTSCs. For one of the two genes tested (Cdx2), the frequency at which a preferential polar distribution occurs is higher than that one observed in the blastocyst. This could suggest that the TE of blastoids obtained with plTSCs are no longer equivalent to a 3.5 blastocyst but to a later stage.

7

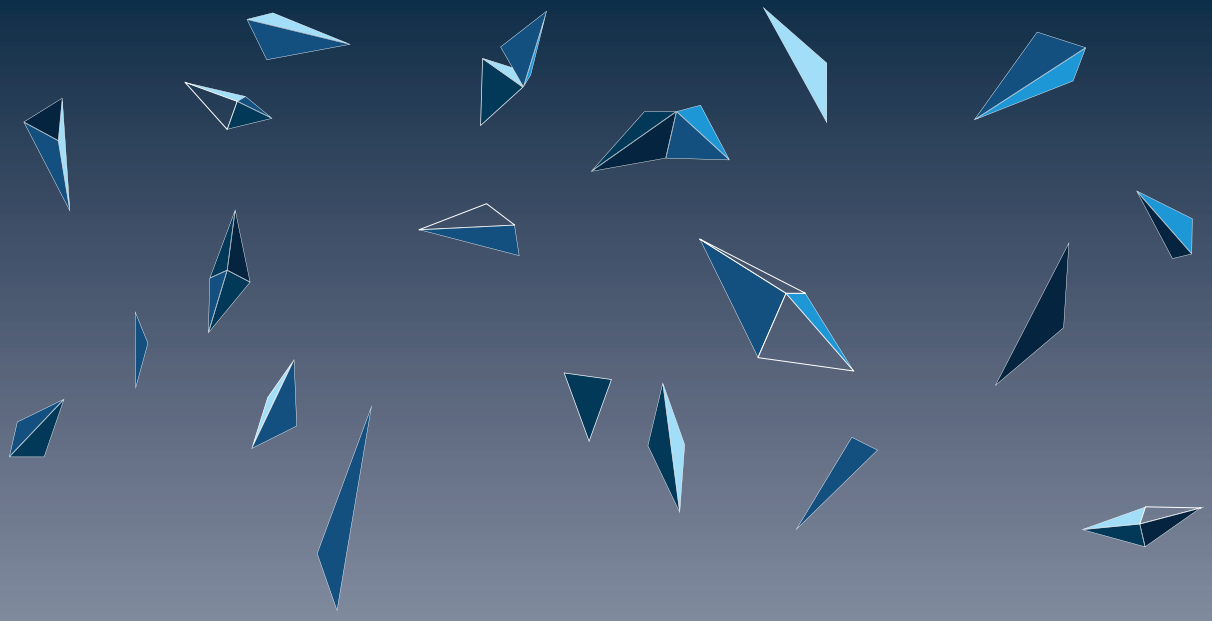

Addendum.

- English summary
- Nederlandse samenvatting
- Resumen en español
- Acknowledgements
- List of publications
- Biography

English summary

Mouse embryonic development spans over a period of 21 days. During this time, as cells proliferate, they also specialize in order to carry out different functions. After egg fertilization, the zygote undergoes a series of symmetric divisions until the morula stage. All the cells included in the early morula have the potential to specialize (or differentiate) into any cell type. The process of differentiation is gradual and goes through several partially differentiated states only present in the embryo. It is at the morula stage that the first differentiation occurs, in a process known as the first lineage commitment, event leading to differentiation into Inner Cell Mass (ICM) and Trophectoderm (TE). While the ICM represents the embryonic compartment, precursor of all the tissues present in the adult, the TE represents the first extraembryonic compartment which will develop into the placenta. After the first lineage commitment, the TE remains surrounding the ICM and cavitates leading to a cystic structure. This morphology gives the name to the next embryonic stage known as the blastocyst. Until this stage, the embryo has not yet implanted in the uterus. Such implantation is mediated by the TE and for it to occur, partial differentiation needs to occur in both embryonic and extraembryonic compartment. Differentiation of a subset of cells in the TE is necessary for initial attachment and invasion of the endometrium.

We are capable of culturing *in vitro* the analogues of the cells in the ICM and the TE. Embryonic Stem Cells (ESCs) are the analogues of the embryonic compartment while Trophoblast Stem Cells (TSCs) represent the extraembryonic counterpart. Both of these are stem cells, meaning that are cells with the potential to differentiate into all specialized derivatives. Although the ESCs and TSCs are representative of the cells in the ICM and TE respectively, the TSCs we are capable of culturing show certain aberrations when directly compared with the TE cells.

In the first two experimental chapters of this thesis, we focused on characterizing those TSC aberrations as well as trying to correct for them. In order to do so we relied on the expression of a set of genes which serve as a reliable approximation for checking the differentiation state of TSCs. One of those genes is known as Cdx2. By looking for regulators capable of increasing the expression of Cdx2 in our TSCs culture, we were able to find new culture conditions that make the cells more comparable that those present in the TE.

Our group previously managed to develop a protocol which under specific conditions combines ESCs and TSCs leading to structures functionally and morphologically comparable to the mouse blastocyst. We called this structures "blastoids". Importantly, blastoids are capable of implanting in the uterus of females triggering a response in the endometrium only comparable to the one observed upon implantation of real embryos.

Blastoids can be generated in large numbers. This attribute makes the blastoid a suitable tool for genetic or pharmacological screenings as well as for studying the interaction between

embryonic and extraembryonic compartments. In Chapter 4 we made use of the blastoid for identifying a pathway that originates from the embryonic compartment and leads to proliferation and cavitation of the TE-like cyst.

Although the blastoid have an extremely promising potential in the fields of developmental biology, in vitro fertilization and pharmaceutics, the efficiency at which we obtain blastoids is suboptimal since only 10 to 15% of the structures we recover show the correct morphology and cell distribution. We hypothesized that an improvement of the culture of TSCs would ultimately lead to an increase in blastoid formation efficiency. By using the Cdx2 regulators we discovered in chapter 3, we were able to generate new culture conditions that lead to cells more comparable to the cells in the TE. We could confirm that these new TSCs have a better communication with ESCs making them significantly more efficient at generating blastoids.

By studying the nature of those blastoids, we were able to observe that the extraembryonic compartment of blastoids generated with the new TSCs autonomously show partial differentiation in the trophoblastic layer, a process necessary for attachment to the endometrium.

The work described in this book represents an improvement in the culture of TSCs, making them more suitable for their use as a model for studying trophoblastic lineage development as well as for the generation of more reliable *in vitro* models such as the blastoid.

Nederlandse samenvatting

De ontwikkeling van een muizenembryo duurt 21 dagen. Tijdens deze ontwikkeling proliferereren de cellen in het embryo zich. Tegelijkertijd specialiseren de cellen zich ook, zodat ze hun specifieke taken kunnen uitvoeren. Nadat de eicel bevrucht is, ondergaat de zygote een aantal symmetrische delingen, zodat de zygote zich ontwikkelt tot een morula. Alle cellen in de jonge morula hebben de potentie om zich te specialiseren (of te differentiëren) in iedere celtype. Het proces van deze differentiatie is geleidelijk, en tijdens dit proces ondergaan de cellen meerdere fases van differentiatie die alleen in het embryo plaatsvinden. Tijdens het morula stadium beginnen de eerste cellen zich te differentiëren. Dit proces wordt ook wel de eerste lineage commitment genoemd. Hiermee wordt bedoeld dat de cellen hun eerste stappen van differentiatie ondergaan, en zich beginnen toe te spitsen op hun specialisatie. Deze fase leidt tot differentiatie van de binnenste zogeheten Inner Cell Mass (ICM) en het Trophectoderm (TE). De ICM is de massa die later het embryo zelf zal vormen en bevat de voorlopercellen van alle weefsels die later in het volwassen organisme aanwezig zullen zijn. Het TE vormt zich rondom de ICM, en vormt later de placenta. Tijdens het eerste lineage commitment vormt het TE zich om de ICM en maakt een bolvormige structuur, zoals een cyste. Deze bolvormige structuur wordt ook wel de blastocyste genoemd. Tot aan dit stadium heeft het embryo zich nog niet genesteld in de baarmoeder. Deze innesteling wordt verzorgd door het TE. Om dit te laten gebeuren is het nodig dat zowel het ICM als het TE deels gedifferentieerd zijn. Differentiatie van een deel van de cellen in het TE is nodig voor initiële binding en het zich ingraven in de baarmoederwand.

Wij zijn in staat om in vitro analogen van de ICM en TE cellen te kweken. Embryonale stamcellen (ESCs) zijn de analogen van het embryonale deel, het ICM, terwijl de Trofoblast stamcellen (TSCs) het extra-embryonale deel, het TE, representeren. Beide celtypen zijn stamcellen. Dit betekent dat deze celtypen de mogelijkheid hebben om naar alle gespecialiseerde celtypen te differentiëren. Hoewel de ESCs en TSCs de cellen van het ICM en het TE representeren, zijn er voornamelijk enkele verschillen tussen gekweekte TSCs en de TE-cellen.

In de eerste twee hoofdstukken van dit proefschrift focussen we ons op de karakterisatie van de verschillen tussen TSCs en TE cellen. Ook proberen we deze verschillen te corrigeren. Hiervoor hebben we de expressie van een set genen gekozen die kunnen worden gebruikt om de staat van differentiatie van TSCs te bepalen. Één van de genen in die set is Cdx2. Door naar regulatoren te kijken die de expressie van Cdx2 verhogen in gekweekte TSCs, konden we nieuwe kweekcondities vinden die de TSCs meer op TE cellen laten lijken.

Onze onderzoeksgroep heeft een protocol ontwikkeld met specifieke kweekcondities waardoor de ESC en TSC gecombineerd een structuur vormen die functioneel en morfologisch vergelijkbaar is met de blastocyste van de muis. We noemen deze structuren “blastoïden”. De blastoïden zijn in staat om zich te nestelen in de baarmoeder van de muis, met als gevolg dat er een reactie plaatsvindt in het endometrium. Deze reactie lijkt sterk op de reactie die

plaatsvindt wanneer er een echt embryo zich innestelt.

De blastoïden kunnen worden gekweekt in grote aantallen. Deze eigenschap is ideaal voor genetische of farmacologische studies, of voor het bestuderen van de interactie tussen de embryonale en extra-embryonale onderdelen. In hoofdstuk 4 maken we gebruik van de blastoïde voor het identificeren van een signaaltransductieroute dat stamt van het embryonale deel, en wat leidt tot de proliferatie en de vorming van de holte in een TE-achtige cyste.

Hoewel de blastoïde een veelbelovende nieuwe techniek is in het onderzoeksveld van de ontwikkelingsbiologie, in vitro fertilisatie en farmacologie, is de efficiëntie waarmee we blastoïden kunnen kweken suboptimaal. Slechts 10 tot 15 procent van de structuren die we overhouden in de kweek vertonen het juiste aantal cellen en de correcte morfologie. Wij veronderstelden dat een verbetering van de kweekcondities van de TSCs zou leiden tot een verhoogde efficiëntie van blastoïde-formatie. Door Cdx2-regulatoren te gebruiken, zoals te lezen in hoofdstuk 3, kwamen we erachter dat dit tot verbeterde kweekcondities leidde, en dat de cellen meer vergelijkbaar waren met het TE. We bevestigden dat deze nieuwe TSCs een verbeterde communicatie hadden met de ESCs, waardoor ze significant beter waren in het genereren van blastoïden.

Door de blastoïden te bestuderen, zijn we erachter gekomen dat de extra-embryonale structuur van de blastoïden die met deze nieuwe TSCs waren gekweekt een gedeeltelijke differentiatie naar de trofoblastische laag vertonen. Dit proces is cruciaal voor de verbinding met het endometrium.

Dit proefschrift toont een verbetering aan wat betreft de kweekcondities van TSCs, waardoor deze meer geschikt zijn voor het gebruik als model voor de ontwikkeling van de trofoblastische cellen. Daarnaast wordt er aangetoond dat er hierdoor een verbeterd in vitro model zoals de blastoïde kan worden gegenereerd.

Resumen en español

El desarrollo embrionario en ratón dura 21 días. Durante este tiempo, mientras las células proliferan, también se especializan para llevar a cabo distintas funciones. Después de la fertilización del óvulo, el zigoto experimenta una seria de divisiones celulares simétricas hasta el estadio de mórula. Todas las células que forman parte de la mórula tienen el potencial de especializarse (o diferenciarse) en cualquier tipo celular. Este proceso de diferenciación es un proceso gradual, pasando por múltiples estadios parcialmente diferenciados que solo se dan en el embrión. Durante el estadio de mórula, ocurre el primer proceso de diferenciación, un evento que da lugar a la Masa Celular Interna (MCI) y al Trophectodermo (TE). Mientras que la MCI representa el linaje embrionario, precursor de los tejidos presentes en el adulto, el TE representa el linaje extraembrionario, precursor de la placenta. Tras comprometerse a uno de esos dos linajes, las células del TE quedan rodeando las células de la MCI y empiezan a generar una cavidad dando lugar a una estructura cística. Esta forma es la de que da nombre al siguiente estadio embrionario, conocidos como blastocisto. Hasta este punto, el embrión aún no se ha implantado en el útero. Dicha implantación es llevada a cabo por el TE y para que ocurra, es necesario que se dé una diferenciación parcial tanto en el linaje extraembrionario como en el embrionario. La diferenciación parcial en un grupo de células del TE es crucial para que haya un contacto inicial entre endometrio y embrión.

Es posible cultivar in vitro los análogos de las células la MCI y de el TE. Las células madre embrionarias (CMEs) son los análogos de las células de la MCI mientras que las células madre trofoblásticas (CMTs) son los análogos de las células del TE. Estos dos tipos celulares, como células madre, tienen el potencial de diferenciarse en otros tipos celulares derivados. Aunque las CMEs y las CMTs representan las células de la MCI y del TE respectivamente, las CMTs que podemos cultivar a día de hoy muestran ciertas aberraciones cuando las comparamos directamente con las células del TE.

En los dos primeros capítulos experimentales de esta tésis, nos centramos en caracterizar y corregir las aberraciones que observamos en las CMTs. Para ello, nos hemos fijado en la expresión de un grupo de genes que nos sirve como aproximación para comprobar el estado de diferenciación de las CMTs. Uno de esos genes es Cdx2. Buscando moduladores de la expresión de Cdx2 en nuestro cultivo de CMTs, conseguimos encontrar nuevas condiciones de cultivo que permiten obtener células más similares a aquellas presentes en el TE.

Nuestro grupo ha conseguido desarrollar un protocolo que bajo ciertas condiciones, combina CMEs y CMTs dando lugar a estructuras funcional y morfológicamente comparables al blastocisto. Hemos llamado a estas estructuras ¨blastoides¨. Los blastoides son capaces de implantar en el útero de hembras, generando una reacción en el endometrio solo comparable a la observada cuando un verdadero embrión se implanta.

Podemos generar blastoides en grandes cantidades. Esta propiedad hace de los blastoides una

herramienta adecuada para su uso en estudios genéticos y farmacológicos además de para estudiar la interacción entre linajes embrionario y extraembrionario. En el capítulo 4 hicimos uso de los blastoides para identificar una ruta de señalización con origen en la MCI que promueve la proliferación y cavitación del cisto del TE.

Aún a pesar de que el blastoide tiene un potencial muy prometedor en los campos de biología del desarrollo, fertilización in vitro y farmacología, la eficacia a la que obtenemos los blastoides es sub-óptima ya que solo el 10-15% de las estructuras que recuperamos muestran la morfología y organización celular correcta. Generamos la hipótesis de que una mejoría en el cultivo de CMTs llevaría a un incremento en la eficacia a la hora de generar blastoides. Usando los moduladores de expresión de Cdx2 que descubrimos en el capítulo 3, pudimos generar nuevas condiciones de cultivo que dan lugar a células más similares a las células del TE. Pudimos confirmar que estas nuevas CMTs muestran mejor comunicación con las CMEs, haciéndolas más eficientes a la hora de formar blastoides.

Estudiando la naturaleza de los blastoides generados con las nuevas CMTs, pudimos observar que las células de linaje extraembrionario generaron de manera autónoma una diferenciación parcial, un proceso necesario para el contacto inicial con el endometrio.

El trabajo descrito en este libro representa una mejoría en el cultivo de CMTs, haciéndolas mejores en su uso como modelo para estudiar el linaje trophoblástico en biología del desarrollo así como para la generación de nuevos modelos in vitro de más confianza como el blastoide.

Acknowledgements

Nicolas, I want to express my most sincere gratitude to you for giving me the chance to work in such an interesting and groundbreaking field. During these 6 years, I have done nothing but learn from or with you and it feels like I might have been part of something truly special. It has not always been easy as you know, but I am sure I will remember my times at your lab with a sense of satisfaction. Apart from the many lab skills I have learned over these years, I take with me the perseverance, confidence and the clarity with which you approach science.

Thanks a lot **Niels** for hosting me at your lab and help with guidance over these years. I do really appreciate you trying to help in the difficult times. Some of the best friends I have made during my times in Utrecht have been coworkers at your lab. You clearly have a good eye for recruiting good people. Thanks **Clemens** for supporting our projects as well as allowing me to stay for a couple years more in order to make a satisfactory thesis.

Thanks to the Hubrecht Institute and everyone in it. It is truly a fantastic place for research and even though I was only a guest, I leave with a very strong sense of attachment after all these years. I never stopped learning from the research happening in such a leading institute. Thanks to the MERLN as well for making it possible for us to develop our research from the distance, I'm sure this wasn't always easy to handle.

To the Rivron group labmates: Thanks for the help and your trust. **Erik**, I admire your work and findings done at the lab, which clearly will push the blastoid to reach further developmental stages. Apart from your thesis being a guide for me to write mine, I always found scientific discussions with you to be extremely helpful. **Linfeng**, thanks a lot for helping with my project and for nice talks during our teaching times together, I am sure you will be successful wherever you end up. **Yvonne**, form what I can see in our short lab overlap, I can tell that you are very well suited for this job and I can only hear great things about you! **Delia**, you are the first in a new era in the Rivron lab, and you clearly are the most indicate for the job. I really admire how much of an optimist and perfectionist you are. I wish our overlap would have been a bit longer. I hope my frustration does not condition the way you see this new stage on your career. To **Maarten** and **Frank**: you guys helped a lot with the earlier stages of the research described in this book. I hope I didn´t make it too difficult for both of you. Thanks as well to all the others who helped with my research. **Jeroen**, I know I wasn't always the easiest when handling the AMS. It has been a pleasure to learn some techniques from you. **Anna A**: Te estoy muy agradecido por tu ayuda con el análisis y con todo lo que me ha ayudado hablar contigo de las movidas del trabajo. Me alegra muchísimo haber pasado contigo todas esas buenas tardes en el Lebowski, Cubanita u Olympos. Puedes contar conmigo para cuidar de ti en cualquier fiesta que quieras. **Abel**, **Onur, Adi** and **Isabel**, it was also a pleasure to work and learn from all of you.

From the Geijsen lab, a few people have had to deal with me in a different way. **Nune**, **Sonja** and **Melissa**: thanks a lot for dealing with the complications involving my stay at the Geijsen lab, I am sure it has not been easy to keep full track of it. I am extremely thankful to the three of you for making it all so easy. You were very willing to help anytime I needed something like a last minute order or help for the hundredth time at the Magazijn. Apart from the professional level you three have been great to be around and I have learnt a great deal on aspects such as organization and authority from you all! Many of the friends I have made these last few years belonged to the Geijsen lab. **Maaike**, although it has been a while, I will always remember you as the stem cell expert to go to. Very few people I know are as cheerful and easy to talk to as you are. I really appreciated having you around at the beginning. Just so you know, sometimes I still come across some glitter from your book. **Oliver**, our overlap was relatively short, but it´s awesome to catch up with you every once in a while. I remember our early days working for way too long in the cell culture. You are one of the hardest working persons I know. **Ator**, you have been of great help. First with Bram and Bella who often tell me how much they miss you, but also during lunch time, you are such a show! Never forget the Tiger mama situation! I also love our complain sessions,. All together it has always been great to share a big part of my PhD next to you! I hope we get to stay in touch wherever we end. **Axel**, you also are part of the old guard. It has been great to share these times with you. This includes: ski trips, board game nights, crazy engineered drinking games or introductions to German traditions such as the feuerzangenbowle, one of my favourite winter things ever since I tried it. **Sonja**, you are one of the most cheerful people I know. I am still amazed at how well you managed to handle things in the lab while being so young (so so young). I am sure Vienna will be another amazing step in your career. **Peng**, you are an amazing guy, thanks a lot for all the times you helped in the lab. You are such a pro! I am sure that the future of the Geijsen´s lab is safe with people like **Jorik**, **Fanny**, **Darnell**, **Ada**, **Lin** and **Pascale**. Also was nice to share the lab with older members: **Stefan**, **Diego**, **Chen**, **Clara**, **Manda**, **Sandra**...

Chloé, **Lorenzo**, **Lennart**, **Arianna**, **Hesther** and **Annette**: I am glad I could share one of the early years being part of the PV with you guys. I had an amazing time with such a great group of people. I don't think

Thanks all the Futsal buddies: **PJ**, **Guy**, **Joppe**, **Max**, **Oliver**, **Charles**, **Axel** , **Alex**, **Maartje**, **Wim**, **Lucas**, **Saman**, **Mauro**, **Frans**, **Lorenzo**, **Geert**, **Lucas K.**, **Samu**, **Enric**, **Deepak**, **Abel**, **Margit**, **Sonja**, **Nico Lansu**, **Pim**, **Wouter**, **Axel R**, **Frank**, **Jens**, **Lars**, **Cayetano**, **Tim**, **Erik** and many other that I am probably forgetting. It was great to share so many Tuesday/Wednesday or Labs United matches with you guys.

To my festival and concert companion: **PJ**, **Maartje**, **Tim**, **Anna**, **Bas**, **Oliver**, **Elke**, **Stefan**, **Frerik**, **Charlotte**, **Sara**, **Geert**, **Kay**, **Emily**, **Sebas**, **Koen**, **Teije**, **Nicolas**, **Euclides** and **Lorenzo**. Thanks you all! You guys made the camp weekends and the nights at Tivoli or Ekko unforgettable.

Thanks to all the Florin pubquiz team members! **Bas**: Even though I don´t often agree with neither your team name ideas nor your guess for our ranking every other Tuesday, I have to say that it was amazing to spend so many Wednesdays sharing beers with such a great group. You are the eternal captain! **Wim**, in my mind you were always the second in command. As you can see, I don´t have anything against you after those murder attempts at the Ardennes.

Both of you southerners always were the perfect company for sharing beers mid-week. Thanks as well to many of the regulars: **Tim**, **Alex**, **Margit**, **Annabel**, **Jeff**, and many others.

Thanks for the poker, bbq and vintage videogame and Kung Fury nights. **Mauro**, although we have lost some of the main attendants for some of these, I hope we get to repeat them some time and I hope we both stay as loyal customers of beefensteak.nl. **Kay**, I am glad you can no longer say that you win 100% of the games you play with Law. I admire your persistency. **Chloé**: it has been great to have so many parties next to you! I trust you to pass on the ostrich thing; I expect to see your future colleagues do it whenever I come to Boston. You clearly are the natural heir. **Freddy**, I haven't gone out as much as with these other guys, but it has been great fun the few times we have hanged out. I hope we get to spend many more evenings eating lamb or sharing beers.

Thanks as well to many of the old building´s third floor colleagues. **Annabel**: it has been great to spend coffee breaks, SinterKlaas and pubquiz evenings as well as many other events with you. You are an amazing person, always willing to help and listen. This was truly appreciated. **Lorenzo** and **Euclides**, you guys are the perfect mediterraneans. Even though it´s at your own rhythm (and after working way too much), you guys always surround yourselves with the best kind of people. I always liked our quick catch-up conversations at the coffee machine or at the elevator on the way to your smoke break. **Anna K.**: Thanks for the good times at concerts, festivals, coffee houses, borrels…it was always great to share all those great times with such a nice person like you. You are clearly the new concert addict! Thanks also to **Tota**, **Caro**, **Ilia**, **Erik** and many other third floor people! Thanks also to the new third floor colleagues **Carlo**, **Niels**, **Yike, Christian, Peter, Erika** and **Valerio**. Although we didn't spend much time in the new room, I can already tell that this would have been a great place to work at. Thanks **Marjon, John** and **Wouter T.**, for helping us out in the new space!

The borrels were always a very important part of the week. This is the place where I forged many of the friendships I hope to retain. **Ajit**: you were the essence of the borrel, always in a great mood and with a secret beer stash. You were exactly what most of us needed at 5 o'clock on a Friday. Wish you all the luck with your new project, but I hope you know that you are a huge loss for the Hubrecht. Thanks **Tim** for all the good times with a beer in our hands since as early as our dutch course. **Rob**: Thanks for all the chats and help at the mouse house. You are one of the most cheerful guys to talk to on a Friday night. Cheers to other borrel regular attendandts: **Bas M.**, **Sara** (Ciao bella!), **Spiros**, **Corina**, **Kim**, **Charlotte**, **Susanne**, **Peter**, **Maya**, **Anna A.**, **Cristoph**, **Eirinn**, **Luca, Lotte, Laura, Colinda** and many others!

Gracias a los perfectos anfitriones! Me alegra muchísimo poder contar con vosotros como amigos por aquí. Siempre que nos reunimos para comer o cenar, conseguís que nos sintamos como en casa y que nos cueste mucho tener que irnos (ya sea por estar pasándolo bien o por lo que cueste levantarse tras esas cantidades de comida y Mastiha). **Enric**, siempre me ha parecido increíble cuanto te gusta hablar de política, aunque soy un tanto ignorante en el panorama político español, siempre he podido aprender de ti. Espero que tras estos años lo hayas cogido un poco más de cariño a los madrileños. **Miriam**, muchas veces cuando hablo de ti te describo como una alemana más española que yo. Sé que no es difícil, pero siempre me ha parecido curioso. De algún modo me haces estar aún más orgulloso de ser español. Mil gracias por todas esas reuniones de amigos. **Geert**, you are such an amazing guy! I love how

you are always up for a meeting with friends. You were always a must have person in all those meetings happening around food or football. I don't think I have ever seen you saying a bad word about anything nor anyone, I admire that! I am glad I got to spend so many great times next to you!

For the perfect **PJ** and **Maartje**: thanks for all the moments we have shared in Utrecht and surroundings. Be sure I will try to visit you guys regularly so we can enjoy some more good times together. I will always admire the way you guys are, how much you are able to work and your thirst for science. These attributes will clearly allow you to do whatever you want, you deserve it. It is clear that you guys left a mark in many of the Hubrecht workers, but I keep you in a very special place in my mind.

Alex, thanks for all the good times together: nights out, parties at your place, concerts, festivals, futsal afternoons, beers at Olympos, Pub quiz nights, meals at home, Ardennes weekends, Derrick nights… The list is endless man…You will always remain as my beer commander. I hope we get to visit each other every now and then.

Gracias a mis amigos en España. Gracias por visitar, por hacer un hueco para verme en esas visitas fugaces o por contar conmigo para ir a vuestras bodas. Gracias **Teru**, **Joel**, **Anita**, **Javi** (awesome), **Alfonso**, **Mónica**, **Paula**, **Ale** y **Heidi**. Me alegra mucho ver que a todos os está yendo bien!

A mi familia: Gracias por todo el apoyo que me habeis prestado durante estos 6 años. Siento haberme ido tan lejos para continuar mi trayectoria profesional, pero de algún modo me ha servido para apreciar aún más lo que tengo en España. Siempre habéis hecho todo lo posible para que me sintiera cómodo cuando volvía por vacaciones. ¡Que sepáis que me mimáis demasiado! Gracias por preocuparos por mi situación personal y profesional a lo largo de estos años, y por tantos consejos que solo vienen con las mejores intenciones. Siento mucho haberme perdido ciertos momentos importantes en los últimos años, tanto los buenos como los malos pero aunque no sé dónde acabaré, espero poder ir a visitar más a menudo. Papá y mamá, aunque seguro que lo sabéis, es gracias a vosotros que he llegado hasta aquí. **Papá**, sé que siempre vas a preocuparte por mi situación tanto laboral como personal, lo agradezco de veras. **Mamá**, ya ves que aunque dijera que nunca fuese a hacer una tesis debido al trauma que me causó la tuya, opté por hacer mi propio doctorado. **Laura**, siento mucho haberme perdido gran parte de los primeros años de Alicia, me encantaría poder ayudar un poco más en ese sentido. Pero me alegra muchísimo el ver que has creado tu propia familia. **Sole**, en muchos aspectos sigues tratándome igual que cuando tenía tres años. Que sepas que nadie me echa tantos piropos como tú. Sois vosotros cuatro los que me habéis demostrado lo que es ser una buena persona y me habéis enseñado los valores necesarios para ir por la vida con una conciencia tranquila. Aunque estoy seguro que todavía me queda mucho que aprender de vosotros. ¡Gracias! **Alicia**, espero que en el futuro pueda estar un poco más involucrado en tu vida. Que sepas que no me importa tener que ganarme tu confianza cada vez que voy, merece la pena! **Marcos**, me alegra mucho que seas el padre de mi sobrina. Por lo que puedo ver cada vez que voy, podemos contar contigo en las reuniones familiares, aunque requieran 4 horas de viaje. Gracias **Luke**, pocos me prestan tanta atención y se alegran tanto de verme como tú. Gracias al resto de la familia por hacerme sentir como si nunca me hubiese ido. No me quiero perder ni una de las reuniones familiares en navidades.

Bram and **Bella**: thanks for your attention. It is very special for me to share a home with the two of you. It is simply amazing the healing effect that you have on me.

Judith, you are by far the person that has helped me the most in these last years. Getting close to you is my most proud achievement. I am extremely happy that our paths crossed here and that (already almost two years ago) we moved together to a house so we could make it our home. Your support has been crucial for me to survive these last few years, you have always managed to calm me down at the end of a bad day. I admire how much of a hard worker you are and how you are not to too scared to start new things ("let's make a company out of this") and all this without losing touch with your best friends. Although we have started with Spain, there are so many places I would like to see next to you! I am sure we will get to start many adventures together! Ik hou van je!

List of publications

Frias Aldeguer J, Kip M, Vivié J, Li L, Alemany A, Korving J, Darmis F, van Blitterswijk CA, van Oudenaarden A, Geijsen N and Rivron NC . Polar-like trophoblast stem cells form an embryonic-abembryonic axis in blastoids. bioRxiv 510362 (2019). doi:10.1101/510362

Vrij EJ, Scholte op Reimer Y, **Frias Aldeguer J**, Misteli Guerreiro I, Kind J, Koo BK, van Blitterswijk CA and Rivron NC. Self-organization of post-implantation-like embryonic tissues from blastoids. bioRxiv 510396 (2019). doi:10.1101/510396

Rivron NC, **Frias Aldeguer J**, Vrij EJ, Boisset JC, Korving J, Vivié J , Truckenmüller RK, van Oudenaarden A, van Blitterswijk CA and Geijsen N. Blastocyst-like structures generated solely from stem cells. Nature 557, 106–111

Basak O, Krieger TG, Muraro MJ, Wiebrands K, Stange DE, **Frias Aldeguer J**, Rivron NC, van de Wetering M, van Es JH, van Oudenaarden A, Simons BD and Clevers H. Troy+ brain stem cells cycle through quiescence and regulate their number by sensing niche occupancy. Proc. Natl. Acad. Sci. U. S. A. 115, E610–E619 (2018).

Lonardo E, **Frias Aldeguer J**, Hermann PC. and Heeschen C. Pancreatic stellate cells form a niche for cancer stem cells and promote their self-renewal and invasiveness. Cell Cycle 11, 1282–1290 (2012).

Garcia-Silva S, **Frias Aldeguer J**, and Heeschen C. Stem cells & pancreatic cancer. Pancreatology 13, 110–113 (2013).

Biography

Javier Frias Aldeguer was born in Madrid (Spain) on October 17th 1987. He grew up in Madrid in a family of 4. In Madrid he attended primary, secondary and high school at Colegio Virgen de Mirasierra and later on at Colegio Base. In 2005 he started his bachelor in biochemistry at Universidad Autónoma de Madrid. During his bachelor studies, he obtained an Erasmus internship grant for performing the bachelor´s thesis in Vienna at the lab of Gerhard Wiche (Max. F. Perutz laboratories) studying microtubule dynamics. After finishing the bachelor in Biochemistry, Javier continued with a master in biotechnology at Universidad Autónoma de Madrid, including an internship at Christopher Heeschen´s lab (Centro Nacional de Investigaciones Oncológicas) studying pancreatic cancer stem cells and their cross-communication with the microenvironment.

In 2013 Javier moved to Utrecht for doing a PhD under the supervision of Dr. Nicolas Rivron and Prof. Dr. Clemens A. van Blitterswijk first affiliated to Twente University and then Maastricht University. All worked was performed as a guest at the Geijsen lab at the Hubrecht Institute. The results of such PhD are described in this book.